SYNTHESIS AND BIOLOGICAL EVALUATION OF ZWITTERIONIC POLYSACCHARIDES

By

JOHNY M. NGUYEN

Dissertation

Submitted to the Faculty of the

Graduate School of Vanderbilt University

in partial fulfillment of the

requirements for the degree of

DOCTOR OF PHILOSOPHY

in

CHEMISTRY

March 31st, 2022

Nashville, Tennessee

Approved:

Steven D Townsend, Ph.D.

Nathan D. Schley, Ph.D.

Lars Plate, Ph.D.

Jennifer A. Gaddy, Ph.D.

To my parents,

for their unconditional love and support.

Có công mài sắt có ngày nên kim – *Vietnamese Proverb*

Literal translation: If you are persistent enough, you can make needles out of metal bars.

Lesson: Perseverance can turn any dreams into reality.

ACKNOWLEDGMENTS

First and foremost, I would like to thank my mentor and advisor, Prof. Steven D. Townsend, for his unwavering support and enthusiasm over the past five years. Looking back, I am still not exactly sure what he saw in me, but I am forever thankful for his immense patience and kindness. I am grateful also for his evaluation of my numerous ideas that I presented to him and for his vast knowledge in the realm of organic chemistry and more importantly, life. Conversations with Steve often deviate from chemistry to talk about our families and personal struggles growing up in socially and economically disadvantaged communities. I am thankful for his faith in me, especially when I was close to losing faith in myself. Over the more recent years, Steve has continued to be a mentor, role-model, and friend to me. Being a part of the Townsend group has been a great honor. Although I am quite sad to be leaving, I look forward to seeing what other luxury goods Steve will be buying, as well as what is in store for the future of the Townsend lab.

Furthermore, I would like to thank the other professors who have greatly contributed to my growth, education, and success while at Vanderbilt: Nathan D. Schley, Lars Plate, and Jennifer A. Gaddy. They have constantly pushed me to be a more critical thinker and helped me become an independent scientist. Moreover, I am grateful for their numerous scientific insights, especially during my candidacy and IRP exams. Individually, I would like to thank Jen for her generous support, mentoring and interest in my mental well-being.

I owe a great deal of gratitude to my mentors, Dr. David B.C. Martin and Dr. Richmond Sarpong, for their continual support. My roots as a chemist come from Prof. David B.C. Martin at UC Riverside and Dr. Richmond Sarpong at UC Berkeley. Dave fostered a great learning environment and spent an enormous amount of time working with me throughout my first couple of years at UC Riverside. Learning synthesis from Dave first-hand was certainly one the most valuable and fun experiences I've had and without

it, I wouldn't have pursued graduate education. My internship experience at Berkeley with Richmond, gave me a profound sense of appreciation for the art of total synthesis. Moreover, his love for teaching and organic synthesis was truly inspiring.

During my time at Vanderbilt, I have been fortunate to have a supportive group of people around me in the chemistry department. I would like to thank personally: Josh Elder, Cal Larson, Danielle Penk, Chris Sharp, and Dr. Isaiah Speight, and Dr. Ross Koby. I am thankful for y'all and our insightful conversations both about life and science. I had the privilege of working closely with many great colleagues. I am grateful to Dr. Kelly M. Craft for her guidance and mentorship while I was a junior student in the lab. Her thoughtful comments helped me to critically evaluate the purpose of every reaction and how to problem solve a step at a time. In addition, she was an incredible desk-mate, hood-mate, and friend! I appreciate her for always listening to my morning rants, failures, and triumphs. Moreover, I am greatly indebted to Dr. Eric D. Huseman for everything he has helped me with over the years, especially going over reaction mechanisms, NMRs, and anything related to Taylor Swift and chemistry.

I would like to thank the Townsend group collectively for making our laboratory a safe and great working environment. I am thankful for the many talented colleagues I have had the honor to work with and collaborate on many occasions: Rebecca Moore, Sabrina Spicer, Lianyan Xu, Cleo Evans, Dr. Kerrick Reese and Dr. Jaimin Keith. Additionally, each member of the Townsend lab warrants special mention for their encouragement, insight, helpful discussion, support, and friendship. While my graduate education has had its high moments, it has certainly had its low points. Having friends like Alex Hughes, C. Elizabeth Adams, Dr. Jade Williams, and Nainoa Norman Ing who could pick me up when I was drowning in work or celebrate with me when I had a successful reaction was without a doubt central to my ability to endure graduate school. To my best friends, Alexander H. Nguyen and Gloria Chang, thank you for always checking up on me and for your continual support.

I am beyond thankful for my parents, who have sacrificed everything, including moving to a foreign country to create a better life for my sister and me. Without them, I would be lost. My only big regret in life thus far is that I haven't been able to visit them as often as I can, especially during Covid. I am also grateful for my sister, Kelly. Thank you for holding down the fort while I am away. Although we haven't always seen eye to eye, I am honored to be your brother.

I want to give my deepest thanks to my fiancé, Nhi. She has been my best friend and better half (sometimes three-quarters) for many years, and without her, I would not have made it through graduate school. She has always dragged me out of lab when I needed it and only when I need it! Her love, patience, and sacrifice mean everything to me. I am also grateful for Nhi's family for their support and encouragement. Finally, and most importantly, I am thankful for my relationship with God. He has given me strength, love, and guidance during the darkest days in my graduate career.

This work was supported by predoctoral fellowships from the Gates Millennium Scholars program and the Vanderbilt University Provost Graduate Research Fellowship. I appreciate the efforts of the Gates Millennium Scholars program to help alleviate the financial burden of individuals from underrepresented areas to pursue higher education. Without the Gates Millennium Scholars program, I wouldn't have been able to afford a college education.

TABLE OF CONTENTS

LIST OF FIGURES

LIST OF SCHEMES

LIST OF TABLES

LIST OF ABBREVIATIONS

Note: For chemicals, CAS number given in square bracket when available.

Ac	acetyl
Å	angstrom (10^{-10}meter)
Ac_2O	acetic anhydride [108-24-7]
AcOH	acetic acid [64-19-7]
aq.	Aqueous
BDMA	benzaldehyde dimethyl acetal [1125-88-8]
$BF3•OEt_2$	boron trifluoride diethyl etherate [109-63-7]
BnBr	benzyl bromide [100-39-0]
Bn	benzyl
Bz	benzoyl
BzCl	benzoyl chloride [98-88-4]
BRSM	based on recovered starting material
°C	degrees Celsius
cat.	Catalytic
CAM	ceric ammonium molybdate (TLC stain)
CAN	ceric ammonium nitrate [16774-21-3]
$CDCl_3$	chloroform-*d* [865-49-6]
CH_3CN	acetonitrile [75-05-8]
CH_3OH	methanol [67-56-1]
CH_2Cl_2	methylene chloride [75-09-2]
CCl_3CN	trichloroacetonitrile [545-06-2]
CF_3CO_2H	trifluoroacetic acid [76-05-1]

conc	concentrated
COSY	homonuclear correlation sprectroscopy
CSA	10-camphorsulfonic acid [3144-16-9]
δ	chemical shift in ppm
d	doublet
DBU	1,8-diazobicyclo[5.4.0]undec-7-ene [6674-22-2]
dd	doublet of doublets
ddd	doublet of doublet of doublets
DMAP	4-dimethylaminopyridine [1122-58-3]
DMF	*N*-*N*-dimethylformamide [68-12-2]
DMSO	dimethyl sulfoxide [67-68-5]
dt	doublet of triplets
eq.	equivalent
Et	ethyl
Et_3N	triethylamine [121-44-8]
Et_2O	diethyl ether [60-29-7]
EtOAc	ethyl acetate [141-78-6]
EtOH	ethanol [64-17-5]
Et_3SiH	triethylsilane [617-86-7]
g	gram
H_2O	water [7732-18-5]
hr	hour
HCl	hydrochloric acid [7647-01-0]
HMBC	heteronuclear multi-bond correlation spectroscopy

HRMS	high-resolution mass spectrum
HSQC	heteronuclear mass spectrometry
imH	imidazole [288-32-4]
I_2	iodine [7553-56-2]
Ir	Iridium
J	coupling constant
L	liter(s)
m	milli, multiplet (NMR)
M	moles per liter
mCPBA	meta-chloroperoxybenzoic acid [937-14-4]
Me	methyl
MHz	megahertz
min	minute(s)
mol	mole(s)
mp	melting point
NaOH	sodium hydroxide [1310-73-2]
$NaOCH_3$	sodium methoxide [124-41-4]
$NaBH_3CN$	sodium cyanoborohydride [25895-60-7]
$NaHCO_3$	sodium bicarbonate [144-55-8]
NaH	sodium hydride [7646-69-7]
NaN_3	sodium azide [26628-22-8]
Na_2S_2O3	sodium thiosulfate [7772-98-7]
Na_2SO_4	sodium sulfate [7757-86-2]
NH_4Cl	ammonium chloride [12125-02-9]

NIS	*N*-iodosuccinimide [516-12-1]
NOESY	nuclear Overhauser effect spectroscropy
NMR	nuclear magnetic resonance
OAc	acetoxy
OTf	trifluoromethanesulfonate
P_2O_5	phosphorus(V) pentoxide [1314-56-3]
Pd/C	palladium on carbon [7440-05-3]
$Pd(OH)_2$	palladium hydroxide [12135-22-7]
PEtN	phosphoethanolamine
Piv	pivaloyl
PMP	para-methoxy phenyl
PPh_3	triphenylphosphine [603-35-0]
ppm	parts per million
p-TsOH	p-toluenesulfonic acid [104-15-4]
p-Thiocresol	4-methylbenzenethiol [106-45-6]
PhSH	thiophenol [108-98-5]
pyr	pyridine [110-86-1]
RBF	round bottom flask
R_f	retention factor (TLC)
rt	room temperature
q	quartet
s	singlet
SM	starting material
sat.	saturated

TEAB	triethylammonium bicarbonate
TBAI	tetra-*n*-butylammonium iodide [311-28-4]
TBS	*tert*-butldimethylsilyl
TBHP	*tert*-butyl hydroperoxide [75-91-2]
TEMPO	2,2,6,6-tetramethyl-1-piperdinyloxy [2564-83-2]
THF	tetrahydrofuran [109-99-9]
TMS	trimethylsilyl
TMSOTf	trimethylsilyl trifluoromethanesulfonate [27607-77-8]
TfOH	triflic acid [1493-13-6]
Tf_2O	triflic anhydride [358-23-6]
Tr	trityl
ZPS	zwitterionic polysaccharide

Chapter 1

Cellulose as an Architectural Component in Bacterial Biofilms

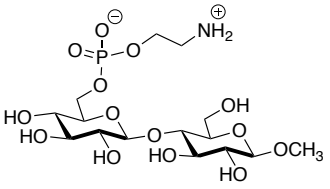

pEtN Cellobiose

1.1 Abstract

Bacteria thrive in diverse environments by establishing biofilms, a collection of surface associated communities of microbial cells encased in an extracellular polymeric matrix. These cells are a concern in the medical field due to their increased resistance to antibiotics. Bacteria found in biofilm can have antibiotic resistance 10-1000 times that of their planktonic counterparts.[1] As a result, it is important to study the formation of biofilms. Cellulose biofilms are predominantly formed by *Enterobacteriaceae*, such as *Salmonella* and *Escherichia coli* (*E. coli*) spp. strains. Biofilms contribute to these species by providing antimicrobial protection, colonization of bacterial communities, and the promotion of DNA exchange.[1] Current studies suggest that the glycopolymer cellulose, and its functionalized derivatives, plays an important role in the formation of *E. coli* biofilms. While bacterial cellulose was first discovered in the 19th century, it was not until this last decade that studies emerged to provide insight into the biosynthesis and production of bacterial cellulose. This chapter examines recently published research on how cellulose-based polymers modulate bacterial cell processes including alterations in cellular metabolism, extracellular matrix secretion, surface organelle biogenesis, cellular adhesion, and biofilm formation.

1.2 Introduction

Cellulose, an unbranched extracellular polysaccharide, is the most abundant and sustainable biopolymer found on Earth.[2] Cellulose is found in plants, fungi, algae, flagellates, and in some animals. It is the main component of the cell wall in plants and in many natural fibers, such as wood (90% of wood contains cellulose), cotton, and jute. Additionally, plant cellulose is associated with other materials in the cell wall, such as hemicelluloses and lignins. At the structural level, cellulose is a polysaccharide composed of glucans, linked via β-(1→4) glycosidic bonds (Figure 1A).[3] Cellulose chains are linear, with aggregation occurring through intra- and intermolecular hydrogen bonds and van der Waals forces (Figure 1B). These plant microfibrils are commonly 10 nm in diameter and particularly long relative to their width (10-50 mm). When grouped, these microfibrils form macro-fibrils, or cellulosic fibers.

Cellulose was first discovered by Aneselme Payen in 1838, where a white crystalline substance resembling starch was extracted from wood.[4] Furthermore, it was not until years later that the structure and molecular weight of cellulose was confirmed by Hermann Staudinger.[5-6] Staudinger showed that the viscosity of the polymer is directly proportional to its molecular weight and as a result, the equation for this relationship is known as the *Staudinger equation*.[6] Despite its ubiquitous presence in plants, it is reported to exist in a variety of bacteria. Although the molecular formula of both plant and bacterial cellulose are the same, their chemical and physical features are different.[7-8] One key difference lies in the highly ordered structure of these celluloses. Distinctive from plant cellulose, bacterial cellulose is

secreted in the form of a ribbon, composed of bundles of microfibrils.[9-13] These fibers are very thin with a width that is only one-hundredth that of plant cellulose. A shared feature among the cellulose biosynthetic machinery is the coupling of glucose polymerization reactions with secretion of the polymer in either the extracellular matrix or the cell's envelope.[13-15]

Cellobiose, a β-1,4-linked glucose dimer, is the structural unit of cellulose and the major product in enzymatic or acid hydrolysis of cellulose. Cellobiose is a repeating unit and is incorporated at varying degrees of polymerization. When considering the structure of cellobiose, the molecule is highly oxygenated bearing eight free alcohols along with a hemiacetal group.[8] These functional groups provide cellobiose with the ability to form strong inter- and intramolecular hydrogen bonds.

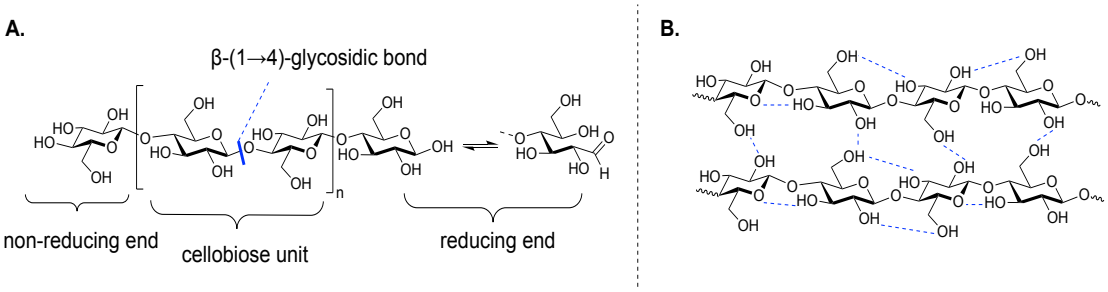

Figure 1.1. Properties of cellulose polymers in nature: (**A**) Molecular structure of cellulose polymer with cellobiose as a repeating unit. (**B**) Inter-and intramolecular hydrogen bonds in cellulose.

1.3 Synthesis and Degradation of Cellulose

1.3.1 Synthesis of Cellulose

The biosynthesis of plant-derived cellulose takes place in the plasma membrane in plants, Golgi apparatus in algae, and acquired extracellular in bacteria (Figure 1.2. A).[8,10-12] While cellulose predominantly exists as an essential structural component in plants, bacteria synthesize cellulose to provide a protective coat around the cell (i.e., exopolysaccharides). Bacterial cellulose (BC) was initially discovered by A.J. Brown in 1886 from *Acetobacter xylinum*, who noticed the growth of unbranched pellicles that displayed similar structural features to the plant-derived cellulose.[7] Despite the initial discovery, it was not until the 20th century that more in-depth research on BC was accomplished. From the onset, a wide variety of bacteria was discovered to produce cellulose including *Enterobacter*, *Agrobacterium*, *Dickeya*, *Rhizobium, Achromobacter*, *Pseudomonas*, *Komagataeibacter* (formerly *Gluconacetobacter*), *Gluconacetobacter* (formerly *Acetobacter*), *Alcaligenes*, *Aerobacter*, *Azotobacter*, *Agrobacterium*, *Dickeya*, *Rhizobium, Burkholderia*,

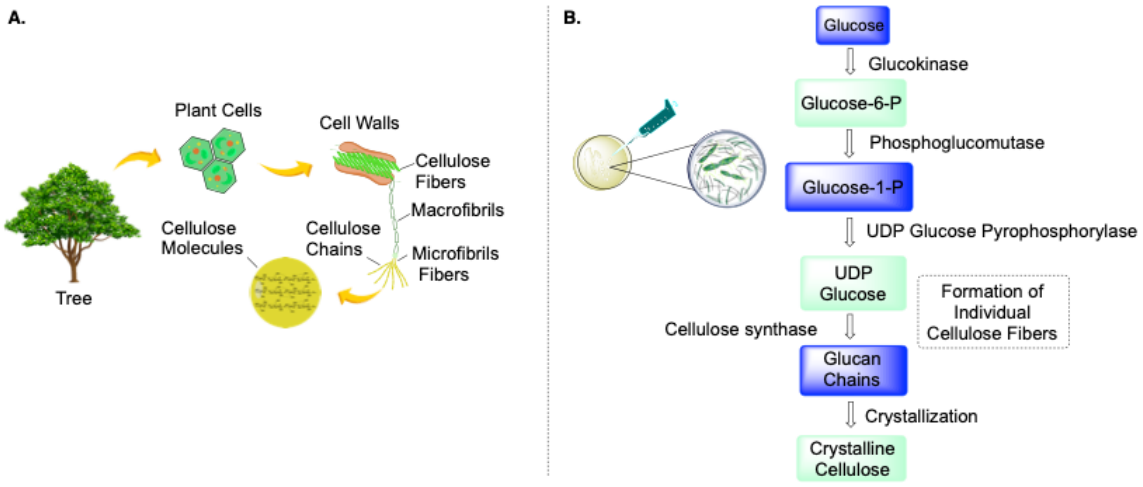

Figure 1.2. Natural sources of cellulose: (**A**) Cellulose contained in plants or trees. (**B**) Cellulose found in bacteria.

Salmonella, *Sarina* and *Escherichia coli*.[9-20]

Contrary to plant-derived cellulose, BC is a pure crystalline material with a high degree of polymerization and surface area and is free of hemicellulose and lignin. The degree of crystallinity represents the relative number of crystalline regions in the cellulose polymer, but also helps quantify changes in cellulose structure stemming from physiochemical, biological, and chemical treatments.[21-26] More importantly, the β-(1→4) glucan chain in cellulose corresponds strongly via hydrogen bonding and is responsible for maintaining the high degree of crystallinity and stability of cellulose.[27-28] Taking inspiration from the seminal work of A.J. Brown, the Tokoh group began to further characterize BC and has shown it produces an interesting three-dimensional fibers network with fibers diameter of approximately 30-50 nm.[29] These ribbon-like microfibrils are much thinner compared to plant cellulose, making BC a more porous material. The unique physical properties along with the ease of production have prompted many uses of BC fibers in the medical field, such as wound care treatment.[30] Since its discovery, there is a growing body of work on the production of modified bacterial cellulose and its applications. Table 1.1. compares the differences in growth and production between bacterial and plant-derived cellulose fibers.

Table 1.1. Comparison criteria for the synthesis of bacterial and plant-derived cellulose fibers.

Criteria	Bacteria-derived cellulose	Plant-derived cellulose
Composition	Pure cellulose produced after bacterial cells removal, no hemicellulose or other components present	Primarily wood components: lignin, hemicellulose, and cellulose
Growth conditions	Sugars used from agricultural and food wastes, controlled bioreactor conditions: temperature, pH, mixing, nutrients, and aeration	Nutrients, climate conditions, soil type, and susceptible to insect infestation
Production time	Days, depending on bacterial species and growth rate	Years, depending on tree species

Bacterial cellulose biosynthesis, applications, and production have been reported in detail by many groups around the world.[31-33] Cellulose biosynthesis entails two key steps: step one entails the polymerization of β-(1→4) glucan chain to cellulose, and step two involves cellulose chain crystallization and assembly. Figure 1.2.B shows a schematic diagram of the BC biosynthesis.[34] Cellulose microfibrils are synthesized inside the bacteria and extrude between the outer and cytoplasmic membranes of the cell. These ribbon-like structures are composed of approximately 25-50 microfibrils. Bacteria that produce cellulose metabolize glucose via the Krebs cycle or the pentose-phosphate cycle, depending on the physiological state of the cell coupled with gluconeogenesis.[32] The biosynthesis of cellulose is a multi-step sequence involving different enzymes, catalytic complexes, and regulatory proteins. The four major enzymatic steps for the synthesis of BC from

glucose are: (1) the phosphorylation of glucose by glucokinase, (2) the transformation of glucose-6-phosphate (Glc-6-P) to glucose-1-phosphate (Glc-1-P) by phosphoglucomutase, (3) the synthesis of uridine diphosphoglucose (UDP-Glc) by UDP glucose pyrophosphorylase (UGPase), and (4) cellulose synthase, a membrane bound enzyme that catalyzes the polymerization of glucose using UDP-Glc as its donor.[21-22]

The synthesis of cellulose occurs when glucose is polymerized into a β-(1→4) chain, which incorporates other neighboring chains and protrudes from the cell as fibrils.[29, 31] This coupling step needs to occur for the biosynthesis of cellulose. Among the characterized microorganisms with respect to cellulose synthesis, *G. xylinus* is the most extensively studied.[23-24] During initial investigation on BC production by this bacterium, it was determined that the BC biosynthesis system is composed of *bcs* operons, which is vital for cellulose synthesis and its activation. Furthermore, the *bcs* operon is assembled by *bcsA*, *bcsB*, *bcsC* and *bcsD*.[22] Through further analysis, it was understood that *bcsA* is responsible for the polymerization of UDP-Glc; *bcsB,* a subunit of cyclic D-guanosine monophosphate, is an activator of cellulose and bcsC and *bcsD* are responsible for the crystallization and extrusion of cellulose. The repeating unit, cellobiose, is also derived biosynthetically from cellulose and relies on cellulase, an enzyme that hydrolyzes β-(1→4) glycosidic bonds.

1.3.2 Degradation of Cellulose

The degradation of cellulose to produce biomaterials is typically prepared industrially by subjecting the material to a strong acid under strict control of temperature, agitation, and hydrolysis time. The differing hydrolysis conditions and sources of cellulose can generate diverse cellulose nanomaterials (CN) with unique morphologies.[35] Additionally, it has been studied that the hydronium ions penetrate the loosely bundled and disordered amorphous region instead of the tightly bound crystalline area.[36] The preparation of CNs generally use hydrochloric acid or sulfuric acid. Interestingly, hydrolysis of cellulose using sulfuric acid can create rod-like materials with negative charges (OSO_3^-/H^+), whereas treatment with hydrochloric acid generates neutral materials and minimizes their dispersion ability.[35]

Enzymatic hydrolysis of cellulose is also known via a multi-step heterogeneous reaction in which cellulose is cleaved by complex enzymes such as, endoglucanase, cellobiase, and cellobiohydrolase that work synergistically with each other.[37] Particularly, fungi, especially *Penicillium*, *Aspergillus*, and *Trichoderma* species, produce commercial cellulases.[38] Currently, *Trichodermareesei* (*T.reesei*) is the most efficient producer of extracellular cellulase enzymes and is the preferred choice of enzyme for CNs production industrially.[37] Lastly, the enzymatic hydrolysis of cellulose is dependent on the surface area of the substrate, concentration of the enzyme, reaction temperature, and duration of enzyme activity.[39]

1.4 Bacterial Biofilm and Extracellular Matrix

To cooperate and coordinate within a community, microorganisms form aggregates of cells encased in a rigid but dynamic extracellular matrix that is commonly referred to as a biofilm. Biofilms are complex cellular structures that are governed by tightly controlled regulation of gene expression of biofilm-associated factors. The shift from planktonic to sessile life occurs due to a variety of environmental factors which are sensed by the cell; triggering alterations in transcriptional and metabolic processes leading to enhanced cellular adhesion.

Biofilms serve several functions that facilitate bacterial colonization and survival in the environment. The tenacious extracellular matrix of the biofilm serves to increase bacterial survival of antimicrobial challenges including antibiotics. Biofilms also help bacteria evade host immune responses including phagocytosis by innate immune cells. Additionally, the community of bacterial cells that is housed in a biofilm is protected from various environmental stressors, such as desiccation or osmotic pressure. Thus, bacterial biofilm formation is critical for microbes to create and maintain a replicative niche.

The self-produced biofilm matrix, composed of extracellular polymeric substances (EPS), is critical to structural integrity, protection, surface adhesion and survival. This hydrated matrix, which accounts for over 90% of the total biofilm mass, is composed of exopolysaccharides, nucleic acids (RNA and extracellular DNA), lipids, and amyloid-like proteins.[40-41] The structural morphology of the matrix is highly varied and can indicate the extent of a biofilm virulence or stage of formation. Initially, biofilms appear smooth and flat in their microcolonies, but later can become

rough and wrinkled, often progressing into mushroom-like macro-colonies.[41]

EPS mediates cell-to-cell communication interactions called quorum sensing as a result of the close proximity of the cells within the matrix. The EPS matrix is particularly effective in protecting microorganisms against hostile stressors including ultraviolet radiation, variations in temperature, and pH. Moreover, protection against antimicrobial agents is afforded as the matrix acts as a structural barrier.[42] The reduced diffusion of antimicrobial agents across the matrix contributes to the spread of antibiotic resistant strains of bacteria. In addition to the physical barrier of the matrix, anionic molecules within the EPS bind to charged antibiotics, effectively deactivating them.[43]

As outlined above, the biofilm matrix is an integral part of these cellular communities. Furthermore, it has been demonstrated that the transition from planktonic to sessile life is regulated by a complex network of polysaccharide biosynthetic genes, and as such, it is important that the polysaccharide components of it are explored in depth.[44] The function and subsequent components of these extracellular polysaccharides vary greatly between microbes but can generally be separated into two distinct categories: those associated with the cellular surface, and those that are secreted extracellularly.[40] The polysaccharides described below are those implicated in biofilm formation in *E. coli* (Figure 1.3.).

Capsular polysaccharides (CPS) are one of the primary virulence factors associated with the pathogenesis of a myriad of species. These protective glycans are tightly bound to the bacterial cell surface through covalent attachments to phospholipid or lipid-A moieties. These hydrated molecules are structurally diverse

with more than 80 unique CPSs identified in *E. coli*.[45] Despite the structural variability, CPS can be classified into four groups based on the location of the biosynthesis gene cluster, biosynthesis processes, and mode of transport and regulation.[46] As a first line of defense against the host immune response, these capsules are often targeted for treatment and prevention of infection.

Cell surface polysaccharides are associated with bacterial adhesion, biofilm stability, and bacteria-mediated immune responses.[40] One adhesive structure found on many biofilm-producing bacteria is pili. Also termed fimbriae, these proteinaceous appendages are made up of interacting pilin subunits, and are integral in cellular adhesion, host cell invasion, biofilm formation and cell motility.[47] Binding of the proteins located on the tip of the pilus to specific receptors on the host cell initiates cellular adherence. Moreover, pili interacts with structural units of neighboring pili to instigate auto aggregation of bacterial cells in the beginning stages of biofilm formation. Mediating this attachment is a linear glucosaminylglycan, polysaccharide intercellular adhesin (PIA, **1.1**) (Figure 1.3.). It has been shown that PIA is implicated in early stages of adherence to host tissues.[48] Additional studies have found PIA to play an integral role in moderating the host cell immune response.[49-50] Implicated tightly in *S. aureus* and *S. epidermidis* biofilm formation among others, PIA is responsible for the intracellular bacterial adhesion found in mature biofilms.[51]

While many polysaccharides implicated in the biofilm matrix serve to promote bacterial cell adherence, others help to mediate microbial protection from host and environmental challenges. One such polysaccharide is alginate, a linear chain of 1→4 linked mannuronic acid and l-guluronic acid.[52-53] Alginate (**1.2**) was originally

studied due to its large role in cystic fibrosis lung infections of *P. aeruginosa.*[54] While it was originally thought that alginate promoted bacterial attachment and biofilm formation, upon more recent study, it has been determined that due to its highly hygroscopic properties, alginate is responsible for promoting antimicrobial and host immune protections.[55]

Structurally composed of a glucose, galactose, fucose, and glucuronic acid core, colanic acid (**1.3**) is an additional cell-associated, branched polysaccharide. Moreover, other branched polysaccharides that are known contributors to biofilms are curdlan (**1.4**) and dextran (**1.5**) (Figure 1.3.). The production of this protective capsule provides defense against extreme environmental stressors, such as extreme temperatures, osmotic shock, and dehydration.[56-57] Colanic acid expression is not critical for initial microbial adhesion, however, has been shown necessary for the maturation of three-dimensional biofilms.[58-60]

Finally, cellulose plays a key role in the structural integrity of the biofilm structures formed across species.[53] Initial reports of cellulose-mediated biofilm formation cite the contribution of cellulose to cell aggregation in *G. xylinus.* Cellulose (**1.6**) in various *Enterobacteriaceae* has been shown to interact with curli, protein fibers, to develop the mature biofilm matrix.[61] Additionally, the production of bacterial cellulose initiates binding of epithelial cells and suppresses the immune response to *E. coli* Nissle 1917.[62] Taken together, all these functions set up an important framework for a symbiotic relationship between host surface and bacterium. Most interestingly, cellulose is a ubiquitous polysaccharide used by many bacteria for a wide array of different functions, highlighting the structural and functional diversity

of polysaccharides implicated in the biofilm matrix.[53]

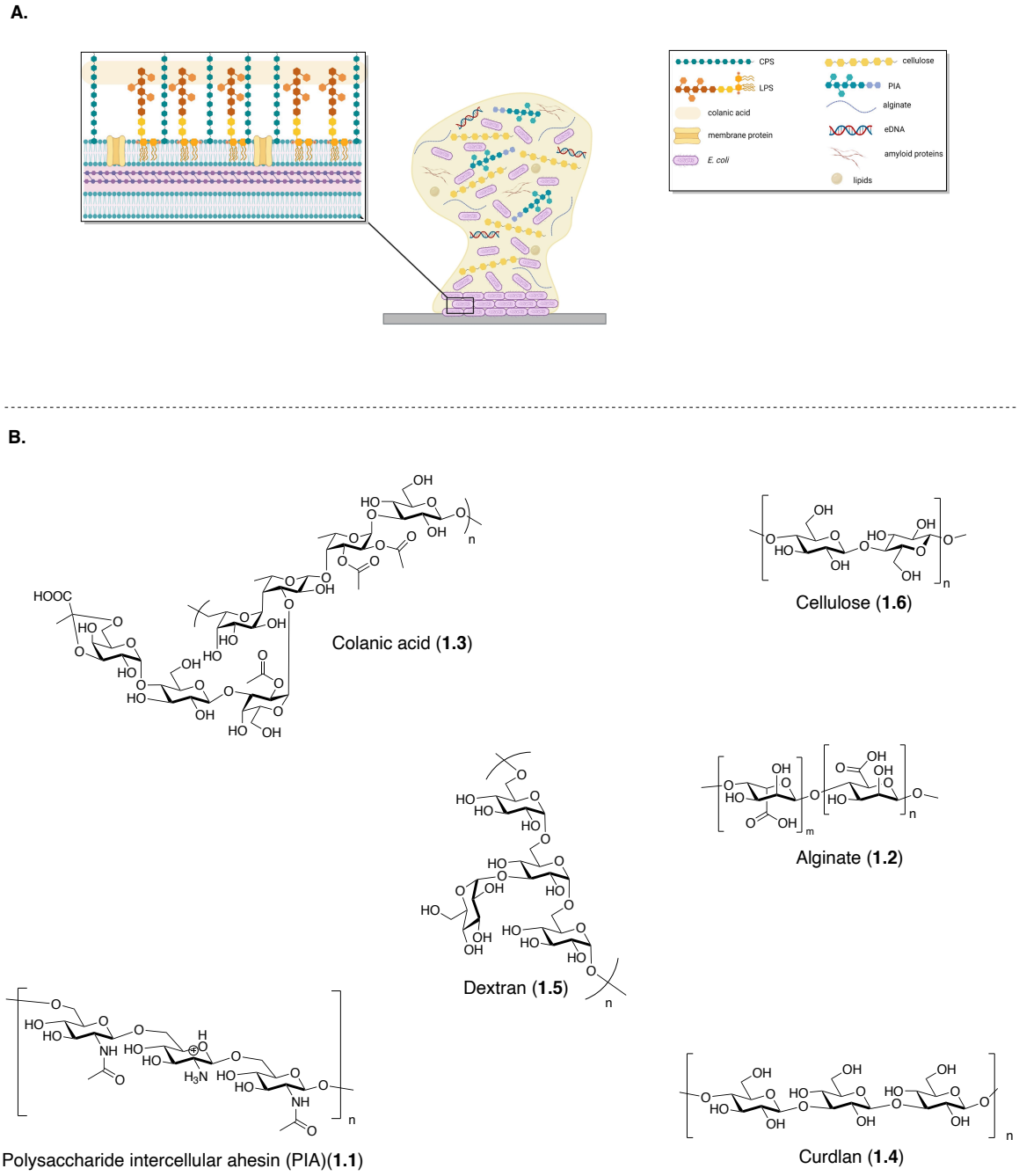

Figure 1.3. (**A**) Extracellular polymeric substances (EPS) matrix. (**B**) Polysaccharides associated with bacterial biofilm and extracellular matrix.

1.5. Chemical and Enzymatic Modification to Cellulose Fibers

Cellulose is a versatile bio-based material with the potential to be used in a variety of applications. In the past decade, the race to develop sustainable and biodegradable materials have led to the rapid growth in cellulose-focused research with the aim of replacing petroleum-based materials. As an excellent alternative, cellulose is a naturally abundant polymer that could be used for this purpose because of its low-cost of production, easily modifiable chemical functionality, and strong physical properties, which makes it an ideal feedstock to manufacture new materials. Moreover, the core structure of cellulose allows for convenient modification via a chemical or enzymatic reaction. Importantly, the functional groups available on cellulose serve as handles that can be altered using various methods including sulfonation, oxidation, phosphorylation, etherification, esterification, silylation, carbamation, and nucleophilic substitution (Figure 1.4.).[63-64]

Depending on the preferred site of transformation, the primary or secondary alcohols of cellulose can be functionalized. As a result, these structural modifications can greatly improve the versatility of cellulose-based materials. In this section, we discuss some literature examples of regioselective and site-specific chemical and enzymatic modification of cellulose.

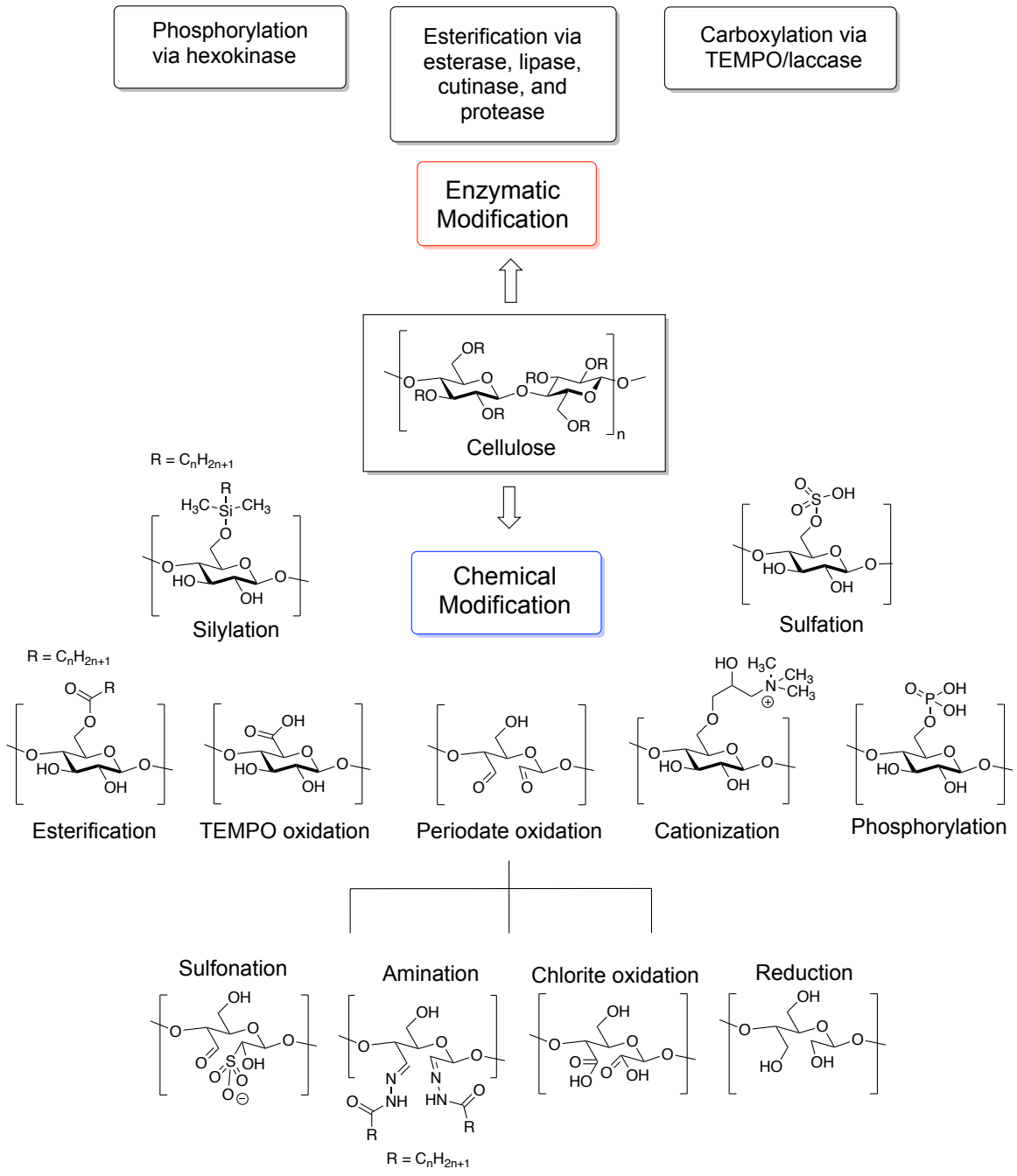

Figure 1.4. Enzymatic and chemical modification of cellulose.

1.5.1 Chemical Modification of Alcohols

One of the first implemented strategies to modify cellulose is through the oxidation of the C-6 primary alcohol and the oxidative cleavage between the C-2 and C-3 carbon bond in β-*D*-glucose monomer of cellulose to access carboxycellulose. The presence of the negative charge on the carboxylic acid group is deleterious to cellulose crystalline structure due to the enhanced repulsive interactions between charges. Published work has shown that an increase in the degree of oxidation will result in a decrease of crystallinity leading to a more amorphous-like cellulose material.[65-66]

Although many strategies exist for the oxidation of alcohols, two known methods to access carboxycellulose fibers include: the periodate-chlorite and 2,2,6,6-tetramethyl-1- piperidinyloxy (TEMPO) oxidation reactions. Periodate-chlorite mediated oxidation of cellulose is achieved by an initial oxidative cleavage of the vicinal diols (C-2 and C-3 alcohols) in β-*D*-glucose monomer of cellulose resulting in the formation of 2, 3, dialdehyde cellulose (DAC). From here, sodium metaperiodate in an aqueous solution can regioselectively oxidize the C-2 and C-3 alcohols to provide Dicarboxyl acid cellulose (DCC) fibers.[65-66]

The use of the organocatalyst TEMPO and its analogous have opened a new area of efficient and selective functionalization of alcohols to ketones, aldehydes, and carboxylic acids. This catalytic oxidative reaction offers a mild protocol to functionalized complex molecules. Specifically, De Nooy *et al.* first applied TEMPO-mediated oxidation to water soluble carbohydrates, such as pullulan (**1.7**), starch

(**1.8**), dextrin (**1.9**) and cellulose for the regioselective conversion of C-6 primary alcohol to a carboxylic acid moiety (Figure 1.5.).[67]

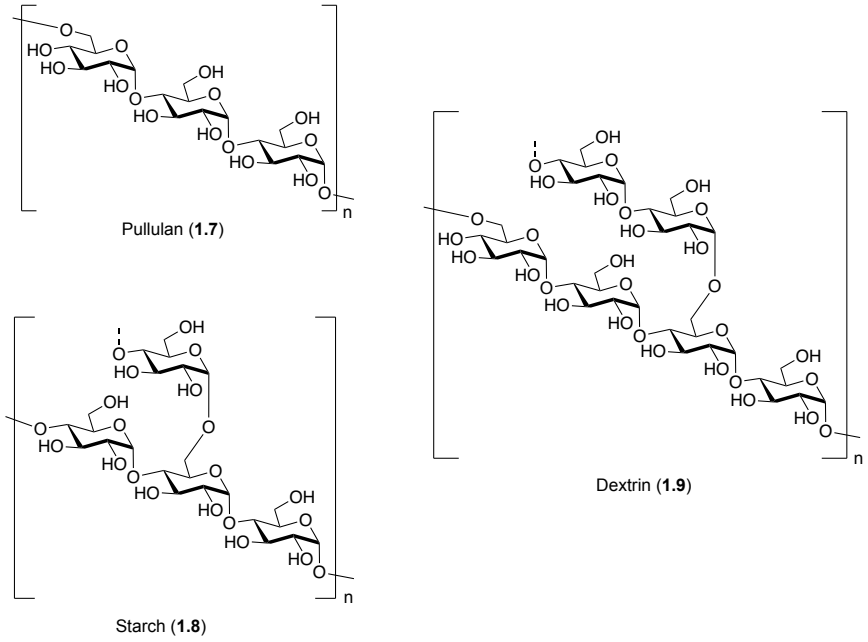

Figure 1.5. Structures of Pullulan (**1.7**), Starch (**1.8**), and Dextrin (**1.9**). Pullulan, starch, and dextrin have been successfully functionalized via TEMPO-mediated oxidation.

In this reaction, catalytic amounts of TEMPO and NaBr were dissolved in a solution of cellulose at pH 10-11, and oxidation commenced by the addition of a solution of NaClO as the primary oxidant.[65-66] This sustainable and efficient reaction for the conversion of the primary alcohol to the carboxylate is believed to proceed to the mechanism shown in Figure 1.6. Mechanistically, TEMPO reacts with the oxidant to create a nitrosium ion intermediate that then transforms the C-6 alcohol into an aldehyde. Next, the aldehyde group undergoes further oxidation to access the carboxylic acid group. Various TEMPO-mediated oxidation reactions of complex mono-, oligo- and polysaccharides have been achieved thus far. The TEMPO-

mediated oxidation reaction remains one of the most popular reactions for oxidizing cellulose in industry since it is thoroughly studied and cost-effective.

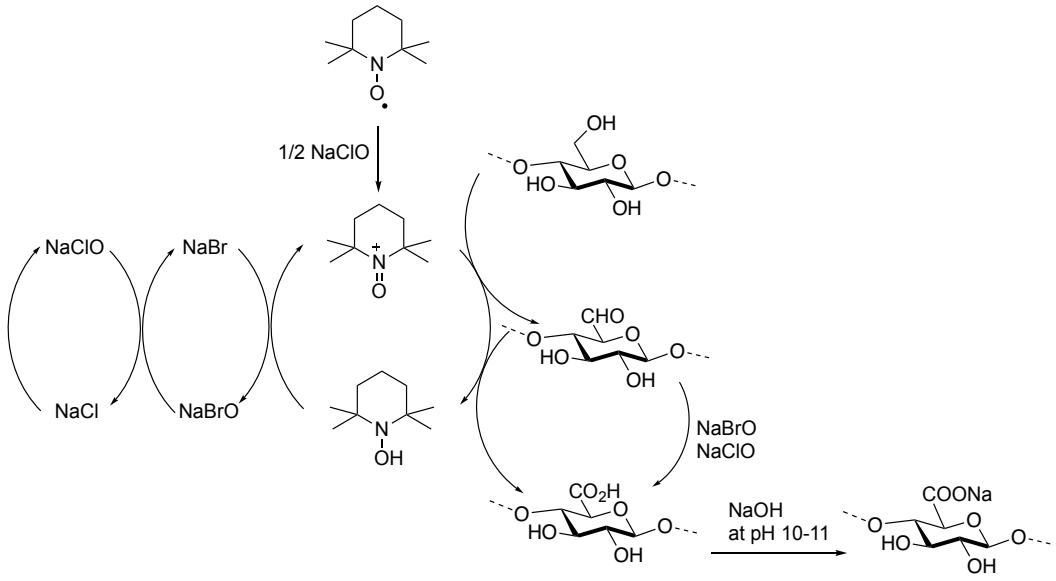

Figure 1.6. Mechanism of selective oxidation of C-6 alcohols of cellulose to carboxylate groups by TEMPO/NaBr/NaClO in aqueous solution.

Additional approaches for the chemical modification of cellulose have also used DAC as an important intermediate (Figure 1.7.). DAC can be functionalized to form cationic quaternized (CDAC) cellulose through use of Girard's reagent ((2-hydrazinyl-2- oxoethyl)-trimethylazanium chloride).[64] Alternatively, introduction of sulfur atoms on cellulose fibers can also be achieved via a sulfonation reaction by treating DAC with bisulfite to form adducts to give anionic sulfonated cellulose (ADAC).[68]

Among the diverse set of chemical modifications of cellulose, esterification represents one of the most promising methods, which was adopted by van de Ven *et al*. to access cellulose derivatives.[63] The first step of the reaction involves the treatment of an alcohol with sodium hydroxide, followed by S_N2 displacement with monochloroacetic acid to provide the carbomethylated cellulose fibers. Interestingly, other methods to modify the C-6 position of cellulose fibers include phosphorylation and silyl ether formation. To date, more than 100 different methods of converting cellulose into new materials have been achieved.

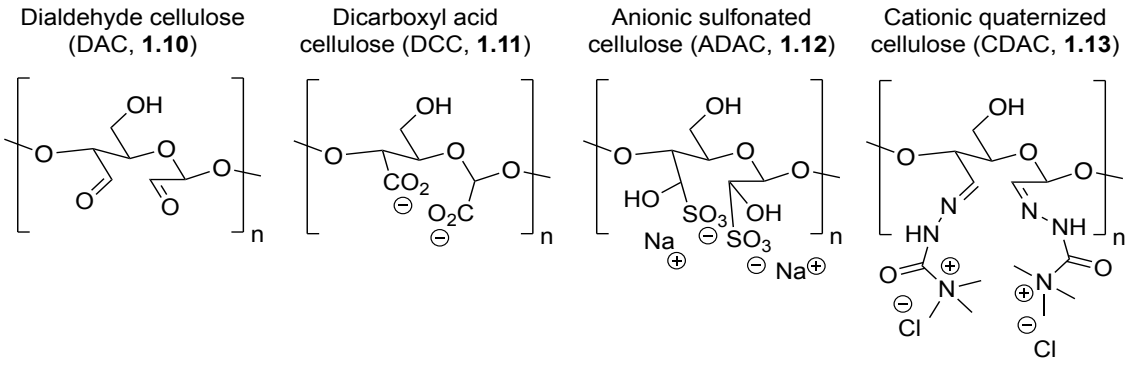

Figure 1.7. Key intermediates and products from cellulose functionalization.

1.5.2 Enzymatic Modification of Alcohols

Enzymatic modification of cellulose fibers is a viable greener method when compared to the traditional route using chemical synthesis.[69] Cellulose material functionalized with enzymes has a significant advantage since it avoids the production of toxic byproducts as well as using harmful reagents. To date, chemical synthesis to esterify cellulose uses toxic anhydrides, acid catalysts, and non-green solvents. The introduction of enzymes, such as esterases, and in particular, lipases

has been used successfully for the regio- and stereo selective esterification of complex molecules and sugars.[70-71] Furthermore, one of the earliest examples of enzymatic esterification of cellulose was accomplished by Sereti *et al.*, where cellulose fatty esters were synthesized.[72]

More recently, enzymatic phosphorylation of cellulose has been reported by Cavaco-Paulo *et al.* This phosphorylation involves hexokinase by which it catalyzes the phosphoryl transfer from adenosine-5'-triphosphate (ATP) to the 6-alcohol of cellulose.[73] This method is also applicable to various furanose and pyranose compounds as well. The ability to enzymatically phosphorylate cellulose rather than chemical phosphorylation cuts down many complicated steps that would otherwise require additional protection and deprotection sequences in chemical synthesis. Enzymatic phosphorylation allows for a facile and efficient synthesis, while eliminating many of these costly and unwanted steps.

Furthermore, the carboxylation of cellulose through a chemo-enzymatic process has also been well-studied by Kokol *et al*. in which they used laccase as the biocatalyst and TEMPO as the mediator in this reaction.[74] From their studies, it was shown that laccase was more productive and had a higher oxidation rate than alternative chemical peroxides at near neutral or slightly acidic environments, and under mild conditions. This is an ecologically and economically friendly alternative as compared to traditional chemical oxidative conditions of cellulose fibers.

1.6 Targeting Cellulose as an Anti-biofilm Strategy

While it has been outlined in detail the ways in which cellulose can be chemically manipulated, it is important to contextualize the reason behind such modifications. As discovered by Cegelski and co-workers, *E. coli* biofilms not only contain curli fibers, but also produce pEtN cellulose within their extracellular matrix.[75] Additional discoveries from this study confirm the synergistic relationship between pEtN cellulose and curli within the biofilm to elicit structural integrity of the architecture. Our recent efforts confirm this discovery, highlighting that increases in *E. coli* biofilm production across multiple strains correlate with supplementation of a phosphoethanolamine cellobiose (pEtN) tool compound.[76] To expand on this further, it is also determined that not only is biofilm production increasing, but also the presence of curli binding within the extracellular matrix, making pEtN also responsible for changes in biofilm architecture. The relationship between pEtN cellulose, curli, and subsequent biofilm formation offers a unique targeting opportunity for biofilm producing microbes and highlights the importance of glycobiology in the pathogenesis of said organisms.

In the United States, hospital-acquired infections account for more deaths per year than those from human immunodeficiency virus (HIV/AIDS), cancer, and vehicle accidents combined. Of these invasive infections, catheter associated urinary tract infections (CAUTIs) and hospital-acquired pneumonias (HAPs) rank among the most prevalent and deadly. Hospital-acquired infections are most usually caused by instrumentation use, specifically long-term catheter, and ventilator use, wherein the infectious bacteria form biofilms to the mentioned abiotic surfaces and

are introduced to the patient during treatment. We hypothesize that employing cellulose targeted strategies against biofilm forming bacteria on abiotic hospital surfaces will lead to the decrease and potential eradication of cell surface adhesion, offering unique opportunities for prophylactic antimicrobial intervention.

1.7 Biogenesis of Bacterial Surface Organelles

The complex nature of the extracellular matrix that gives rise to biofilm formation is unique to each bacterium within the biofilm and can be characterized by distinct component communities within the matrix.[77] Specific to *Enterobacteriaceae,* such as *Salmonella* and *Escherichia* spp., the extracellular biofilm matrix is predominantly composed of curli. Curli, an amyloid-type fiber, is an extracellular protein produced by many enteric bacteria such as *Escherichia coli* (*E. coli*) and *Salmonella* species. Curli fibers serve to promote biofilm formation, cell aggregation, and adhesion to surfaces. Structurally, curli belongs to a large class of fibers known as amyloids. Amyloid fiber formation is associated with Alzheimer's and Huntington's diseases, although the in vivo formation of amyloids is not fully studied.

Specifically, *E. coli* produces an extracellular matrix that consists of curli as the major proteinaceous component and cellulose being the second in the matrix. Curli provides a unique avenue to study the pathogenesis of diseases and how it interacts with flagella, pili, and exopolysaccharides to enable biofilm development. Furthermore, curli's role in the pathogenesis of diseases has not been fully elucidated, but several factors suggest that curli has an important role in the initial step of infection (i.e., attachment phase). Understanding the key structures that

actively help promote biofilm formation, such as curli and the role that cellulose plays in curli formation, is vital towards developing therapeutics that can negate host colonization and biofilm formation.

Enteric bacteria express curli, proteinaceous amyloid proteins, to promote community behavior and host colonization within the produced biofilms.[78] Curli production and biogenesis are highly regulated by the bacteria and have been shown to initiate under stressful conditions that favor biofilm formation over planktonic cell growth. While implicated in cell communication and host colonization, curli production is regulated by curli-specific gene (*csg*) operons, some of which are integral in discerning the bacterial transition from motile to attached bacterial behaviors, and as such, afford curli as the responsible component for the three-dimensional structure of the biofilm architecture.[79] It has been previously demonstrated that *E. coli* lacking curli-specific genes are unable to form three-dimensional structures, and as such, only grow in a single layer.[77]

1.8 Synthetic Phosphoethanolamine Cellobiose by Nguyen and co-workers

In our previous studies, we reported the synthesis and evaluation of a minimal zwitterionic pEtN ability to promote cellular adhesion and biofilm formation in *E. coli*.[76] The strategy was to synthesize a structurally defined tool compound to mimic the naturally occurring polymer, which is difficult to acquire and characterize in a heterogenous mixture (Figure 1.8.).

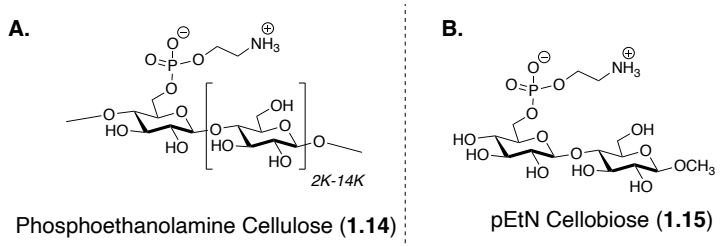

Figure 1.8. Phosphoethanolamine Cellulose (**1.14**) glycopolymer from *E.coli* and pEtN Cellobiose (**1.15**).

The impact of synthetic pEtN cellobiose on biofilm was examined via colorimetric assays, which revealed an increase in cellular adhesion to an abiotic substrate compared to untreated sample.[76] Additionally, we confirmed this through high-resolution field-emission scanning electron microscopy analyses, which showed that pEtN cellobiose supplementation increases adhesion within the biofilm matrix (Figure 1.9.).

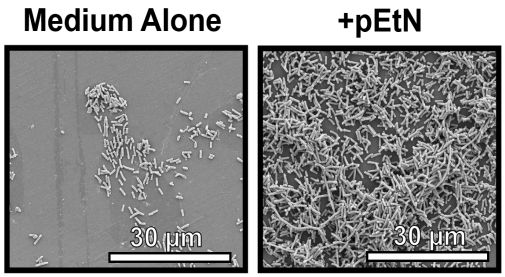

Figure 1.9. High resolution scanning electron microscopy demonstrates that exposure to phosphoethanolamine (+pEtN) enhances *E. coli* biofilm compared to samples cultured in medium alone without pEtN (Medium Alone).

The synthesis commenced with fully protected D-methyl cellobiose **1.17**, prepared in 6 steps from D-cellobiose **1.16** (Scheme 1.1.). Next, regioselective reductive opening of the benzylidene acetal allows access to the C6' alcohol in excellent yield to provide **1.18**. To introduce the phosphoethanolamine moiety at C6', phosphoramidite donor **1.19** was synthesized, which functioned well when using tetrazole as an activator. Coupling of intermediate **1.18** with **1.19**, followed by oxidation at phosphorous using mCPBA gave the desired phosphodiester **1.20** in 80 % yield over two steps. With the fully protected disaccharide **1.20** in hand, hydrogenolysis with Pd/C in methanol and formic acid furnished **1.15** in quantitative yield.

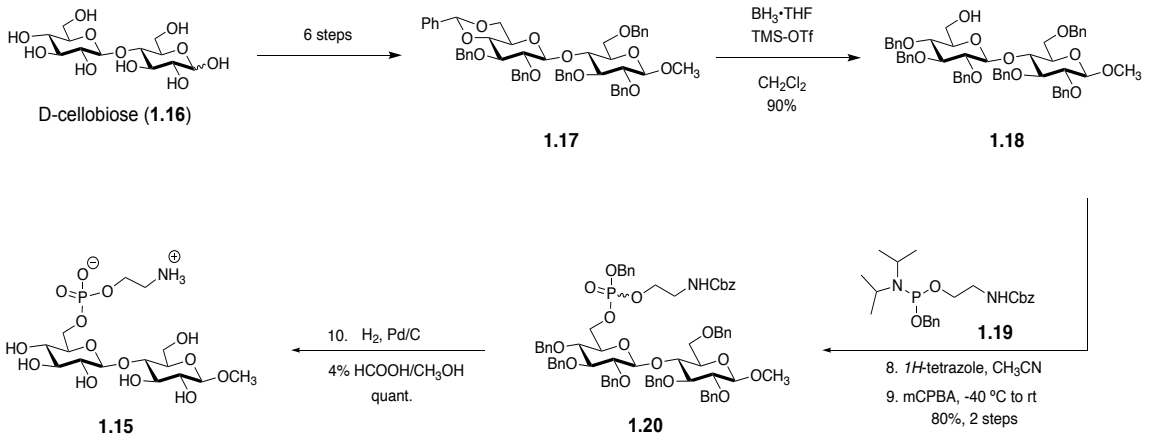

Scheme 1.1. The synthesis of pEtN cellobiose methyl acetal

1.9 Conclusion and Future Outlook

As the most abundant natural polymer on the planet, cellulose has gained considerable attention due to its excellent physical and chemical properties, low cost, and recyclability. Specifically, BC has a broad spectrum of application for many industries, allowing for further research and development of new cellulose-based materials. The use of biocatalysis provides a simpler and green approach to perform these complex chemical transformations, offering sustainable and innovative solutions to specially modify cellulose. The present chapter reports details on the advance in the preparation, modification, and employment of cellulose as a target for anti-biofilm strategy. Polysaccharides play an integral role in biofilm formation and assembly, with cellulose and its derivatives additionally critical to modulating numerous cellular processes. While current studies have provided in-depth information about cellulose's role in biofilm architecture, additional work is needed to keep pace with the continued development of diseases associated with biofilms.

1.10 References

1. Sharma, D.; Misba, L.; Khan, A. U. Antibiotics versus biofilm: an emerging battleground in microbial communities. *Antimicrobial Resistance & Infection Control* **2019**, *8*, 76.

2. Djalal, T.; Hussin, M. H.; Chuin, C. T.H.; Sabar, S.; Fazita, M.R.N.; Taiwo, O. F.A.; Hassan, T.M.; Haafiz, M.K.M. Microcrystalline cellulose: Isolation, characterization, and bio-composites application—A review. *International Journal of Biological Macromolecules* **2016**, *93*, 789-804.

3. Ummartyotin, S.; Manuspiya, H. A critical review on cellulose: From fundamental to an approach on sensor technology. *Renewable and Sustainable Energy Review* **2015**, *41*, 402-412.

4. Philips, M. Anselme Payen, distinigushed French chemist and pioneer investifator of the chemistry of lignin. *Journal of the Washington Academy of Science* **1940**, *30* (2), 65-71.

5. Percec, V.; Xiao, Q. The legacy Of Hermann Staudinger: Covalentyly Linked Macromolecules. *Chem* **2020**, *6*, 11, 2855-2861.

6. Oberlerchner, J. T.; Rosenau, T.; Potthast, A. Overview of Methods for the Direct Molar Mass Determination of Cellulose. *Molecules* **2015**, 20, 10313-10341.

7. Brown, A.J. XLIII.–On an acetic ferment which forms cellulose. *J.Chem.Soc., Trans.* **1886**, *49*, 432-439.

8. Shoda, M.; Sugano, Y. Recent advances in bacterial cellulose production. *Biotechnol. Bioprocess Eng.* **2005**, *10,* 1-8.

9. Jonas, R.; Farah, L. F. Production and application of microbial cellulose. *Polymer Degradation and Stability.* **1998**, *59*, (1-3), 101-106.

10. Deinema, M. H.; Zevehvizen, L. Formation of cellulose fibrils by gram-negative bacteria and their role in bacterial flocculation. *Arch. Microbiol.* **1971**, *78*, 42-51.

11. Orlando, I.; Basnett, P.; Nigmatullin, R.; Wang, W.; Knowles, J.C.; Roy, I. Chemical Modification of Bacteria Cellulose for the Development of an Antibacterial Wound Dressing. Front. Bioeng. Biotechnol. **2020**, *8*, 1-19.

12. Römling, U. Molecular biology of cellulose production in bacteria. *Res. Microbiol.* **2002**, *153*, 205-212.

13. Yoshinaga, F.; Tonouchi, N.; Watanabe, K. Research progress in production of bacterial cellulose by aeration and agitation culture and its application as a new industrial material. *Biosci. Biotech. Biochem.* **1997**, *61*, 219-224.

14. Fontana, J. D., Souza, A.M.; Fontana, C.K.; Torrianio, I.L.; Moreschi, J.C.; Galloyi, N.J.; Souza, S.J.; Narcisco, C.P.; Bichara, J.A.; Farah, L. F. X. Acetobacter cellulose pellicle as a temporary skin substitute. *Appl. Biochem. Biotechnol.* **1990**, *24(25),* 253-264.

15. Nishi, Y.; Uryu, M.; Yamanaka, S.; Watanabe, K.; Kitamura, N.; Iguchi, M.; Mitsuhashi, S. The structure and mechanical properties of sheets prepared from bacterial cellulose. *J. Mater. Sci.* **1990**, *25*, 2997-3001.

16. Vandamme, E. J.; Beats, S.D.; Vanbalen, A.; Joris, K.; Wulf, P.D. Improved production of bacterial cellulose and its application potential. Polymer Degrad. Stabil. **1998**, *59*, 93-99.

17. Delmer, D. P. Cellulose biosynthesis. *Annu. Rev. Plant Physiol.* **1987**, *38*, 259-290.

18. Swissa, M.; Aloni, Y.; Weinhouse, H.; Benziman, M. Intermediatry steps in Acetobacter xylinum cellulose synthesis: Studies with whole cells and cell-free preparations of the wild type and a celluloseless mutant. *J. Bacteriol*. **1980**, *143*, 1142-1150.

19. Wong, H. C., Fear, A.L.; Calhoon, R.D.; Eichinger, G.H.; Mayer, R.; Amikam, D.; Benziman, M.; Gelfand, D.H.; Meade, J.H.; Emerick, A. W.; Bruner, R.; Ben-Bassat, A.; Tal, R. Genetic organization of the cellulose synthase operon in Acetobacter xylinum. *Proc. Natl. Acad. Sci. USA* **1990**, *87*. 8130-8134.

20. Saxena, I. M.; Kudlicka, K.; Okuda, k.; Brown, R.M. Jr. Characterization of genes in the cellulose-synthesizing operon (acs operon) of Acetobacter xylinum: implications for cellulose crystallization. *J. Bacteriol.* **1994**, *176*, 5735-5752.

21. Volman, G.; Ohana, P.; Benziman, M. Biochemistry and molecular biology of cellulose biosynthesis. *Carbohydrates* **1995**, *20*, 20-27.

22. Tal, R.; Wong, H.C.; Calhoon, R.; Gelfand, D.; Fear, A.L.; Volman, G.; Mayer, R.; Ross, P.; Amikam, D.; Weinhouse, H.; Cohen, A.; Sapir, S.; Ohana, P.; Benziman, M. Three cdg operons control cellular turnover of cyclic diGMP in

Acetobacter xylinum: Genetic organization and occurrence of conserved domains in isoenzymes. *J. Bacteriol.* **1998**, *180*, 4416-4425.

23. Ross, P., Weinhouse, H.; Aloni, Y.; Michaeli, D.; Weinberger-Ohana, P.; Mayer, R.; Braun, S.; de Vroom, E.; van der Marel, G.; H. van Boom, J.; Benziman, M. Regulation of cellulose synthesis in Acetobacter xylinum by cyclic diguanylic acid. *Nature* **1987***, 325*, 279-281.

24. Standal, R.; Inversen, T.G.; Coucheron, D.H.; Fjærvik, E.; Blatny, J.; Valla, S. A new gene required for cellulose production and a gene encoding cellulolytic activity in Acetobacter xylinum are colocalized with the bcs operon*. J. Bacteriol.* **1994**, *176*, 665-672.

25. Nakai, T., Moriya, A.; Tonouchi, N.; Tsuchida, T.; Yoshinaga, F.; Horinouchi, S.; Sone, Y.; Mori, H.; Sakai, F.; Hayashi, T. Expression and characterization of sucrose synthase from mungbean seedlings in Escherichia coli. *Gene* **1998**, 213, 93-100.

26. Nakai, T.; Nishiyama, Y.; Kuga, S.; Sugano, Y.; Shoda, M. ORF2 gene involves in the construction of high-order structure of bacterial cellulose. *Biochem. Biophys. Res. Commun.* **2002**, *295*, 458-462.

27. Klemm, D.; Kramer, F.; Moritz, S.; Lingstrom, T.; Ankerfors, M.; Gray, D.; Dorris, A. Nanocelluloses: A new family of nature-based materials. *Angewandte Chemie (International Edition)* **2011**, *50,* 5438-5466.

28. Son, H. J.; Kim, H.G.; Kim, K.K.; Kim, H,S,; Kim, Y. G.; Lee, S. J. Increased production of bacterial cellulose by *Acetobacter sp.* VR in synthetic media under shaking culture conditions. *Bioresource technology*. **2003**, *86*, 215-9.

29. Tokoh, C.; Takabe, K.; Fujita, M.; Saiki, H. Cellulose synthesized by *Acetobacter xylinum* in the presence of acetyl glucomannan. *Cellulose* **1998**, 249-261.

30. Orlando, I.; Basnett, P.; Nigmatullin, R.; Wang, W.; Knowles, J. C.; Roy, I. Chemical Modification of Bacterial Cellulose for the Development of an Antibacterial Wound Dressing. *Front. Bioeng. Biotechnol.* **2020**, *24*, 1-19.

31. Chawla, P. R.; Bajaj, L. B.; Survase, S. A.; Singhal, R. S. Microbial cellulose: Fermentative production and applications. *Food Technology and Biotechnology* **2009**, *47*, 107-124.

32. Ross, P.; Mayer, R.; Banziman, M. Cellulose biosynthesis and function in bacteria. *Microbiological Reviews* **1991**, *55*, 35-58.

33. Lin, S. P.; Loira Calvar, I.; Catchmark, J.; Liu, J.R.; Demirci, A.; Cheng, K.C. Biosynthesis, production and applications of bacterial cellulose. *Cellulose* **2013**, *20*, 2191-2219.

34. Lee, K. Y.; Buldum, G.; Mantalaris, A.; Bismarck, A. More than meets the eye in bacterial cellulose: Biosynthesis, bioprocessing, and applications in advanced fiber composites. *Macromolecular Bioscience* **2014**, *14*, 10-32.

35. Habibi, Y.; Lucia, L. A.; Rojas, O. J. Cellulose nanocrystals: chemistry, self-assembly, and applications. *Chemical Reviews* **2010**, *110*, 3479-3500.

36. De Souza Lima, M. M.; Borsali, R. Rodlike cellulose microcrystals: Structure, properties, and applications. *Macromolecular Rapid Communications* **2004**, *25*, 771-787.

37. Satyamurthy, P.; Jain, P.; Balasubramanya, R. H.; Vigneshwaran, N. Preparation and characterization of cellulose nanowhiskers from cotton fibres by controlled microbial hydrolysis. *Carbohydrate Polymers* **2011**, *83*, 122-129.

38. Chen, X.; Deng, X.; Shen, W.; Jiang, L. Controlled enzymolysis preparation of nanocrystalline cellulose from pretreated cotton fibers. *BioResources **2017**, 7.*

39. George, J.; Siddaramaiah. High performance edible nanocomposite films containing bacterial cellulose nanocrystals. *Carbohydrate Polymers* **2012**, *87*, 2031.

40. Karygianni, L.; Ren, Z.; Koo, H; Thurnheer, T. Biofilm Matrixome: Extracellular Components in Structured Microbial Communities*. Trends in Microbiology* **2020**, *28(8),* 668-681.

41. Flemming, H.C.; Wingender, J. The biofilm matrix. *Nature Reviews Microbiology **2010**, 8,* 623-633.

42. Koerdt, A.; Godeke, J.; Berger, J.; Thorman, K. M.; Albers, S.V. Crenarchaeal Biofilm Formation under Extreme Conditions. *PLoS One*. **2010**, *5(11).*

43. Yin, W.; Wang, Y.; He, J. Biofilms: The Microbial “Protective Clothing” in Extreme Environments. *Int J Mol Sci*. **2019**, *20(14),* 3423.

44. Goodman, A. L.; Merighi, M.; Hyodo, M.; Ventre, I.; Filloux, A.; Lory, S. Direct interaction between sensor kinase proteins mediates acute and chronic disease phenotypes in a bacterial pathogen. *Genes & development*. **2009**, *23(2),* 249–259.

45. Whitfield, C. Structure and Assembly of *Escherichia coli* Capsule. *EcoSal Plus.* **2021***, 3 (2).*

46. Azurmendi, H.F.; Veeramachineni, V.; Freese, S.; Lichaa, F.; Freedberg, D.; Vann, W.F. Chemical structure and genetic organization of the E.colo O6:K15 capsular polysaccharide. *Scientific Reports* **2020**, *10*, 12608.

47. Lukaszczyk, M.; Pradhan, B.; Remaut, H. The Biosynthesis and Structures of Bacterial Pili. *Subcell Biochem.* **2019**, *92*, 369-413.

48. Arciola, C.R.; Campoccia, D.; Ravaioli, S.; Montanaro, L.; Polysaccharide intercellular adhesin in biofilm: structural and regulatory aspects. *Front. Cell. Infect. Microbiol.* **2015**, *5 (7),* 1-10.

49. Costa, A.R.; Henriques, M.; Oliveira, R.; Azeredo, J. The role of polysaccharide intercellular adhesin (PIA) in *Staphylococcus epidermidis* adhesion to host tissues and subsequent antibiotic tolerance. *Eur. J. Clin. Microbiol. Infect. Dis.* **2009**, *28 (6*), 623-9.

50. Spiliopoulou, A.I.; Krevvata, M.I.; Kolonitsiou, F. An extracellular *Staphylococcus epidermidis* polysaccharide: relation to Polysaccharide Intercellular Adhesin and its implication in phagocytosis. *BMC Microbiol* **2012**. *12,* 76.

51. Boles, B.R.; Horswill, A.R.; Staphylococcal biofilm disassembly. *Trends Microbiol.* **2011**, *19(9),* 449-55.

52. Rohde, H.; Burandt, E.C.; Siemssen, N.; Frommelt, L.; Burdelski, C.; Wurster, S.; Scherpe, S.; Davies, A.P.; Harris, L.G.; Horstkotte, M.A.; Knobloch, J.K.; Ragunath, C.; Kaplan, J.B.; Mack, D. Polysaccharide intercellular adhesin or protein factors in biofilm accumulation of *Staphylococcus epidermidis* and *Staphylococcus aureus* isolated from prosthetic hip and knee joint infections. *Biomaterials*. **2007,** *28(9),*1711-20.

53. Limoli, D. H.; Jones, C. J.; Wozniak, D. J. Bacterial Extracellular Polysaccharides in Biofilm Formation and Function. *Microbiology spectrum*. **2015**, *3*(3).

54. Franklin, M. J.; Nivens, D. E.; Weadge, J. T.; Howell, P. L. Biosynthesis of the *Pseudomonas aeruginosa* Extracellular Polysaccharides, Alginate, Pel, and Psl. *Frontiers in microbiology* **2011**, *2*, 167.

55. Hentzer, M.; Teitzel, G.M.; Balzer, G.J.; Heydorn, A.; Molin, S.; Givskov, M.; Parsek, M.R. Alginate overproduction affects *Pseudomonas aeruginosa* biofilm structure and function. *J Bacteriol.* **2001**, *183(18),* 5395-401.

56. Pier, G.B.; Coleman, F.; Grout, M.; Franklin, M.; Ohman, D.E. Role of alginate O acetylation in resistance of mucoid *Pseudomonas aeruginosa* to opsonic phagocytosis. *Infect Immun.* **2001**, *69(3),*1895-901.

57. Gottesman, S.; Stout, V. Regulation of capsular polysaccharide synthesis in *Escherichia coli* K12. *Molecular Microbiology* **1991**, *5*, 1599-1606.

58. Stevenson, G.; Andrianopoulos, K.; Hobbs, M.; Reeves, P.R. Organization of the *Escherichia coli* K-12 gene cluster responsible for production of the extracellular polysaccharide colonic acid. *Journal of Bacteriology* **2021**, *178(16).*

59. Hanna, A.; Berg, M.; Stout, V.; Razatos, A. Role of capsular colanic acid in adhesion of uropathogenic *Escherichia coli. Applied and environmental microbiology* **2003**, *69(8),* 4474–4481.

60. Danese, P. N.; Pratt, L. A.; Kolter, R. Exopolysaccharide production is required for development of *Escherichia coli* K-12 biofilm architecture. *Journal of bacteriology* **2000**, *182(12),* 3593–3596.

61. Cook, K.E.; Colvin, J.R. Evidence for a beneficial influence of cellulose production on growth of *Acetobacter xylinum* in liquid medium. *Curr Microbiol.* **1980**, *3*, 203–205.

62. Monteiro, C.; Saxena, I.; Wang, X.; Kader, A.; Bokranz, W.; Simm, R.; Nobles, D.; Chromek, M.; Brauner, A.; Brown, R.M.; Römling, U. Characterization of cellulose production in *Escherichia coli* Nissle 1917 and its biological consequences. *Environ Microbiol.* **2009**, *11*, 1105–1116.

63. Tavakolian, M.; Jafari, S. M.; van de Ven, T. G.M. A Review on Surface-Functionalized Cellulosic Nanostructures as Biocompatible Antimbacterial Materials. Nano-Micro Lett. **2020**, *73*, 1-25.

64. Sivio, J.; Honka, A.; Liimatainen, H.; Niinimaki, J.; Hormi, O. Synthesis of highly cationic water-soluble cellulose derivative and its potential as novel biopolymeric flocculation agent. *Carbohydrate Polymer*. **2011**, *86*, 266-270.

65. Isogai, A.; Hänninen, T.; Fujisawa, S.; Saito, T. Review: Catalytic oxidation of cellulose with nitroxyl radicals under aqueous conditions. *Prog. Polym. Sci.* **2018**, *86*, 122–148.

66. Shinoda, R.; Saito, T.; Okita, Y.; Isogai, A. Relationship between Length and Degree of Polymerization of TEMPO-Oxidized Cellulose Nanofibrils. *Biomacromolecules* **2012**, *13*, 842–849.

67. De Nooy, A. E. J.; Besemer, A. C.; van Bekkum, H. On the Use of Stable Organix Nitroxyl Radicals for the Oxidation of Primary and Secondary Alcohols. *Synthesis* **1996**, *10*, 1153-1176.

68. Shaabani, A.; Rahmati, A.; Badri, Z. Sulfonated cellulose and starch: New biodegradable and renewable solid acid catalyst for efficient synthesis of quinolines. *Catalysis Communication*, **2008**, *9*, 13-16.

69. Martinelli, A.; Giannini, L.; Branduardi, P. Enzymatic Modifications of Cellulose To Unlock Its Exploitation in Advanced Materials. *ChemBioChem* **2021**, *22*, 974.

70. Xie, J.; Hsieh, Y.L. Enzyme-catalyzed transesterification of vinyl esters on cellulose solids. *J. Polym. Sci. Part* A **2001**, 39, 1931–1939.

71. Ibinga, S.K.K.; Fabre, J.F.; Bikanga, R; Mouloungui, Z. Atypical Reactions Media and Organized Systems for the Synthesis of Low-Substitution Sugar Esters. *Front. Chem.* **2019**, 7, 587.

72. Sereti, V.; Stamatis, H.; Koukios, E.; Kolisis, F.N. Enzymatic acylation of cellulose acetate in organic media. *Journal of Biotechnology,* **1998**, *66 (2-3)*, 219-223.

73. Tzanov, T.; Stamenova, M.; Cavaco-Paulo, A. Phosphorylation of Cotton Cellulose with Baker's Yeast Hexokinase. *Macromol. Rapid Commun.* **2002**, *23*, 962-964.

74. Jausovec, D.; Vogrincic, R.; Kokol, V. Introduction of aldehyde vs. carboxylic groups to cellulose nanofibers using laccase/TEMPO mediated oxidation. *Carbohydrate Polymer* **2015**, *116*, 74-85.

75. Hollenbeck, E.C.; Antonoplis, A.; Chai, C.; Thongsomboon, W.; Fuller, G.G.; Cegelski, L. Phosphoethanolamine cellulose enhances curli-mediated adhesion of uropathogenic *Escherichia coli* to bladder epithelial cells. *Proc Natl Acad Sci U S A*. **2018**, *2*, 115(40), 10106-10111.

76. Nguyen, J.M.; Moore, R. E.; Spicer, S. K.; Gaddy, J. A., Townsend, S. D. Synthetic Phosphoethanolamine Cellobiose Promotes *Escherichia coli* Biofilm Formation and Congo Red Binding. *ChemBioChem***. 2021**, *22*, 15, 2540-2545.

77. Hung, C.; Zhou, Y.; Pinkner, J. S.; Dodson, K. W.; Crowley, J. R.; Heuser, J.; Chapman, M. R.; Hadjifrangiskou, M.; Henderson, J. P.; Hultgren, S. J. *Escherichia coli* biofilms have an organized and complex extracellular matrix structure. *mBio* **2013**, *4*(5), e00645-13.

78. Barnhart, M. M.; Chapman, M. R. Curli biogenesis and function. *Annual review of microbiology* **2006**, *60*, 131–147.

79. Tursi, S. A.; Tükel, Ç Curli-Containing Enteric Biofilms Inside and Out: Matrix Composition, Immune Recognition, and Disease Implications. *Microbiology and molecular biology reviews* ***2018****, 82(4),* e00028-18.

1.11. Experimental Methods

General. All moisture-sensitive reactions were performed in flame-dried or oven-dried glassware under an atmosphere of argon. Reaction temperatures were controlled and monitored using a hot plate stirrer with a thermocouple thermometer. Analytical thin-layer chromatography (TLC) was performed on Sorbtech Silica XHL UV254, glass-backed, 250 μm plated, and visualized using UV, cerium ammonium molybdate stain or ninhydrin stain. Yields were reported as purified and isolated compounds. Solvents were dried through a Braun MB-SPS solvent system and used immediately or stored over 3 Å or 4 Å molecular sieves. Instrumentation: ^{1}H, ^{13}C, ^{1}H-^{13}C HSQC and ^{31}P NMR spectra were recorded in the Vanderbilt Small Molecule NMR Facility on a Bruker 400 and 600 MHz. Chemical shifts are reported in parts per million (ppm) of the δ scale. Spectra were recorded in $CDCl_3$ by using the solvent residual peak chemical shift as the internal standard ($CDCl_3$: 7.26 ppm ^{1}H, 77.0 ppm ^{13}C) or in D_2O using the solvent as the internal standard in ^{1}H NMR (D_2O: 4.79 ppm ^{1}H). 1H NMR spectral data are presented as follows: Chemical shifts (δ ppm), multiplicity (s = singlet, d = doublet, dd = doublet of doublets, t = triplet, q = quartet, br = broad, m = multiplet) coupling constants (Hz), integration. High-resolution mass spectra (HRMS) were obtained from the Department of Chemistry, Vanderbilt University using a Synapt G2-S HDMS (Milford, Ma, USA) mass spectrometer.

Preparative Procedures

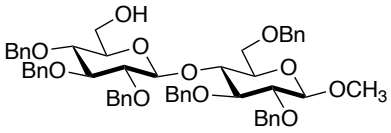

1.18

Methyl 2,3,4-tri-*O*-benzyl-β-D-glucopyranosyl-(1→4)-2,3,6-*O*-benzyl-β-D-glucopyranoside (**1.18**): A solution of methyl 4,6-O-benzylidene acetal-2-*O*-benzyl-β-D-glucopyranosyl-(1→4)-2,3,6-*O*-benzyl-β-D-glucopyranoside (**1.17**) (1.0 equiv., 2.50 g, 3.07 mmol) in anhydrous CH_2Cl_2 (60.0 mL) was added BH3·THF (5.0 equiv., 15.4 mL, 15.4 mmol) and a solution of TMSOTf (0.25 equiv., 0.15 mL, 0.768 mmol, 15 % in anhydrous CH_2Cl_2) at 0 °C under an argon atmosphere. The reaction mixture was stirred for 1.5 h while warming to room temperature. The reaction mixture was cooled to 0 °C and quenched by the addition of methanol and Et_3N. The reaction was concentrated then co-evaporated with methanol to remove residual borate esters. The crude reaction mixture was purified by silica gel flash column chromatography (30:70 EtOAc/hexanes) to give methyl 2,3,4-tri-*O*-benzyl-β-D-glucopyranosyl-(1→4)-2,3,6-*O*-benzyl-β-D-glucopyranoside **1.18** (2.50 g, 2.79 mmol, 90%) as a white solid; ^{1}H NMR (600 MHz, $CDCl_3$): δ ^{1}H NMR (600 MHz, $CDCl_3$) δ 7.31 – 7.08 (m, 30H), 4.90 – 4.60 (m, 9H), 4.51 (dd, *J* = 11.6, 7.3 Hz, 2H), 4.37 (d, *J* = 7.9 Hz, 1H), 4.36 (d, *J* = 12.1 Hz, 1H), 4.22 (d, *J* = 7.8 Hz, 1H), 3.84 (t, *J* = 9.5 Hz, 1H), 3.73 (dd, *J* = 10.9, 4.0 Hz, 1H), 3.62 (dd, *J* = 10.9, 1.8 Hz, 1H), 3.54 (dd, *J* = 12.0, 2.7 Hz, 1H), 3.49 (s, 1H), 3.48 – 3.39 (m, 2H), 3.41 – 3.21 (m, 5H), 3.05 (ddd, *J* = 9.7, 5.1, 2.7 Hz, 1H); ^{13}C NMR (151 MHz, $CDCl_3$) δ 139.13, 138.63, 138.54, 138.39, 138.12, 138.10, 128.46, 128.43, 128.36, 128.33, 128.06, 127.92, 127.85, 127.82, 127.79, 127.69, 127.67, 127.64, 127.60, 127.54, 127.18, 104.74, 102.47, 84.74, 82.75, 82.71, 81.66, 77.98, 75.70, 75.23, 75.04, 75.01, 74.87, 73.35,

67.94, 61.82, 57.09; ESI-HRMS calcd for $C_{55}H_{60}O_{11}Na^+$ (m/z): [M+Na^+] 919.4033, found: 919.4032.

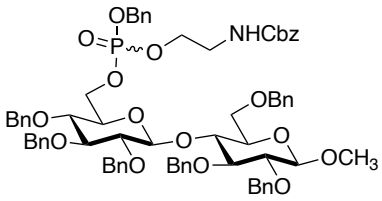

1.20

Methyl 6-*O*-{benzyloxy-2 [N(benzyloxycarbonyl) amino]ethylphosphate}-2,3,4-tri-*O*-benzyl-β-D-glucopyranosyl-(1→4)-2, 3, 6-*O*-benzyl- β-D-glucopyranoside (**1.20**): Methyl 2,3,4-tri-*O*-benzyl-β-D-glucopyranosyl-(1→4)-2,3,6-*O*-benzyl-β-D-glucopyranoside **1.18** (1.50 g, 1.67 mmol) and phosphoramidite **1.19** (1.45 g, 3.34 mmol) were coevaporated (3 ×) from toluene and dried overnight in vacuo. The compounds were dissolved in CH_2Cl_2 (65 mL) and a solution of 3% tetrazole solution in anhydrous CH_3CN (3.0 equiv., 12.1 mL, 5.02 mmol). The solution was allowed to stir at room temp, for 3 h. The solution was cooled to -40 °C and mCPBA (1.92 g, 8.36 mmol) was added to the reaction mixture. The solution was allowed to warm to room temp for 1 h, after which it was diluted with CH_2Cl_2 (10 mL), washed with 10% Na_2SO_3 (2 × 3 mL), dried with Na_2SO_4, filtered and evaporated. The crude reaction mixture was purified by silica gel flash column chromatography (10:90 EtOAc/hexanes) to give methyl 6-*O*-{benzyloxy-2 [N(benzyloxycarbonyl) amino]ethylphosphate}-2,3,4-tri-*O*-benzyl-β-D-glucopyranosyl-(1→4)-2, 3, 6-*O*-benzyl- β-D-glucopyranoside **1.20** (1.48 g, 1.19 mmol, 72%, mixture of phosphate diastereomers) as a clear oil. ^{1}H NMR (600 MHz, $CDCl_3$): 7.42 – 7.15 (m, 40H), 5.13 – 4.60 (m, 17H), 4.55 (d, *J* = 7.7 Hz, 1H), 4.51-4.48 (m, 1H), 4.32 (d, *J* = 7.7 Hz, 1H), 4.23 – 3.97 (m, 4H), 3.97 – 3.69 (m, 4H), 3.59 (s, 3H), 3.57 – 3.47 (m, 2H), 3.42-3.33 (m, 4H); ^{13}C NMR (151 MHz, $CDCl_3$) δ 156.33, 138.94, 138.61, 138.42, 138.32, 138.07, 137.92, 136.66, 135.74, 135.69,

128.64, 128.50, 128.47, 128.44, 128.38, 128.27, 128.19, 128.11, 128.06, 127.91, 127.89, 127.82, 127.77, 127.75, 127.70, 127.68, 127.54, 104.79, 102.03, 84.69, 82.88, 82.60, 81.59, 77.17, 76.01, 75.62, 75.41, 74.97, 74.94, 74.89, 74.75, 73.56, 73.34, 69.56, 69.52, 68.10, 66.61, 57.02, 41.08, 41.04; 31P NMR (162 MHz, CDCl3) δ -0.54, -0.14; ESI-HRMS calcd for $C_{72}H_{78}NO_{16}PNa^+$ (m/z): [M+Na$^+$] 1266.4955, found: 1266.4956.

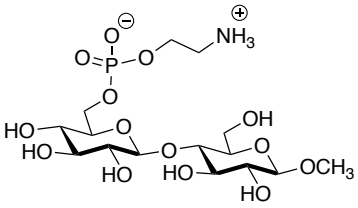

1.15

Phosphoethanolamine Cellobiose (**1.15**): A solution of methyl 6-*O*-{benzyloxy-2 [N(benzyloxycarbonyl) amino]ethylphosphate}-2,3,4-tri-*O*-benzyl-β-D-glucopyranosyl-(1→4)-2, 3, 6-*O*-benzyl- β-D-glucopyranoside (**1.20**) (1.25 g, 1.00 mmol), in 4% HCOOH in MeOH (20 mL), 10% Pd/C (1.07 g) was added and the mixture was hydrogenated at room temp for 48 h. The reaction mixture was filtered over celite and concentrated in vacuo yielded **1.15** quantitatively (445 mg, 0.928 mmol). ^{1}H NMR (600 MHz, D2O) δ^1H NMR (600 MHz, D_2O) δ 4.32 (d, *J* = 8.0 Hz, 1H), 4.20 (d, *J* = 8.0 Hz, 1H), 3.98 (ddd, *J* = 11.5, 5.2, 2.2 Hz, 1H), 3.95 – 3.83 (m, 2H), 3.79 (dd, *J* = 12.3, 1.9 Hz, 1H), 3.61 (dd, *J* = 12.3, 4.7 Hz, 1H), 3.45 – 3.39 (m, 4H), 3.37 (s, 3H), 3.36 – 3.27 (m, 2H), 3.26 – 2.93 (m, 4H); ^{13}C NMR (151 MHz, D_2O) δ 103.01, 102.80, 79.37, 75.25, 74.62, 74.51, 74.34, 73.04, 72.80, 69.01, 64.42, 61.88, 60.02, 57.21, 40.01; ^{31}P NMR (162 MHz, D_2O) δ 1.58; ESI-HRMS calcd for $C_{15}H_{30}NO_{14}P^+$ (m/z): [M+H]$^+$ 479.1403, found: 480.1477.

Bacterial Strains and Culture Conditions

The bacterial strains used in this study were all *Escherichia coli* strains: ATCC 11775T, a type strain urinary isolate (serovar O1:K1: H7); ATCC 700414, ATCC 700415, and ATCC 700416, all urinary isolates (serovar O4:H5); ATCC 700928, a urinary isolate (serovar O6: H1); and ATCC 25922, a control strain (serovar O6:H1). *E. coli* strains were grown on tryptic soy agar plates supplemented with 5% sheep blood (blood agar plates) at 37°C in ambient air overnight. The strains were subcultured from the blood agar plates into 5 mL of Todd-Hewitt broth (THB) and incubated under shaking conditions at 180 rpm at 37°C in ambient air overnight. Following overnight incubation, bacterial density was quantified through absorbance readings at an optical density at 600 nm (OD_{600}) using a Promega GloMax-Multi Detection System plate reader. Bacterial numbers were determined using the predetermined coefficient of 1 OD_{600}=109 CFU/mL.

Bacterial Biofilm Assays

E. coli was grown overnight as described above and used to inoculate fresh THB or THB+1% glucose at a multiplicity of infection (MOI) 10^6 colony forming units (CFUs) per 200 µL of growth medium in 96 well tissue culture treated, sterile polystyrene plates. pEtN methyl cellobiose was dissolved in DI water to achieve a concentration of 50 mg/mL and filtered through a 0.2 µm syringe filter. pEtN methyl cellobiose was added to achieve a final concentration of ca. 5 mg/mL. Bacteria grown in THB or THB+1% glucose in the absence of any pEtN methyl cellobiose served as the

controls. Cultures were incubated under static conditions at 37°C in ambient air for 24 h. Bacterial growth was quantified through absorbance readings at an optical density of 600 nm (OD_{600}). Following growth quantification, the culture medium was removed, and wells were washed gently with phosphate buffered saline (PBS, pH 7.4) to remove nonadherent cells. The remaining biofilms were stained with a 1% crystal violet solution for 10 min. Following staining, wells were washed with PBS and allowed to dry at room temperature for at least 30 min. The remaining crystal violet stain was solubilized with 200 µL of 80% ethanol/20% acetone solution. Biofilm formation was then quantified through absorbance readings at an optical density of 560 nm (OD_{560}). Results are expressed as biofilm/biomass ratios (OD_{560}/OD_{600}).

Bacterial Growth Assays

E. coli was grown overnight as described above and used to inoculate fresh THB at a multiplicity of infection (MOI) of 10^6 colony forming units per 200 µL of growth medium in 96 well tissue culture treated, sterile polystyrene plates (Corning, Inc). pEtN cellobiose was dissolved in DI water to achieve a concentration of 50 mg/mL and filtered through a 0.2 µm syringe filter. pEtN cellobiose was added to achieve a final concentration of ca. 5 mg/ mL. Bacteria grown in THB in the absence of pEtN cellobiose served as the control. Cultures were grown under static conditions at 37°C in ambient air for 24 h. Growth was quantified through spectrophotometric reading at OD600 with readings taken at 0, 2, 4, 6, 7, and 8 hours then a final reading at 24 hours.

Scanning Electron Microscopy Analysis of E.coli cultured in the absence or presence of pEtN

Scanning electron microscopy analysis of *E. coli* cultured in the absence or presence of pEtN *E. coli* was grown on plastic coverslips in 1 mL THB media in the presence or absence of ca. 5 mg/mL pEtN cellobiose. Cultures were grown under static conditions at 37°C in ambient air for 24 h. The following day, samples were fixed in a solution of 2.0% paraformaldehyde, 2.5% glutaraldehyde in a 0.05 M sodium cacodylate buffer at pH 7.4 for 24 h as previously described. After primary fixation, samples were subjected to sequential dehydration with increasing concentrations of ethanol and dried at the critical point using a Tousimis Critical Point Dryer machine. Samples were mounted onto aluminum stubs, sputter coated with 20 nm of gold-palladium, and painted at the sample edge with a small stripe of colloidal silver to facilitate charge dissipation. Samples were imaged with an FE-IQuanta 250 field-emission gun scanning electron microscope to evaluate biofilm architecture and bacterial cell ultrastructure.

Appendix A1:

Spectra Relevant to Chapter 1

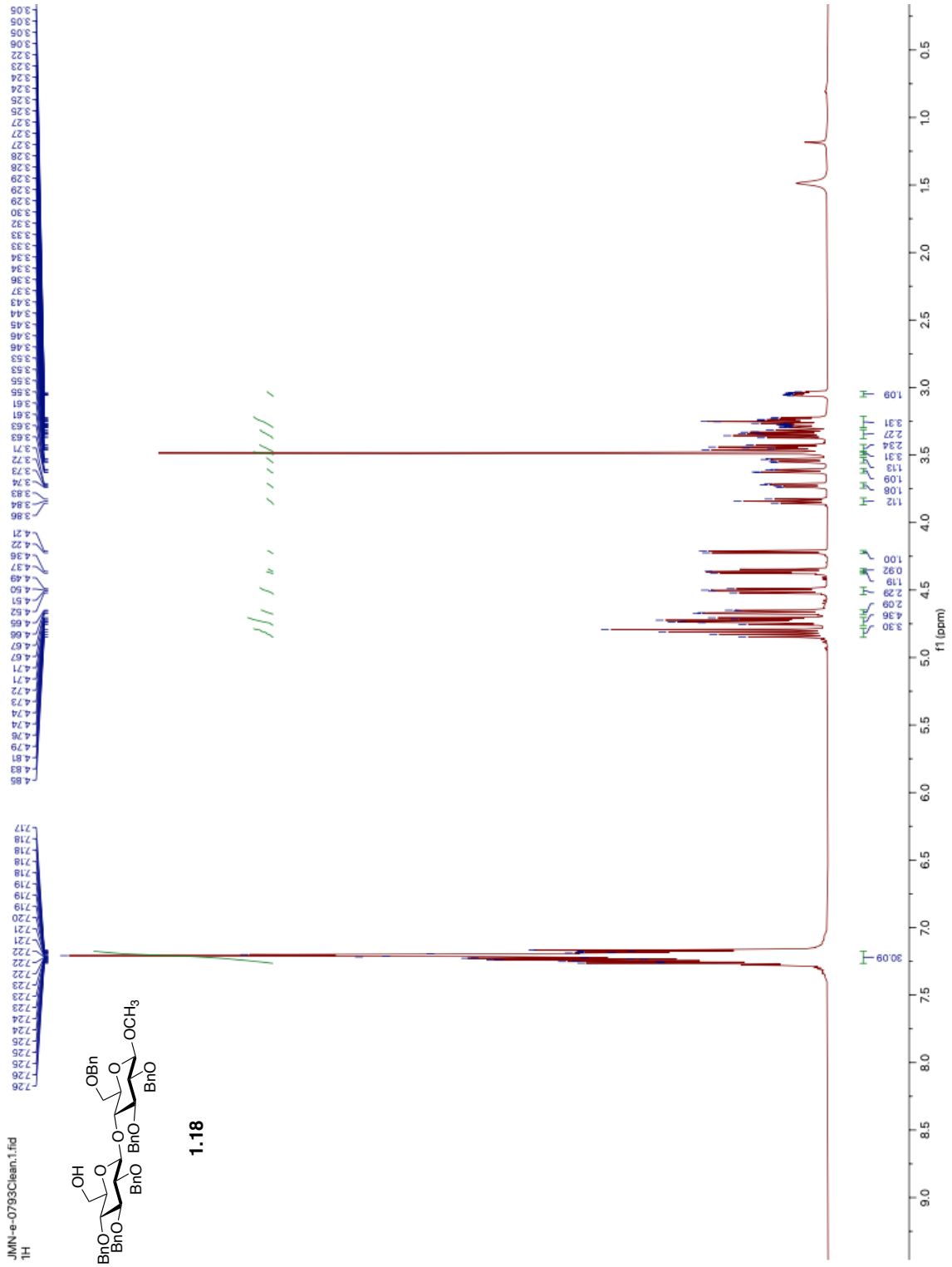

Figure A1.1. ^{1}H NMR (600 MHz, $CDCl_3$) of compound **1.18**

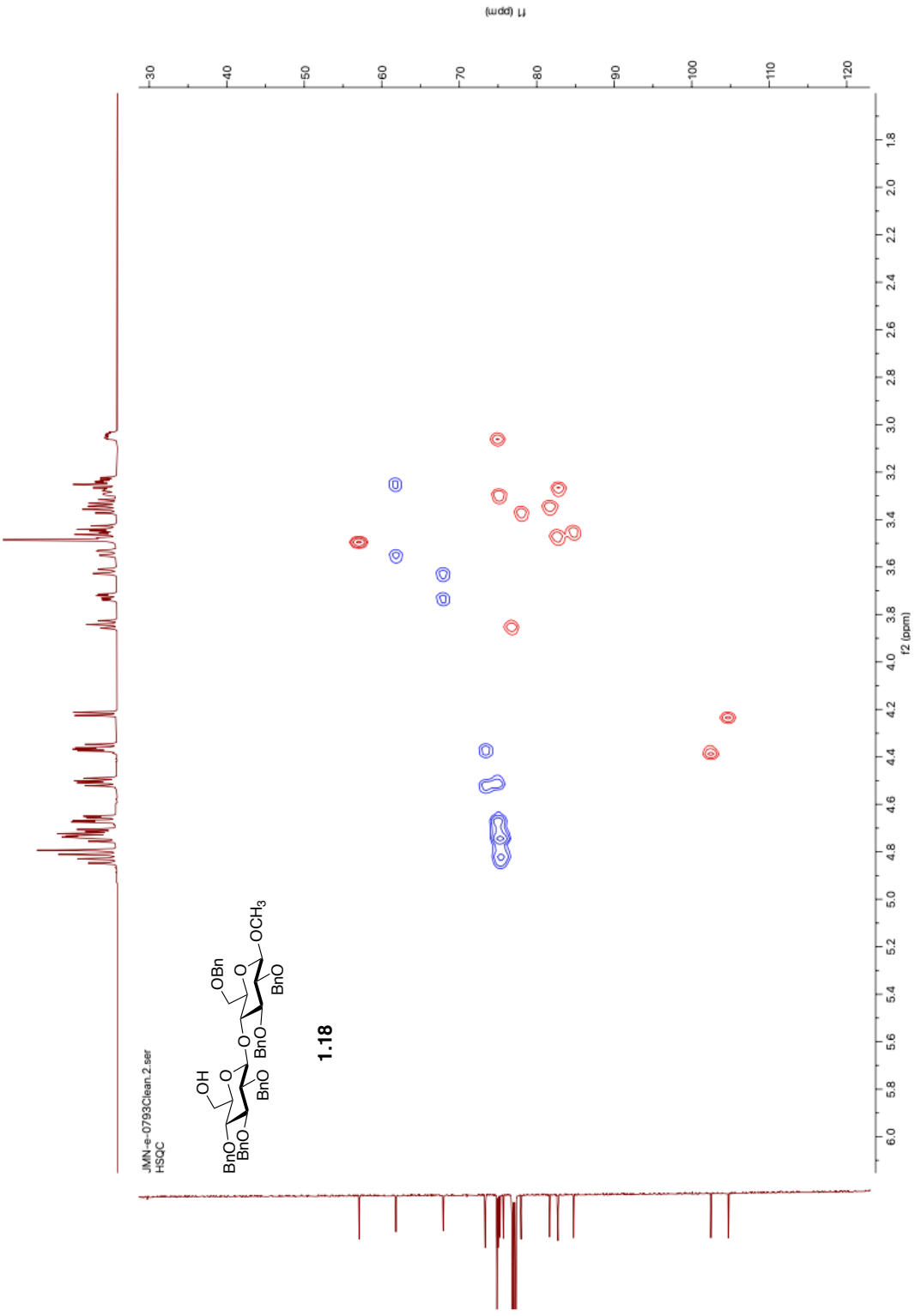

Figure A1.2. ^{1}H-^{13}C HSQC NMR (600 MHz, $CDCl_3$) of compound **1.18**.

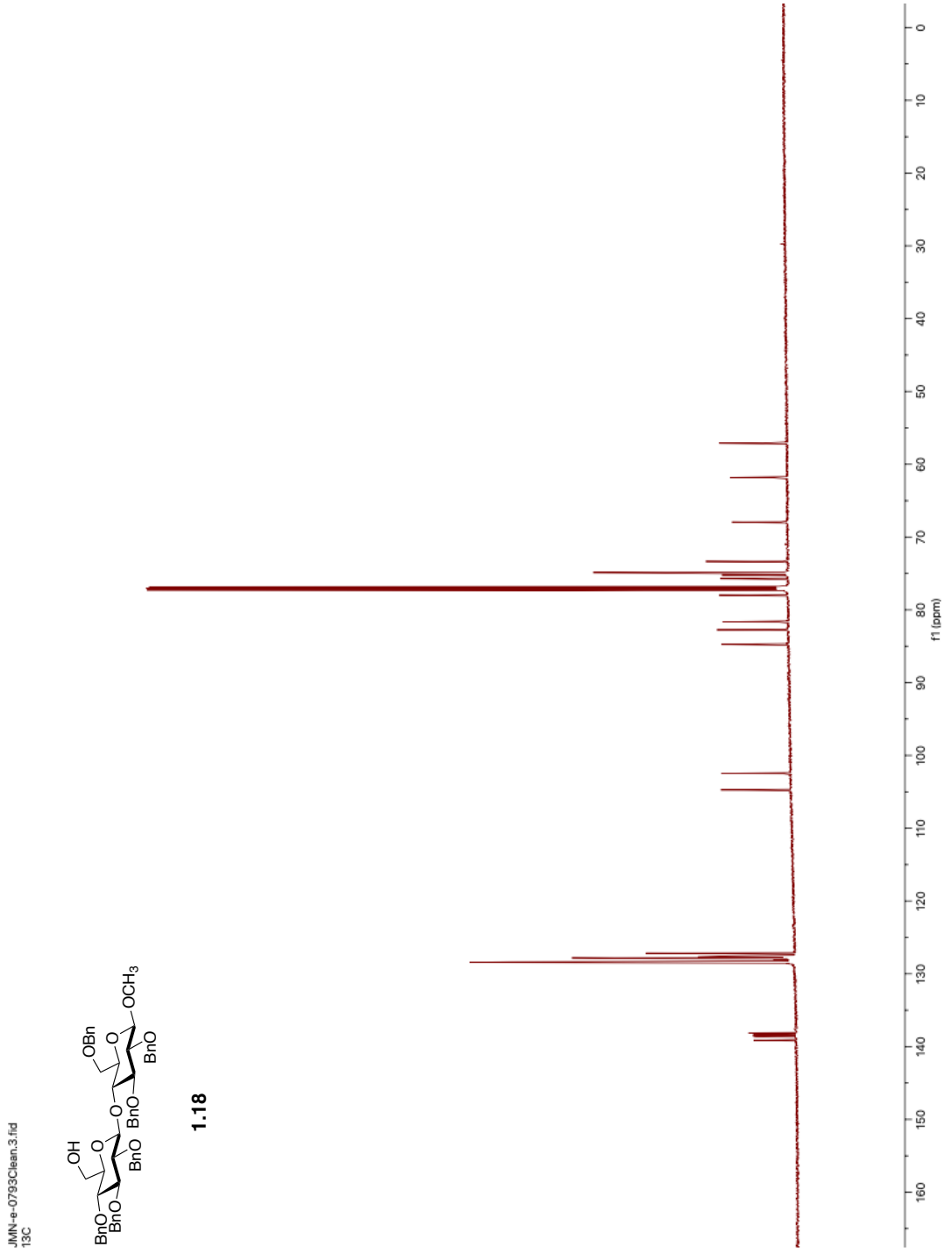

Figure A1.3. ^{13}C NMR (151 MHz, $CDCl_3$) of compound **1.18**.

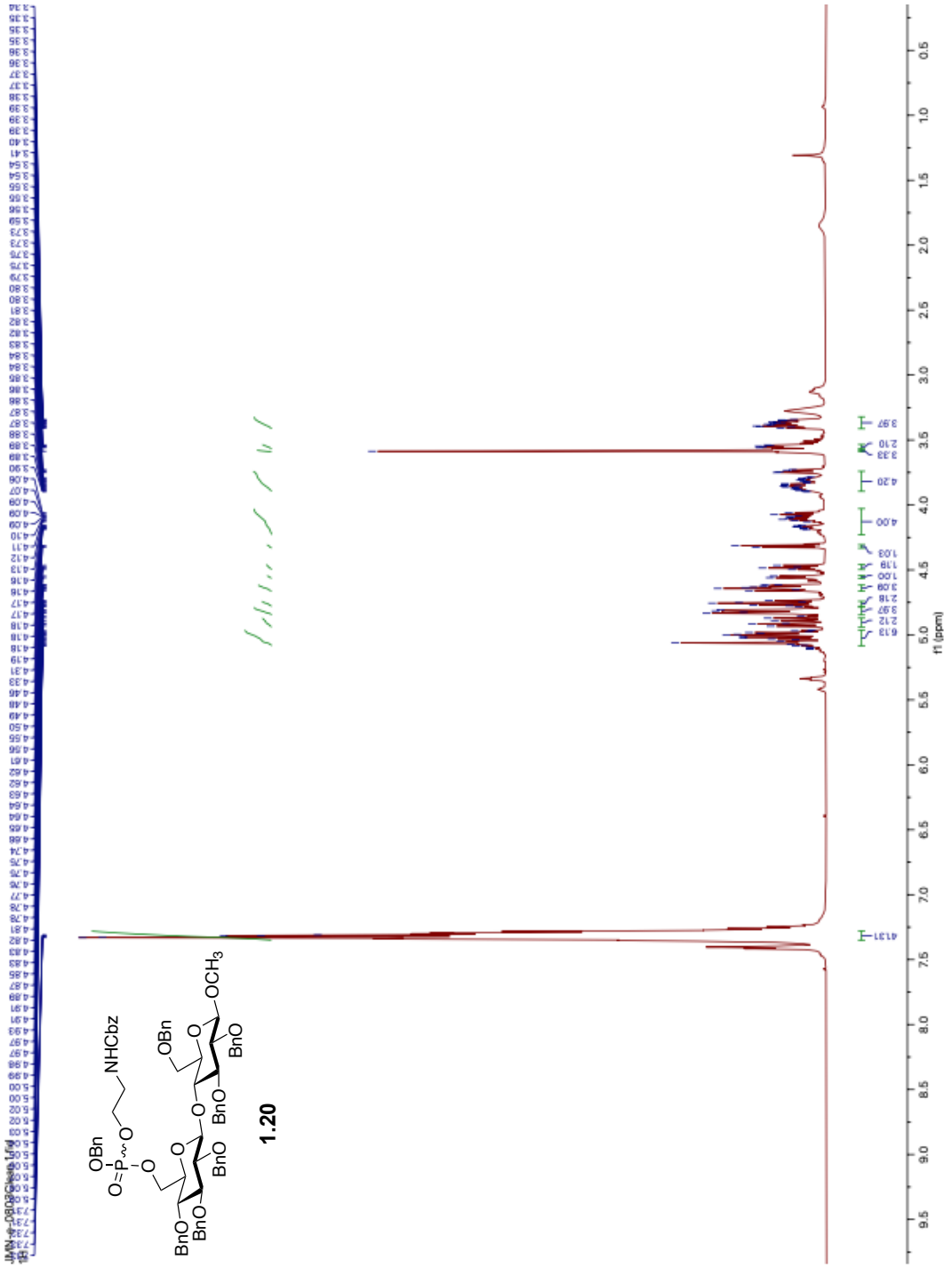

Figure A1.4. ^{1}H NMR (600 MHz, $CDCl_3$) of compound **1.20**.

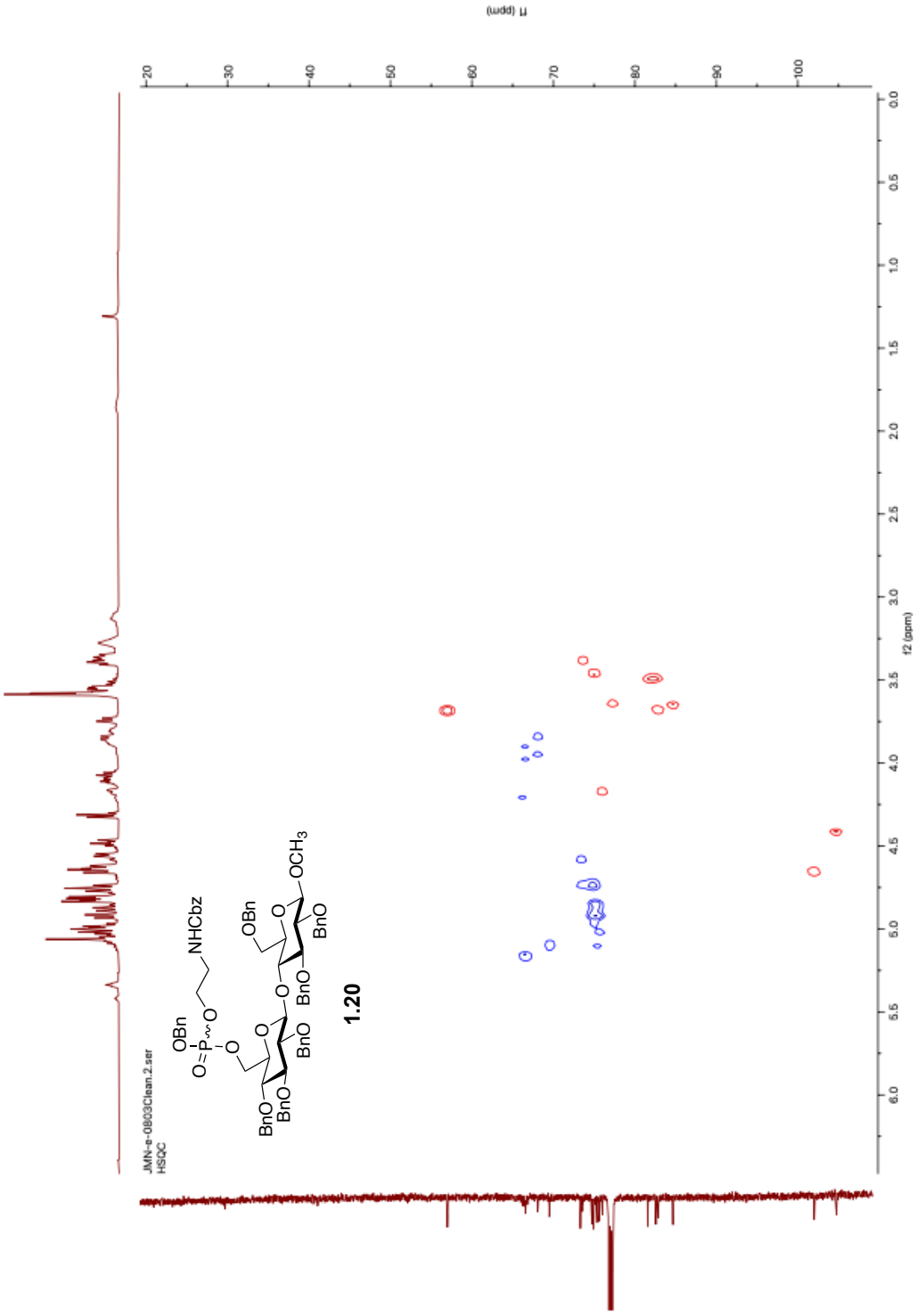

Figure A1.5. ^{1}H-^{13}C HSQC NMR (600 MHz, $CDCl_3$) of compound **1.20**.

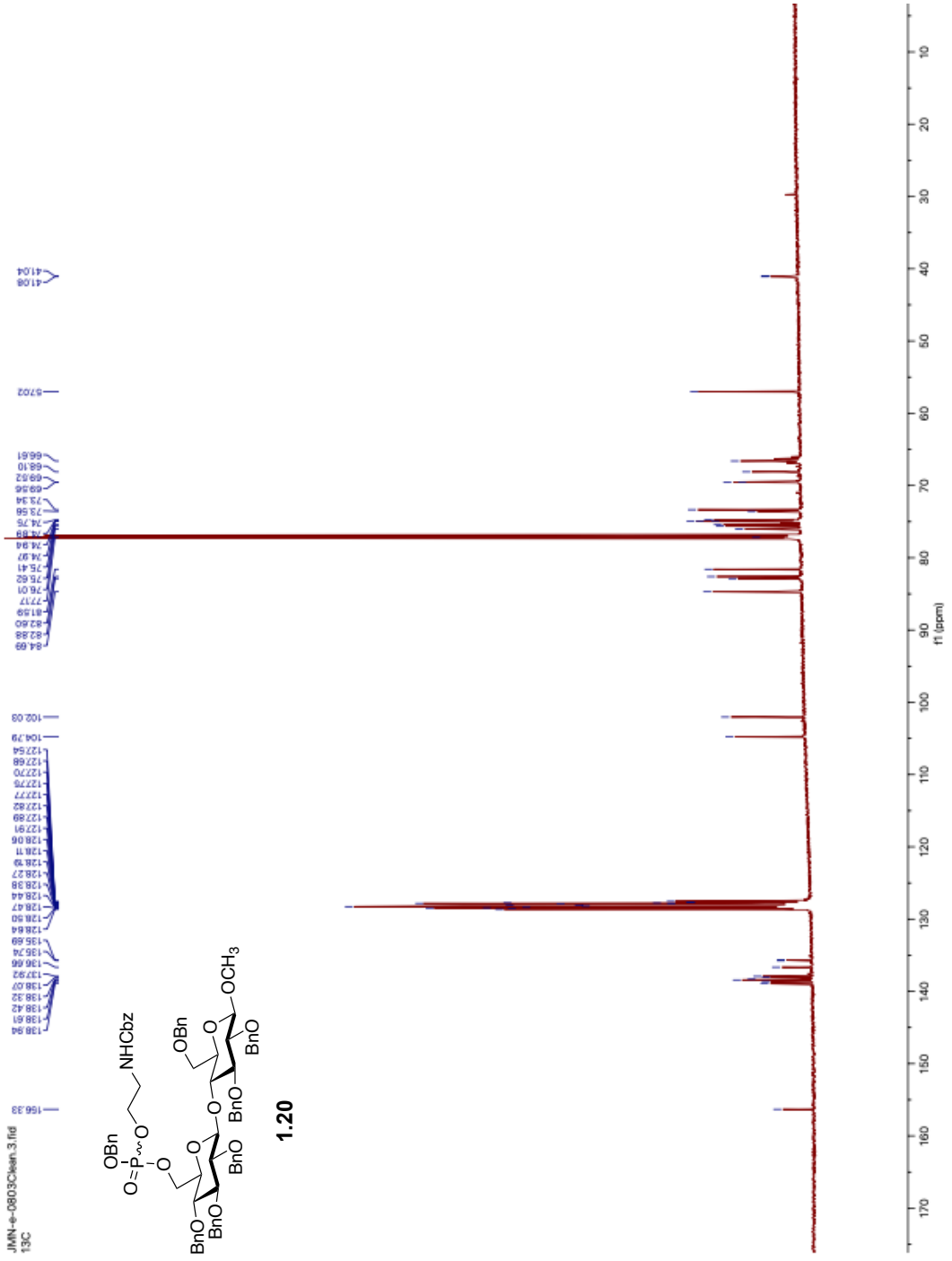

Figure A1.6. ^{13}C NMR (151 MHz, $CDCl_3$) of compound **1.20**.

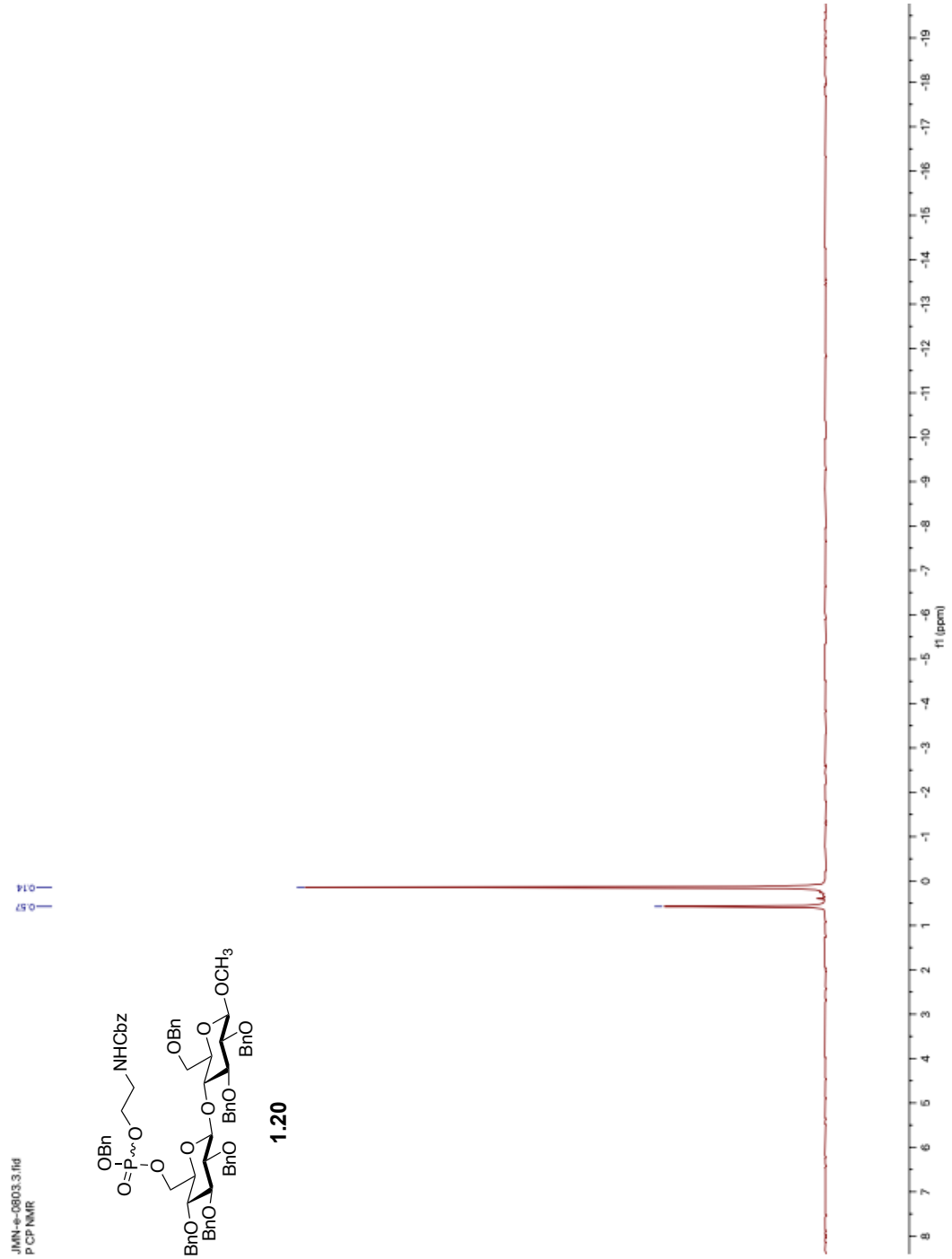

Figure A1.7. ^{31}P NMR (162 MHz, $CDCl_3$) of compound **1.20**

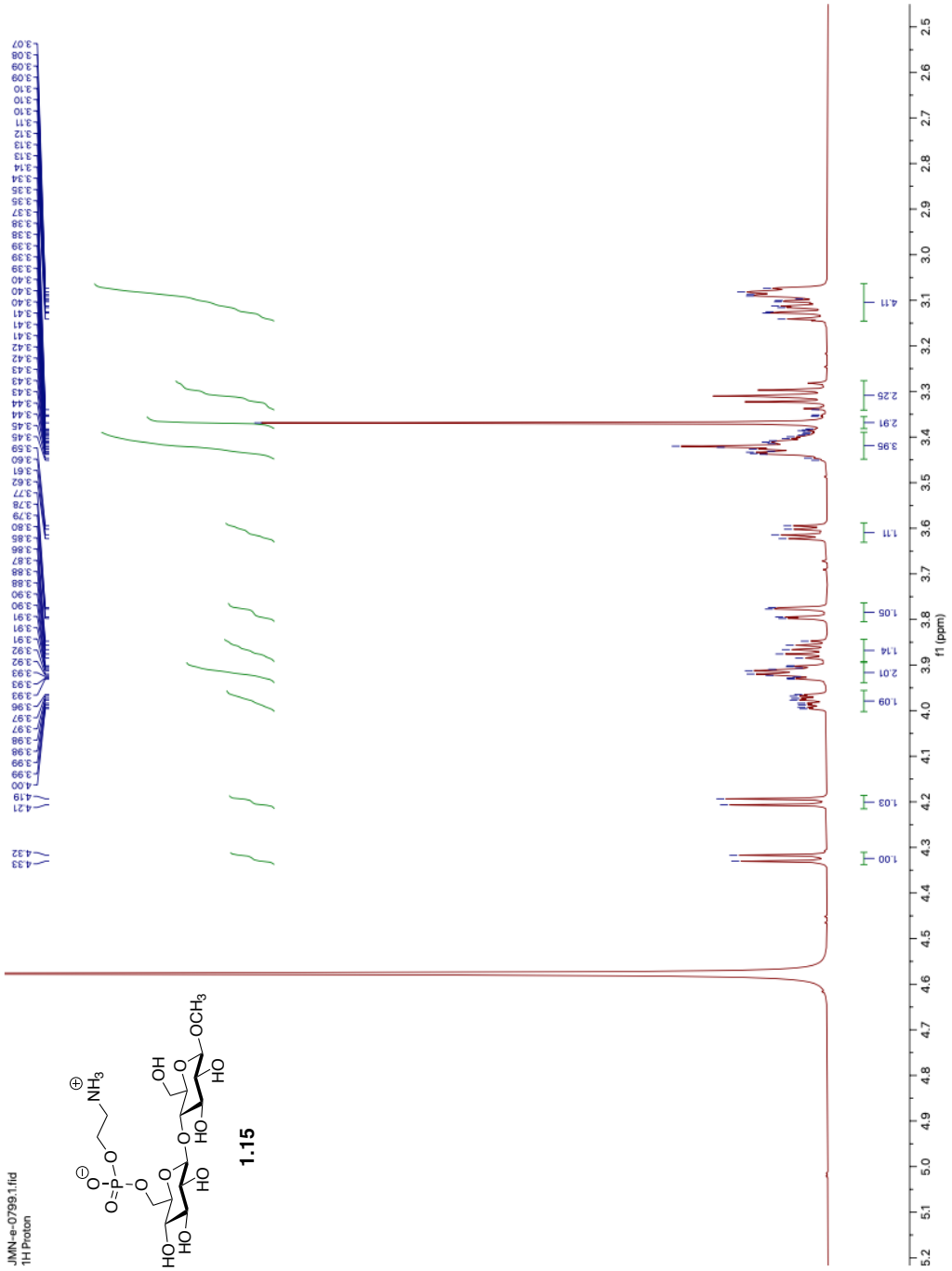

Figure A1.8. ^{1}H NMR (600 MHz, D_2O) of compound **1.15**.

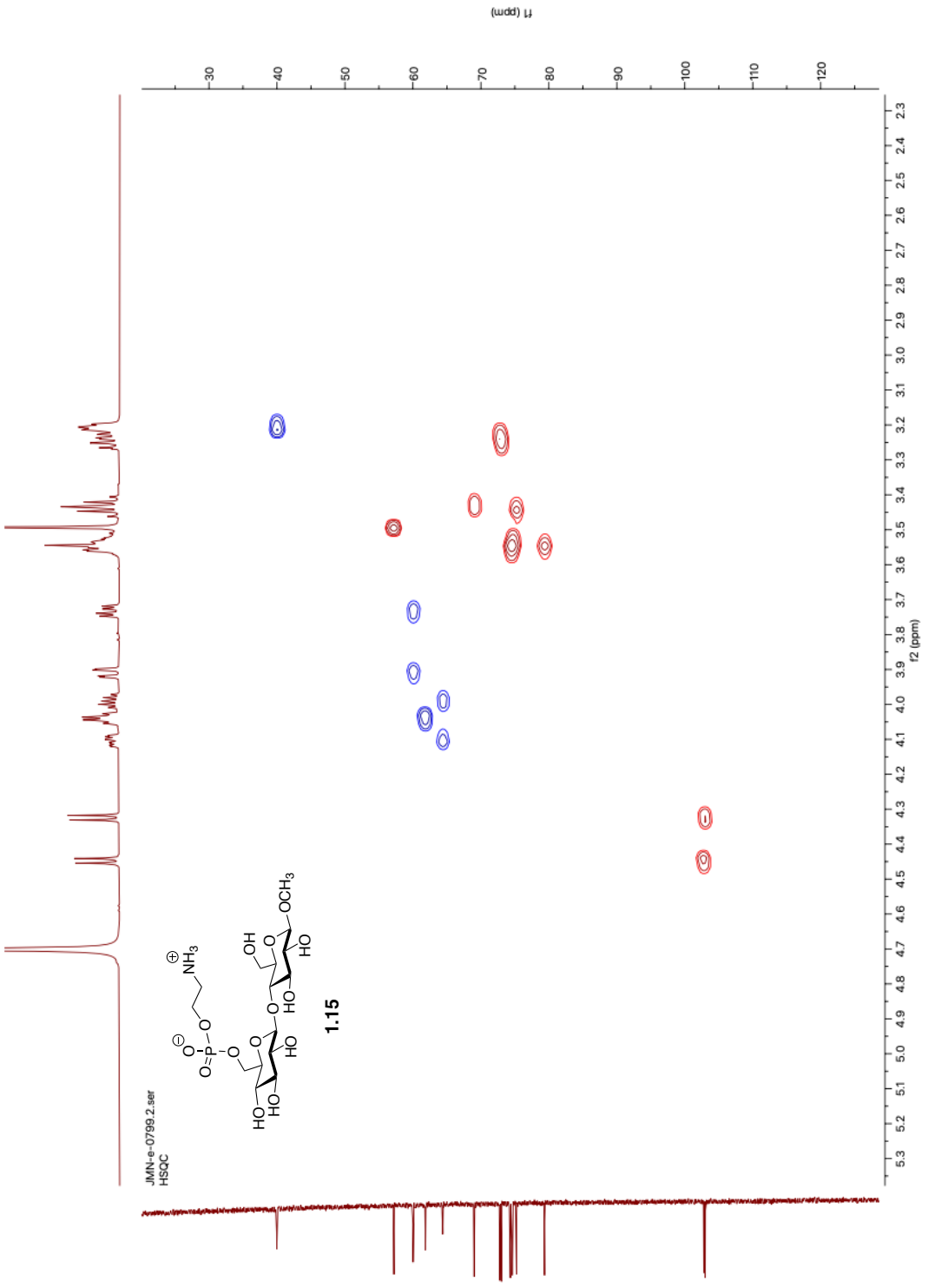

Figure A1.9. ^{1}H-^{13}C HSQC NMR (600 MHz, D_2O) of compound **1.15**.

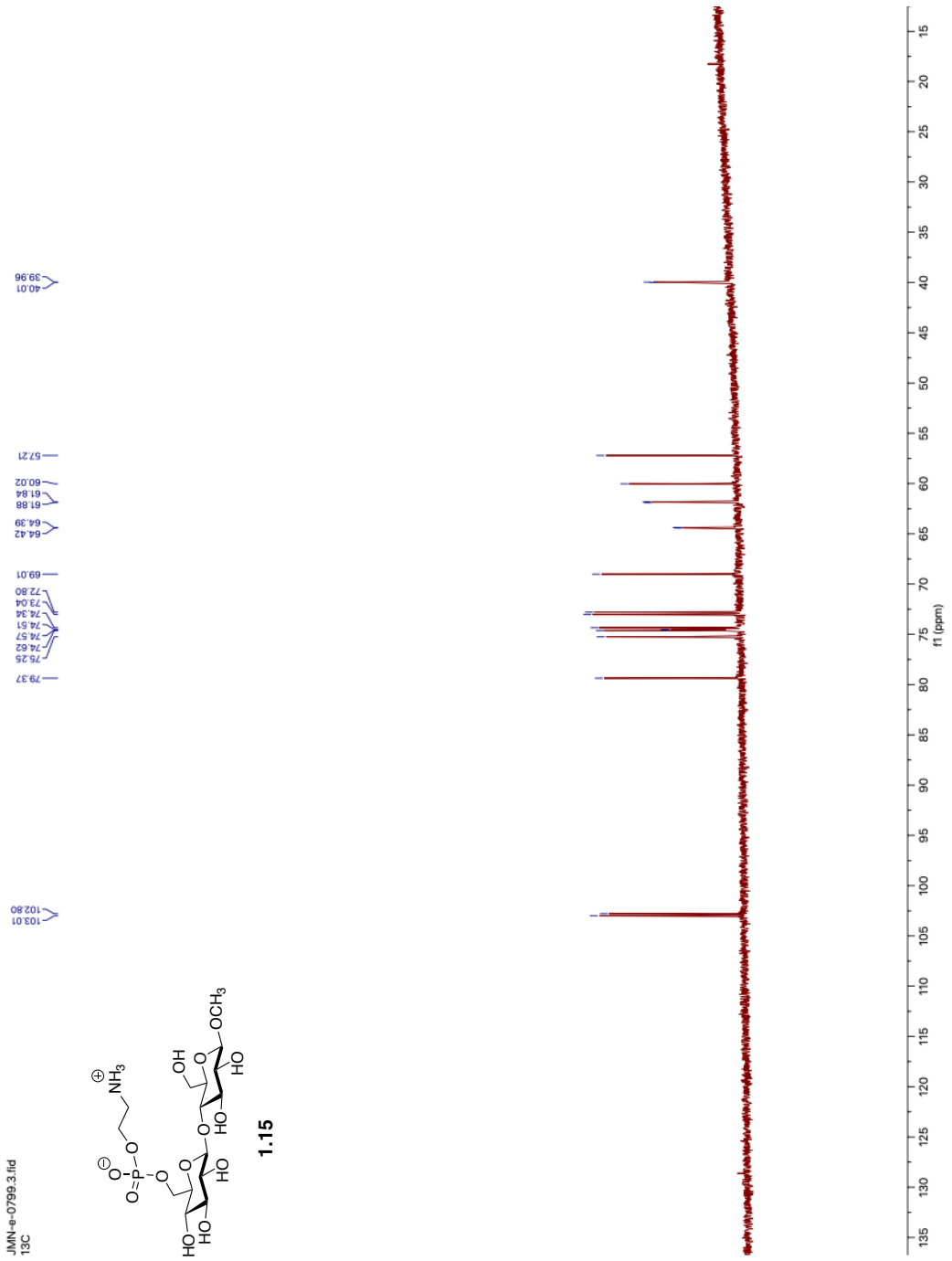

Figure A1.10. ^{13}C NMR (151 MHz, D_2O) of compound **1.15**.

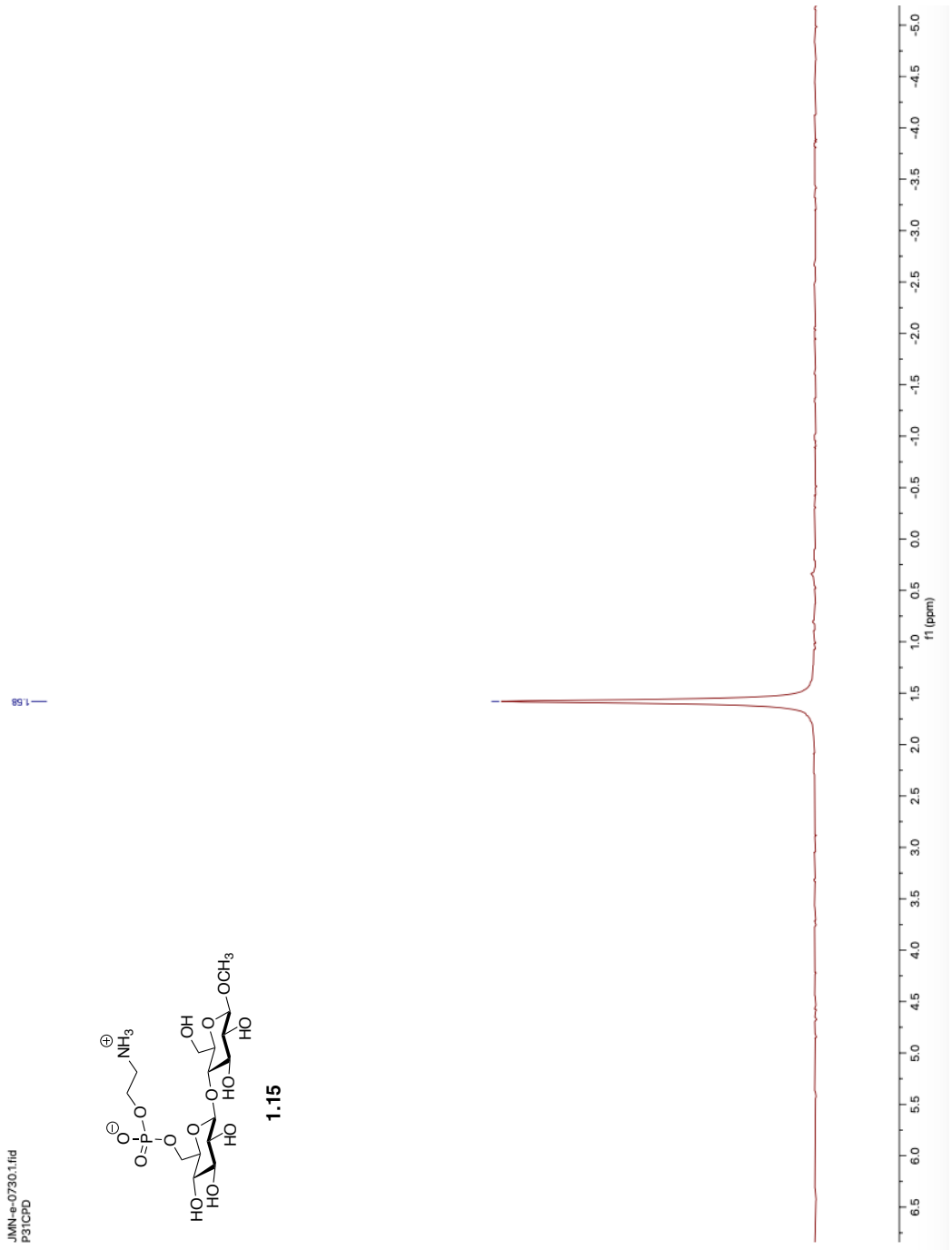

Figure A1.11. ^{31}P NMR (162 MHz, D_2O) of compound **1.15**

Chapter 2

Synthesis of Deoxy-amino Sugars and Their Applications in Total Synthesis

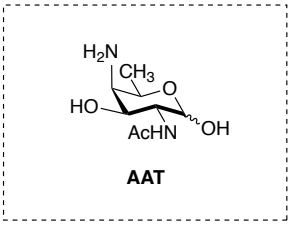

AAT

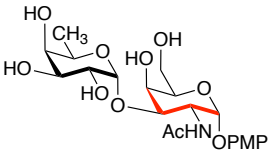

A. veronii strain Bs8 OPS
Repeating Unit

2.1 Introduction

Bacterial deoxy-amino sugars are a vital structural component of several extracellular polysaccharides (EPS), lipopolysaccharides (LPS), glycoconjugates and secondary metabolites, including antibiotics.[1-6] These monosaccharides are ubiquitously dispersed on the cell surface of polysaccharides and are produced by numerous pathogenic bacterial strains including: *Psuedomonas aeruginosa*, *Streptoccocus pneumonia*, *Bacteroides fragilis*, and *shigella sonnei*; however, they are absent in the human metabolism.[5-10] Different from their eukaryotic counterparts, bacterial glycans can be exploited for target specific drug discovery since their structural differences help differentiate between the host cell and pathogen and is quintessential for drug development.

While the biological activity of these deoxy-amino sugars is noteworthy, they are not available from natural sources. As such, the procurement of these highly orthogonally protected glycans via chemical synthesis has therefore received notable attention. To this end, a variety of methods have been developed by groups around the world to access these rare sugars using both carbohydrate and non-carbohydrate starting materials.

The introduction of an amine group into pentose or hexose sugars can greatly affect their physiochemical properties, and in consequence, can change their biological activity. The most desirable sugars include, 2-acetamido-4-amino-2,4,6-trideoxy-D-galactose (AAT, **2.1**)[9], *N*-acetyl fucosamine (FucNAc, **2.2**)[10], 2,4-diacetomido-2,4,6-tridoexy-D-galactose (DATDG, **2.3**)[11], D-xylo-6-deoxy-4-ketohexosamine (DKH, **2.4**)[12] and bacillosamine (Bac, **2.5**)[13] among the selected

from Table 2.1 (Figure 2.1). Synthetic methods to access these compounds in suitable quantity and stereochemical purity is of great importance because it will provide tool compounds to investigate the role of bacterial glycans in the pathogenesis of virulent bacteria. In this chapter, we will discuss the biological importance of bacterial deoxy-amino sugars, their biosynthesis, and current methods for their preparation and application in total synthesis. Chapter 2 of this thesis will also delineate our laboratory's work in the area of deoxy-amino sugar synthesis; this work has resulted in the first total synthesis of the *Aeromonas veronii strain Bs8 OPS* disaccharide repeating unit, as well as a scalable synthesis of an AAT derivative.

IUPAC name	Common name	Constituent of	Sources
2-amino-2-deoxy-D-galactose	D-galactosamine	bacterial cell wall chondroitin sulfate	*Bacillus subtilis,* mammalian glycosaminoglycans
2-amino-2,6-dideoxy-D-galactose	D-fucosamine	teichuronic acid (component of cell wall)	*Bacillus subtilis*
2-acetamindo-4amino-2,4,6-trideoxy-D-galactose	AAT	zwitterionic polysaccharides	*Shigella sonnei, Streptococcus pneumonia, Bacteriodes fragilis, Streptococcus mitis, Proteus vulgaris*
2,4-diacetamino-2,4,6-trideoxy-D-galactose	DATDG	polysaccharides	*Staphlyococcus aureus*
5,7-diacetamido-3,5,7,9-tetradeoxy-l-glycero-α-l-manno-nonulosonic acid	Pseudaminic acid	polysaccharides	*P. aeruginose, Shigella boydii*
D-xylo-6-deoxy-4-ketohexosamine	DKH	lipopolysaccharides	*Yersinia enterocolitica*
2-acetamindo-2,6-dideoxy-L-galactose	N-acetyl-L-fucosamine	lipopolysaccharides	*Pseudomonas aeruginosa*
2-amino-2-deoxy-D-mannose	D-mannosamine	amphotericin B, nystatin, trichomycine A, pimaricin	human plasma
3-amino-3,6-dideoxy-D-mannose	D-mycosamine	N-acetylneuraminic acid sialic acid	*Streptomycetes*
4-amino-4,6-dideoxy-D-mannose	D-perosamine	O-antigen, perimycin	*Vibrio cholerae, Streptomyces coelicolor*
2-amino-2-deoxy-D-gulose	D-gulosamine	streptothricins	*Actinomycetes*
2-amino-2-deoxy-D-talose	D-talosamine	chondroitin sulfate	*Sheep cartilage*
3-amino-3-deoxy-D-ribose	D-ribosamine	puromycine	*Streptomyces alboniger*
4-amino-4-deoxy-L-arabinose	—	lipopolysaccharides	*Salmonella minnesota*
3-amino-2,3,6-trideoxy-L-lyxo-hexose	L-daunosamine	daunomycine	*Streptomyces spp.*
3-amino-2,3,6-trideoxy-L-ribose	L-ristosamine		*Streptomyces spp.*
3-amino-2,3,6-trideoxy-L-arabinose	L-acosamine		*Streptomyces spp.*
2-acetamido-2,6-dideoxy-L-galactose	L-fucosamine	polysaccharides	*Yersinia enterocolitica, Plesiomonas shigelloides, Staphylococcus aureus, Pseudomonas chloraphis, Pseudomonas aeruginosa*
2-acetamido-2,6-dideoxy-L-glucose	L-quinovosamine	polysaccharides	*Vibrio vulnificus, Shewanella putrefaciens*
2-acetamido-2,6-dideoxy-L-talose	N-acetyl L-pneumosamine	polysaccharides	*P. shigelloides, Alteromonas nigrifaciens*
2-acetamido-2,6-dideoxy-L-rhamnose	L-rhamnosamine	polysaccharides	*V. vulnificus, P.vulgaris*
2,3,4,6-tetra-deoxy-4-(methoxycarbonylamino)-3-C-methyl-3-nitro-D-xylo-hexapyranose	D-kijanose	kijanimicin A	*Actinomadura kijaniata*
2-amino-2-deoxy-D-glucose	D-glucosamine	chitosan	*Mucor rouxii*
2-methylamino-2-deoxy-L-glucose	N-methyl-L-glucosamine	streptomycin	*Actinomycetes*
2-acetamido-2-deoxy-D-glucose	N-acetyl-D-glucosamine	chitin, murein, hyaluronic acid, glycoproteins	Crustaceans, insects, fungal and bacterial cell wall
2-amino-2,6-dideoxy-D-glucose	D-quinosamine	lipopolysaccharides	*Vibrio cholerae*
2,4-diamino-2,4,6-trideoxy-D-glucose	D-bacillosamine	polysaccharides	*Bacillus subtilis*
2,4-diacetamido-2,4,6-trideoxy-D-glucose	—	polysaccharides	*Bacillus licheniformis, C.jejuni*
3-amino-3-deoxy-D-glucose	D-kanosamine	unbound, kanamycine A	*Streptomyces kanamyceticus, Bacillus spp.*
6-amino-6-deoxy-D-glucose	—	kanamycine A	*Streptomyces kanamyceticus*
3,6-dideoxy-3-dimethylamino-D-glucose	D-mycaminose	leucomycines, tylosin	*Streptomyces kitasatoenis Hata*
3-(dimethylamino)-3,4,6-trideoxy-D-glucose	D-desoamine	erythromycin	*Streptomyces erytherus, Streptomyces venezuleae*
4-(dimethylamino)-2,3,4,6-tetradeoxy-D-erythro-hexose	D-forosamine	spinosyns	*Saccharopolyspora spinosa*

Table 2.1. The natural origin of deoxy-amino sugars.[14-42]

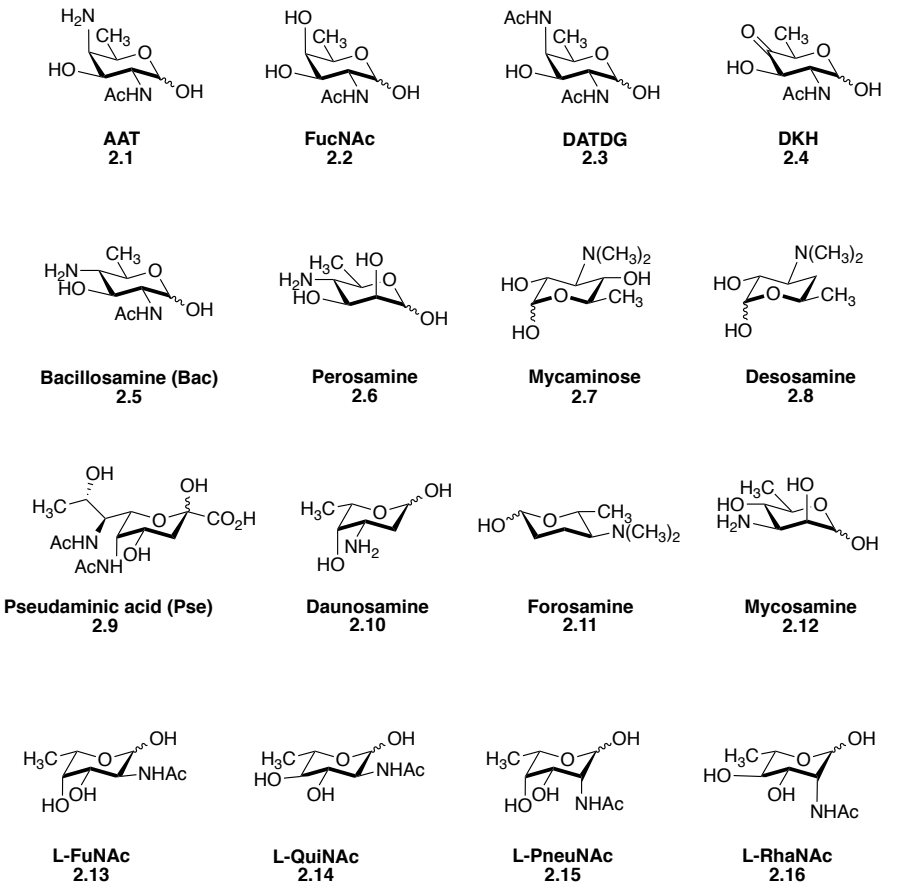

Figure 2.1. Representative examples of rare deoxy-amino sugars from bacteria.

2.2 The natural origins of deoxy-amino sugars

Deoxy-amino sugars are an important class among deoxy-sugars and are synthesized by a diverse range of microorganisms. Naturally abundant glycans, such as D-mannosamine (ManN), D-galactosamine (GalN), D-glucosamine (GlcN) and their *N*-acetyl derivatives (GalNAc, ManNAc, and GlcNAc) are products of primary metabolism.[43-44] For example, chitin, the second most abundant biopolymer on Earth after cellulose, is a β-1,4 linked GlcNAc homopolymer.[45] These *N*-acetyl deoxy-amino sugars are also present in the microbial cell wall, where they are a key

structural component of the peptidoglycan layer. Furthermore, they are also a major constituent of bacterial glycoproteins and are linked to pathogen-associated targets. Indeed, pathogenic bacteria can synthesize glycoproteins and is more than often related to their ability to cause disease.

In contrast, other deoxy-amino sugars, such as perosamine (**2.6**), mycaminose (**2.7**), desosamine (**2.8**), daunosamine (**2.10**), forosamine (**2.11**), and mycosamine (**2.12**) are products of secondary metabolism (Figure 2.1).[46-49] They are components of several antibiotics. For example, **2.8** is present in erythromycin, **2.7** in tylosin, and **2.12** in amphotericin B, respectively. Although more than fifty amino sugars have been described in the literature, only the most relevant and important are listed in Table 2.1**.** At present, deoxy-amino sugars are important for biological activity and further investigation of these rare sugars will enable access to new glycoconjugate-based vaccines.

2.3 Deoxy-amino sugar biosynthesis

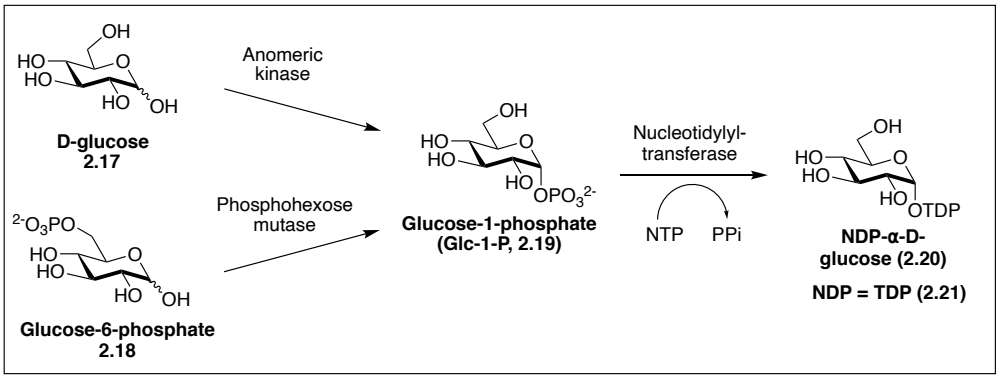

Scheme 2.1. Activation of key glycolytic intermediates D-glucose (**2.17**) and glucose-6-phosphate (**2.18**).

The origin of most deoxy-amino sugars produced by bacteria biosynthetic pathways are derived from α-D-glucose-1-phosphate, which in turn, is initially from D-glucose (**2.17**).[50-51] From here, direct anomeric phosphorylation is catalyzed by an anomeric kinase to allow access to glucose-1-phosphate (**2.19**). Alternatively, glucose-6-phosphate (**2.18**) upon treatment with a phosphohexose mutase can also arrive at the same key intermediate (**2.19)**. Next, a nucleotide monophosphate (NMP) group from nucleotide triphosphate (NTP) could then be coupled with nucleotidylyltransferase to provide NDP-glucose (**2.20**). Although deoxy-amino sugars from primary metabolites can be activated by NDP groups, majority of all bacterial deoxyamino-sugars featured in complex molecules, such as antibiotics, are primarily produced via the secondary metabolism pathway. They are derived biosynthetically from TDP-α-D-glucose (**2.21**).[52-53]

From here, **2.20** and **2.21** can be subjected through a series of enzymatic reactions that lead to a key reduction (dehydration), resulting in the displacement of one or two alcohols with hydrogens. Moreover, an important step in the synthesis of

deoxy-amino sugars involves a transamination reaction that converts the ketone for an amine. Consequently, the genes that are involved in the biosynthesis of deoxy-amino sugars are often grouped and located nearby other genes required for the synthesis of the corresponding sugar.[49] These clustered genes share a commonality, as they contain genes encoding isomerases, aminotransferases, amidotransferases, dehydratases, glycosyltransferases, and methyltransferases. Furthermore, chemical synthesis of deoxy-amino sugars is possible through routes involving the use of carbohydrate starting material or via a *de novo* route that highlights precursors, such as amino acids, alcohols, carboxylic acids, esters, lactones, and aldehydes. In both cases, a regio- and stereospecific reaction would be required to introduce an amino functionality into the appropriate site on the molecule.

2.3.1. Deoxy-amino sugars derived from primary metabolism

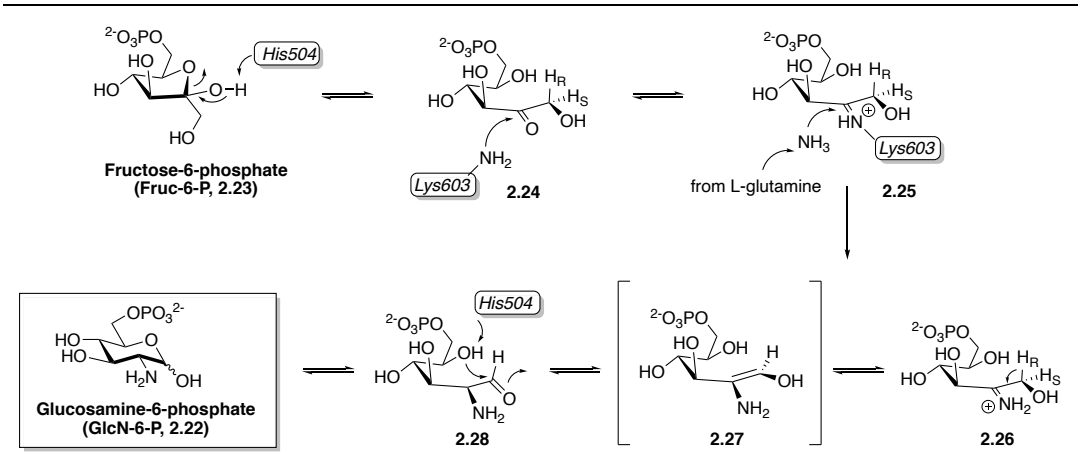

Scheme 2.2. Proposed mechanism of amino transfer and sugar isomerization by GlcN-6-P synthase in primary metabolism.

The transfer of an amine group from an amino acid donor, such as L-glutamine or L-glutamate to a ketose derivative in the open form or to the closed

form of an aldose derivative is an important initial step in the biosynthesis of deoxy-amino sugars in primary metabolism. This stereospecific reaction is driven via enzymatically by an independent amidotransferase or a dependent aminotransferase. In general, the acceptor is a sugar nucleotide or a sugar phosphate. The synthesis of D-glucosamine-6-phosphate (GlcN-6-P, **2.22**) from L-glutamine and D-fructose-6-phosphate (Fruc-6-P, **2.23**) is a prime example of deoxy-amino sugars synthesized from primary metabolism.[49] The enzyme responsible for this transformation is fructose-6-phosphate amidotransferase, also known as glucosamine-6-phosphate (GlcN-6-P) synthase, which is a ubiquitous enzyme in nature and is prevalent among all living organisms. This irreversible enzymatic reaction with GlcN-6-P synthase does not require any coenzymes and proceeds through transferring an amide of L-glutamine to Fruc-6-P followed by isomerization of the fructose intermediate as shown in Scheme 2.2.[50-53]

Upon completion of **2.22**, the newly synthesized glycan can then proceed downstream through the Leloir pathway, which is a series of three consecutive reactions to access UDP-GlcNAc. From here, the UDP-GlcNAc can serve as a donor in the biosynthesis of other structurally complex polysaccharides and glyco-conjugates. Nevertheless, UDP-GlcNAc can also be functionalized by other enzymes, such as epimerases to access *N*-acetyl galactosamine (GalNAc) and mannosamine (ManNAc) deoxy-amino sugars. Additionally, UDP-GlcNAc can be used for the synthesis of the rare sugar, *N*-acetyl-L-fucosamine, which is shown in numerous polysaccharides.[49-50]

2.3.2 Deoxy-amino sugars derived from secondary metabolism

The biosynthesis of deoxy-amino sugars via the secondary metabolism pathway is often associated with a variety of genes and enzymes. Bacterial glycan featured in complex molecules are functionalized from enzymes, such as isomerase, dehydratases, methyltransferases, glycosyltransferases, and aminotransferases.[51] An overview of the enzymes and genes required for the biosynthesis of selected monosaccharides is shown in Table 2.2.

Complex Molecules	Deoxy-amino sugar	Isomerase	Glycotransferase	4,6-Dehydratase	Aminotransferase	Methyltransferase	3,4-dehydratase
Erythromycine	D-desosamine	EryCII	EryCIII	Gdh	EryCI	EryCVI	EryCIV
Spinosyns	Forosamine	NI	SpnP	Gdh	SpnR	SpnS	SpnQ
Polyene macrolides	Mycosamine	NI	AmphDI, CanG, NysDI, PimK	AmphDIII, CanM, NysDIII, PimJ	AmphDII, CanA, NysDII, PimC	NI	Ni
Daunorubicin	L-daunosamine	NI	DnmS	DnmM	DnmJ	NI	NI
Tylosin	Mycaminose	NI	TylM2	TylA2	TylB	TylMI	NI

Table 2.2. Summary of common enzymes in the biosynthetic pathways of key deoxy-amino sugars in bacteria. *NI* Not Identified.[49]

In general, the biosynthesis of deoxy-amino sugar requires the activation of a precursor monosaccharide followed by coupling with nucleotidylyltransferase to access NDP-α-D-glucose.[49] From the latter intermediate, the biosynthetic pathway for this glycan can vary, since the next steps could involve a reduction, isomerization, and dehydration reaction. Eventually, a key transamination step will convert the deoxy-sugar to a deoxy-amino sugar by an aminotransferase. However, deoxy-amino sugars produced in bacterial secondary metabolism exclusively use TDP-α-D-glucose (**2.21**) as the primary intermediate for further enzymatic modifications. Indeed, rare bacterial sugars, such as mycaminose (**2.7**),

desosamine (**2.8**), and forosamine (**2.11**) can be accessed from **2.21** (Scheme 2.3). While most deoxy-amino sugar moieties (i.e., **2.8, 2.11, and 2.12**) in macrolides originate from **2.21**, deoxy-amino sugars from polyene macrolides, specifically perosamine (**2.6**) and mycosamine (**2.12**) are believed to arise from GDP-D-mannose (**2.44**, Scheme 2.4).

To date, erythromycin, 3-(dimethylamino)-3,4,6-trideoxy-D-glucose, is one of the most widely studied antibiotics and is produced by *Saccharopolyspora erythraea.* Erythromycin contains two deoxy-sugars (L-cladinose and D-desosamine) linked to a 14-membered ring, respectively. The biosynthesis of TDP-D-desosamine (**2.39**) requires the early activation of glucose-1-phosphate (**2.19**) by TDP-glucose synthase to provide **2.21**, followed by dehydration at the C-4 and C-6 positions by TDP-D-glucose 4,6 dehydratase to access **2.29**.[54] From here, an additional four enzymatic steps, including a key aminotransferase reaction will provide TDP-D-desosamine (**2.39**). Conveniently, mycaminose and forosamine can also be synthesized in three and five steps by the same key dehydrated intermediate **2.29** (Scheme 2.3).[55-56]

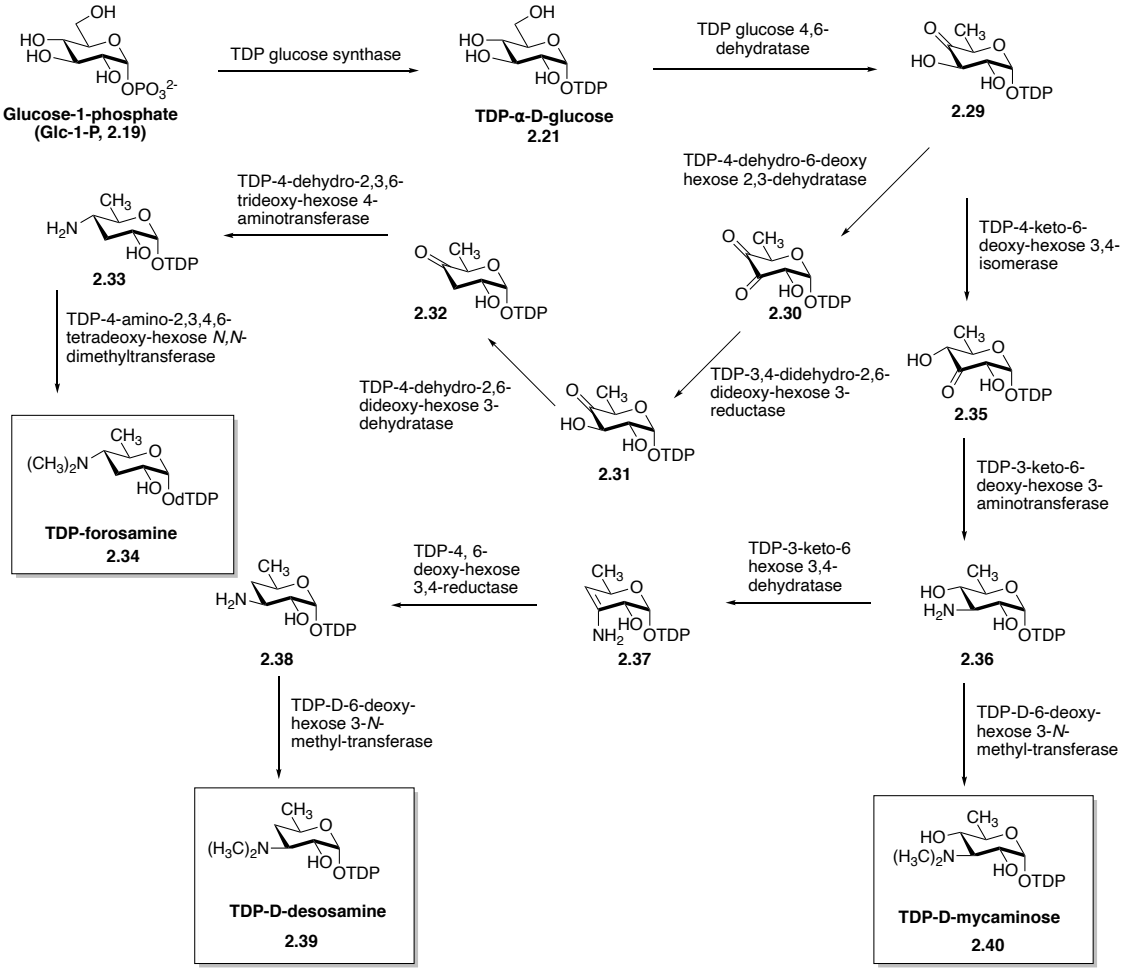

Scheme 2.3. Proposed biosynthetic pathway for D-desosamine, D-mycaminose, and D-forosamine.

Other deoxy-amino sugars derived from microbial secondary metabolism, such as **2.6** and **2.12** are mainly associated with polyene macrolide antibiotics, such as nystatin, amphotericin B, and candicidin, which are produced by *S. noursei, S. nodosus,* and *S. griseus*.[57] The proposed biosynthetic pathway for both **2.6** and **2.12** is shown in **Scheme 2.4**. Different from other deoxy-amino sugars synthesized by secondary metabolism, **2.6** and **2.12** is synthesized via the GDP-mannose pathway.[57-58] Accordingly, GDP-D-mannose is synthesized by enzymes involved in

primary metabolism, starting from fructose-6-phosphotase (**2.23**). From here, transformation of GDP-D-mannose to GDP-D-perosamine (**2.46**) and GDP-D-mycosamine (**2.49**) would entail a few additional steps starting from a reaction with GDP-4,6-dehydratase, followed by a key transamination step to afford **2.46** and **2.49**.

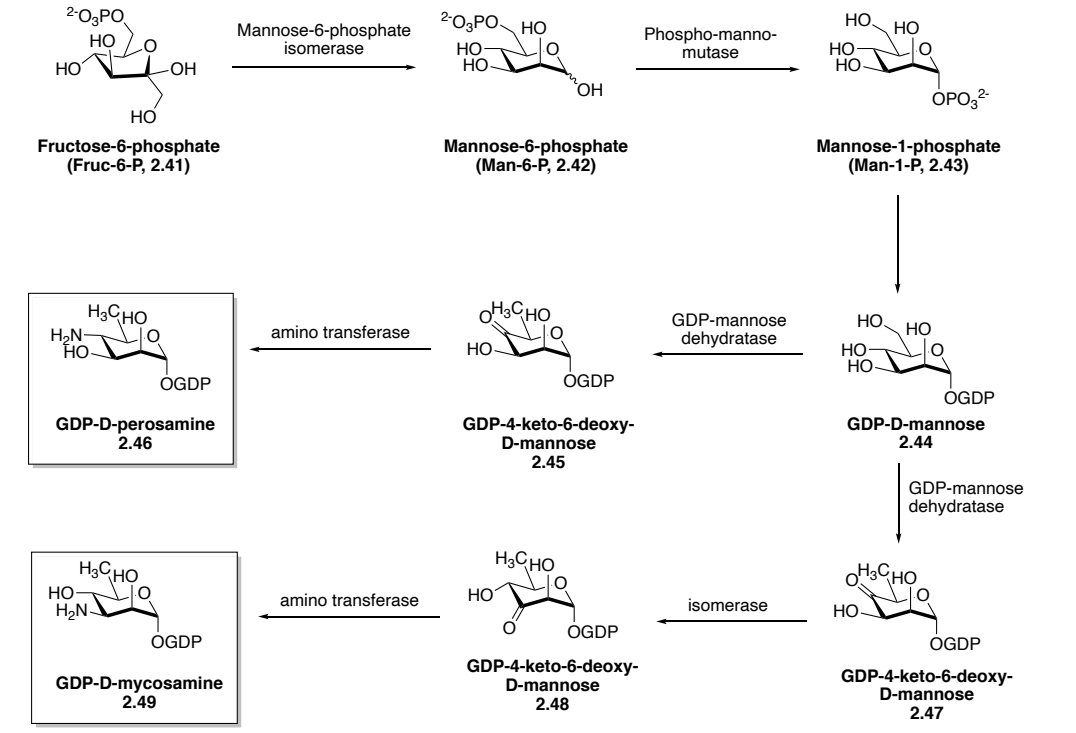

Scheme 2.4. Proposed biosynthetic pathway for D-perosamine and D-mycosamine.

2.4. Chemical synthesis of deoxy-amino sugars

Current strategies to combat against bacterial diseases have heavily relied on blockbuster antibiotics, such as Penicillin and Vancomycin, to inhibit the enzymes responsible for peptidoglycan biosynthesis.[59] Although these therapies have been effective at saving numerous lives, recent emergence of the World Health Organization antibiotic resistant “priority pathogen” list has called for an inquiry into alternative treatment.[60]

An ongoing impediment in bacterial disease treatment have largely been due to the paucity of knowledge around bacterial glycoproteins and glycosyltransferases. Particularly, the lack of specific probes for diagnosis and treatment against pathogenic bacteria in a selective manner is a major setback. To address this issue, recent work showed that deoxy-amino sugars found exclusively on pathogenic bacteria can used as a basis for a target therapy. Moreover, these bacterial sugars have been linked to bacterial fitness and pathogenesis, respectively making them great targets. Undeniably, a quick survey of the literature has shown that peptidoglycan formed improperly can experience osmotic lysis and altered lipopolysaccharides can be dismantled by the host’s immune system.[61] These examples reveal that deoxy-amino sugars have a critical function and are linked to pathogenicity. Remarkably, targeting these structures could alleviate the urgent need to develop new diagnostic and antibiotics for bacterial diseases.

Therefore, access to these bacterial sugars in sizeable quantity and stereochemical purity can be highly attractive. As a result, the development of efficient synthetic methods and strategies to acquire these structurally diverse

deoxy-amino sugar is of great importance. For example, *Pseudomonas aeruginosa* links *N*-acetyl fucosamine (FucNAc, **2.2**) residues[62], *Bacteroides fragilis* attaches 2-acetamido-4-amino-2,4,6-trideoxy-galactose (**AAT, 2.1**)[9] onto its cell surface zwitterionic polysaccharides, and *Neisseria meningitidis* use bacillosamine (2,4, diamino-2,4,6-trideoxy-D-glucose, **Bac, 2.5**)[63] as a key structural component of its long polymeric filamentous glycoproteins (Figure 2.1). For more than three decades, there has been an earnest attempt to synthesize these unique bacterial sugars to access aforesaid synthetic targets. Given their biological importance, these complex glycoconjugates and molecules represented in Figure 2.2 are interesting targets for chemical total synthesis.

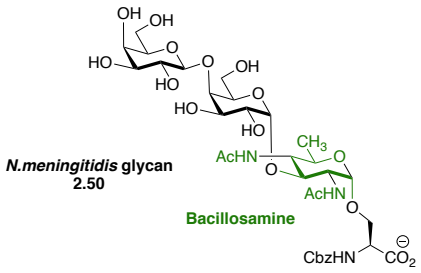

***N.meningitidis* glycan**
2.50

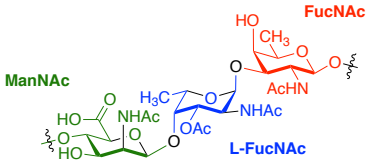

***S. aureus* type 5 CPS**
2.51

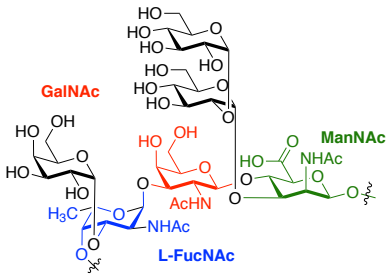

***S. pneumoniae* serotype 12F CPS**
2.52

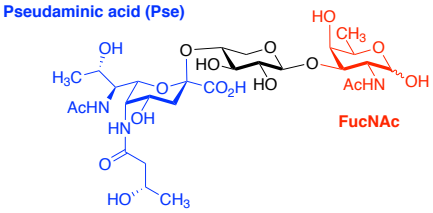

***P. aeruginosa 1244* pilin glycan trisaccharide**
2.53

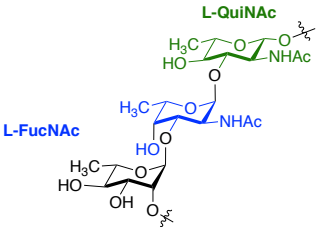

***P. chlororaphis subsp. aureofaciens* strain M71**
2.54

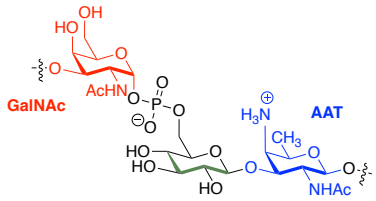

***H. parainfluenzae strains 20* ZPS**
2.55

Figure 2.2. Part A. Structures of representative glycans found on bacterial cells, with exclusively bacterial sugar highlighted in color.

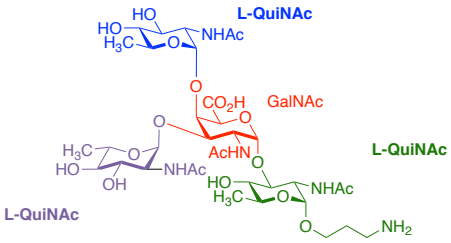

***V. vulnificus* MO6-24 polysaccharide**
2.56

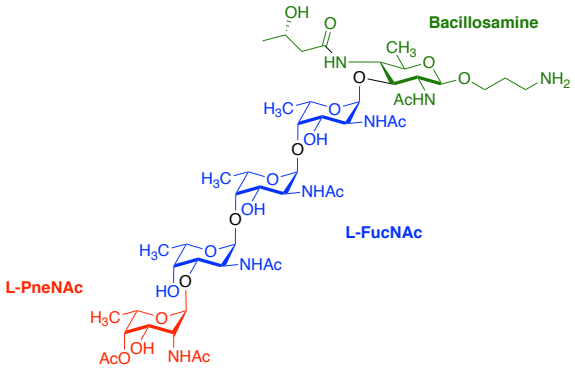

***P. shigelloides* Strain 302-73 (Serotype O1)**
2.57

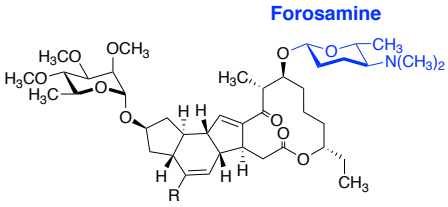

R = H: (-)-Spinosyn A, 2.58
R = CH_3: (-)-Spinosyn D, 2.59

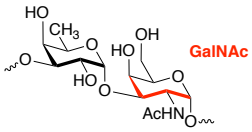

***A. veronii* strain Bs8 OPS**
2.60

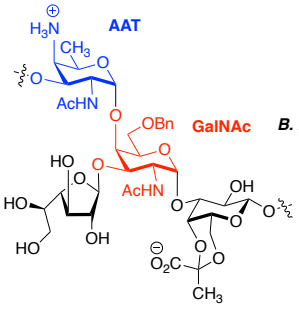

***B. fragilis* ZPS A1**
2.61

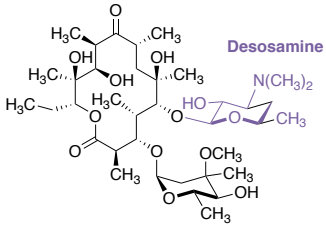

Erythromycin
2.62

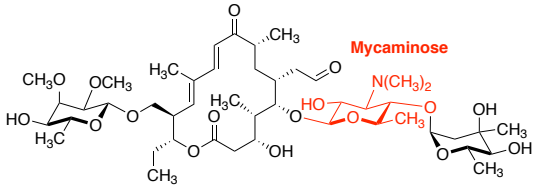

Tylosin
2.63

Figure 2.2. Part B. Structures of representative glycans found on bacterial cells, with exclusively bacterial sugar highlighted in color.

Considerable attention has been dedicated toward the syntheses of these rare bacterial monosaccharides, exploiting both non-carbohydrate and carbohydrate starting materials. Given the inherent difficulty of synthesizing these glycans, some strategies still require lengthy multistep procedures, along with low overall yields and use of expensive starting materials. New methodology employing modern chemistry and enantioselective catalysis would allow for an efficient and facile method to synthesize these structurally diverse molecules. The section below will provide an overview on the various approaches toward the synthesis of deoxy-amino sugars, but also include an in-depth analysis of modern approaches that employs *de novo* strategies.

2.4.1 Overview of D-fucosamine chemical synthesis

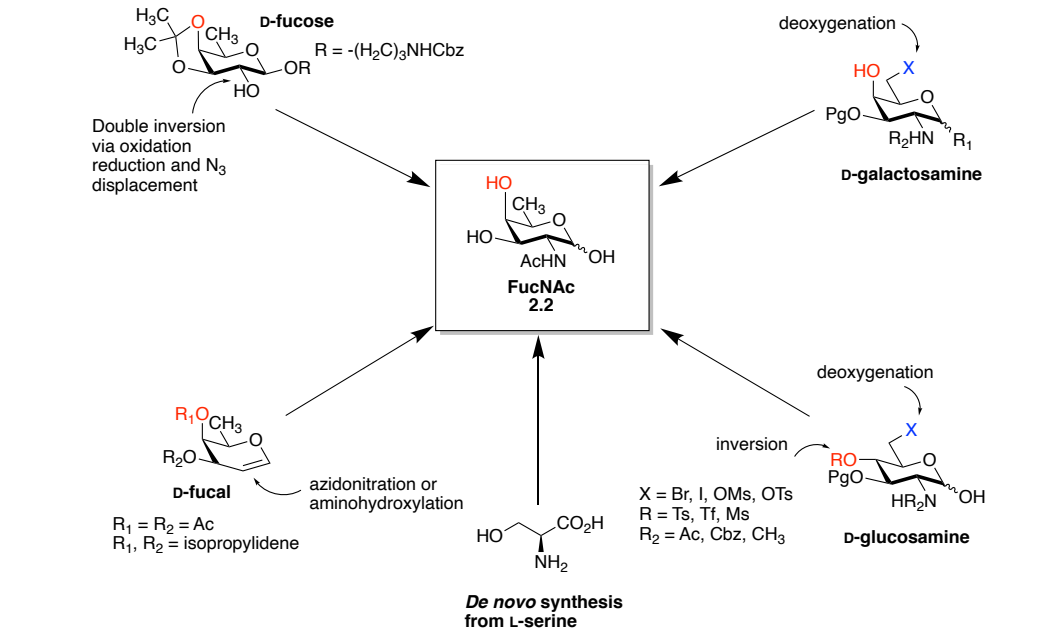

Figure 2.3. Synthetic strategies for the synthesis of D-fucosamine (FucNAc) derivatives.

Among the methodology that has been developed for the synthesis of D-fucosamine (FucNAc, **2.2**), a common strategy involves the deoxygenation on D-galactosamine at the C-6 position. This protocol would require a reduction of an alkyl halide at C-6 with a hydride source or using classical Barton-McCombie conditions.[64-68] Because D-galactosamine is significantly more expensive when compared to D-glucosamine, the latter is frequently used as an alternative. Strategies for the use of D-glucosamine would require an additional two-step procedure that consists of an S_N2 displacement of a triflate or mesylate at the C-4 position followed by nucleophilic attack with benzoate.[69-71] From here, deoxygenation at C-6 with conditions mentioned above would provide D-fucosamine derivatives (Figure 2.3).

A closer examination at the literature reveals chemistry developed by the Shibaev[72] and Carreira[73] groups have used D-fucal as a starting material, whereby an azidonitration or aminohydroxylation reaction would allow access to D-fucosamine derivatives. In a different approach, elegant work by Adamo and co-workers showed that functional group interconversion at the C-2 position via a double inversion oxidation-reduction reaction followed by azide displacement can afford the deoxy-amino sugar.[74]

2.4.2 Overview of D-bacillosamine chemical synthesis

Previous chemistry that has been developed for the synthesis of D-fucosamine can be applied toward the synthesis of D-bacillosamine (**2.5**) by using D-fucal[75], D-glucosamine[76-77], and D-galactosamine[78] as the starting materials. A fruitful route to access D-fucosamine would entail a tosylation, mesylation, or

triflation reaction on the secondary alcohol at C-4 and subsequent nucleophilic displacement with an amine source will afford the desired D-bacillosamine building block (Figure 2.4).

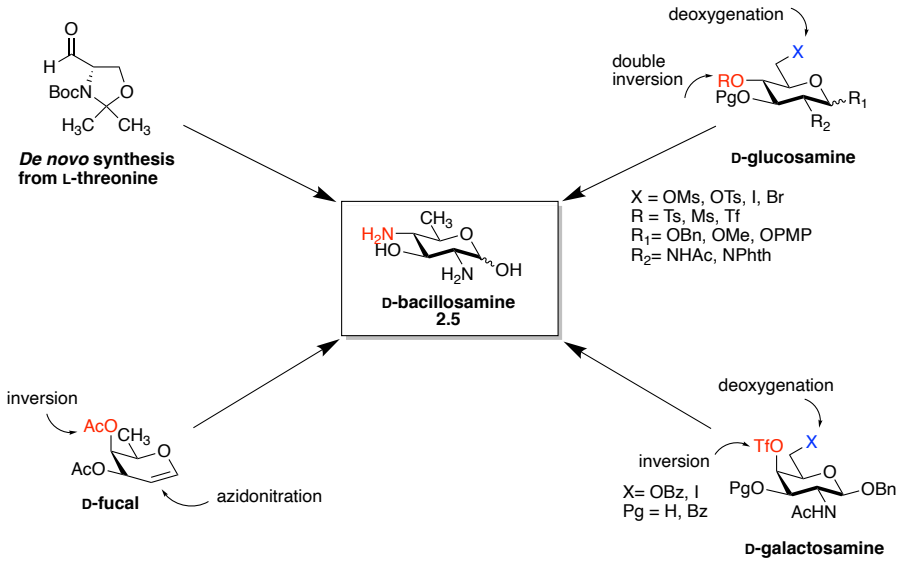

Figure 2.4. Synthetic strategies employed for D-bacillosamine (Bac) derivatives.

2.4.3 Overview of AAT and DATDG chemical synthesis

With so many unique and diverse complex molecules containing AAT and DATDG, it is not surprising that several syntheses of these key building blocks have been reported.[79-85] The first synthesis of an orthogonally protected **AAT** building block was achieved by Loongren and co-workers in 1984, where D-glucosamine was used as the key starting material for their total synthesis of a capsular polysaccharide antigen of *Streptococcus pneumoniae*.[80] At the start of their work, they employed the popularized two-step Mitsunobu protocol to set the desired stereocenter on their AAT building block. D-glucosamine is the most suitable

material for the synthesis of **2.1** and **2.3** since the necessary amine at C-2 has graciously been installed beforehand (Figure 2.5). In a similar approach for the syntheses of **2.2** and **2.5**, deoxygenation at C-6 will be necessary to afford **2.1** and **2.3**.

Tremendous and continuous research effort for the synthesis of **2.1** and **2.3** was accomplished by van Boom and co-workers using D-mannose as their starting material.[86-87] This method would consist of a stepwise approach to install the amine at the C-4 and C-2 positions. Since the discovery of these rare deoxy-amino sugars, more than ten groups around the world have successfully synthesized **2.1** and **2.3** by various chemistries, including a concise approach that was developed by our group. Furthermore, we will enumerate the application of these chemistries in the context of total synthesis to highlight both classical and *de novo* approaches to deoxy-amino sugars.

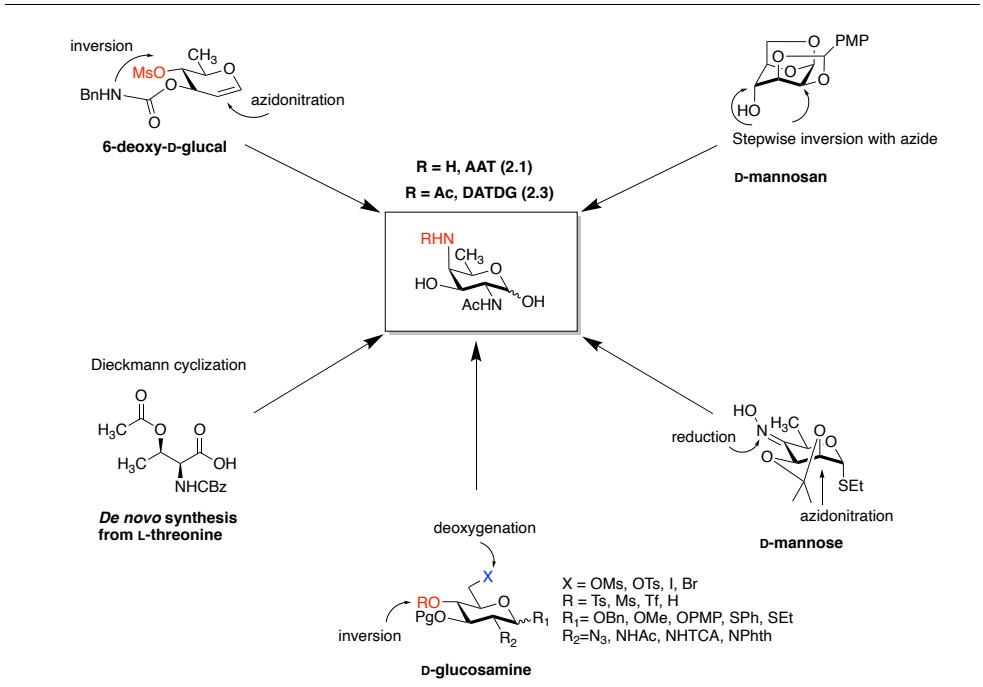

Figure 2.5. Known synthetic strategies for AAT and DATDG derivatives.

2.4.4 General approaches for rare deoxy-amino sugar chemical synthesis

*Adamo and co-workers' 2012 synthesis of D-FucNAc acceptor **2.68**.*[74]

In their 2012 total synthesis of *Staphylococcus aureus* type 5 capsular polysaccharide (CPS) repeating unit (**2.51**), Adamo and co-workers reported a synthesis of a D-FucNAc derivative using peracetylated D-fucose (**2.64**) as their starting material. The synthesis of the D-FucNAc acceptor **2.68** commenced with the installment of a benzyl(*N*-(hydroxylpropyl) carbamate at the anomeric position to afford **2.65** in a 72% yield, exclusively as the β-product (Scheme 2.5). Next, deacetylation of **2.65** under Zemplén condition and isopropylidene protection provided compound **2.66** (87% yield over two steps). To install the amine moiety at C-2, the next steps consist of a Swern oxidation and subsequent reduction with $NaBH_4$, leading stereoselectivity to the *talo* configuration in 87% yield over two steps. At this stage, *O*-triflation of the C-2 alcohol followed by displacement with sodium azide provided **2.67** in excellent 90% yield. Finally, removal of the isopropylidene protecting group and regioselective protection of the C-4 alcohol through a sequence of four steps provided the desired accepter **2.68**.

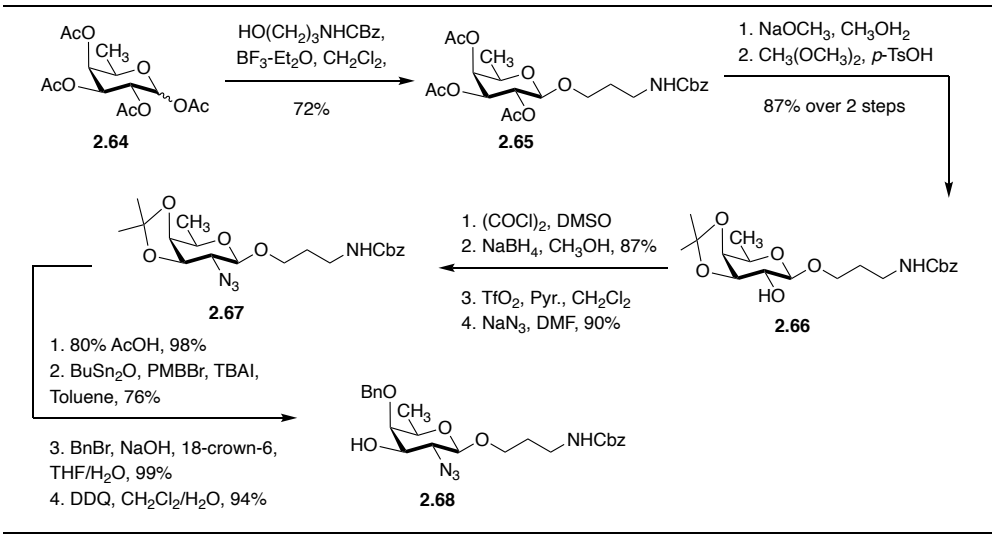

Scheme 2.5. Synthesis of D-FucNAc (**2.2**) from D-galactose by Adams and co-workers.

*Seeberger's 2010 de novo synthesis of AAT (**2.1**) from L-threonine*[88-89]

Although majority of carbohydrate building block synthesis proceeds through the classical approach of using carbohydrate as a starting material, *de novo* approaches have attracted much interest from the synthetic community. The advantage of such an approach for total synthesis are often atom economics by avoiding protecting group manipulations and pre-functionalization, which is notorious in carbohydrate synthesis. Recent *de novo* approaches have explored the use of aldehydes, alcohols, esters, ketones, lactones, and amino acid as starting materials.

In 2010, Seeberger and co-workers developed an elegant and efficient synthesis of AAT via a *de novo* route. Seeberger's synthesis commenced with commercially available Cbz-L-threonine **2.69** (Scheme 2.6). First, routine esterification and alcohol acetylation provided cyclization precursor **2.70**, which underwent the key Dieckmann cyclization upon treatment with LiHMDS. Methylation

of the cyclized product with dimethyl sulfate gave the vinylogous carbonate **2.71** in 73% yield over two steps. Next, DIBAL-H mediated lactone reduction in a 1,2-fashion and upon acidic workup, provided the rearranged enone intermediate. Reduction of the carbonyl via a diastereoselective Luche reduction afforded allylic alcohol **2.72** in an excellent 77% yield over two steps. Protection of the free C-3 alcohol as its acetate followed by azidonitration to install the C-2 amine functionality gave anomeric nitrate **2.74.** For the construction of an imidate donor, p-TolSH mediated anomeric denitration and subsequent treatment with $F_3CC(NPh)Cl$ provided AAT donor **2.75**.

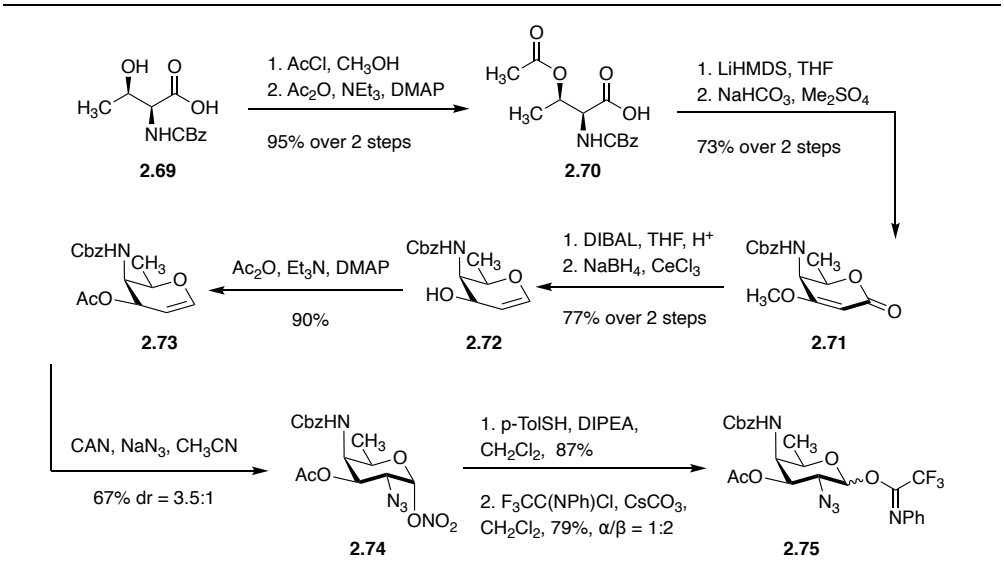

Scheme 2.6. *De novo* synthesis of orthogonally protected AAT (**2.1**) by Seeberger and co-workers.

Myer's 2016 de novo synthesis of D-desosamine acceptor 2.82 [90]

Since the characterization of D-desosamine (**2.8**) in 1962, a variety of syntheses of this monosaccharide have been reported, including three stereospecific approaches. The first reported synthesis of **2.8** was achieved by

Richardson et. al. in 1964, where the group highlighted an 8-steps approach from commercially available methyl 3-acetamido-4,6-O-benzylidene-3-deoxy-α-D-glucopyranoside. Furthermore, a *de novo* route was established in 2004 by McDonald and Davidson, who reported an 11-steps synthesis *from (R)*-3-*tert*-butyldimethylsiloxy-butanal that highlighted a key tungsten-catalyzed alkynol cycloisomerization step. More recently in 2016, Myer's *de novo* route toward a D-desosamine derivative was achieved in a mere 4 steps, making this route the most efficient and concise approach. The synthesis of D-desosamine acceptor **2.82** began with the transformation of methyl vinyl ketone (**2.76**) to a 4-nitro-2-butanone compound (**2.77**) (Scheme 2.7). Next, an enantioselective reduction step was employed that featured the Corey-Bakshi-Shibata oxazaborolidine catalyst (**2.78**) to afford the alcohol (**2.79**) in 75% yield and 87% ee. In the key step, coupling of the nitro alcohol with glyoxal (trimeric form) mediated by an aqueous solution of cesium carbonate furnished the desired crystalline sugar (**2.80**) in 50% yield after filtration. Completion of **2.8** was achieved by a sequential nitro reduction and reductive amination reaction. To access the desired donor **2.82**, a two-step protocol was implemented that consists of a benzoylation reaction to give the fully protected compound **2.81** followed by treatment with 2-mercaptopyrimidine and BF_3•OEt_2 to provide thioglycoside **2.82**.

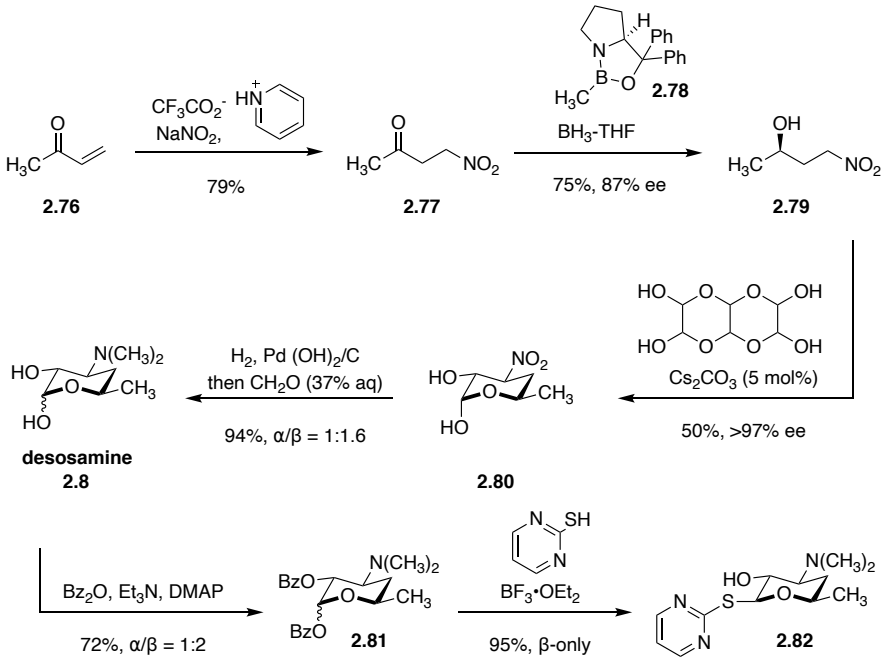

Scheme 2.7. A 4 steps *de novo* synthesis of D-desosamine by Myers and co-workers.

Schmid's 2013 de novo synthesis of DATDG[91]

Owing to the development of using L-threonine (**2.83**) as a chemical precursor for the synthesis of rare bacterial sugars, Schmid's 2013 *de novo* synthesis of DATDG demonstrated the versatility of using amino acid starting material. Their synthetic venture commenced with L-threonine (**2.83**), which proceeded through Garner's protocol to obtain aldehyde (**2.84**). Next, a nitro aldol reaction with 2-nitroacetaldehyde diethyl acetal under basic condition provided the carbon scaffold **2.85** in 74% yield. From here, subsequent nitro reduction with Raney nickel gave the free amine, which was acetylated to afford the fully protected ketal **2.86**. Global deprotection at high temperature and concurrent O to N acetate migration under aforesaid conditions directly furnished DATDG derivative **2.3** in 37% yield.

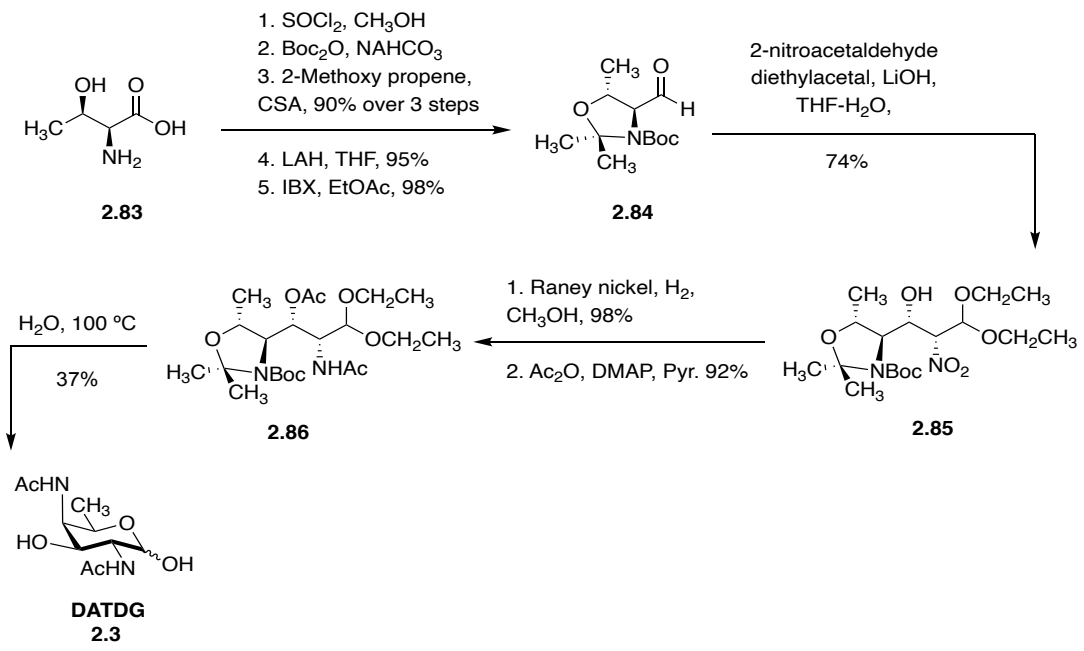

Scheme 2.8. Schmid's *de novo* synthesis of DATDG (**2.3**).

*Lowry's synthesis of methyl L-daunosamine (**2.91**) via formation of an aziridine ring*[92]

In 2006, Lowry reported an alternative approach to L-daunosamine that employed a key photo-induced acylnitrene aziridination. The synthetic route that provided access to L-daunosamine (**2.91**) is shown in Scheme 2.9. The synthesis commenced with known L-t*hreo*-hex-2-enopyranoside derivative **2.87**, which was previously prepared in 6 steps from L-rhamnose. Treatment of **2.87** under modified Bergmeir and Stanchina conditions provided the corresponding acyl azide **2.88** in an excellent 98% yield over two steps. Next, photochemical generation of an acylnitrene intermediate upon exposure to UV light provided aziridine derivative **2.89** in 74% yield. At this stage, a regioselective ring opening of the aziridine ring via hydrogenolysis with palladium on carbon furnished the desired 3,4-carbamate-protected methyl glycoside of daunosamine **2.90**. Finally, deprotection of the carbamate with barium hydroxide in water quantitatively yield methyl L-

daunosamine **2.91**.

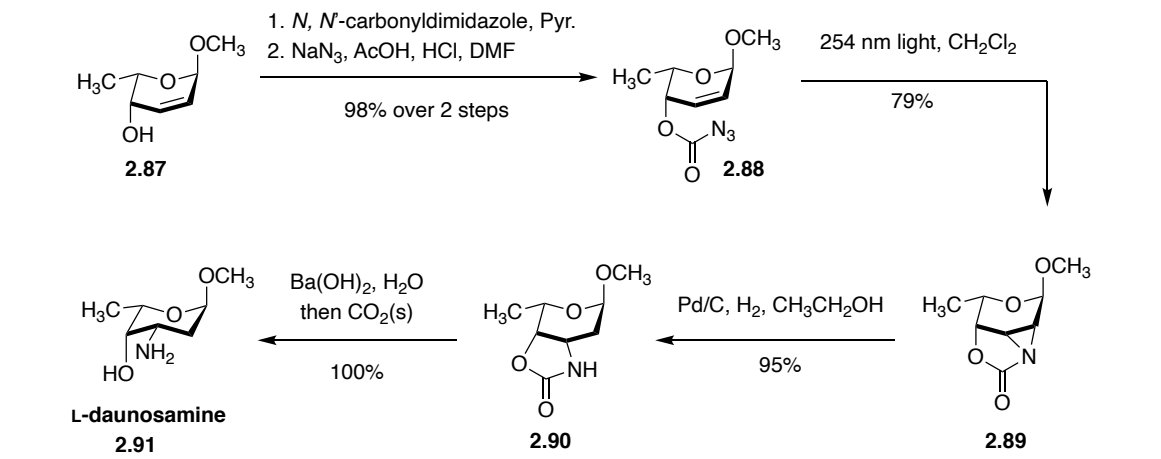

Scheme 2.9. Synthetic strategies to access L-daunosamine via formation of aziridine ring.

Seeberger's 2013 divergent de novo synthesis of orthogonally protected FucNAc, DKH, and Bac derivatives[93]

The stereoselective synthesis of deoxy-amino sugars from non-carbohydrate sources is a valuable synthetic strategy. Among the various functional groups available, aldehydes are the most frequently used, specifically Garner aldehyde. For example, the Seeberger group developed the syntheses of FucNAc, DKH, and Bac derivatives using commercially available L-Garner aldehyde **2.83** while applying chelation-controlled organometallic additions to aforesaid substrate (Scheme 2.10). Beginning with aldehyde **2.83**, reaction with propynyl magnesium bromide afforded the propargyl alcohol and subsequent selective reduction of the alkyne with Red Al provided the desired trans allylic alcohol. Exposure of this compound to *O*-alkylation conditions will afford *E*-olefin **2.84**. Furthermore, cleavage of the acetonide followed by DMP oxidation will generate aldehyde **2.85**. Upjohn dihydroxylation of **2.85** and

intramolecular cyclization gave the desired D-fucosamine derivative **2.86**. To access the DKH derivative, the free C-4 alcohol was oxidized with DMP to give DKH derivative **2.87**. Alternatively, triflation of **2.86** and inversion with azide gave D-bacillosamine derivative **2.88**. Applying this method, Seeberger and co-workers were able to selectively functionalize the **2.86** to access three different valuable deoxy-amino sugars.

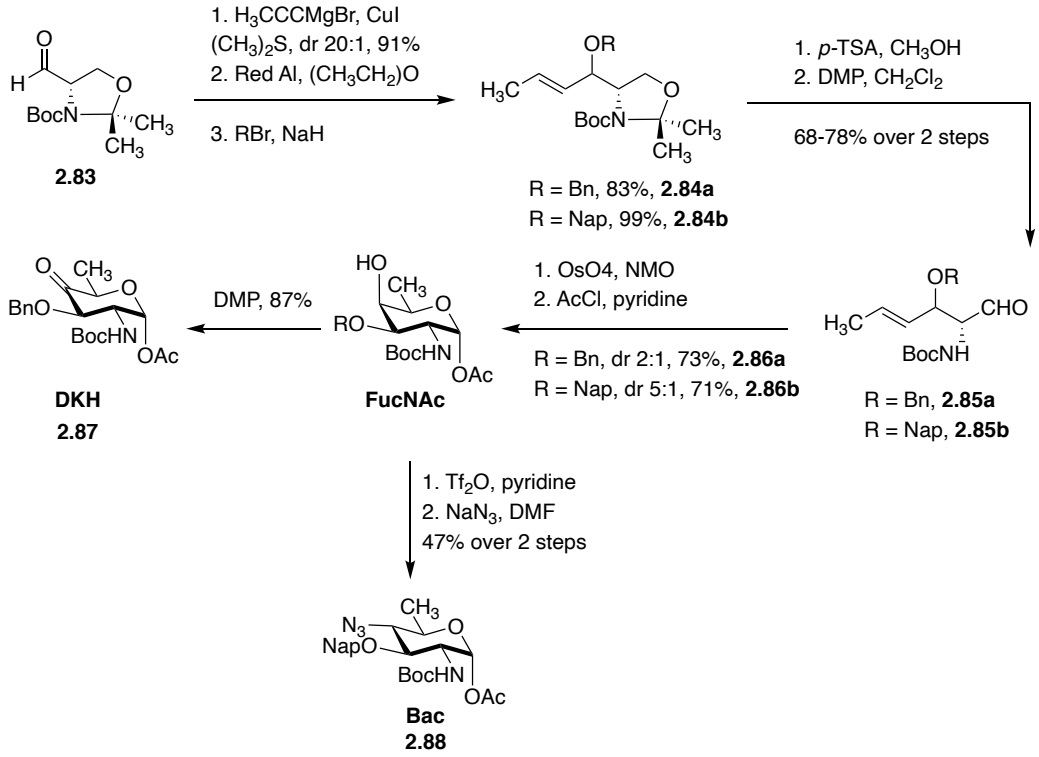

Scheme 2.10. *De novo* synthesis of FucNAc (**2.86**), DKH (**2.87**), and Bac (**2.88**) derivatives by Seeberger and co-workers.

Gao's 2021 synthesis of L-QuiNAc toward the Tetrasaccharide Haptens of Vibrio vulnificus MO6-24[94]

In their 2021 total synthesis of the tetrasaccharides haptens of *Vibrio vulnificus* MO6-24, Gao and co-workers constructed the carbon backbone of the L-QuiNAc sugar in a manner reminiscent of Kulkarni's 2016 work. They began from known β-L-thiorhamnoside **2.89**, which was treated with dimethyltin dichloride to mediate a regioselective benzoylation of the C-3 alcohol to afford alcohol **2.90** in 79% yield (Scheme 2.11). Next, **2.90** was converted to the corresponding triflate using triflic anhydride and pyridine. Substitution of the triflate with sodium azide provided orthogonally protected 2-azido-L-QuiN **2.91** in 62% yield over two steps. The author postulated that the observed β-anomeric configuration of **2.91** was key for the S_N2 reaction to occur, since the α-confirmation would have an unfavorable repulsive interaction with the thiomethyl group, and the incoming nucleophile would have a deleterious pyranosidic vicinal axial effect that would lead to decomposition of the intermediate compound. With the skeleton of **2.91** in place, further treatment with Lewis-acid and thiophene provided the desired linker-equipped monosaccharide **2.92** in 83% yield. Finally, treatment with Zemplén conditions provided the acceptor building block **2.93** an excellent 91% yield.

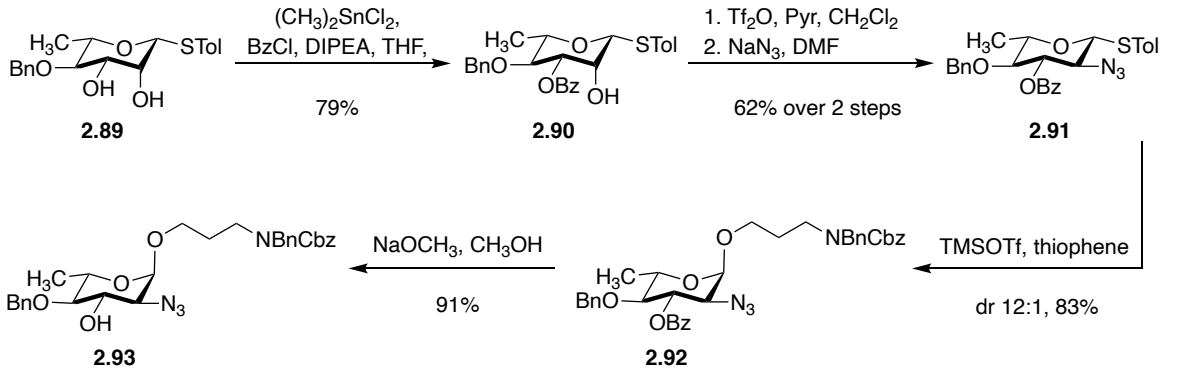

Scheme 2.11. Synthesis of L-QuiNAc acceptor (**2.93**) from L-rhamnose by Gao and co-workers.

Kulkarni's divergent synthesis of L-mycosamine, L-fucosamine, and L-quinovosamine derivatives[95]

In 2016, Kulkarni reported a divergent total synthesis of L-deoxy-amino sugars, which are virtually absent in the human metabolism and difficult to isolate in nature. This efficient and expedient methodology to access L-mycosamine, L-fucosamine, and L-quinosvosamine derivatives from readily available starting material is advantageous toward the total synthesis of complex molecules. They began from commercially available β-L-thiorhamnoside **2.94** and upon exposure to triflic anhydride and catalytic Me_2SnCl_2, regioselective triflation of the C-3 alcohol was successful (Scheme 2.12). Next, acetylation of the 2,4 alcohols and subsequent displacement with $TBANO_2$ gave 6-deoxy-l-altroside **2.95** in 40% yield over 3 steps. At this stage, triflation of the C-3 alcohol of **2.95** and concomitant displacement with azide fashioned L-mycosamine derivative **2.96** (47% over 2 steps).

Alternatively, treatment of **2.94** under a highly regioselective

monobenzoylation using Me_2SnCl_2 and benzoyl chloride provided intermediate **2.97**. For the synthesis of L-fucosamine derivative, **2.97** was treated with triflic anhydride in pyridine to give rise to 2,4-bis-triflate, which upon treatment with stoichiometric amount of tertbutyl ammonium azide in acetonitrile lead to regioselective inversion of the C-2 triflate to the corresponding alcohol. In the same pot, increasing stoichiometric amount $TBANO_2$ enable the displacement of C-4 triflate via a Lattrel-Dax reaction to afford L-fucosamine acceptor **2.98** (57% yield over 3 steps).

To this end, compound **2.97** can also be used to access L-quinovosamine through a series of three additional steps. These steps first consist of a *tert*-butyldimethyl silyl protection of the C-4 alcohol to obtain intermediate **2.99**. Similarly, a two-step inversion using triflic anhydride and sodium azide gave fruitful access to L-quinovosamine derivative **2.100**.

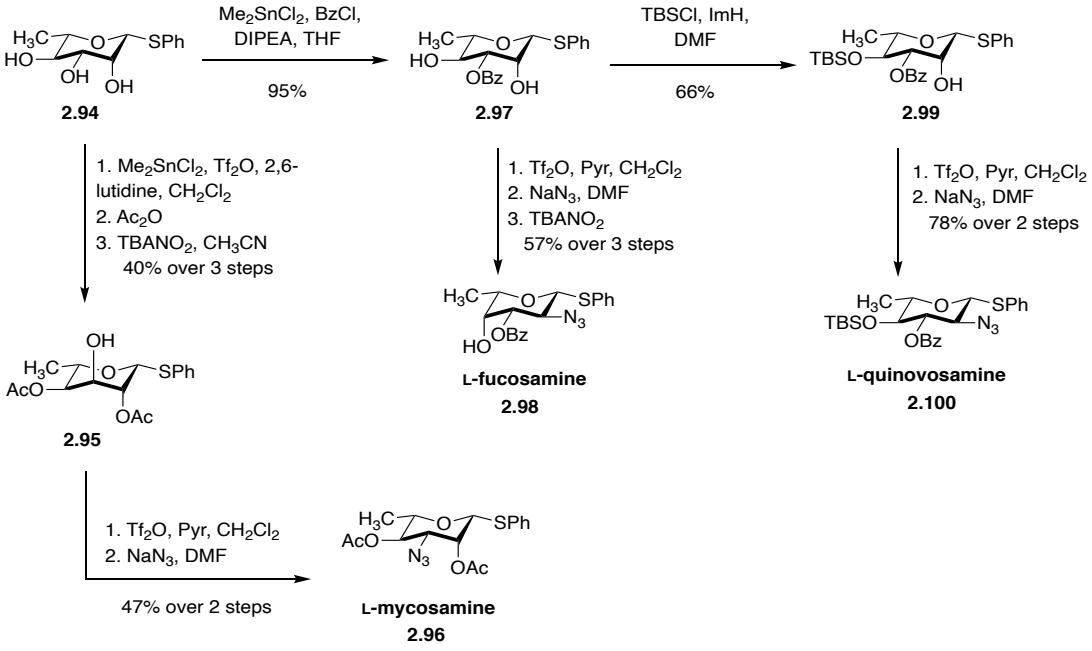

Scheme 2.12. Kulkarni's divergent synthesis of L-quinovosamine (**2.96**), L-fucosamine (**2.98**) and L-mycosamine (**2.100**) derivatives.

2.4.5 Nguyen and Townsend's 2021 Gram scale synthesis of an orthogonally protected AAT donor and acceptor [96]

In designing our synthesis of a suitable 2-acetamido-4-amino-2,4,6-trideoxy-D-galatose (AAT, **2.1**) donor and acceptor, we surveyed the literature of this particularly rare deoxy-amino sugar. We found that AAT serves as a key glycan in the structures of numerous zwitterionic polysaccharides (ZPSs) from bacteria (i.e., *Bacteroides fragilis, Photorhabdus temperata, Bacillus cereus,* and *Providencia alcalifaciens*).

As noted above (See section 2.4.3), various groups have previously synthesized AAT from either a carbohydrate source or by a *de novo* route. To this end, we envisioned that AAT derivative **2.105** would serve as an ideal intermediate target as it possesses a modifiable reducing end that can proceed through an oxidative cleavage to transform into a variety of glycosidic donors, and benzoyl removal at C-3 would provide a suitable acceptor. We were inspired by chemistry developed by the Mulard and Schmidt group that used D-glucosamine as the carbohydrate starting material. The advantage of using D-glucosamine as the requisite material consists of a pre-installed C-2 amine and ease of large-scale material throughput.

We drew inspiration for our approach from previous syntheses of AAT, as well as syntheses related to deoxy-amino sugars DATDG, D-fucosamine, and D-bacillosamine. We note that synthetic target **2.105** differs only from its nitrogen protecting at the C-2 position from chemistry employed by Schmidt in the syntheses of D-AAT acceptor. This strategic choice arose from (1) concerns that an azide at

C-2 in previous AAT syntheses would not provide the desired β-selectivity in our total synthesis pursuit of *Photorhabdus temperata* repeating unit and (2) the ability to use our key AAT building block as both an acceptor and donor, which would require a robust capping group at the anomeric position that would survive our planned synthetic route, but also can be selectively cleaved.

To implement this strategy, our synthesis of AAT donor **2.106** and acceptor **2.107** began with known triol **2.101**, available in 4 steps from commercially available D-glucosamine•HCl (**Scheme 2.13**). Next, functional group interconversion to the 6-iodo glucoside **2.102** was subsequently exposed to a $NaBH_3CN$ facilitated the desired reduction, providing **2.103** in 80% yield. With the diol in hand, regioselective benzoylation of the C-3 alcohol gave **2.104**. Having established the full carbon skeleton, our next task was to convert **2.104** to the corresponding triflate using triflic anhydride and pyridine. Substitution of the triflate with sodium azide provided the fully orthogonally protected AAT intermediate **2.105**. At this stage of the synthetic campaign, we elected to push forward to synthesize the desired AAT donor **2.106** with a 2-step sequence. First, oxidative cleavage of the *p*-methoxyphenyl ether (PMP) acetal with ceric ammonium nitrate (CAN) and conversion of the resulting alcohol to its trichloroacetimidate gave **2.106**, primarily as the α-anomer, in 70% yield.

Alternatively, we can access the desired AAT acceptor via exposure of **2.105** with sodium methoxide in methanol to obtain **2.107** in an excellent 90% yield. While this synthesis of AAT donor and acceptor is not radically different from established routes, we highlight that this synthesis is operable on gram scale and is currently

the shortest route toward AAT known in the literature.

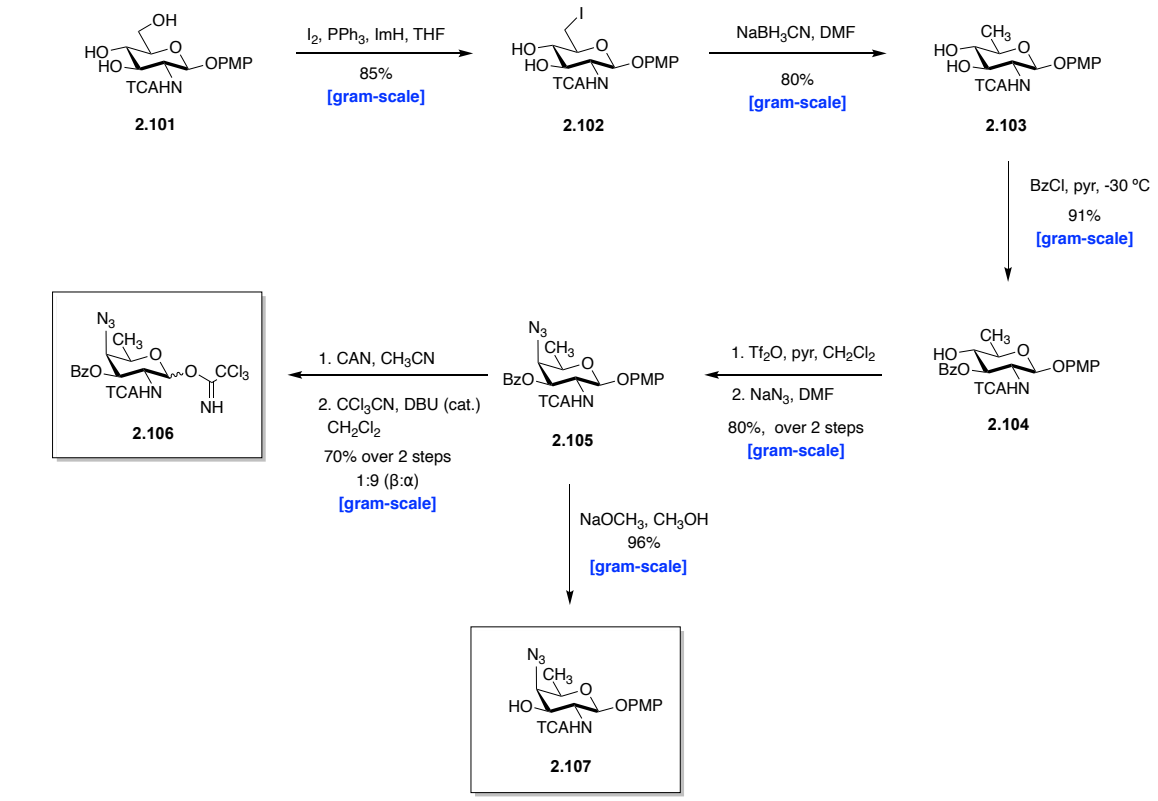

Scheme 2.13. Nguyen and Townsend's gram scale synthesis of AAT donor **2.106** and acceptor **2.107**.

2.5 Applications to total synthesis of glycoconjugates

*Seeberger's 2011 Synthesis of Bacteroides fragilis ZPS A1 Repeating Unit (**2.114**)*[88-89]

In 2011, Seeberger and co-workers reported the first total synthesis of PS A1, highlighting an elegant *de novo* approach toward the synthesis of AAT. As initial attempts to form the desired glycosidic linkage with AAT donor in a late-stage approach proved ineffective, the authors elected to implement the union of *N*-phenyl trifluoroacetimidate (**2.75**) and D-galactosamine acceptor (**2.108**) earlier, which proved to be successful (Scheme 2.14). Accordingly, **2.75** donor was activated with TMSOTf and coupled with **2.108** to form the desired disaccharide in great yields and diastereoselectivity.

Next, naphthyl cleavage and subsequent glycosylation with **2.110** followed by anomeric functional group interconversion provided trisaccharide (**2.111)**. Exposure to dimethyl(methylthio)sulfonium triflate (DMTST)/TTBP mediated glycosylation of **2.111** with acceptor **2.112** afforded the corresponding tetrasaccharide (**2.113**) in 58% yield. Finally, global deprotection was carried out over four additional steps to access tetrasaccharide repeating unit of PS A1 of *B. fragilis* **2.114**.

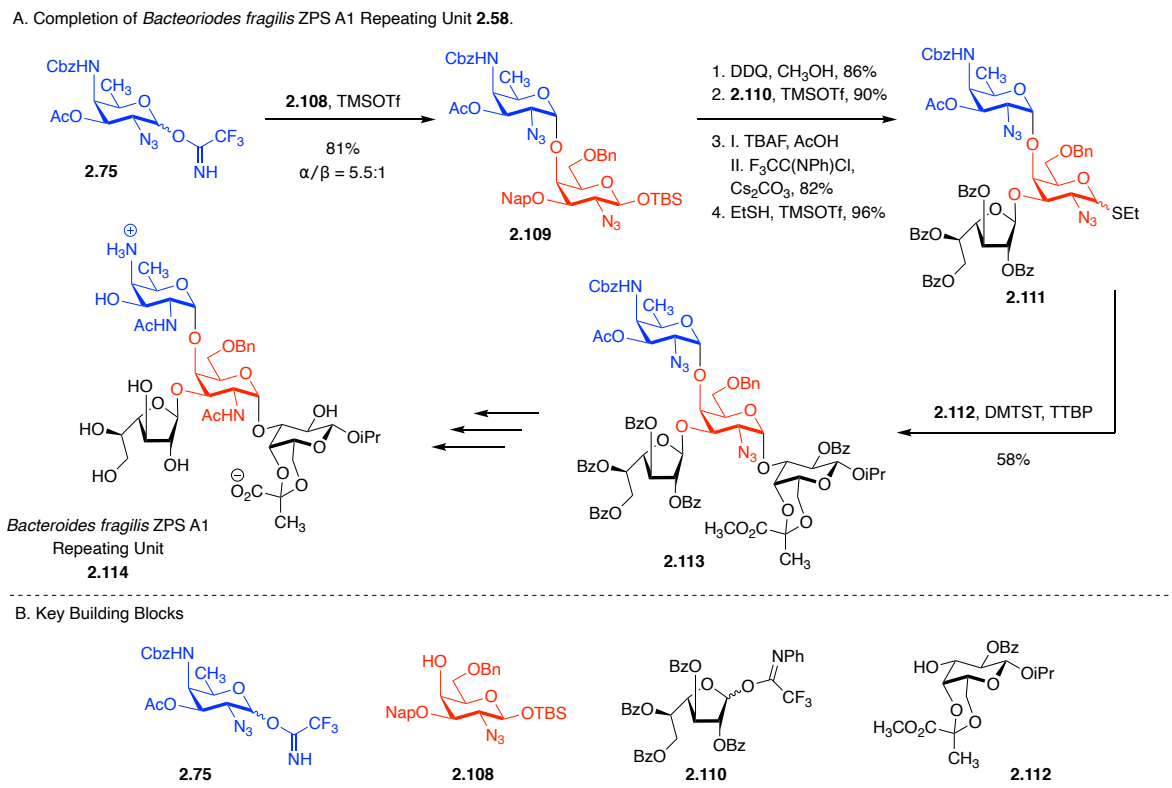

Scheme 2.14. Synthesis of PS A1 ZPS of *B. fragilis* by Seeberger and co-workers.

Adamo's 2012 Synthesis of Staphylococcus aureus type 5 repeating unit[74]

Adamo's synthesis of *Staphylococcus aureus* type 5 was completed in 2012, which featured a novel strategy for the synthesis of rare L and D-FucNAc building block. Elaborating further on this work, Adamo and co-workers employed these key pieces to complete the total synthesis of capsular polysaccharide from *Staphylococcus aureus.* Furthermore, the monumental step for this synthesis involved the formation of a required α-glycosidic bond, which was achieved by coupling of donor **2.115** with acceptor **2.68** to obtain trisaccharide **2.116** in good selectivity (α:β 2.8:1). Global deprotection of the trisaccharide **2.116** afforded the final

target compound in good yields (**Scheme 2.15**).

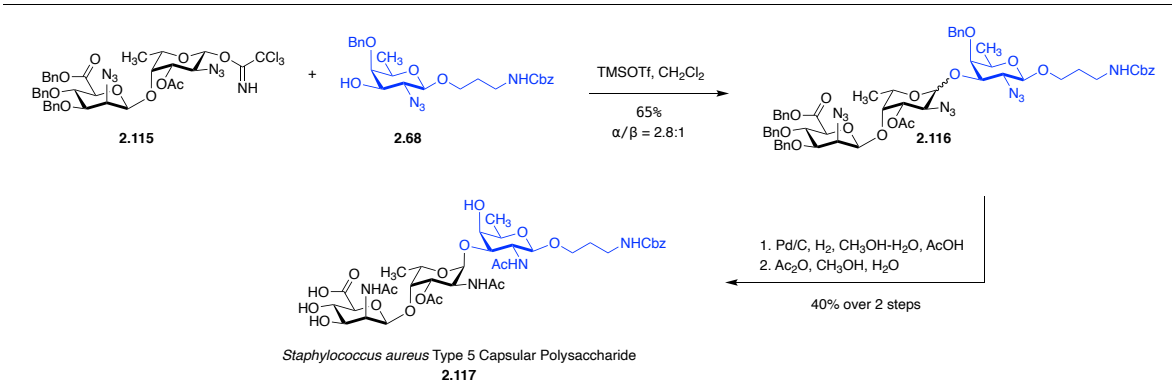

Scheme 2.15. Synthesis of the repeating unit of *S. aureus* by Adamo and co-workers.

Gao's 2021 Synthesis of Tetrasaccharide Haptens of Vibrio vulnificus MO6-24[94]

Recently, in 2021, Gao and co-workers reported the first total synthesis of *Vibrio vulnificus* MO6-24 repeating unit **2.56**, featuring the use of rare L-deoxy-amino sugar, L-QuiNAc **2.9** (Scheme 2.16). Accordingly, disaccharide **2.120** was assembled via AgOTf promoted glycosylation of thioglycoside donor **2.118** and D-galactosamine acceptor **2.119**. Next, regioselective ring opening of the benzylidene acetal upon exposure to triflic acid provided the desired free alcohol, which was subjected to another glycosylation reaction, with **2.121** to give trisaccharide **2.122**.

Oxidative cleavage of the PMP acetal, followed by conversion of the hemiacetal to the imidate donor **2.123** resulted in a 71% yield over 2 steps. Then the corresponding trisaccharide donor **2.123** was activated with TMSOTf and coupled with L-QuiNAc derivative to produce the α linked tetrasaccharide **2.124** in 82% yield. The target tetrasaccharide **2.56** was accomplished by consecutive deprotection of the functional groups.

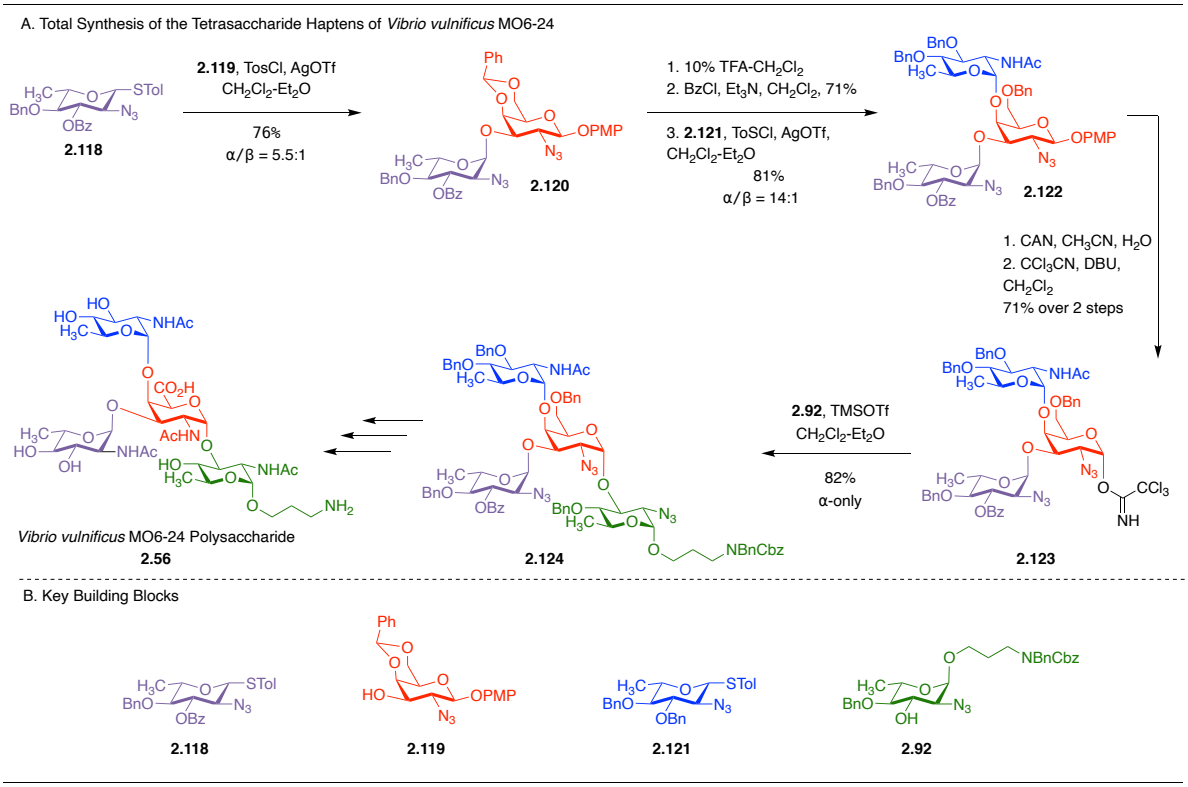

Scheme 2.16. The total synthesis of the tetrasaccharide haptens of *Vibrio vulnificus* MO6-24 by Gao and co-workers.

Kulkarni's 2016 Synthesis of Pseudomonas chloroaphis subsp. aeureofaciens Trisaccharide Repeating Unit [97]

In 2016, Kulkarni and co-workers reported the first total synthesis of *P. chloroaphis subsp. aeureofaciens* trisaccharide repeating unit **2.130**. The total synthesis of L-QuiNAc and L-FucNAc containing trisaccharide is outlined in Scheme 2.17. The major challenges for this synthesis were the construction of the L-deoxy-amino sugars **2.126** and **2.128** and the incorporation of two consecutive α linkages. Coupling of **2.125** with L-FucNAc derivative **2.126** in a stereoselective fashion gave disaccharide **2.127**. Thioglycoside **2.127** was activated by NIS and TMSOTf and coupled with acceptor **2.128** to furnish trisaccharide **2.129** in 58% with clean

selectivity. Global deprotection was done in 3 steps, involving a key reduction of the azide, followed by *N*-acetylation, then hydrogenolysis of all functional groups afforded target molecule **2.130**.

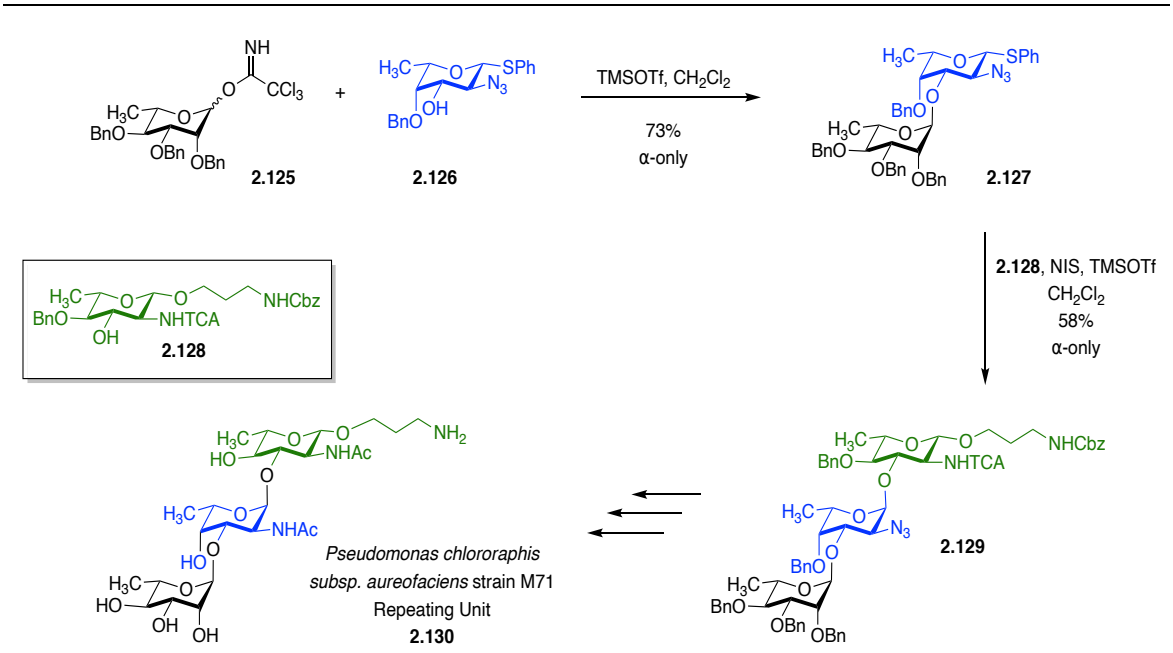

Scheme 2.17. The total synthesis of *Pseudomonas chlororaphis subsp. aureofaciens* repeating unit by Kulkarni and co-workers.

2.6 Nguyen and Townsend's 2021 Total Synthesis of Aeromonas veronii strain Bs8 OPS Repeating Unit

The *Aeromonas* family of gram-negative bacteria is dispersed among freshwater environments and soils, where they are symbionts of zebrafish, mussel, and leech.[98-99] More recently, there has been an increase in *Aeromonas* related research due to the relevance in both veterinarian and human health. Pertaining to human health, *Aeromonas* species are associated with wound infections, gastroenteritis, and sepsis – bacterial blood poisoning. It is important to mention that *Aeromonas* species were the leading cause of skin and soft tissue infections found among the 2004 tsunami survivors in Thailand. [100-103]

In particular, the pathogenesis of *Aeromonas* species includes a series of virulence factors including extracellular enzymes, flagella, and toxins. Moreover, cell surface lipopolysaccharides (LPS) are a key contributor to virulence by interacting with eukaryotic cells.[104-106] For instance, an *O*-specific polysaccharides regulates strain immunospecificity and is the basis for their serological classification.[107-115] While the biological activity of many of these *O*-specific polysaccharides is noteworthy, it is truly their chemical complexity that piqued our interest as synthetic targets.

Herein, we describe the first total synthesis of *A.veronii strain Bs8* disaccharide repeating unit **2.131**, which features the deoxy-amino sugar, D-galactosamine.[116] The major challenges in the synthesis of the disaccharide **2.131** is the formation of the requisite 1,2-cis linkage. Regardless of the conditions, forming glycosidic bonds to C-3 of GalNac with absolute stereocontrol is often

problematic.[117-119] While not achieving complete diastereocontrol, we have had success in forming the desired 1,2 cis linkage by leveraging the equatorial donating effects of thiophene as an addictive, as well as relied on solvent assisted glycosylation conditions to bring our synthetic route to completion.[117] For an efficient and convergent synthesis of disaccharide **2.132**, we envisaged that D-fucose[120] donor could be accessed in 4 steps and D-galactosamine[121] acceptor can acquired in 5 steps from known literature precedent.

In the forward direction, building block synthesis started from D-fucose, which was peracetylated resulting in near quantitative yield. Exposure of the anomeric acetate with ethanethiol and BF_3•OEt_2 gave thioglycoside **2.137**. Lastly, to arm the donor, and to enable a more facile deprotection sequence, all acetates were substituted for electron releasing benzyl ethers. For the GalNAc piece, we first masked the acetamide as its trichloro-derivative using previous chemistry developed in the group. Next, peracetylation provided compound **2.139** in excellent yield (80% over 2 steps). From here, the anomeric acetate was exchanged for a PMP acetal under Lewis acidic conditions to give **2.140**, exclusive as the α-anomer. Saponification of **2.140** and treatment with benzylaldehydedimethylacetal afforded acceptor **2.134** in 75% over two steps. Having access to both key building blocks, we next evaluated the best conditions to yield the best diastereoselectivity. Upon initial screen with select conditions, we found that glycosylation with diethyl ether as the solvent provided the most favorable selectivity and yield. With the fully protected disaccharide in hand, exhaustive hydrogenolysis provided the repeating unit (as its reducing end PMP-acetal) in 85%. This final key reaction removed three benzyl

ethers, one single benzylidiene acetal, and converted the trichloroacetamide to its acetamide. The spectral data for the final compound showed homology with published characterization data for the native polymer.

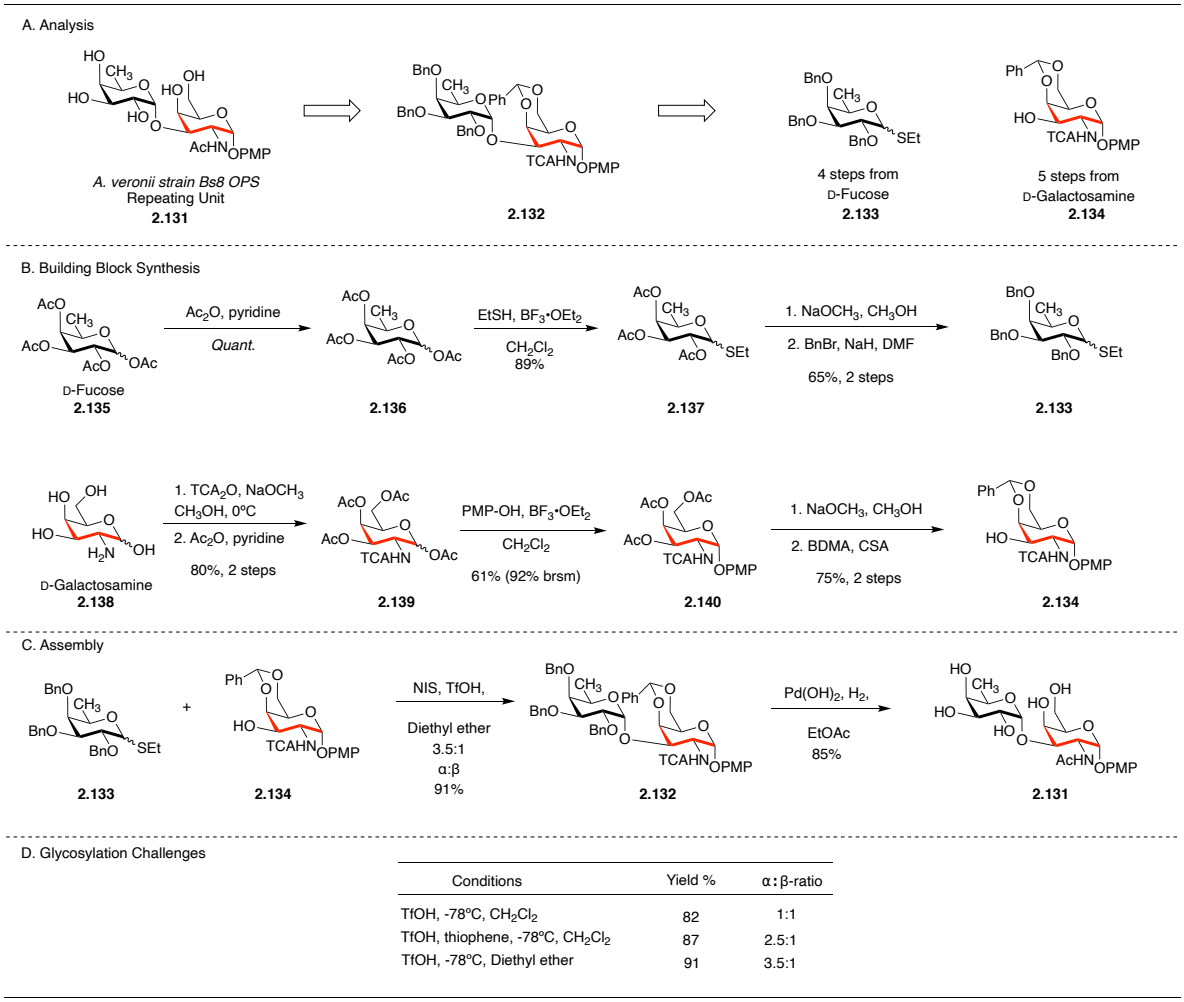

Conditions	Yield %	α:β-ratio
TfOH, -78°C, CH_2Cl_2	82	1:1
TfOH, thiophene, -78°C, CH_2Cl_2	87	2.5:1
TfOH, -78°C, Diethyl ether	91	3.5:1

Scheme 2.18. The total synthesis of the *A. veronii* strain Bs8 disaccharide repeating unit.

2.7 Conclusion

In this chapter, we described the biosynthesis, chemical synthesis, and application of bacterial deoxy-amino sugars in total synthesis. Our goal in this chapter was to provide the reader with a brief overview of known protocols to synthesize both D and L- deoxy-amino sugars and disclose our efforts to the synthesis of the widely studied glycan, AAT. Furthermore, we described the first total synthesis of the *Aeromonas veronii* strain Bs8 disaccharide repeating unit, which contains a D-galactosamine derivative as part of the core structure.

2.8 References

1. Chaudhury, A.; Ghosh, R. A target oriented expeditious approach towards synthesis of a certain bacterial rare sugar derivatives. *Org. Biomol. Chem.* **2017**, *15*, 1444.

2. Dube, D. H.; Champasa, K.; Wang, B. Chemical tools to discover and target bacterial glycoproteins. *Chem. Commun*. **2011**, *47*, 87-101.

3. Emmadi, M.; S. Kulkarni. Recent Advances in Synthesis of Bacterial Rare Sugar Building Blocks and Their Applications. *Natural Products Reports*. **2014**, *31*, 870-879.

4. Longwell, S. A.; Dube, D. H. Deciphering the bacterial glycocode: recent advances in bacterial glycoproteomics. *Curr. Opin. Chem. Biol.* **2013**, **17**, 41-48.

5. Adibekian, A; Stallforth, P.; Hecht, M.-L.; Werz, D. B. Gagneux, P.; Seeberger, P.H. Comparative bioinformatics analysis of the mammalian and bacterial glycomes. *Chem. Sci.* **2011**, *2*, 337-344.

6. Wilkinson, S. G. Bacterial lipopolysaccharides—themes and variations. *Prog. Lipid. Res.* **1996**, *35*, 283-343.

7. Kenne, L.; Lindberg, N.; Petersson, K.; Katzenellenbogen, E.; Romanowska, E. Structural studies of the *O*-specific side chains of the *shigella sonnei* phase 1 lipopolysaccharide. *Carbohydr. Res.* **1980**, *78*, 119-116.

8. Lindberg, B.; Lingqvist, B.; Lonngren, J.; Power, D. A. Structural studies of the capsular polysaccharide from streptococcus pneumoniae type 1. Carbohydr. Res. 1980, 78, 111-117.

9. Baumann, H.; Tzianabos, A. O.; Brisson, J. -R.; Kasper, D. L.; Jennings, H.J. Structural elucidation of two capsular polysaccharide from one strain of *Bacteroides fragilis* using high-resolution NMR spectroscopy. *Biochemistry.* **1992**, *31*, 4081-4089.

10. Castric, P.; Cassels, F. J.; Carlson, R. W. Structural characterization of the *Pseudomonas aeruginosa* 1244 pilin glycan. *J. Biol. Chem.* **2001**, *276*, 26479-26485.

11. Stimson, E.; Virji, M.; Makepeace, K.; Dell, A.; Morris, H. R.; Payne, G.; Saunders, J. R.; Jennings, M. P.; Barker, S.; Panico, M.; Blench, I.; Moxon, E.R. Meningococcal pilin: a glycoprotein substituted with digalactosyl 2,4-diacetamido-2,4,6-trideoxyhexose. *Mol. Microbiol.* **1995**, *17*, 1201-1214.

12. Simemieniuk, R. A. C.; Gregson, D. B.; Gill, M. J. The persisting burden of invasive pneumococcal disease in HIV patients: an observational cohort study *BMC Infect. Dis.* **2011**, *11*, 314-321.

13. Young, N. M.; Brisson, J.-R.; Kelly, J.; Watson, D. C.; Tessier, L.; Lantheir, P. H.; Jarell, H. C.; Cadotte, N.; St. Michael, F.; Aberg, E.; Szymanski, M. Structure of the N-linked glycan present on multiple glycoproteins in the Gram-negative bacterium, Campylobacter jejuni. *J. Biol. Chem.* **2002**, *276,* 26479-26485.

14. Rinaudo, M. Chitin and chitosan: Properties and applications. *Progress in Polymer Science.* **2006**, *31*, 603-632.

15. Kuehl Jr., F. A.; Flynn, E. H.; Holly, F. W.; Mozingo, R.; Folkers, K. Streptomyces Antibiotics V. N-Methyl-l-Glucosamine from Streptomycin. *J. Am. Chem. Soc.* **1946**, *68*, 3, 536.

16. Candy, D. L.; Blumsom, N. L.; Baddiley, J. The biosynthesis of streptomycine. Incorporation of ^{14}C-labelled compounds into streptose and N-methyl-L-glucosamine. *Biochem. J.* **1964**, *91*, 31-35.

17. Peters, W. Occurrence of chitin mollusa. *Comp. Biochem. Physiol.* **1972**, *41*, 541-550.

18. Sugahara, K.; Schwartz, N. B.; Dorfman, A.; Biosynthesis of Hyaluronic Acid by Streptococcus. *J. Biol. Chem.* **1979**, *254*, 6252-6261.

19. Zehavi, U.; Sharon, N.; Structural Studies of 4-Acetamido-2-amino-2,4,6-trideoxy-D-glucose (*N*-Acetyl-bacillosamine), the *N*-Acetyl-diamino Sugar of *Bacillus licheniformis*. J. *Biol. Chem.* **1972**, *248*, 433-438.

20. Liav, A.; Hildesheim, J. Zehavi, U.; Sharon, N. Synthesis of 2,4-diacetamido-2,4,6-trideoxy-D-glucose and its identification with the diacetamido-sugar of *Bacillus licheniformis. J. Chem. Soc. Chem. Commun.* **1973***,* 668-669.

21. Umezawa, S.; Umino, K. Shibahara, S.; Omoto, S. Studies of Aminosugars. XVII. Production of 3-Amino-3-deoxy-D-glucose by Bacillus Species. *Bull. Chem. Soc. Jpn.* **1967***, 40,* 2419-2421.

22. Cron, M. J.; Evans, D. L.; Palermiti, F. M.; Whitehead, D. F.; Hooper, I. R.; Chu, P.; Lemieux, R. U. Kanamycin. V. The Structure of Kanosamine. *J. Am. Chem. Soc.* **1958**, *80*, 4741-4742.

23. Watanabe, T. Studies on leucomycin. IV. Isolation of mycaminose from the acid hydrolysate. *Bull. Chem. Soc. Jpn.* **1961**, *34*, 15-18.

24. Fly, E. H.; Sigal Jr., M. V.; Wiley, P. F.; Gerzon, K. Erythromycin. I. Properties and Degradation Studies. *J. Am. Chem. Soc.* **1954**, *76*, 3121-3131.

25. Newman, H. Degradation and Synthesis of Desosamine. *J. Org. Chem.* **1964**, *29*, 1461-1468.

26. Duckworth, M.; Archibald, A. R.; Baddiley, J. The location of *N*-acetylgalactosamine in the walls of *Bacillus subtilis* 168. *Biochem. J.* **1972**, *130*, 691-696.

27. Janczura, E.; Perkin, H. R.; Rogers, H. J. Teichuronic acid: a mucopolysaccharide present in wall preparations from vegetative cells of *Bacillus subtilis*. *Biochem. J.* **1961**, *80*, 82-93.

28. Sharon, N.; Shif, I.; Zehavi, U.; The isolation of D-fucosamine (2-amino-2, 6-dideoxy-D-galactose) from polysaccharides of *Bacillus*. *Biochem. J*. **1964,** *93*, 210-214.

29. Aono, R.; Uramoto, M. Presence of fucosamine in teichuronic acid of the alkalophilic *Bacillus* strain C-125. *Biochem. J.* **1986**, *233*, 291-294.

30. Horton, D.; Rodemeyera, G.; Saeki, H. A synthesis of 2-acetamido-2,6-dideoxy-D-galactose (N-acetyl-D-fucosamine). *Carbohydr. Res.* **1977**, *59,* 607-611.

31. Comb, D. G.; Roseman, S. Composition and enzymatic synthesis of N-acetylneuraminic acid (sialic acid). *J. Am. Chem. Soc.* **1958**, *80*, 497-499.

32. von Saltza, M.; Dutcher, J. D.; Reid, J.; Wintersteiner, O. Nystatin. IV. The Stereochemistry of Mycosamine. *J. Org. Chem.* **1963**, *27*, 999-1004.

33. Dutcher, J. D.; Walter, D. R., Wintersteiner, O. Nystatin. III. Mycosamine: Preparation and Determination of Structure. *J. Org. Chem.* **1963**, *28*, 995-999.

34. Lee, C. -H.; Schaffner, C. Perimycin: Chemistry of perosamine. *Tetrahedron Lett.* **1966,** *47,* 5837-5840.

35. Els, M. J.; Ganem, B. An improved synthesis of D-perosamine and some derivatives. *Carbohydr. Res.* **1988**, *176*, 316-323.

36. Rivett, R. W.; Peterson, W. H. Streptolin, a New Antibiotic from a Species of Streptomyces. *J. Am. Chem. Soc.* **1947**, *69*, 3006-3009.

37. Van Tamelen, E. E.; Dyer, J. R.; Whaley, H. A.; Carter, H. E. Whitfield Jr., G. B. Constitution of the streptolin-streptothricin group of Streptomyces antibiotics. *J. Am. Chem. Soc.* **1961**, *83*, 4295-4296.

38. Crumpton, M. J. Separation of Talosamine form other 2-Amino Hexoses. *Nature.* **1957**, *180*, 605-606.

39. Waller, C. W.; Fryth, P. W.; Hutchings, B. L.; Williams, J. H. Achromycin. The Structure of the Antibiotics Puromycin. *J. Am. Chem Soc*. **1953**, *75*, 2025.

40. Baker, B. R.; Schaub, R. E.; Jospeh, J. P. Puromycin. Synthetic Studies. II. The Position of Glycosylation of the 6-Dimethylaminopurine Moiety. *J. Org. Chem.* **1954,** *19,* 638-645.

41. Redmond, J. W. The 4-amino sugars present in the lipopolysaccharides of Vibrio cholerae and related vibrios. *Biochem. Biophys. Acta.* **1978**, *542*, 378-384.

42. Trefzer, A.; Salas, J. A.; Bechthold, A. Genes and enzymes involved in deoxysugar biosynthesis in bacteria. *Nat. Prod. Rep.* **1999**, *16*, 283-299.

43. Laurent, T. C.; Laurent, U.B. G.; Fraser, J. R. E. The structure and function of hyaluronan: An overview. *Immunol. Cell. Biol.* **1996,** *74*, A1-A7.

44. Elieh-Ali-Komi, Daniel.; Hamblim, M. R. Chitin and Chitosan: Production and Application of Versatile Biomedical Nanomaterials. *Int J Adv Res*. **2016**, 4(3), 411-427.

45. Burgie, E. S.; Thoden, J. B.; Holden, H. M. Molecular architecture of DesV from *Streptomyces venezuelae*: A PLP-dependent transaminase involved in the biosynthesis of the unusual sugar desosamine. *Protein Sci.* **2007,** *16*, 887-896.

46. Burgie, E. S.; Holden, H. M. Three-Dimensional Structure of DesVI from *Streptomyces venezuelae*: A Sugar *N*,*N*-Dimethyltransferase Required for dTDP-Desosamine Biosynthesis. *Biochemistry* **2008**, *47*, 3982-3988.

47. Cook, P. D.; H. M. Holden. GDP-Perosamine Synthase: Structural Analysis and Production of a Novel Trideoxysugar. *Biochemistry* **2008**, *47*, 2833-2840.

48. Nedal, A.; Sletta, H.; Brautaset, T.; Borgos, S. E. F.; Sekurova, O. N.; Ellingsend, T. E., Zotchev, S. B. Analysis of the Mycosamine Biosynthesis and Attachment Genes in the Nystatin Biosynthetic Gene Cluster of *Streptomyces noursei* ATCC 11455. *Appl. Environ. Microbiol.* **2007**, *73*, 7400-7407.

49. Nedal, A.; Zotchev. Biosynthesis of deoxyaminosugars in antibiotics-producing bacteria. *Appl. Microbiol. Biotechnol*. **2004**, *64*, 7-15.

50. Sharbek, K.; Milewska, M. J. Biosynthetic and synthetic access to amino sugars. *Carbohydr. Res.* **2016**, *434*, 44-71.

51. Durand, P.; Golinelli-Pimpaneau, B.; Mouilleron, S.; Badet, B.; Badet-Denisot, M.-A. Highlights of glucosamine-6P synthase catalysis. *Arch. Biochem. Biophys.* **2008**, *474*, 302-317.

52. Thibodeaux, C. J.; Melancon, C. E.; Liu, H.-w. Unusual sugar biosynthesis and natural product glycodiversification. *Nature*, **446**, 1008-1016.

53. Thibodeaux, C. J.; Melancon, C. E.; Liu, H.-w. Natural product sugar biosynthesis and enzymatic glycodiversification. *Angew. Chem. Int. Ed.* **2008**, *47*, 9814-9859.

54. Vara, J. A.; Hutchinson, C. R. Purification of thymidine-dipho-spho-D-glucose 4,6-dehyratase from an erythromycin-producing strain of *Saccharopolyspora erythraea* by high resolution liquid chromatography. *J. Biol. Chem.* **1988**, *263*, 14992-14995.

55. Gandecha, A. R.; Large, S. L.; Cundliffe, E. Analysis of four tylosin biosynthetic genes from the tylLM region of the *Streptomyces fradiae* genome. *Gene*. **1997**, *184*, 197-203.

56. Mertz, F. P. *Actinomadura fibrosa* sp. Nov. isolates from soil. *Int. J. Syst. Bacteriol.* **1990,** *40*, 28-33.

57. Aparicio, J. F. Caffrey, P.; Gil, J. A., Zotchev, S. B. Polyene antibiotics biosynthesis gene clusters. *Appl. Microbiol. Biotechnol.* **2003**, *61*, 179-188.

58. Reeves, P. R.; Hobbs, M.; Valvano, M. A.; Skurnik, M.; Whifield, C.; Coplin, D.; Kido, N.; Klena, J.; Maskell, D.; Raetz, C. R.; Rick, P. D. Bacterial polysaccharide synthesis and gene nomenclature. *Trends. Micrbiol.* **1996**, *4*, 495-503.

59. Tra, V. N.; Dube, D. H. Glycans in pathogenic bacteria – potential for targeted covalent therapeutics and imaging agents. *Chem. Commun*. **2014**, *50*, 4659.

60. Vaithinathan, A. G.; Vanitha, A. WHO global priority pathogens list on antibiotic resistance: an urgent need for action to integrate One Health data. *Perspect Public Health.* **2018**, *138*(2), 87-88.

61. Auer, G. K.; Weibel, D. B. Bacterial Cell Mechanics. *Biochemistry* **2017**, *56*(29), 3710-3724.

62. Mulrooney, E.F.; Poon, K.K.; McNally, D.J.; Brisson, J.R.; Lam, J.S. Biosynthesis of UDP-N-acetyl-L-fucosamine, a precursor to the biosynthesis of lipopolysaccharide in Pseudomonas aeruginosa serotype O11. *J Biol Chem.* **2005,** *280*(20),19535-42.

63. Emmadi, M.; Kulkarni, S. S. Total synthesis of the bacillosamine containing α-L-serine linked trisaccharide of *Neisseria meningitidis. Carbohydr. Res.* **2014**, *399*, 57-63.

64. Busca, P.; Martin, O. R. Synthesis of UDP-GalNAc analogues as probes for the study of polypeptide-α-GalNAc-transferases. Part 2. *Tetrahedron Lett*. **2004**, *45*, 4433-4436.

65. Zehavi, U.; Sharon, N. Two Related Syntheses of 2-Amino-2,6-dideoxy-D-galactose (D-Fucosamine). *J. Org. Chem*. **1964**, *29*, 3654-3658.

66. Perry, M.; Oust, V. The Methyl Ethers of 2-Amino-2,6-dideoxy-D-galactopyranose (D-Fucosamine). *Can. J. Chem.* **1974**, *52*, 3251-3255.

67. Horton, D.; Rodemeyer, G.; Saeki, H. A synthesis of 2-acetamido-2,6-dideoxy-D-galactose (N-acetyl-D-fucosamine). *Carbohydr. Res*. **1977**, *59*, 607-611.

68. Jones, G. B.; Lin, Y.; Xiao, Z.; Kappen, L.; Goldberg, I. H. Molecular probes of DNA bulges: Functional assay and spectroscopic analysis. *Bioorg. Med. Chem.* **2007**, *15*, 784-790.

69. Burger, P. J.; Nashed, M. A.; Anderson, L. A convenient preparation of 2-acetamido-2,6-dideoxy-d-glucose, some of its alkyl glycosides, and allyl 2-acetamido-2,6-dideoxy-α-d-galactopyranoside. *Carbohydr. Res.* **1983**, *119*, 221-230.

70. Szabo, P.; Charon, D. Synthesis of 2,6-dideoxy-2-(N-methylacetamido)-d-galactose (N-acetyl-N-methyl-d-fucosamine) and of derivatives suitable for 3-O- or 4-O-glycosylation. *Carbohydr. Res.* **1994**, *257*, 145-153.

71. Horton, D.; Saeki, H. Conversion of 2-acetamido-2-deoxy-d-glucose into 2-acetamido-2,6-dideoxy-d-galactose (N-acetyl-d-fucosamine) and its benzyl-3-O-benzyl glycosides. *Carbohydr. Res*. **1978**, *63*, 270-276.

72. Illarionov, P. A.; Torgov, I.; Hancock, I. I.; Shibaev, V. N. A novel synthesis of N-acetyl-α-d-fucosamine 1-phosphate and uridine 5"-diphospho-N-acetyl-α-d-fucosamine. *Russ. Chem. Bull. Int. Ed.* **2001**, *50*, 1303-1308.

73. Carreira, E. M.; Hong, J.; Du Bois, J.; Tomooka, C. S. The application of nitride manganese reagents to the synthesis of protected. *Pure. Appl. Chem.* **1998**, *70*, 1097-1103.

74. Danieli, E.; Proietti, D.; Brogioni, G.; Romano, M. R.; Cappelletti, E.; Tontini, M.; Berti, F.; Lay, L.; Costantino, P.; Adamo, R. Synthesis of *Staphylococcus aureus* type 5 capsular polysaccharide repeating unit using novel L-FucNAc and D-FucNAc synthons and immunochemical evaluation. *Bioorg. Med. Chem.* **2012,** *20*, 6403-6415.

75. Bedini, E.; Esposito, D.; Parrilli, M. A Versatile Strategy for the Synthesis of *N*-Acetyl-bacillosamine-Containing Disaccharide Building Blocks Related to Bacterial O-Antigens. *Synlett.* **2006***, 6,* 825-830*.*

76. Liav, A.; Hildesheim, J.; Zehavi, U.; Sharon, N. Synthesis of 2-acetamido-2,6-dideoxy-D-glucose (*N*-acetyl-D-quinovosamine), 2-acetamido-2,6-dideoxy-D-galactose (*N*-acetyl-D-fucosamine), and 2,4-diacetamido-2,4,6-trideoxy-D-glucose from 2-acetamido-2-deoxy-D-glucose. *Carbohydr. Res.* **1974**, *33*, 217-227.

77. Bundle, D.; Josephson, S. Chlorosulphation of amino sugars: synthesis of methyl 2-acetamido-4-amino-2,4,6-trideoxy-β-D-glucopyranoside (bacillosamine) from a D-glucosamine derivative. *Can. J. Chem.* **1980**, *58*, 2679-2685.

78. Amin, M. N.; Ishiwata, A.; Ito, Y. Synthesis of asparagine-linked bacillosamine. *Carbohydr. Res.* **2006***, 341,* 1922-1929.

79. Liav, A.; Jacobsen, I.; Sheinblatt, M.; Sharon, N. Synthesis of 2,4-diacetamido-2,4,6-trideoxy-D-galactose. *Carbohydry. Res.* **1978**, *66*, 95-101.

80. Lonn, H.; Lonngren, J. Synthesis of a disaccharide component of the capsular polysaccharide antigen of *Streptococcus pneumoniae* type 1. *Carbohydr. Res.* **1984***, 132,* 39-44.

81. Medgyes, A.; Farkas, E.; Liptak, A.; Pozsgay, V. Synthesis of the monosaccharide units of the O-specific polysaccharide of *Shigella sonnei*. *Tetrahedron* **1997***, 53,* 4159-4178.

82. Liang, H.; Grindley, T. B. An Efficient Synthesis of Derivatives of 2-Acetamido-4-amino-2,4,6-trideoxy-D-galactopyranose. *J. Carbohydr. Chem.* **2004***, 23,* 71-82.

83. Cai, Y.; Ling, C. C.; Bundle, D. R. Concise and Efficient Synthesis of 2-Acetamido-2-deoxy-β-D-hexopyranosides of Diverse Aminosugars from 2-Acetamido-2-deoxy-β-D-glucose. *J. Org. Chem.* **2009**, *74,* 580-589.

84. Pederson, C. M.; Figueroa-Perez, I.; Boruwa, J.; Lindner, B.; Ulmer, A. J.; Zahringer, U.; Schmidt, R. R. Synthesis of the Core Structure of the

Lipoteichoic Acid of *Streptococcus pneumoniae. Chem. Eur. J.* **2010***, 16,* 12627-12641.

85. Pedersen, C. M.; Figuoroa-Perez, I.; Lindner, B.; Ulmer, A. J.; Zahringer, U.; Schmidt, R. R. Total Synthesis of Lipoteichoic Acid of *Streptococcus pneumoniae. Angew. Chem. Int. Ed.* **2010***, 49,* 2585-2590.

86. Hermans, J. P. G.; Elie, C. J. J.; van der Marel. G. A.; van Boom, J. H. Benzyl-2, 4-Diacetamido-2, 4, 6-Tri-Deoxy-α (β)-D-Galactopyranoside. *J. Carbohydr. Chem.* **1987***, 6,* 451-462.

87. Smid, P.; Jorning, W. P. A.; van Duuren, A. M. G.; Boons, G. J. P. H.; van der Marel, G. A.; van Boom, J. H. Stereoselective Synthesis of a Dimer Containing an α-Linked 2-Acetamido-4-Amino-2,4,6-Trideoxy-D-Galactopyranose (Sug*p*) Unit. *J. Carbohydr. Chem.* **1992***, 11,* 849-865.

88. Pragani, R.; Stallforth, P.; Seeberger, P. H. De Novo Synthesis of a 2-Acetamido-4-amino-2,4,6-trideoxy-D-galactose (AAT) Building Block for the Preparation of a *Bacteroides fragilis* A1 Polysaccharide Fragment**.** *Org. Lett.* **2010**, *12*, 1624-1627.

89. Pragani, R.; Seeberger, P. H. Total Synthesis of the *Bacteroides fragilis* Zwitterionic Polysaccharide A1 Repeating Unit**.** *J. Am. Chem. Soc.* **2011**, *133*, 102-107.

90. Zhang, Z.; Fukuzaki, T.; Myers, A. G. Synthesis of d-Desosamine and Analogs by Rapid Assembly of 3-Amino Sugars. *Angew. Chem. Int. Ed.* **2016**, *55,* 523 –527.

91. Schmölzer, C.; Nowikow, C.; Kählig, H.; Schmid, W. Gram scale de novo synthesis of 2,4-diacetamido-2,4,6-trideoxy-D-galactose. *Carbohydr. Res.* **2013**, *367*, 1-4.

92. Mendlik, M. T.; Tao, P.; Hadad, C. M.; Coleman, R. S.; Lowary, T. L. Synthesis of l-Daunosamine and l-Ristosamine Glycosides via Photoinduced Aziridination. Conversion to Thioglycosides for Use in Glycosylation Reactions. *J. Org. Chem.* **2006**, *71*(21), 8059-8070.

93. Leonori, D.; Seeberger, P. H. *De Novo* Synthesis of the Bacterial 2-Amino-2,6-Dideoxy Sugar Building Blocks D-Fucosamine, D-Bacillosamine, and D-Xylo-6-deoxy-4-ketohexosamine. *Org. Lett.* **2012**, *14*, 4954- 4957.

94. Zhang, H.; Wang, X.; Meng, Y.; Yang, X.; Zhao, Q.; Gao, J. Total Synthesis of the Tetrasaccharide Haptens of *Vibrio vulnificus* MO6-24 and BO62316 and Immunological Evaluation of Their Protein Conjugates. *JACS Au.* **2022**, *2(*1), 97-108.

95. Sanapala, S. R.; Kulkarni, S. S. Expedient Route To Access Rare Deoxy Amino l-Sugar Building Blocks for the Assembly of Bacterial Glycoconjugates. J. Am. Chem. Soc. ***2016,*** 138 *(14), 4938-4947.*

96. Nguyen, J. M.; Townsend, S. D. Total Synthesis of the *Photorhabdus temperata* ssp. Cinereal 3240 Zwitterionic Trisaccharide Repeating Unit. *Org. Lett.* **2021,** *23* (15), 5922-5926.

97. Sanapala, S. R.; Kulkarni, S. S. Expedient Route To Access Rare Deoxy Amino L-Sugar Building Blocks for the Assembly of Bacterial Glycoconjugates. *J. Am.*

Chem. Soc. **2016**, *138*, 4938-4947.

98. Hanninen, M.L.; Oivanen, P.; Hirvela-Koski, V. *Aeromonas* species in fish, fish-eggs, shrimp and freshwater*. Int J Food Microbiol*. **1997**, *34*(1),17-26.

99. Fauzi, N. Prevalence, antibiotic susceptibility, and presence of drug resistance genes in *Aeromonas* spp. isolated from freshwater fish in Kelantan and Terengganu states, Malaysia*. Vet World*. **2021**, *14*(8), 2064-2072.

100. Marinho-Neto, F.A. Morphological, microbiological and ultrastructural aspects of sepsis by *Aeromonas hydrophila* in Piaractus mesopotamicus*. PLoS One*. **2019**, *14*(9), p. e0222626.

101. Handfield, M. Aeromonas hydrophila isolated from food and drinking water: hemagglutination, hemolysis, and cytotoxicity for a human intestinal cell line (HT-29). *Appl. Environ. Microbiol*. **1996**, *62*(9), 3459-3461.

102. Daily, O.P. Association of *Aeromonas* sobria with human infection. *J. Clin. Microbiol*. **1981**, *13*(4), 769-777.

103. Gray, S.J.; Griffiths, A. Observations on *Aeromonas* species isolated from human faeces*. J. Infect.* **1990**, *20*(3), 267-268.

104. Hatrongjit, R. Genomic Analysis of *Aeromonas veronii C198*, a Novel Mcr-3.41-Harboring Isolate from a Patient with Septicemia in Thailand. *Pathogens*. **2020**, *9*(12).

105. Usui, M. Use of *Aeromonas spp*. as General Indicators of Antimicrobial Susceptibility among Bacteria in Aquatic Environments in Thailand*. Front. Microbiol.* **2016**, *7*, 710.

106. Wangkahad, B. Occurrence of bacteriophages infecting *Aeromonas, Enterobacter, and Klebsiella* in water and association with contamination sources in Thailand. *J. Water. Health.* **2015**, *13*(2), 613-624.

107. Guz, L. Virulence and Antimicrobial Resistance Pattern of *Aeromonas spp*. Colonizing European Pond Turtles Emys orbicularis and Their Natural Environment. First Study from Poland*. Animals (Basel)* **2021**, *11*(10).

108. Froquet, R. Alternative host model to evaluate *Aeromonas* virulence. *Appl. Environ. Microbiol***. 2007**, *73*(17), 5657-5659.

109. Rahman, M. Persistence, transmission, and virulence characteristics of *Aeromonas* strains in a duckweed aquaculture-based hospital sewage water recycling plant in Bangladesh*. Appl. Environ. Microbiol.* **2007**, *73*(5), 1444-1451.

110. Heiss, C. Structure of the capsule and lipopolysaccharide O-antigen from the channel catfish pathogen, *Aeromonas hydrophila. Carbohydr. Res.* **2019**, *486,* 107858.

111. Pakiet, K., et al. Structure of the O-specific polysaccharide from the lipopolysaccharide of *Aeromonas hydrophila* strain K691 containing 4-acetamido-4,6-dideoxy-d-glucose*. Carbohydr. Res*. **2017**, *439*, 23-29.

112. Turska-Szewczuk, A., et al. Structure of the O-specific polysaccharide from the lipopolysaccharide of *Aeromonas sobria* strain Pt312*. Carbohydr. Res.* 2015, *403*,142-148.

113. Turska-Szewczuk, A., et al. Structural analysis of the O-specific

polysaccharide from the lipopolysaccharide of *Aeromonas veronii bv. sobria* strain K49. *Carbohydr. Res*. **2012**, *353*, 62-68.

114. Turska-Szewczuk, A., et al. Structural characterization of the O-specific polysaccharide from the lipopolysaccharide of the fish pathogen *Aeromonas bestiarum strain P1S. Carbohydr. Res.* **2011**, *346*(6), 815-821.

115. Turska-Szewczuk, A., et al. The structure of the O-specific polysaccharide from the lipopolysaccharide of *Aeromonas bestiarum strain 207. Carbohydr. Res*. **2010**, *345*(5), 680-684.

116. Dworaczek, K., et al. Structure of the disaccharide repeating unit of O-specific polysaccharide isolated from *Aeromonas veronii strain Bs8* pathogenic to common carp *(Cyprinus carpio). Carbohydr. Res.* **2021**, *500*, 108210.

117. Keith, D.J.; Townsend, S. D. Total Synthesis of the Congested, Bisphosphorylated *Morganella morganii* Zwitterionic Trisaccharide Repeating Unit. *J. Am. Chem. Soc.* **2019**, *141*(32), 12939-12945.

118. Yi, W., et al. *Escherichia coli O86* O-antigen biosynthetic gene cluster and stepwise enzymatic synthesis of human blood group B antigen tetrasaccharide*. J. Am. Chem. Soc.* **2005**, *127*(7), 2040-1.

119. Hoffmann-Roder, A.; Johannes, M. Synthesis of a MUC1-glycopeptide-BSA conjugate vaccine bearing the 3'-deoxy-3'-fluoro-Thomsen-Friedenreich antigen. *Chem Commun (Camb*). **2011**, *47*(35), 9903-5.

120. J, Cheng., et al. A divergent approach to the synthesis of iGb3 sugar and lipid analogues via a lactosyl 2-azido-spingosine intermediate*. Org. Biomol.*

Chem. **2014**, *12*, 2729-2736.

121. S, Yang., et al. An Investigation of construction of chondroitin sulfate E (CS-e) repeating unit. *Tetrahedron* **2016**, *72*(37), 5659-5670.

2.9 Experimental Methods

General. All non-aqueous reactions were performed in flame-dried or oven dried round-bottomed flasks under an atmosphere of nitrogen or argon, unless otherwise noted. Stainless steel syringes or cannula were used to transfer air- and moisture-sensitive liquids. Reaction temperatures were controlled using a thermocouple thermometer and analog hotplate stirrer. Reactions were conducted at room temperature (rt, approximately 23 °C) unless otherwise noted. The anhydrous solvents used in the reactions were obtained from an MBraun MB-SPS 800 anhydrous Solvent System. Solvent for chromatography were of analytical grade and distilled under reduced pressure prior to use. Commercially available reagents were obtained from Aldrich, Fisher, TCI, TRC, and Carbosynth. Flash column chromatography was conducted as described Still et. al. using silica gel 230-400 mesh.[1] Where necessary, silica gel was neutralized by treatment of the silica gel prior to chromatography with the eluent containing 1% triethylamine. TEAB buffer was prepared by filling TEA (7 mL) in a measuring cylinder and adding water until the total volume reached 500mL. The solution was transferred to a flask and CO_2 was bubbled through the solution for 2 h at 0 °C. The buffer was stored at 4 °C. Thin layer chromatography (TLC) was performed using glass backed 60-F254 silica gel plates obtained from Silicycle. Visualization of TLC plates was performed by UV (215 nm and 254 nm), CAM stain (5% (w/v) ammonium molybdate, 1% (w/v) cerium (III) sulfate and 10% (v/v) sulfuric acid in water) or ninhydrin stain (1.5% (w/v) ninhydrin and 3% (v/v) acetic acid in n-butanol) dipping solutions. Size exclusion chromatography (SEC) was performed using Bio Gel ® P-2 Gel (Bio-Rad). Powdered 4 Å molecular sieves were obtained from Sigma-Aldrich and used

for reactions. Sieves were activated by iterative heating (to 180 °C) and cooling (to 25 °C) cycles (minimum of 3 times). Heating was carried out by microwave irradiation and cooling took place in a desiccator equipped with Drierite™ and P_2O_5.

Instrumentation: ^{1}H NMR, ^{13}C NMR, ^{31}P and 2D NMR spectra were recorded in the Vanderbilt Small Molecule NMR Facility on a Bruker 400 and 600 MHz. Chemical shifts are reported in parts per million (ppm) of the δ scale. Spectra were recorded in $CDCl_3$ by using the solvent residual peak chemical shift as the internal standard ($CDCl_3$: S7 7.26 ppm ^{1}H, 77.0 ppm ^{13}C) or in D_2O using the solvent as the internal standard in ^{1}H NMR (D_2O: 4.79 ppm 1H) unless otherwise stated. ^{31}P NMR spectra 1% H_3PO_4 in D_2O was used as an external standard. 1H NMR spectral data are presented as follows: Chemical shifts (δ ppm), multiplicity (s = singlet, d = doublet, dd = doublet of doublets, dq = doublet of quadruplet, ddd = doublet of doublet of doublet, t = triplet, q = quartet, p = pentet, br = broad, m = multiplet) coupling constants (Hz), integration. High-resolution mass spectra (HRMS) were obtained from the Department of Chemistry, Vanderbilt University using an LTQ-Orbitrap XL mass spectrometer. Optical rotations (OR) were measured with on a AUTOPOL IV digital polarimeter. Concentrations (c) in g/100 mL and solvent are given in parentheses and the reported value is an average of n = 3 independent measurements.

_p_-Methoxyphenyl 2,6-dideoxy-6-iodo-trichloroacetamido-β-D-glucopyranoside (2.102):

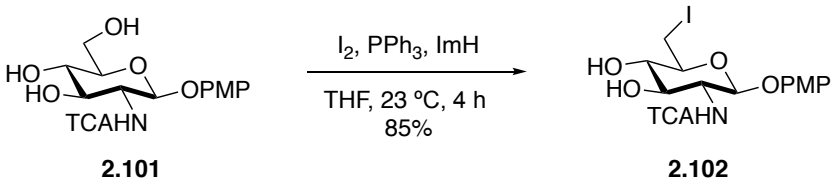

2.101 **2.102**

To a solution of PPh_3 (4.48 g, 17.1 mmol, 1.0 equiv.), imidazole (2.77 g, 40.6 mmol, 2.5 equiv., and I_2 (4.33 g, 17.1 mmol, 1.0 equiv.) in anhydrous THF (81 mL) under an argon atmosphere was added triol **2.101** (7.00 g, 16.3 mmol, 1.0 equiv.). The mixture stirred at room temperature for 4 h. At completion, the reaction mixture was quenched by the addition of satd. aq. $Na_2S_2O_3$ (25 mL × 1) and extracted with CH_2Cl_2 (3 × 50 mL). The combined organic layers were dried over anhydrous Na_2SO_4, filtered, and concentrated *in vacuo*. Flash chromatography of the crude material eluting with EtOAc/Hexane (6:4) gave 6-iodo derivative **2.102** (7.5 g, 16.3 mmol, 85%) as a white foam. 6-iodo derivative **2.102** had R_f 0.42 (EtOAc/Hexane 7:3) visualized with ceric ammonium molybdate stain; $[\alpha]D^{25}$ = -3.9° (c = 0.01, CH_3OH); ^1H NMR (600 MHz, MeOD) δ 7.08 (d, *J* = 9.1 Hz, 2H, Ar), 6.81 (d, *J* = 9.1 Hz, 2H, Ar), 5.02 (d, *J* = 8.4 Hz, 1H, H-1), 3.93 (dd, *J* = 10.5, 8.5 Hz, 1H, H-2), 3.74 (s, 3H, OC*H*$_3$), 3.72 – 3.65 (m, 2H, H-3, H-6), 3.37 – 3.26 (m, 3H, H-4, H-5, H-6); ^{13}C NMR (151 MHz, MeOD) δ 163.2 (NH*C*O), 155.5, 151.7, 118.4, 114.0, 100.4 (C-1), 92.7 (*C*Cl_3), 76.1 (C-5), 74.6 (C-4), 73.1 (C-3), 57.8 (C-2), 54.7 (OC*H*$_3$), 4.3 (C-6); HRMS (ESI) calcd. for $C_{15}H_{16}O_6Cl_3IN$ $(M-H)^-$ 537.9093, found 537.9083 *m/z*.

***p*-Methoxyphenyl 2,6-dideoxy-2-N-trichloroacetamido-β-D-glucopyranoside (2.103):**

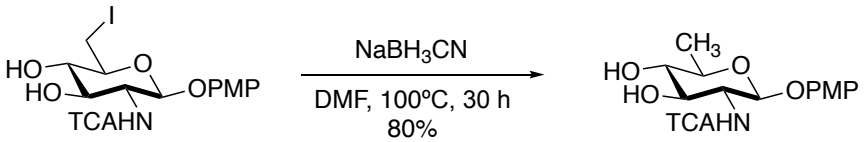

2.102 **2.103**

A solution of 6-iodo derivative **2.102** (10.0 g, 18.5 mmol, 1.0 equiv.) was dissolved in anhydrous DMF (92 mL) under an argon atmosphere. Sodium cyanoborohydride (7.81 g, 211 mmol, 5.0 equiv) was added and the reaction mixture was stirred at 100 °C for 30 h. At completion, the reaction mixture was diluted with H_2O (300 mL) and extracted with CH_2Cl_2 (3 × 100 mL). The combined organic layers were dried over Na_2SO_4, filtered, and concentrated *in vacuo*. Flash chromatography of the crude material eluting with CH_2Cl_2/CH_3OH (95:5) gave diol **2.103** (5.34 g, 12.9 mmol, 70%) as a white foam. Diol **2.103** had R_f 0.33 (CH_2Cl_2/CH_3OH 19:1) visualized with ceric ammonium molybdate stain; $[\alpha]D^{25}$ = -12.5° (c = 0.014, CH_3OH); ^{1}H NMR (600 MHz, MeOD) δ 6.94 (d, *J* = 9.1 Hz, 2H, Ar), 6.81 (d, *J* = 9.1 Hz, 2H, Ar), 5.01 (d, *J* = 8.5 Hz, 1H, H-1), 3.90 (dd, *J* = 10.5, 8.5 Hz, 1H, H-2), 3.74 (s, 3H, OC*H*$_3$), 3.65 (dd, *J* = 10.5, 8.8 Hz, 1H, H-3), 3.46 (dq, *J* = 9.4, 6.1 Hz, 1H, H-5), 3.14 (t, *J* = 9.1 Hz, 1H, H-4), 1.35 (d, *J* = 6.1 Hz, 3H, H-6); ^{13}C NMR (151 MHz, MeOD) δ 163.2 (NH*C*O), 155.4, 151.7, 117.9, 114.0, 100.1 (C-1), 92.8 (*C*Cl_3), 76.1 (C-4), 73.3 (C-3), 72.0 (C-5), 58.0 (C-2), 54.6 (OC*H*$_3$), 16.7 (C-6); HRMS (ESI) calcd. for $C_{15}H_{17}O_6Cl_3N$ $(M-H)^-$ 412.0127, found 412.0127 *m/z*.

_p_-Methoxyphenyl 3-_O_-benzoyl-2,6-dideoxy-2-trichloroacetamido-β-D-glucopyranoside (2.104):

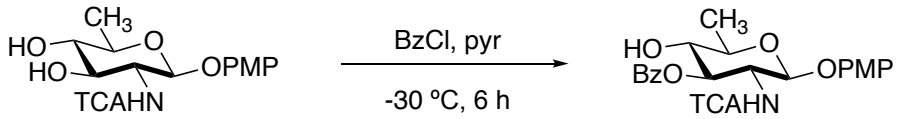

2.103 **2.104**

A solution of diol **2.103** (2.91 g, 6.91 mmol, 1.0 equiv.) was dissolved in anhydrous pyridine (70 mL) under an argon atmosphere and cooled to -30°C. A diluted solution of benzoyl chloride (0.82 mL, 6.9 mmol, 1.0 equiv.) in 1.0 mL pyridine was then added dropwise over 10 min. The reaction mixture was held at -30°C for 6 h. At completion, the solution was diluted with EtOAc (100 mL) and washed with 2M HCl (100 mL × 5), sat. aq. $NaHCO_3$ (100 mL × 1), and brine (100 mL × 1). The combined organic layers were dried over anhydrous Na_2SO_4, filtered, and concentrated *in vacuo*. Flash chromatography of the crude material eluting with EtOAc/Hexane (1:5) gave the 3-O-benzoyl derivative **2.104** (3.31 g, 6.41 mmol, 91%) as a white foam. Alcohol **2.104** had R_f 0.60 (EtOAc/Hexane 3:1) visualized with ceric ammonium molybdate stain; $[\alpha]D^{25}$ = +9.7° (c = 0.0019, $CHCl_3$); ^{1}H NMR (600 MHz, $CDCl_3$) δ 7.97 (dd, *J* = 8.4, 1.4 Hz, 2H, Ar), 7.61 – 7.55 (m, 1H, Ar), 7.41 (dd, *J* = 8.3, 7.4 Hz, 2H, Ar), 7.27 (d, *J* = 9.5 Hz, 1H, NH), 6.96 (d, *J* = 9.1 Hz, 2H, Ar), 6.79 (d, *J* = 9.1 Hz, 2H, Ar), 5.63 (dd, *J* = 10.8, 8.3 Hz, 1H, H-3), 5.13 (d, *J* = 8.4 Hz, 1H, H-1), 4.40 (ddd, *J* = 10.8, 9.1, 8.3 Hz, 1H, H-2), 3.76 (s, 3H, OC*H*$_3$), 3.73 – 3.56 (m, 2H, H-4, H-5), 1.44 (d, *J* = 5.6 Hz, 3H, H-6); ^{13}C NMR (151 MHz, $CDCl_3$) δ 167.9 (*C*OPh), 162.5 (NH*C*O), 155.8, 151.5, 134.0, 130.0, 128.8, 128.7, 118.9, 114.7, 100.5 (C-1), 92.3 (*C*Cl_3), 75.7 (C-3), 74.5 (C-4), 72.4 (C-5), 56.3 (C-2), 55.7 (OC*H*$_3$), 17.8 (C-6); HRMS (ESI) calcd. for $C_{22}H_{21}O_7Cl_3N$ $(M-H)^-$ 516.0389, found 516.0378 *m/z*.

_p_-Methoxyphenyl 3-_O_-benzoyl-4-azido-2,4,6-trideoxy-2-trichloroacetamido-β-D- galactopyranoside (2.105):

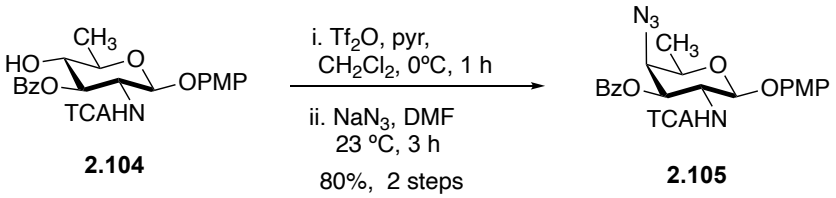

Alcohol **2.104** (1.80 g, 3.50 mmol, 1.0 equiv.) was dissolved in anhydrous CH_2Cl_2 (35 mL) under an argon atmosphere. The reaction mixture was cooled to 0 °C and anhydrous pyridine (0.56 mL, 6.9 mmol, 2.0 equiv.) was added followed by triflic anhydride (0.70 mL, 4.2 mmol, 1.2 equiv.). After stirring for 1 h at 0 °C, the reaction mixture was diluted with CH_2Cl_2 (100 mL) and washed with H_2O (100 mL × 1) and brine (100 mL × 1). The organic layer was dried over anhydrous Na_2SO_4, filtered and concentrated *in vacuo*. The residue was dissolved in anhydrous DMF (30 mL) and NaN_3 (599 mg, 9.22 mmol, 3.0 equiv.) was added. After stirring for 3 h at rt, the reaction mixture was diluted with EtOAc (150 mL) and washed with H_2O (100 mL × 1) and brine (100 mL × 1). The organic phase was dried over anhydrous Na_2SO_4, filtered, and concentrated *in vacuo*. Flash chromatography of the crude material eluting with EtOAc/Hexane (1:4) gave the azido derivative **2.105** (1.30 g, 2.40 mmol, 78%) as a white solid. The trideoxy intermediate **2.105** had $R_f = 0.50$ (EtOAc/Hexane 2:3) visualized with ceric ammonium molybdate stain; $[\alpha]D^{25}$ = -23.3° (c = 0.015, $CHCl_3$); ^1H NMR (600 MHz, $CDCl_3$) δ 8.08 (dd, *J* = 8.3, 1.3 Hz, 2H, Ar), 7.63 – 7.59 (m, 1H, Ar), 7.47 (dd, *J* = 8.3, 7.4 Hz, 2H, Ar), 6.97 (d, *J* = 9.0 Hz, 2H, Ar), 6.88 (d, *J* = 8.6 Hz, 1H, NH), 6.79 (d, *J* = 9.0 Hz, 2H, Ar), 5.77 (dd, *J* = 11.2, 3.6 Hz, 1H, H-3), 5.15 (d, *J* = 8.3 Hz, 1H, H-1), 4.48 (dt, *J* = 11.2, 8.5 Hz, 1H, H-2), 4.03 (dd, *J* = 3.6, 1.3 Hz, 1H, H-4), 3.96 (qd, *J* = 6.3, 1.4 Hz, 1H, H-5),

3.76 (s, 3H, OC*H*$_3$), 1.45 (d, *J* = 6.3 Hz, 3H, H-6); ^{13}C NMR (151 MHz, $CDCl_3$) δ 166.1 (*C*OPh), 162.2 (NH*C*O), 155.8, 151.1, 134.0, 130.1, 128.6, 128.3, 119.1, 114.5, 100.4 (C-1), 92.2 (*C*Cl_3), 72.0 (C-3), 69.6 (C-5), 63.5 (C-4), 55.6 (C-5), 53.3 (O*C*H_3), 17.5 (C-6); HRMS (ESI) calcd. for $C_{22}H_{20}O_6Cl_3N_4$ $(M-H)^-$ 541.0454, found 541.0442 *m/z*.

3-*O*-benzoyl-4-azido-2,4,6-trideoxy-2-trichloroacetamido-β-D-galactopyranosyl *N*-trichloroacetimidate (2.106):

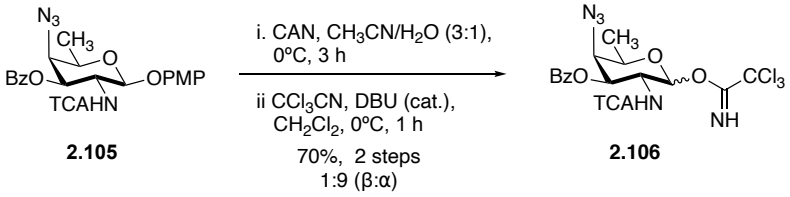

To a solution of compound **2.105** (1.10 g, 2.0 mmol, 1.0 equiv.) in CH_3CN/H_2O (3:1 v/v, 20 mL) at 0 °C under an argon atmosphere was added cerium ammonium nitrate (5.54 g, 10.1 mmol, 5.0 equiv.).[3] The reaction mixture was stirred for 3 h at 0 °C, the reaction mixture was diluted with EtOAc (100 mL) and washed with satd. aq. $NaHCO_3$ (30 mL × 1) and H_2O (30 mL × 1). The organic layer was dried over anhydrous Na_2SO_4, filtered and concentrated *in vacuo*. Flash chromatography of the crude material eluting with EtOAc/Hexane (2:1) as eluent to afford the hemiacetal as a yellow-orange foam. The compound was dissolved in CH_2Cl_2 (50 mL), trichloroacetonitrile (1.0 mL, 10.3 mmol, 5 equiv.) and DBU (50 µL, 0.61 mmol, 0.30 equiv.) were added, and the reaction mixture was stirred at 0 °C for 1 h. The solvent was removed under reduced pressure, and the residue was purified by flash column with EtOAc/hexane (1:1) to yield the trichloroacetimidate **2.106** as a white foam (1.10 g, 1.9 mmol, 70%). The trichloroacetimidate **2.106** had R_f = 0.80 (EtOAc/Hexane 1:1) visualized with ceric ammonium molybdate stain; $[\alpha]D^{25}$ = +7.6° (c = 0.006, $CHCl_3$); ^{1}H NMR (600 MHz, $CDCl_3$) δ 8.79 (s, 1H, OC(N)*H*CCl_3), 8.08 (dd, *J* = 8.4, 1.1 Hz, 2H, Ar), 7.64 – 7.56 (m, 1H, Ar), 7.47 (dd, *J* = 8.3, 7.4 Hz, 1H, Ar), 7.01 (d, *J* = 9.0 Hz, 1H, NH), 6.47 (d, *J* = 3.6 Hz, 1H, H-1), 5.75 (dd, *J* = 11.2, 3.3 Hz, 1H, H-3), 4.91 (ddd, *J* = 11.1, 9.0, 3.6 Hz, 1H, H-2), 4.35 (qd, *J* = 6.4, 1.5 Hz, 1H, H-5), 4.09 (dd, *J* = 3.5, 1.5 Hz, 1H, H-4), 1.40 (d, *J* = 6.4 Hz, 3H,

C-6); ^{13}C NMR (151 MHz, $CDCl_3$) δ 166.9 (*C*OPh), 162.2 (NH*C*O), 160.2 (O*C*(NH)CCl_3), 134.2, 130.3, 128.8, 128.2, 94.9 (C-1), 91.9 (*C*Cl_3), 90.9 (*C*Cl_3), 71.0 (C-3), 68.2 (C-5), 63.8 (C-4), 50.0 (C-2), 17.4 (C-6); HRMS (ESI) calcd. for $C_{17}H_{15}O_6Cl_6N_5Na$ $(M+Na)^+$ 601.9104, found 601.9100 *m/z*.

***p*-Methoxyphenyl 4-azido-2,4,6-trideoxy-2-trichloroacetamido-β-D-galactopyranoside (2.107):**

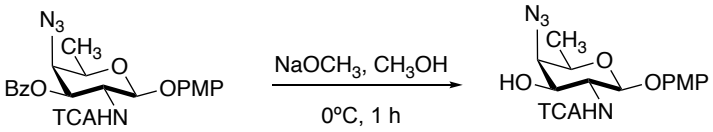

2.105 **2.107**

A solution of **2.105** (125 mg, 0.21 mmol, 1.0 equiv.) in anhydrous CH_3OH (4 mL) under an argon atmosphere was added $NaOCH_3$ solution (0.10 mL, 1.5 mmol, [1.5 M] in CH_3OH) dropwise at room temperature. At 1 h, the pH of the reaction mixture was still >12 and TLC indicated that the starting material had been completely consumed for a more polar spot. The reaction was neutralized by the addition of acidic form Amberlite IR 120 (H+) ion exchange resin. The solution was filtered through a glass fritted funnel with a pad of Celite to remove the resin. The filtrate was concentrated *in vacuo* to give **2.107** (85.0 mg, 0.19 mmol, >95%) as a white foam in quantitative yield. Rf = 0.40 (EtOAc/Hexanes 1:1) visualized with ceric ammonium molybdate stain; $[\alpha]D^{25}$ = -28.9° (c = 0.016, $CHCl_3$); ^1H NMR (600 MHz, $CDCl_3$) δ 7.02 (d, *J* = 6.4 Hz, 1H, NH), 6.97 (d, *J* = 9.1 Hz, 1H, Ar), 6.80 (d, *J* = 9.1 Hz, 1H, Ar), 5.05 (d, *J* = 8.3 Hz, 1H, H-1), 4.45 (ddd, *J* = 10.5, 6.6, 3.7 Hz, 1H, H-3), 3.89 – 3.83 (m, 1H, H-2), 3.83-3.79 (m, 2H, H-4, H-5), 3.76 (s, 3H, -OC*H*$_3$), 3.15 (d, *J* = 6.6 Hz, 1H, O*H*), 1.43 (d, *J* = 6.3 Hz, 3H, H-6); ^{13}C NMR (151 MHz, $CDCl_3$) δ 163.0 (NH*C*O), 155.8, 150.8, 119.1, 114.6, 99.5 (C-1), 92.2 (*C*Cl_3), 70.6 (C-3), 70.0 (C-5), 65.7 (C-4), 57.0 (C-2), 55.6 (O*C*H_3), 17.5 (C-6); HRMS (ESI) calcd. for $C_{15}H_{17}O_5Cl_3N_4Na$ $(M+Na)^+$ 461.0164, found 461.0157 *m/z*.

2,2,2-trichloro-N-((2R,4aR,6S,7R,8R,8aR)-6-(4-methoxyphenoxy)-2-phenyl-8-(((2S,3R,4S,5S,6R)-3,4,5-tris(benzyloxy)-6-methyltetrahydro-2H-pyran-2-yl)oxy)hexahydropyrano[3,2-d][1,3]dioxin-7-yl)acetamide (2.132)

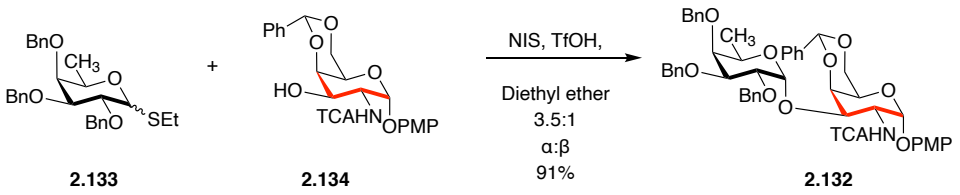

2.133 **2.134** **2.132**

Donor **2.133** (1.0 eq, 0.500g, 1.04 mmol) and acceptor **2.134** (1.5 eq, 0.813g, 1.6 mmol) were coevaporated with benzene (2 x 8 mL) and placed in a vacuum desiccator containing P_2O_5 overnight. The donor/ acceptor mixture was dissolved in diethyl ether (14 mL) and the resulting solution was cannulated into a reaction flask containing 4 Å powdered molecular sieves. The mixture was stirred under argon 1 hour then cooled to -78C and TfOH (0.1 eq, 0.038 mL in 0.2 mL CH_2Cl_2) was added. The reaction was stirred 2 hour then quenched with Et_3N. The reaction was diluted with CH_2Cl_2, filtered through celite, dried ($MgSO_4$), filtered, and concentrated in vacuo. The crude residue was purified via flash column chromatography (2:1 hexanes/EtOAc) to yield diasaccharide **2.132** (0.890g, 0.95 mmol, 91%) as a yellow foam: Rf 0.35 (1:1 hexanes/EtOAc); $[\alpha]D^{25}$ = +38.7° (c = 0.012, $CHCl_3$) (α major product),^{1}H NMR (600 MHz, $CDCl_3$) δ 7.39 – 7.25 (m, 20H), 7.02 (d, *J* = 9.1 Hz, 2H), 6.93 (d, *J* = 8.4 Hz, 1H,-NH), 6.85 (d, *J* = 9.0 Hz, 2H), 5.71 (d, *J* = 3.5 Hz, 1H), 5.26 (s, 1H), 5.16 (d, *J* = 3.5 Hz, 1H), 5.02 (d, *J* = 11.5 Hz, 1H), 4.85 (d, *J* = 11.9 Hz, 1H), 4.79 – 4.77 (m, 1H), 4.75 (d, *J* = 9.2 Hz, 1H), 4.72 (d, *J* = 7.2 Hz, 1H), 4.65 (d, *J* = 11.5 Hz, 1H), 4.62 (d, *J* = 11.4 Hz, 1H), 4.40 (d, *J* = 3.3 Hz, 1H), 4.24 (d, *J* = 13.3 Hz, 1H), 4.20 (dd, *J* = 11.0, 3.2 Hz, 1H), 4.13 (dd, *J* = 10.1, 3.5 Hz, 1H), 4.07 – 4.01 (m, 2H), 3.92 (d, *J* = 13.3 Hz, 1H), 3.80 (m, 1H), 3.78 (s, 3H), 3.64 (m, 1H), 1.20 (d, *J* = 6.6 Hz, 3H). ^{13}C NMR (150 MHz,

$CDCl_3$) δ 161.6, 155.5, 150.4, 138.8, 138.5, 137.5, 128.4, 128.2, 128.2, 128.1, 128.0, 127.4, 117.9, 114.8, 100.6, 97.5, 96.8, 92.6, 78.9, 78.0, 75.9, 75.0, 73.3, 73.1, 72.8, 72.0, 69.2, 67.7, 63.7, 55.6, 50.5, 16.8. HRMS (ESI) calcd for $C_{49}H_{50}Cl_3NO_{11}[M+Na]^+$ 956.2347, found 956.2348.

N-((2R,3R,4R,5R,6R)-5-hydroxy-6-(hydroxymethyl)-2-(4-methoxyphenoxy)-4-(((2S,3R,4S,5R,6R)-3,4,5-trihydroxy-6-methyltetrahydro-2H-pyran-2-yl)oxy)tetrahydro-2H-pyran-3-yl)acetamide (2.131)

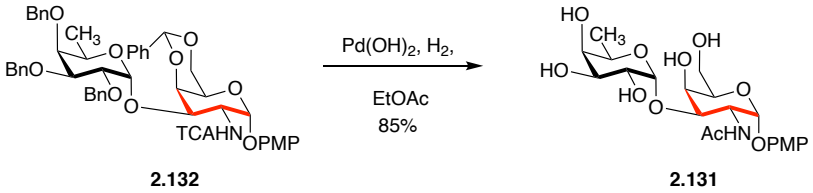

2.132 **2.131**

To a solution of **2.132** (1.0 eq, 0.500 g, 0.535 mmol) in CH_3OH (10 mL) and AcOH (1 mL) and $Pd(OH)_2$ was added (2.0 eq, 0.75g g, 1.07 mmol). The reaction was stirred under H_2 for 3 days then was diluted with CH_3OH, filtered through celite, concentrated in vacuo. The crude material was purified by size exclusion chromatography (Bio-Gel P2 gel) using a 1:1 mixture of deionized H_2O:CH_3OH as an eluant. Fractions containing the desired product (determined from MS) were combined and lyophilized to yield **2.131** (0.214 g, 0.452 mmol, 85%) as a white solid; $[\alpha]D^{25}$ = +60.7° (c = 0.012, CH_3OH), ^1H NMR (600 MHz, CD_3OD) δ 7.18 (d, *J* = 9.2 Hz, 2H), 7.01 (d, *J* = 9.3 Hz, 2H), 5.50 (s, 1H), 5.12 (s, 1H), 4.62 – 4.51 (m, 1H), 4.35 – 4.28 (m, 1H), 4.18-4.12 (m, 2H), 4.06-4.05 (m, 1H), 3.85 (s, 3H), 3.84 – 3.83-3.75(m, 5H), 2.11 (s, 3H), 1.31 (s, 3H). ^{13}C NMR (150 MHz, CD_3OD) δ 175.4, 156.2, 151.8, 120.2, 120.0, 116.3, 98.8, 97.9, 75.8, 73.2, 72.6, 71.0, 69.3, 68.7, 66.7, 62.3, 57.0, 50.2, 23.3, 16.9. HRMS (ESI) calcd for $C_{21}H_{31}NO_{11}$ $[M+Na]^+$ 496.1794, found 496.1101. $[\alpha]D^{25}$ = +60.7° (c = 0.015, $CDCl_3$)

Appendix A2:

Spectra and Table Relevant to Chapter 2

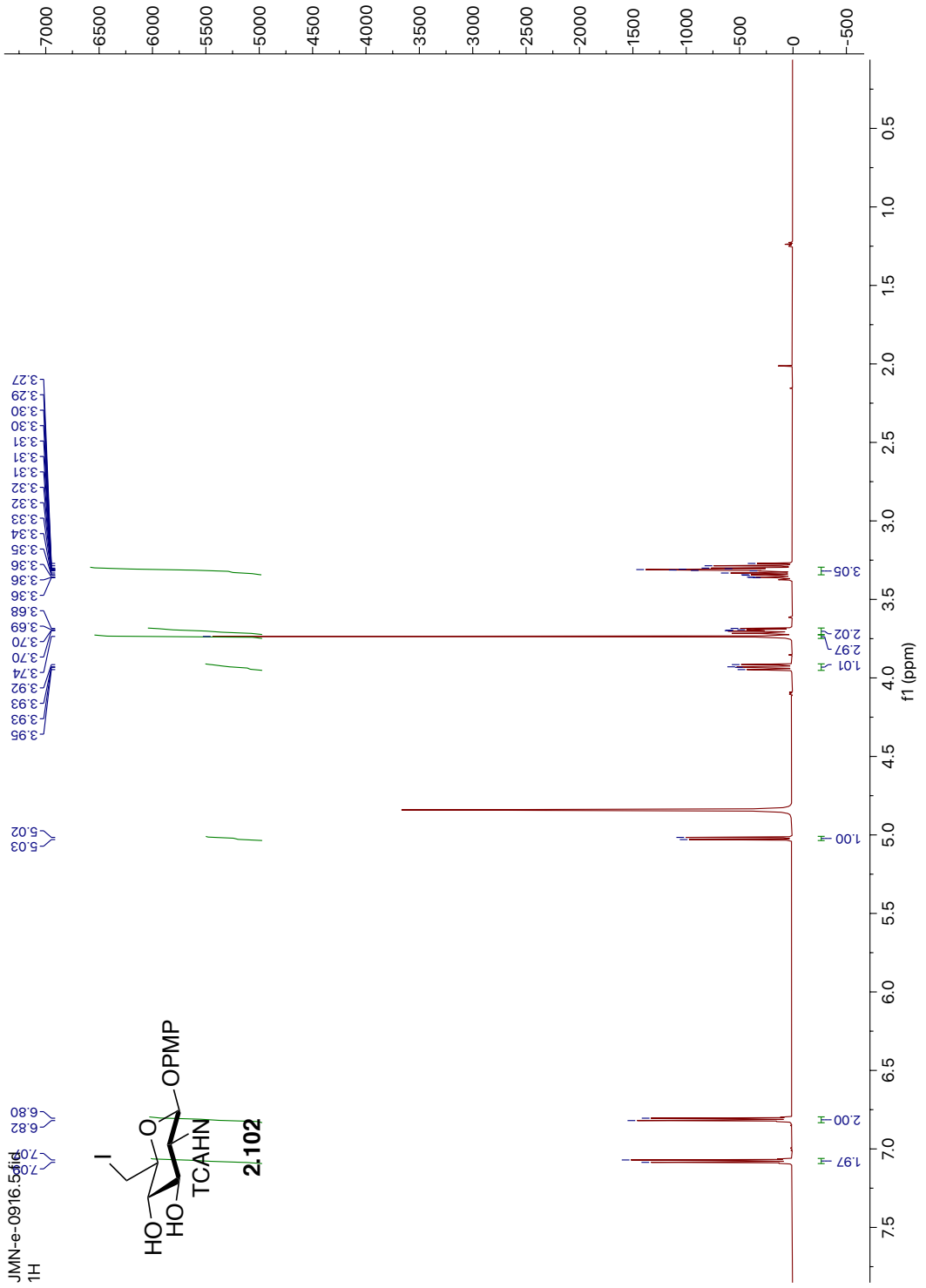

Figure A2.1. ^{1}H NMR (600 MHz, CD_3OD) of compound **2.102**.

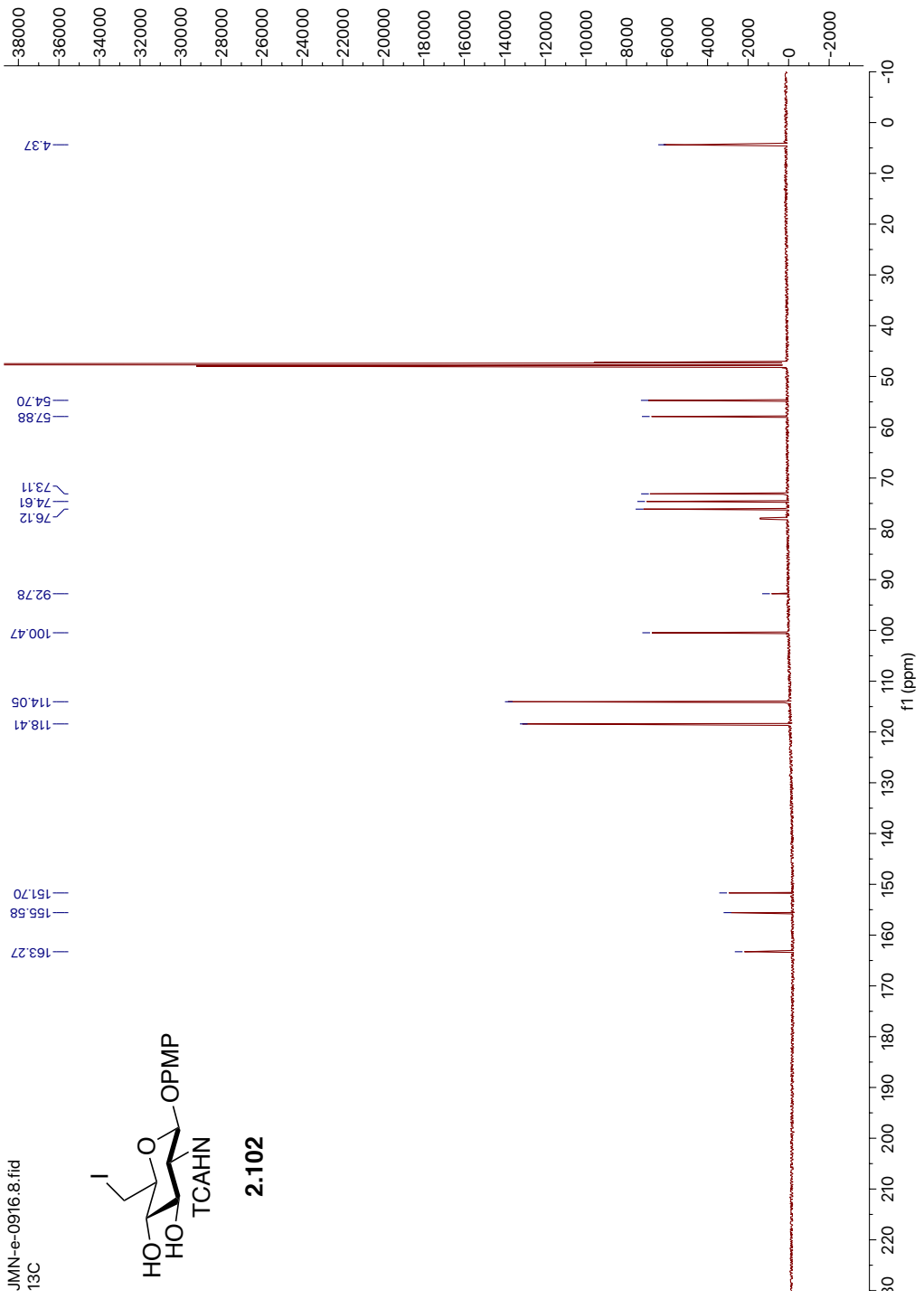

Figure A2.2. ^{13}C NMR (151 MHz, CD_3OD) of compound **2.102**.

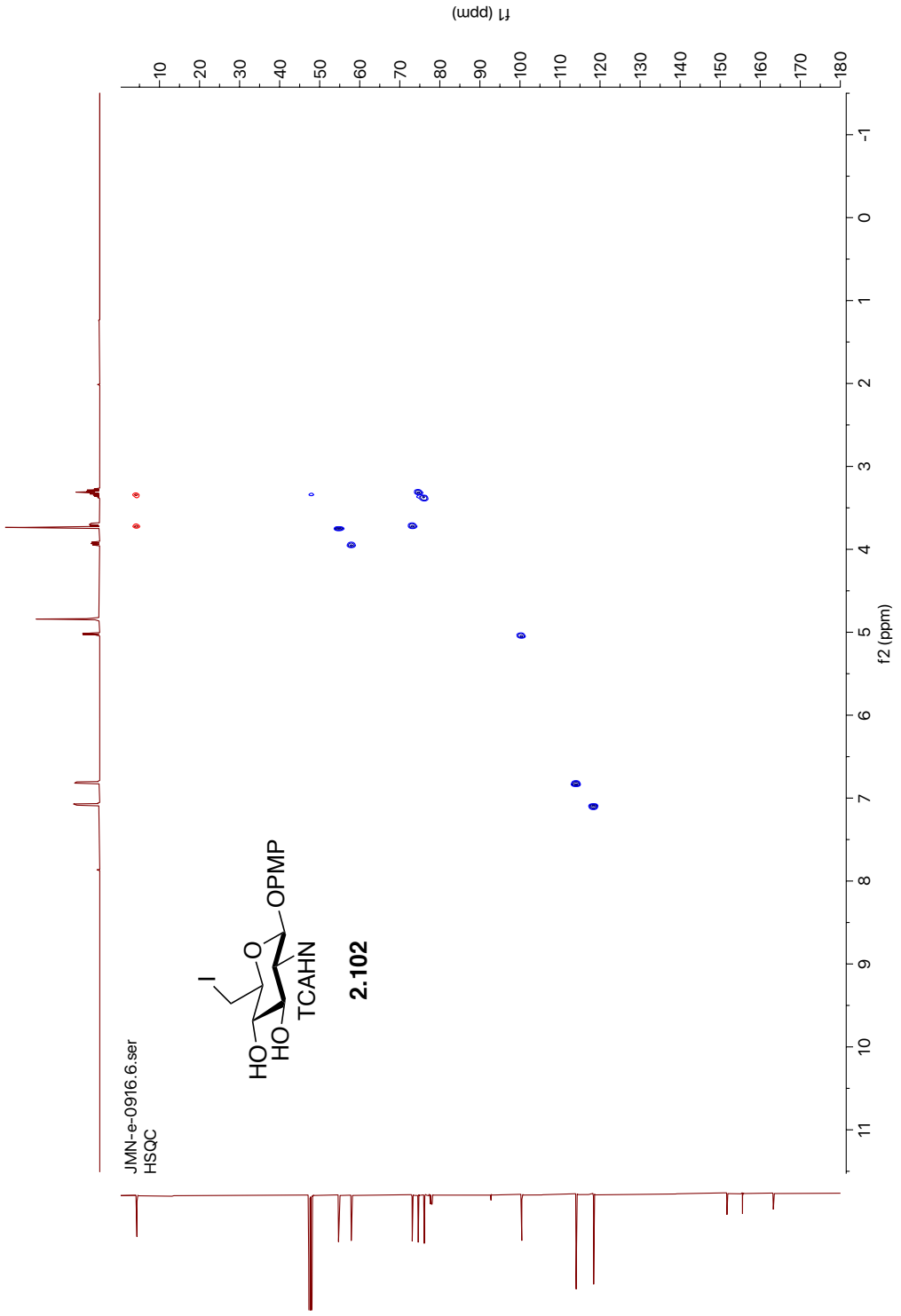

Figure A2.3. ^{1}H-^{13}C HSQC NMR (600 MHz, CD_3OD) of compound **2.102**.

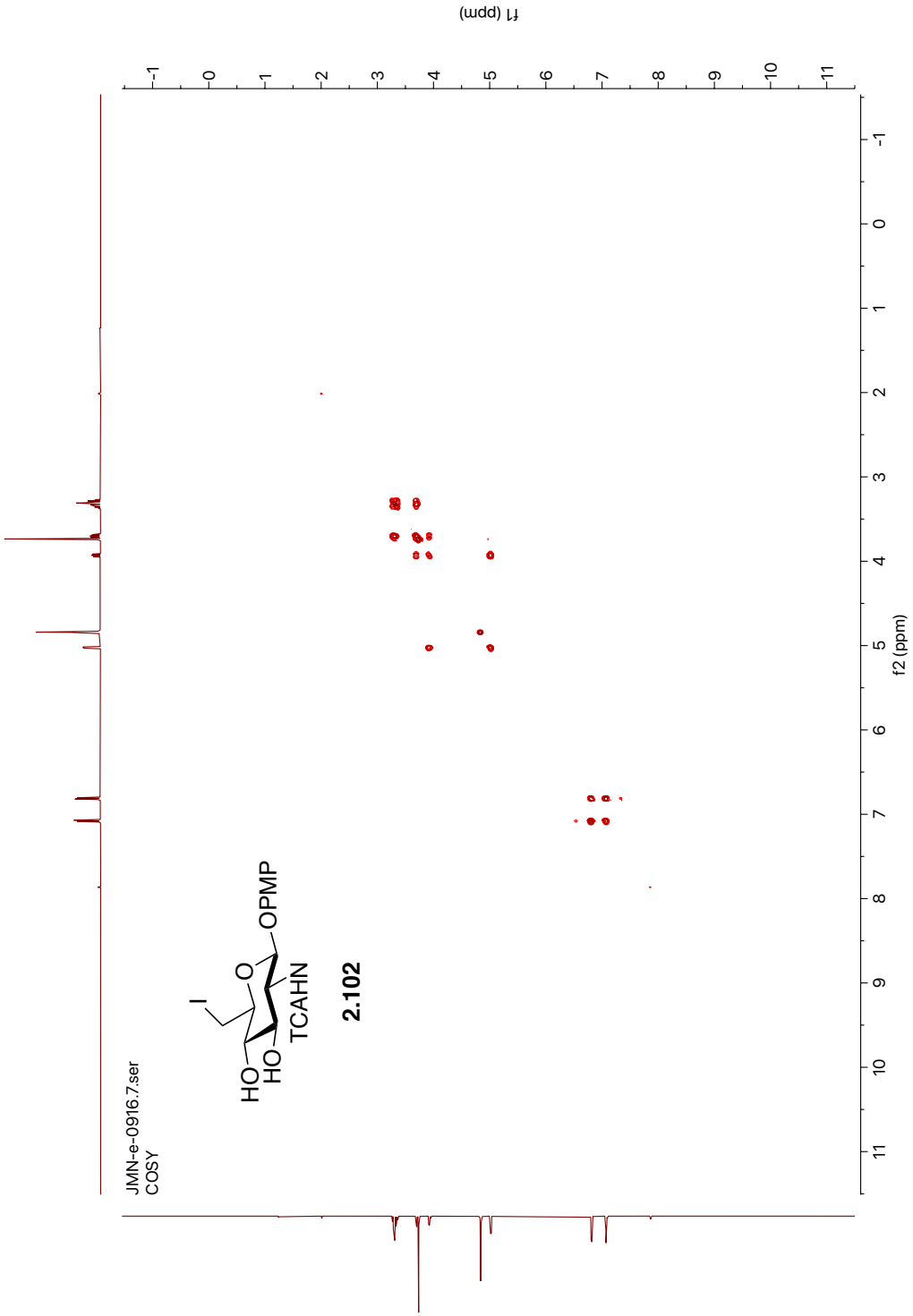

Figure A2.4. ^{1}H-^{1}H COSY NMR (600 MHz, CD_3OD) of compound **2.102**.

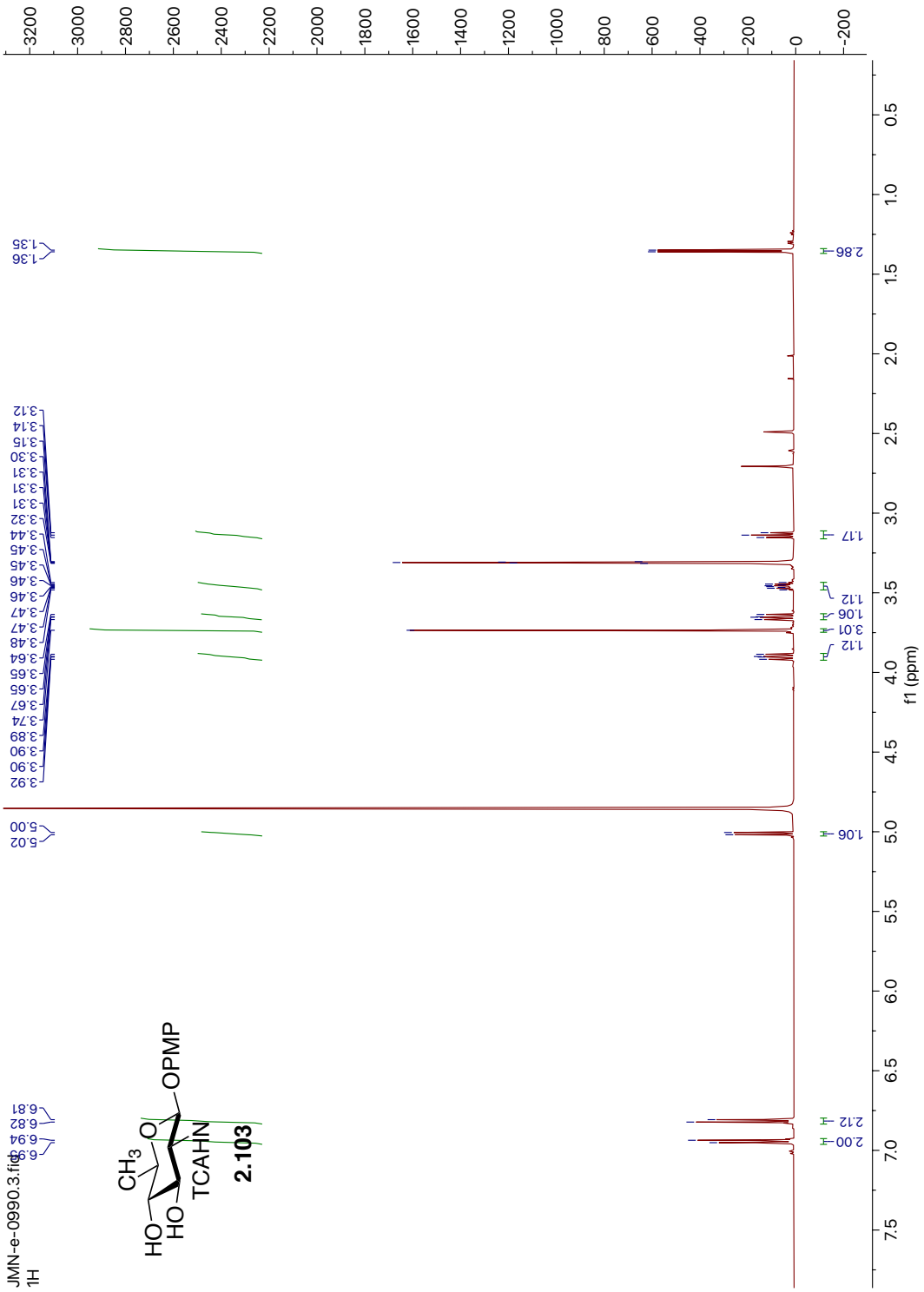

Figure A2.5. ^{1}H NMR (600 MHz, CD_3OD) of compound **2.103**.

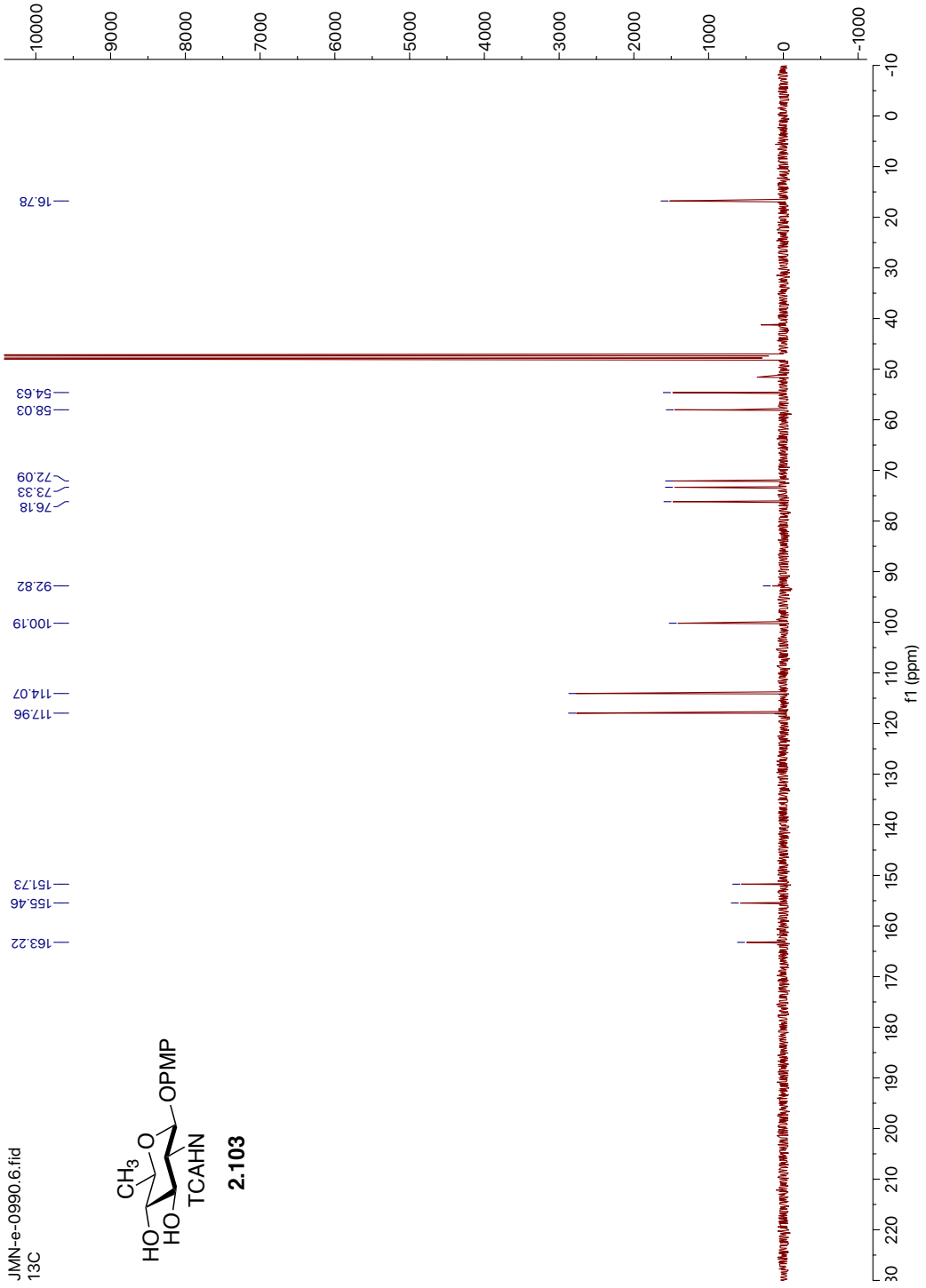

Figure A2.6. ^{13}C NMR (151 MHz, CD_3OD) of compound **2.103**.

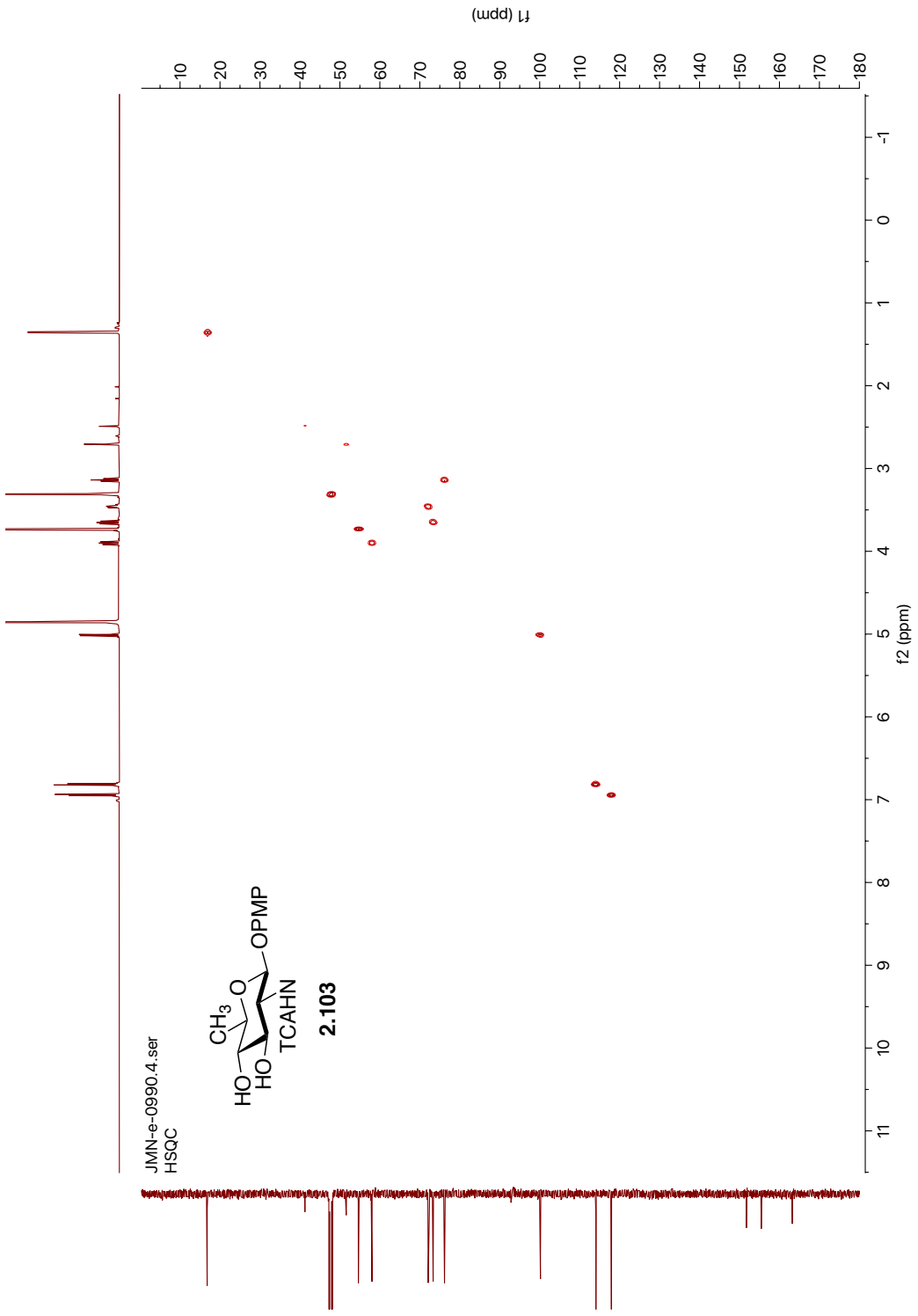

Figure A2.7. ^{1}H-^{13}C HSQC NMR (600 MHz, CD_3OD) of compound **2.103**.

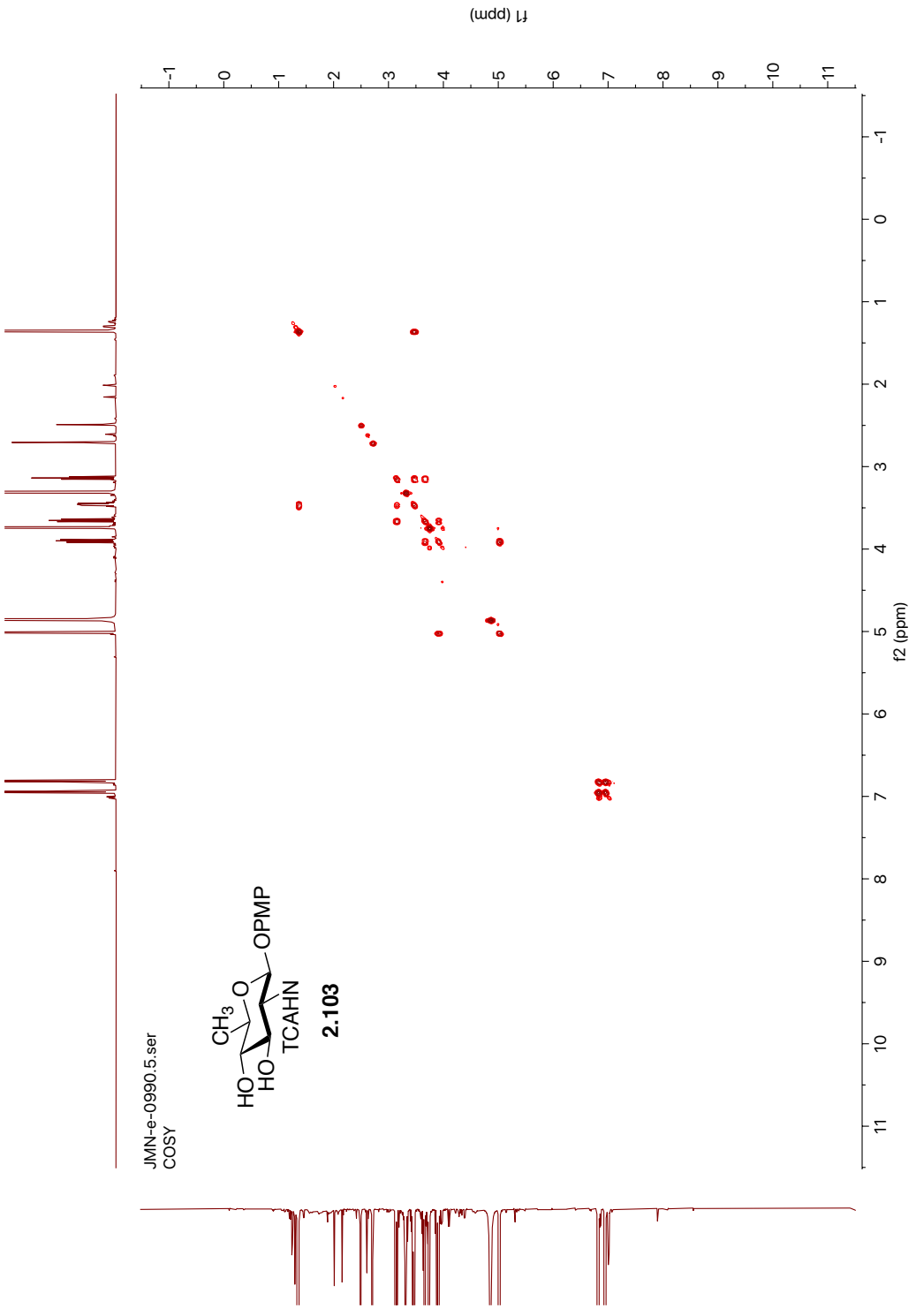

Figure A2.8. ^{1}H-^{1}H COSY NMR (600 MHz, CD_3OD) of compound **2.103**.

.

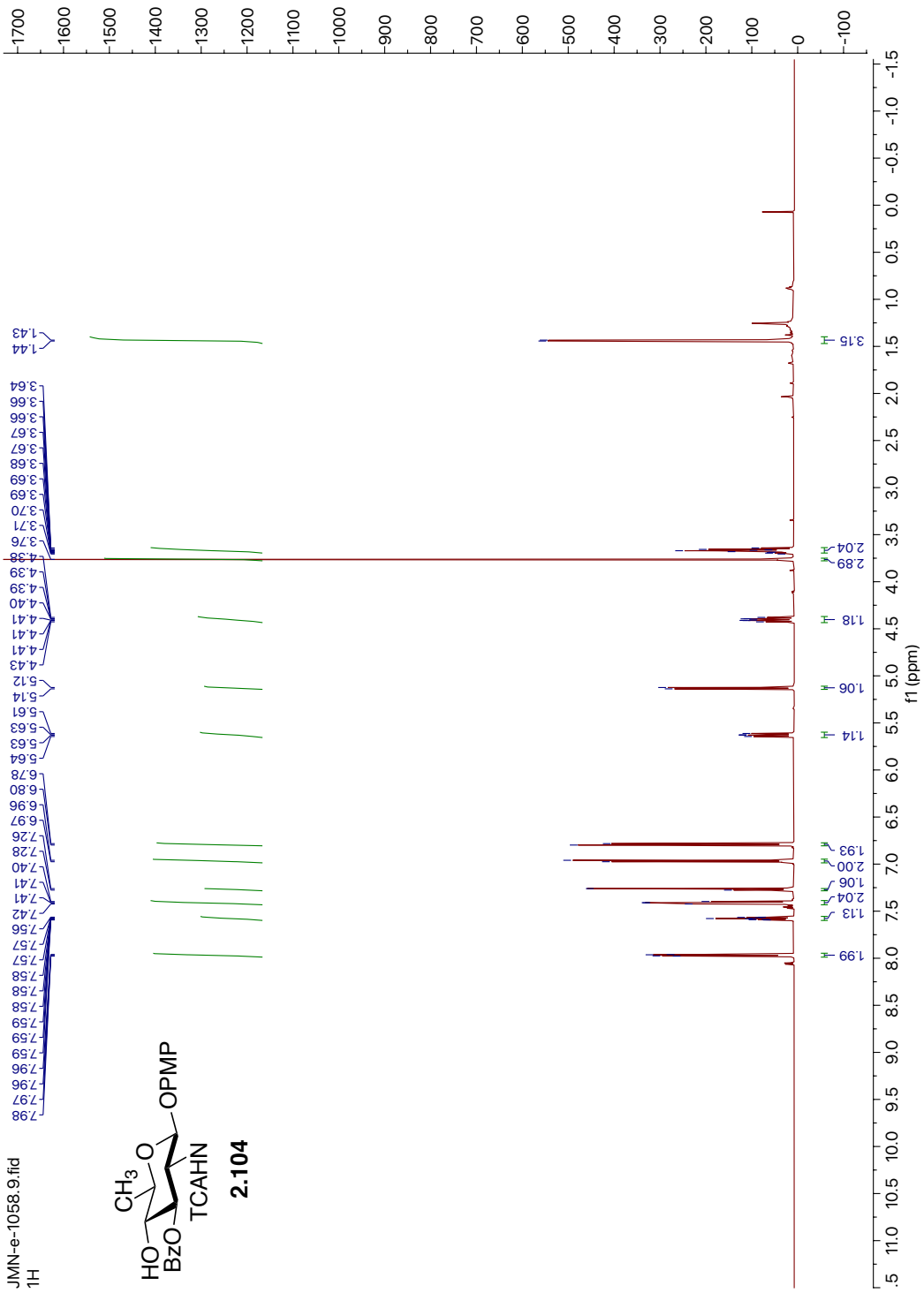

Figure A2.9. ^{1}H NMR (600 MHz, $CDCl_3$) of compound **2.104**.

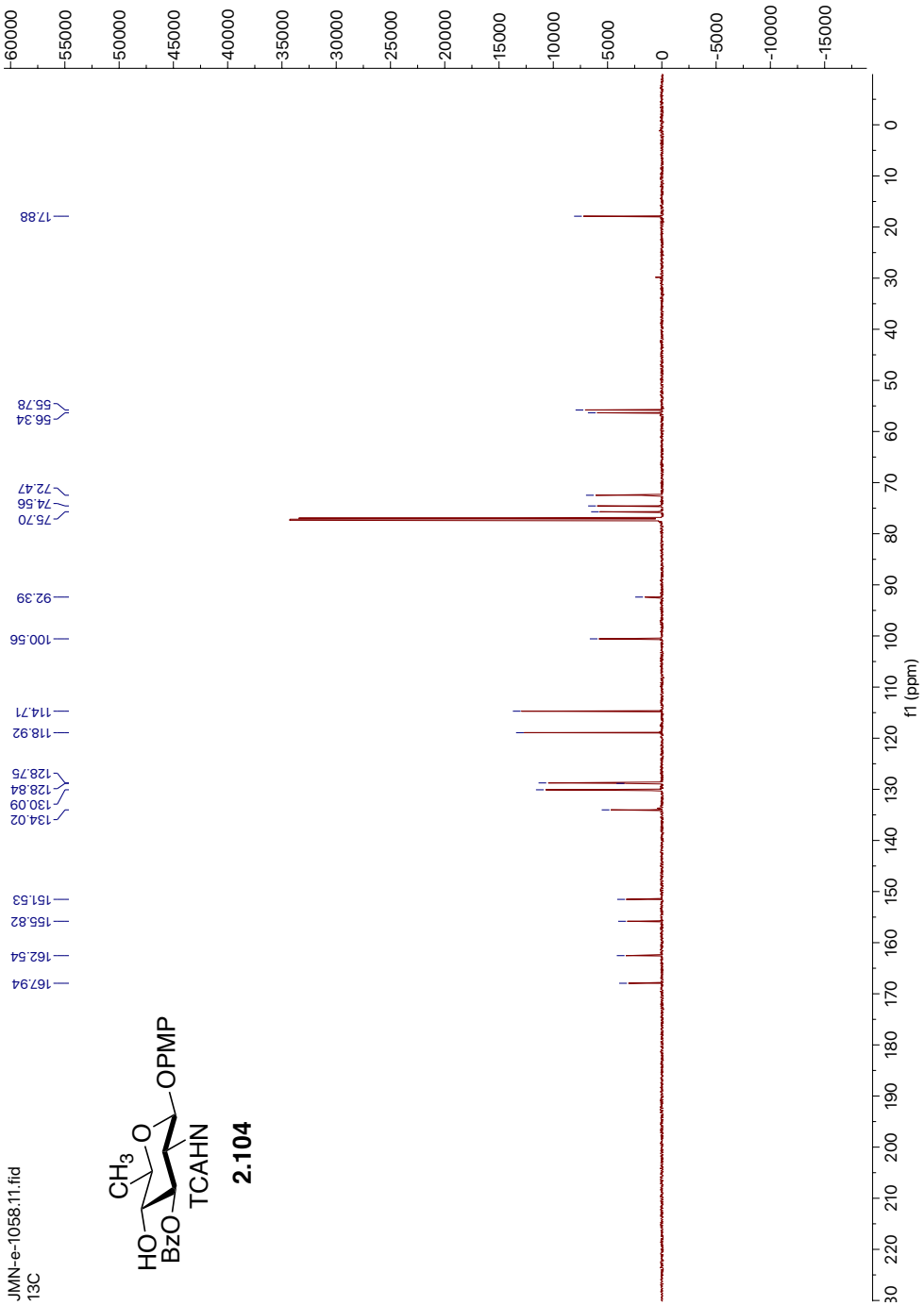

Figure A2.10. ^{13}C NMR (151 MHz, $CDCl_3$) of compound **2.104**.

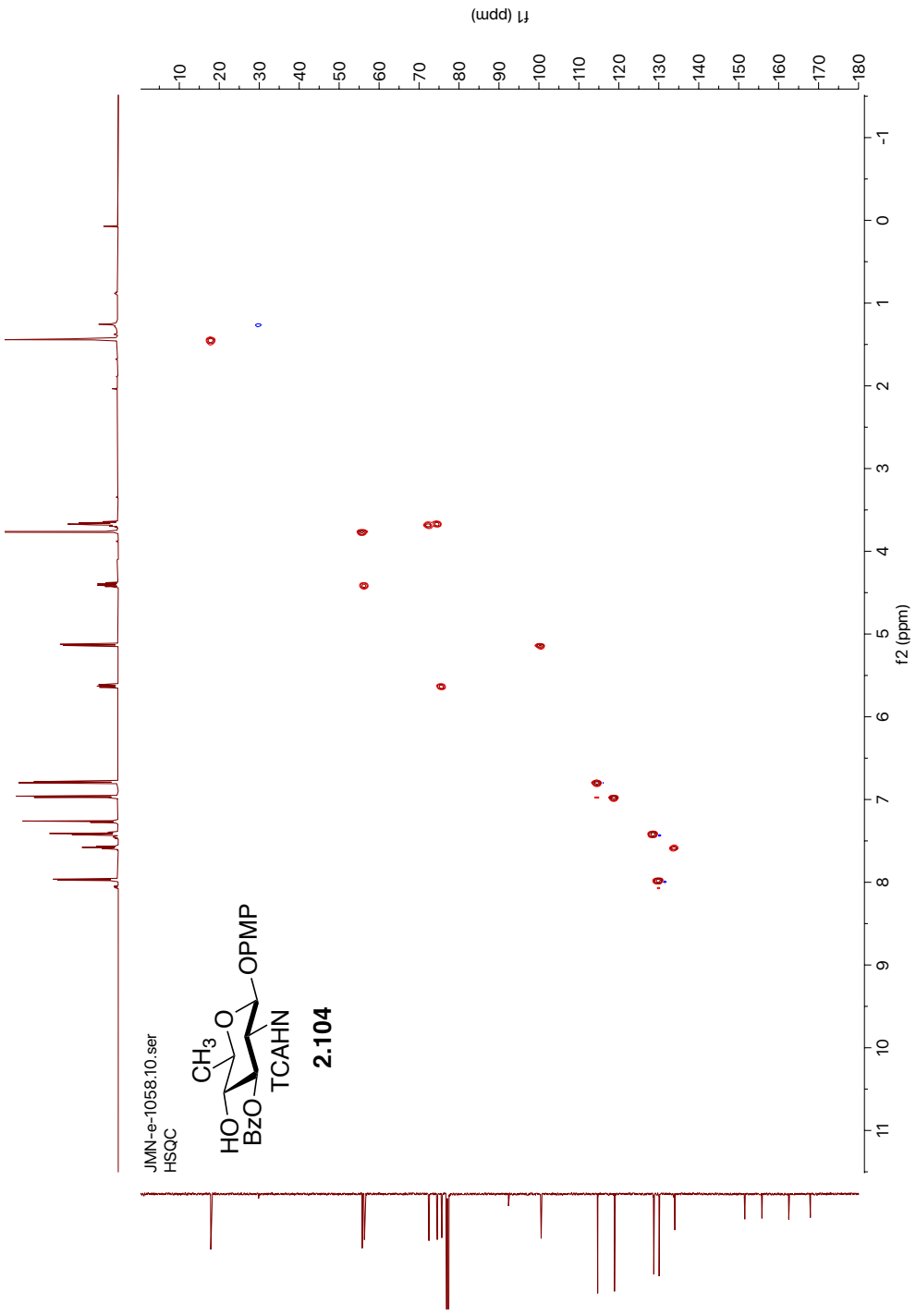

Figure A2.11. ^{1}H-^{13}C HSQC NMR (600 MHz, $CDCl_3$) of compound **2.104**.

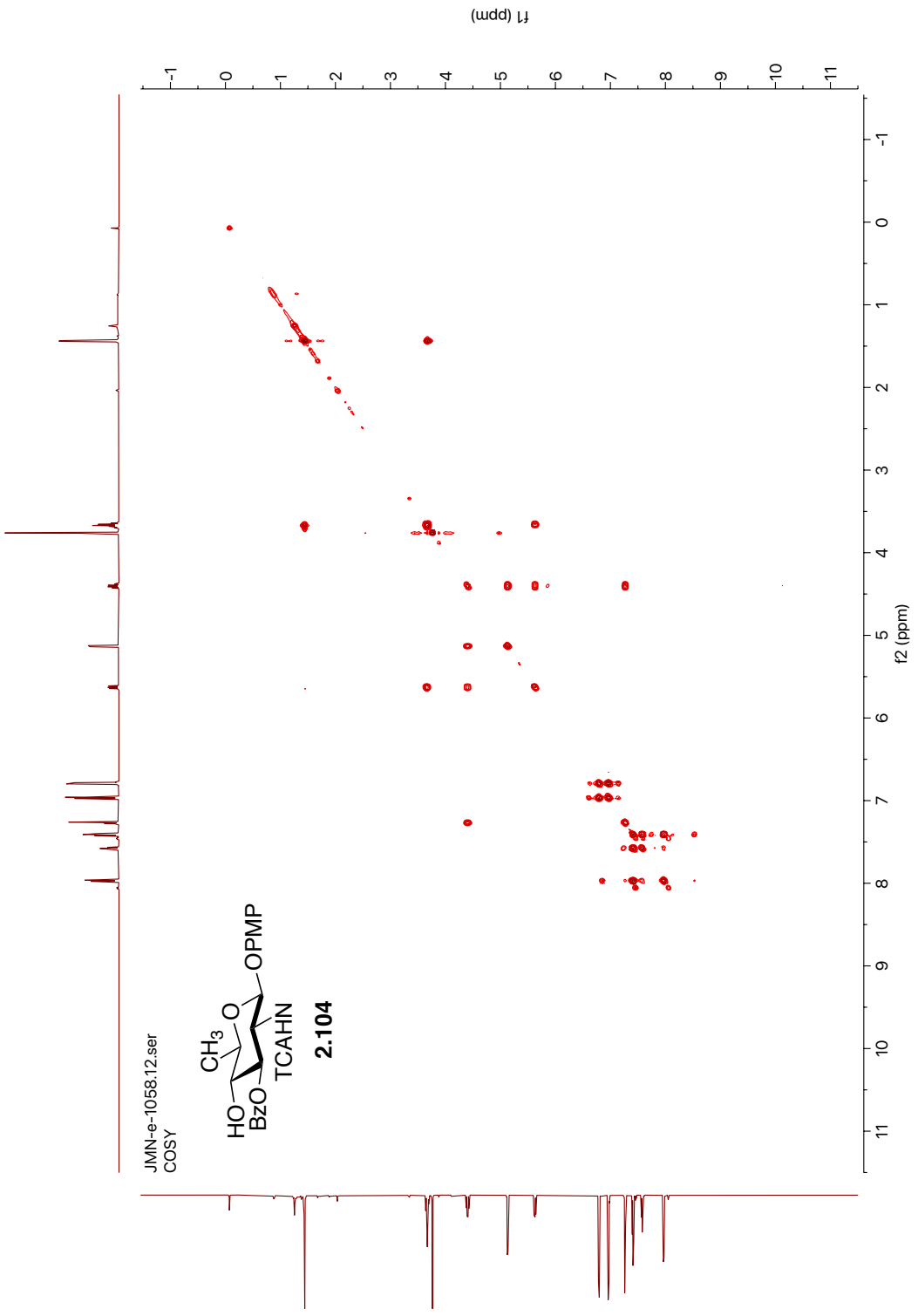

Figure A2.12. ^{1}H-^{1}H COSY NMR (600 MHz, $CDCl_3$) of compound **2.104**.

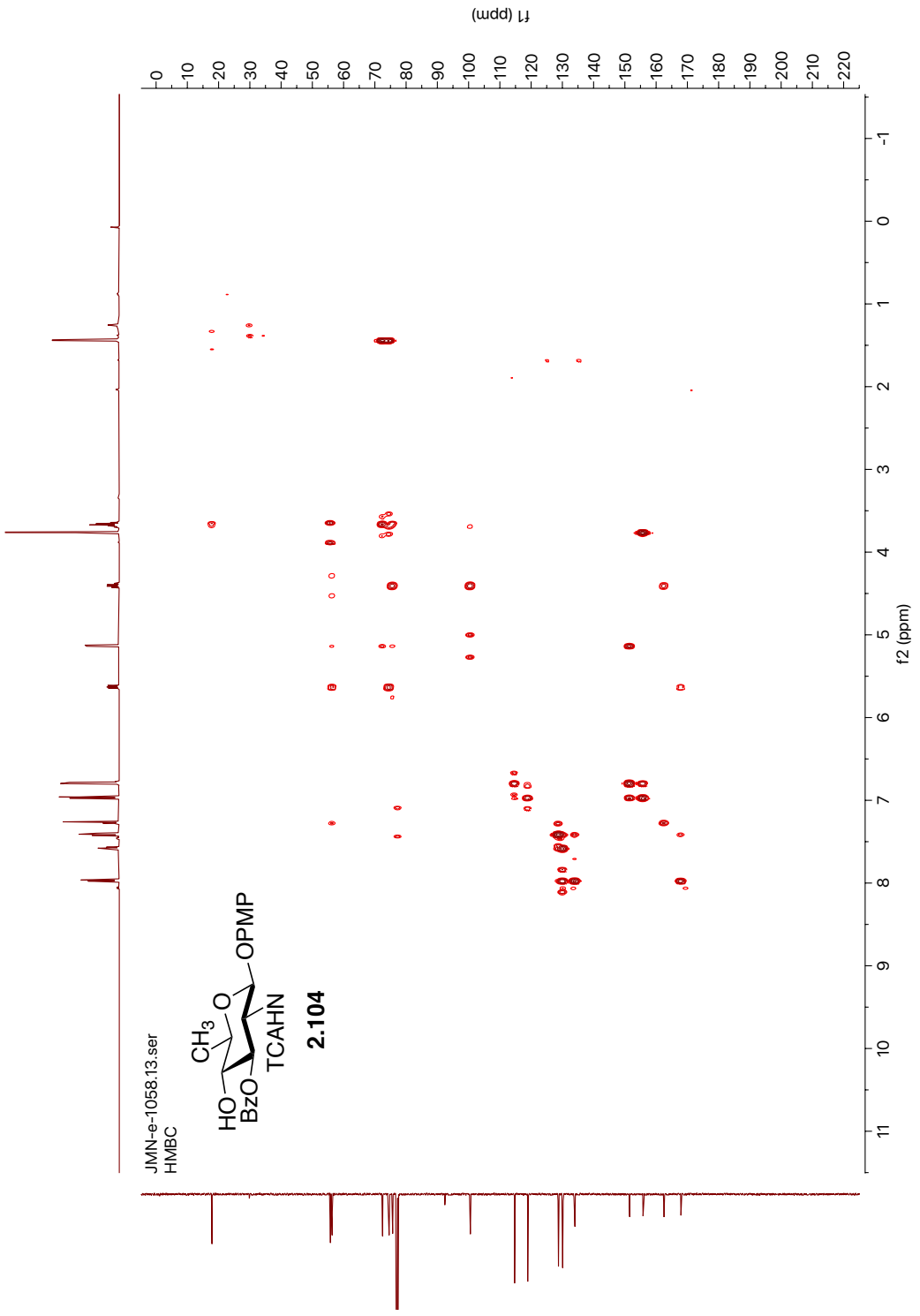

Figure A2.13. ^{1}H-^{13}C HMBC NMR (600 MHz, $CDCl_3$) of compound **2.104**.

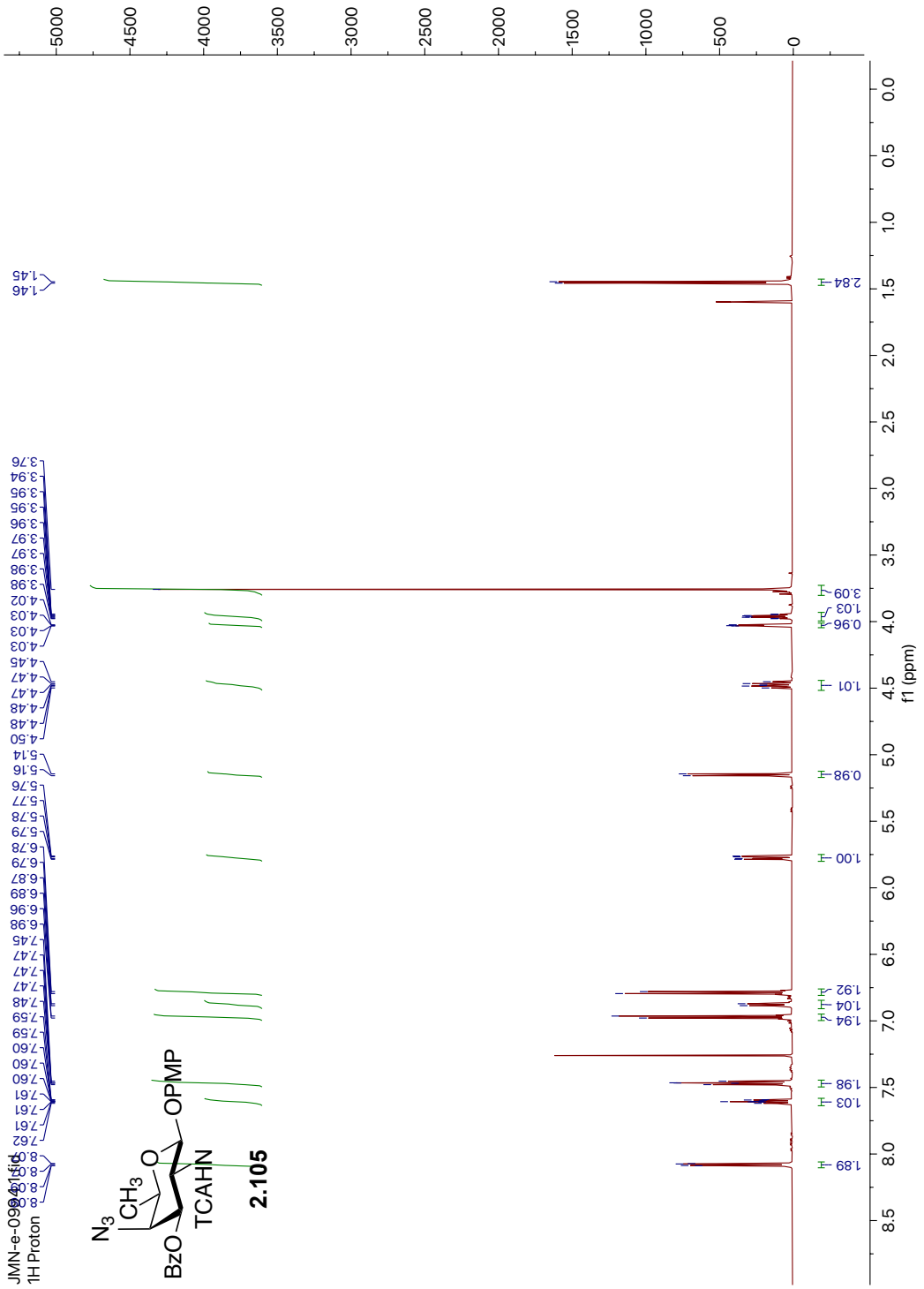

Figure A2.14. ^{1}H NMR (600 MHz, $CDCl_3$) of compound **2.105**.

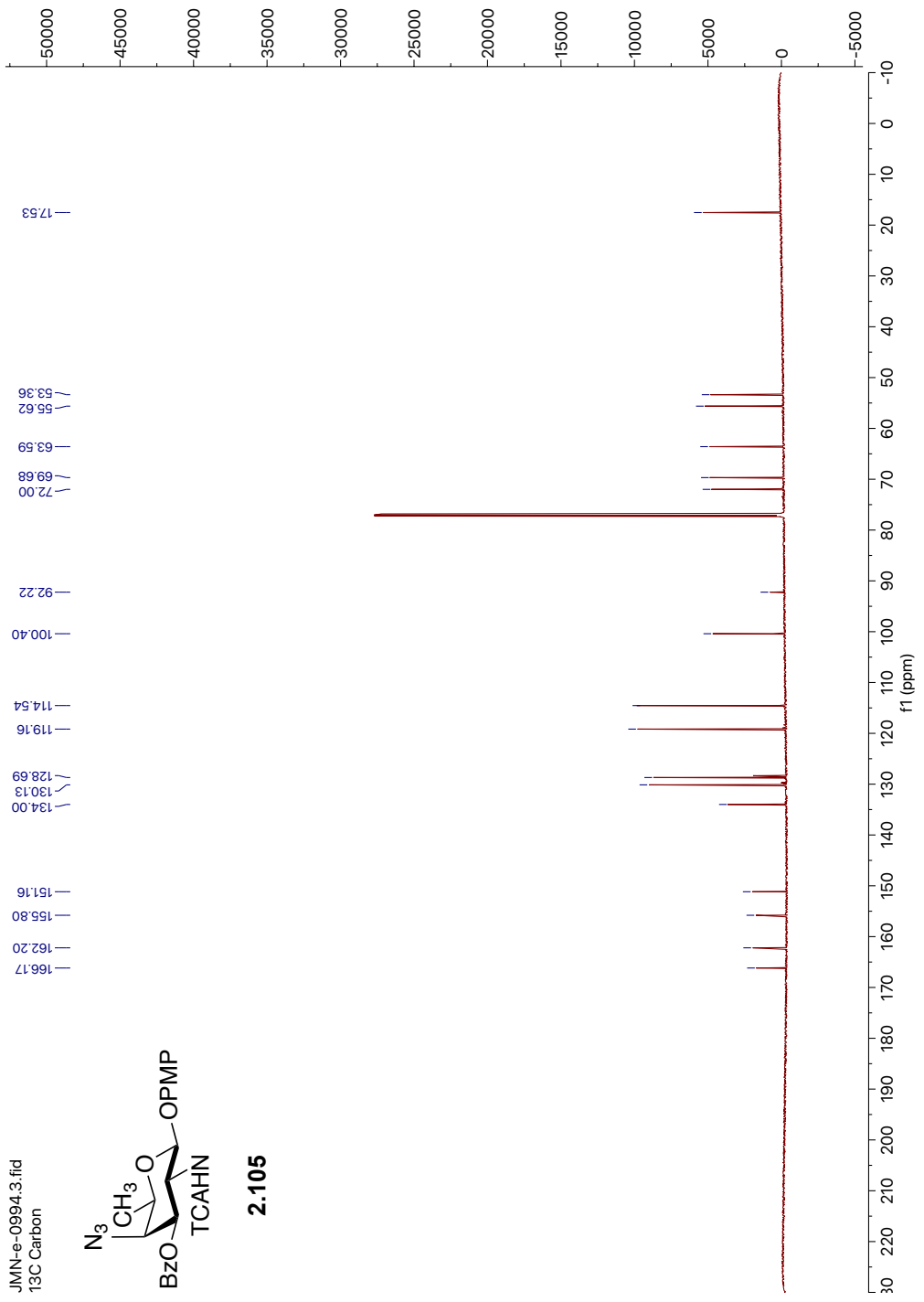

Figure A2.15. ^{13}C NMR (151 MHz, $CDCl_3$) of compound **2.105**.

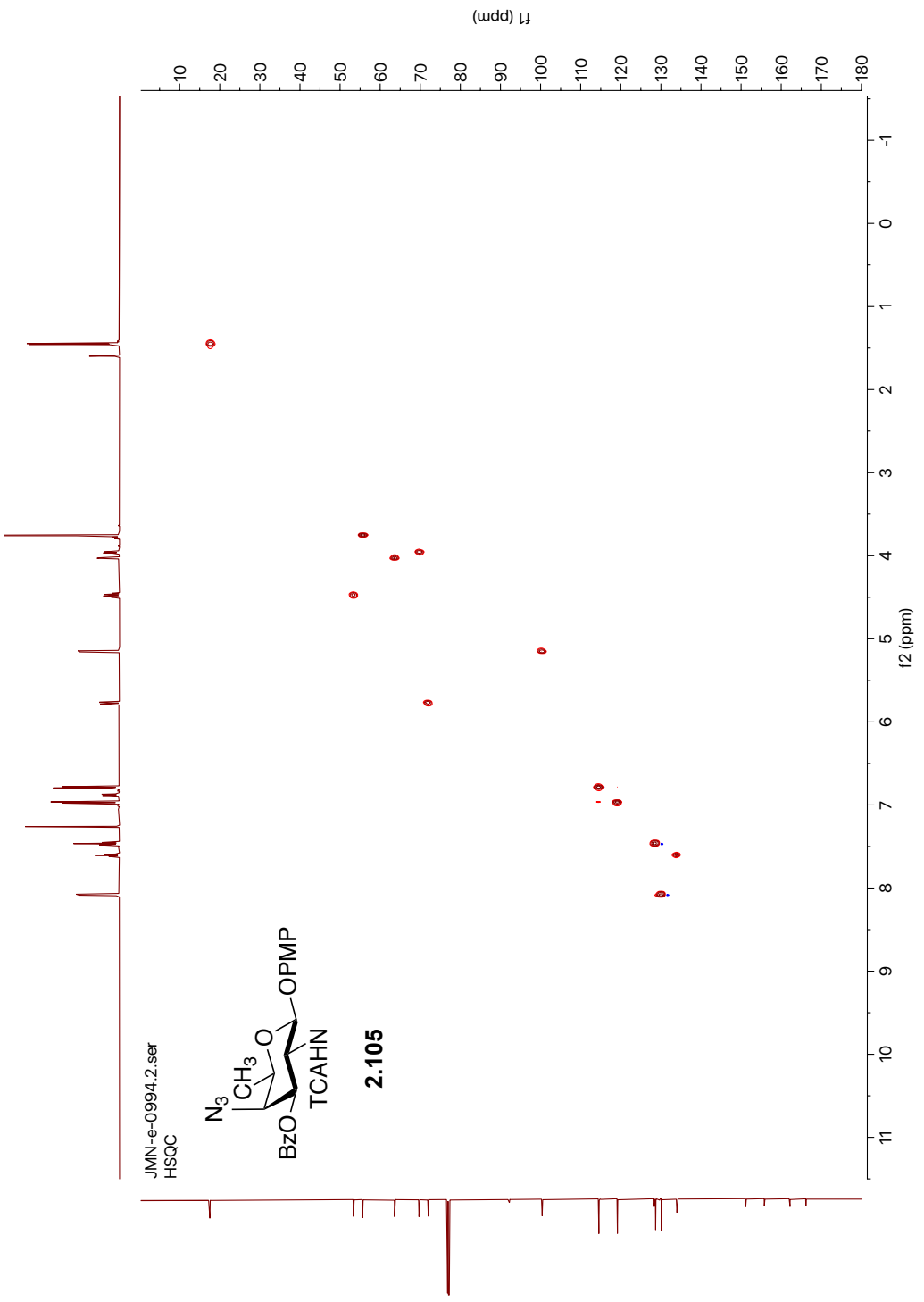

Figure A2.16. ^{1}H-^{13}C HSQC NMR (600 MHz, $CDCl_3$) of compound **2.105**.

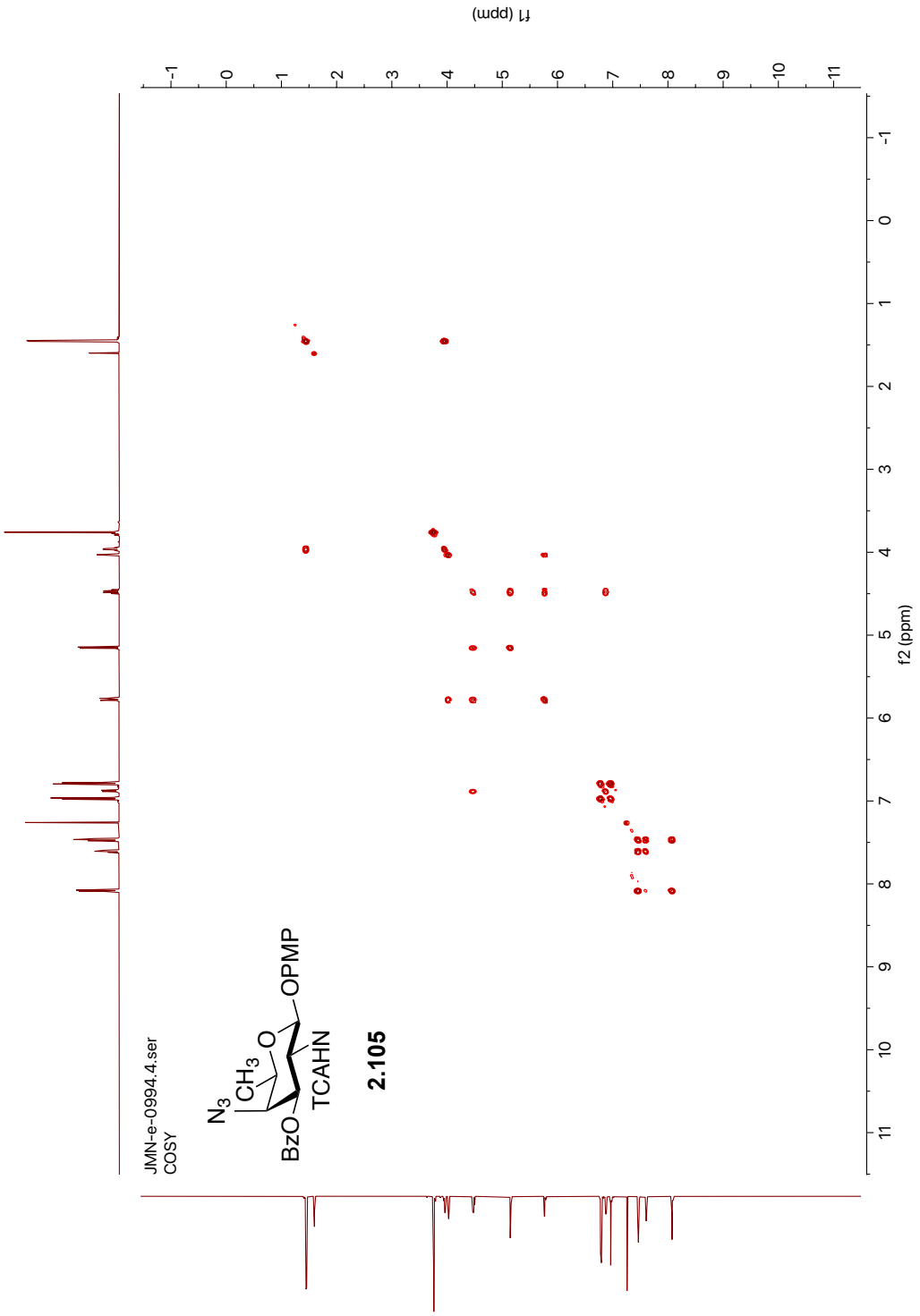

Figure A2.17. ^{1}H-^{1}H COSY NMR (600 MHz, $CDCl_3$) of compound **2.105**.

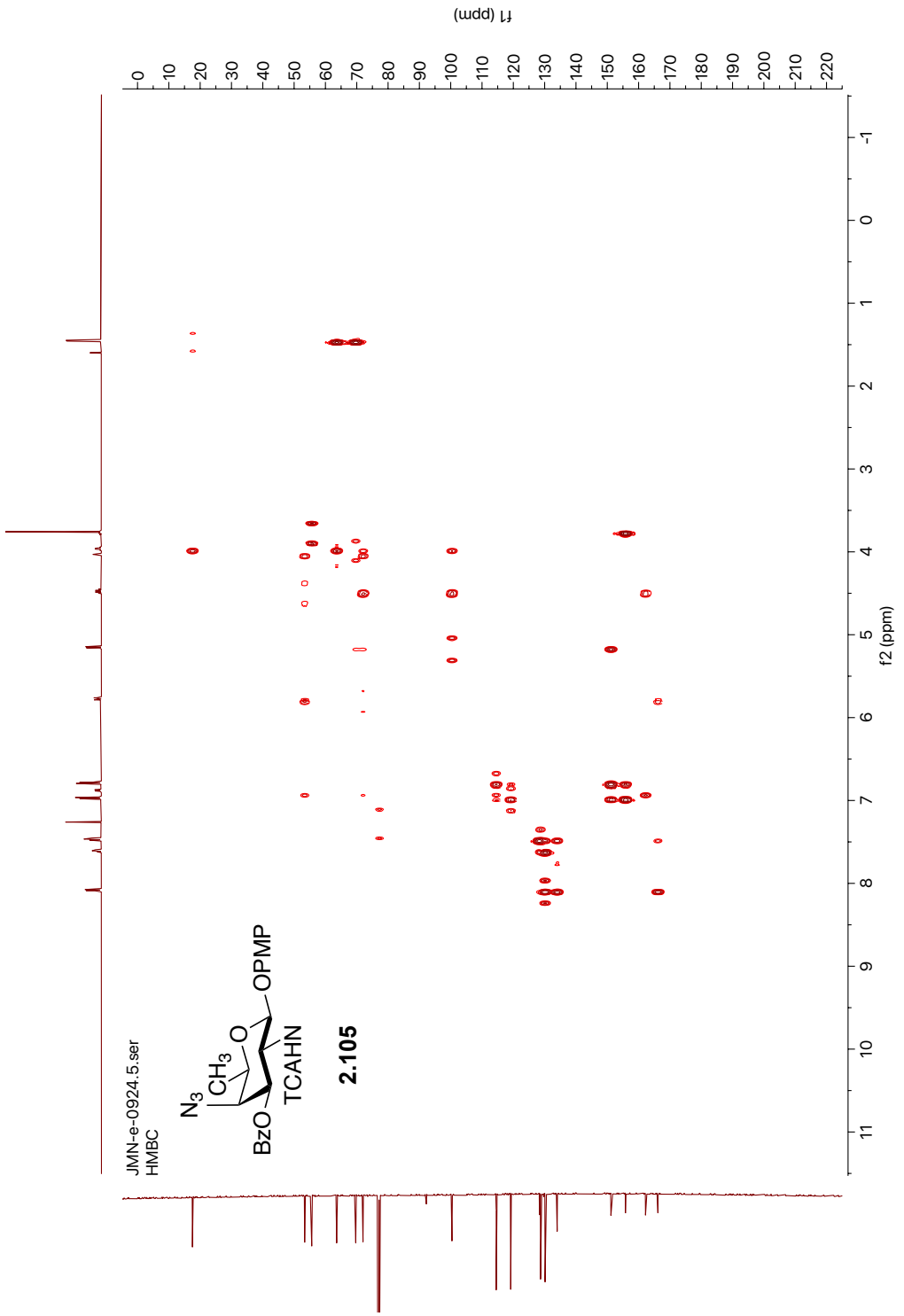

Figure A2.18. ^{1}H-^{13}C HMBC NMR (600 MHz, $CDCl_3$) of compound **2.105**.

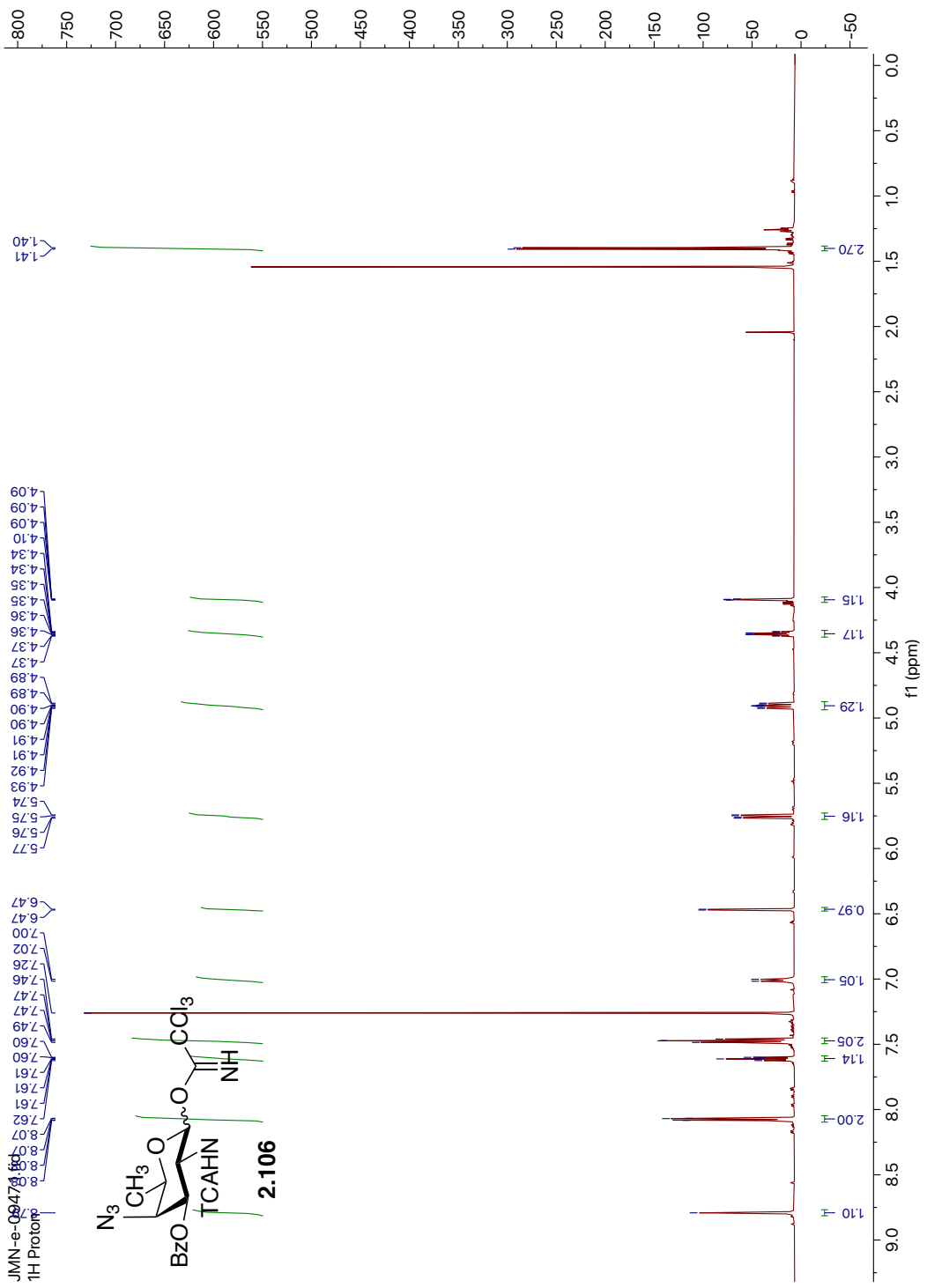

Figure A2.19. ^{1}H NMR (600 MHz, $CDCl_3$) of compound **2.106**

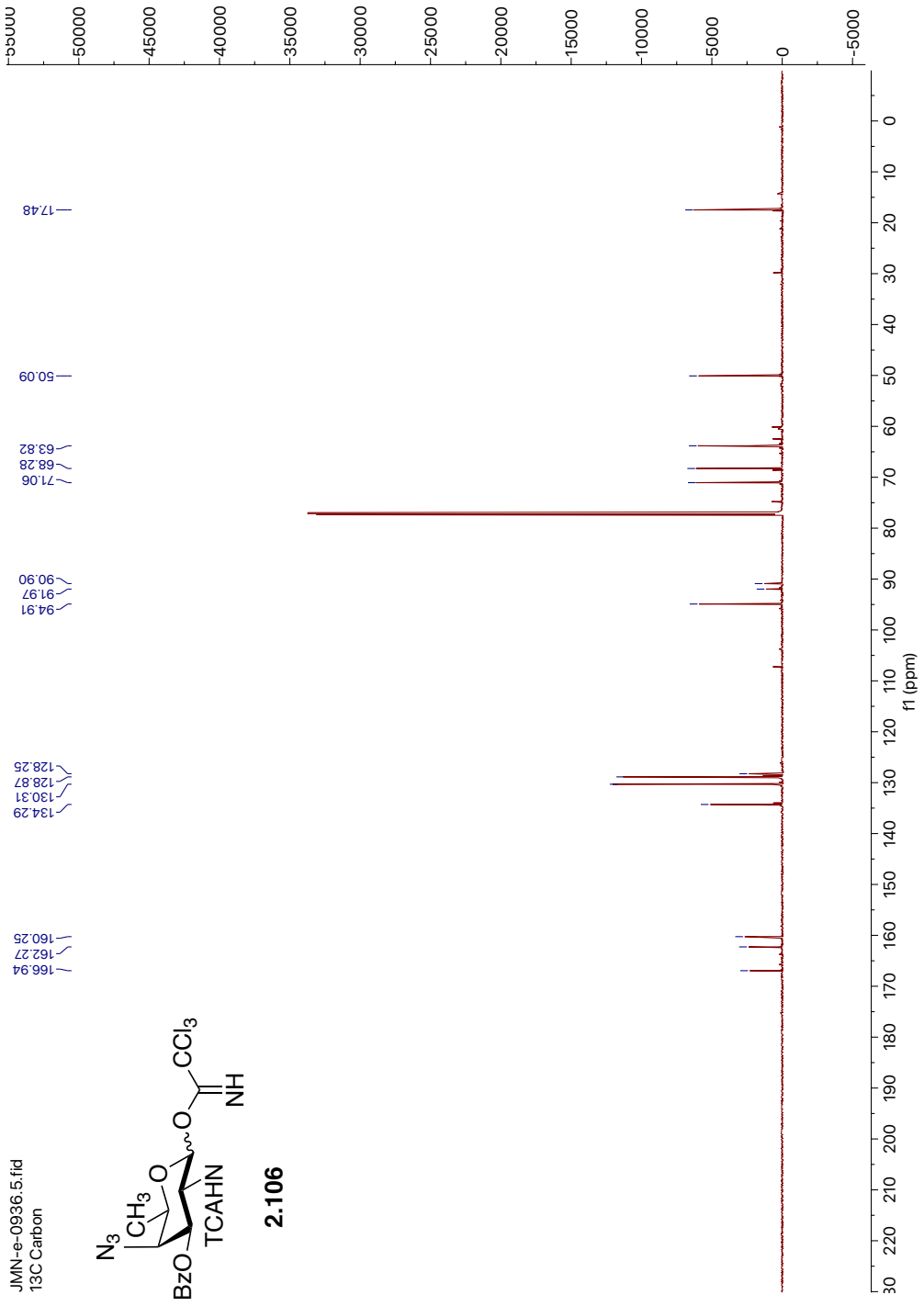

Figure A2.20. ^{13}C NMR (151 MHz, $CDCl_3$) of compound **2.106**

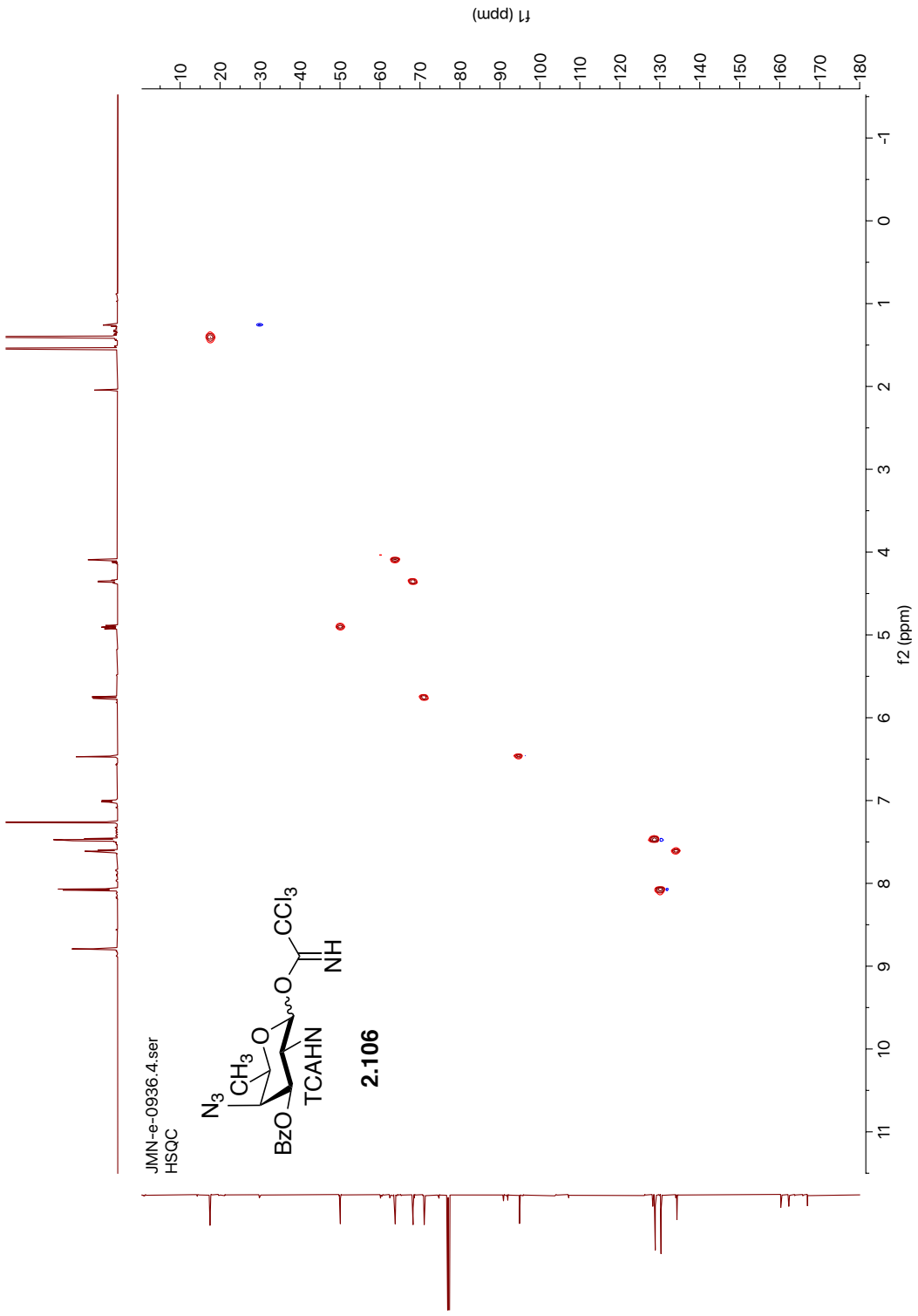

Figure A2.21. ^{1}H-^{13}C HSQC NMR (600 MHz, $CDCl_3$) of compound **2.106**.

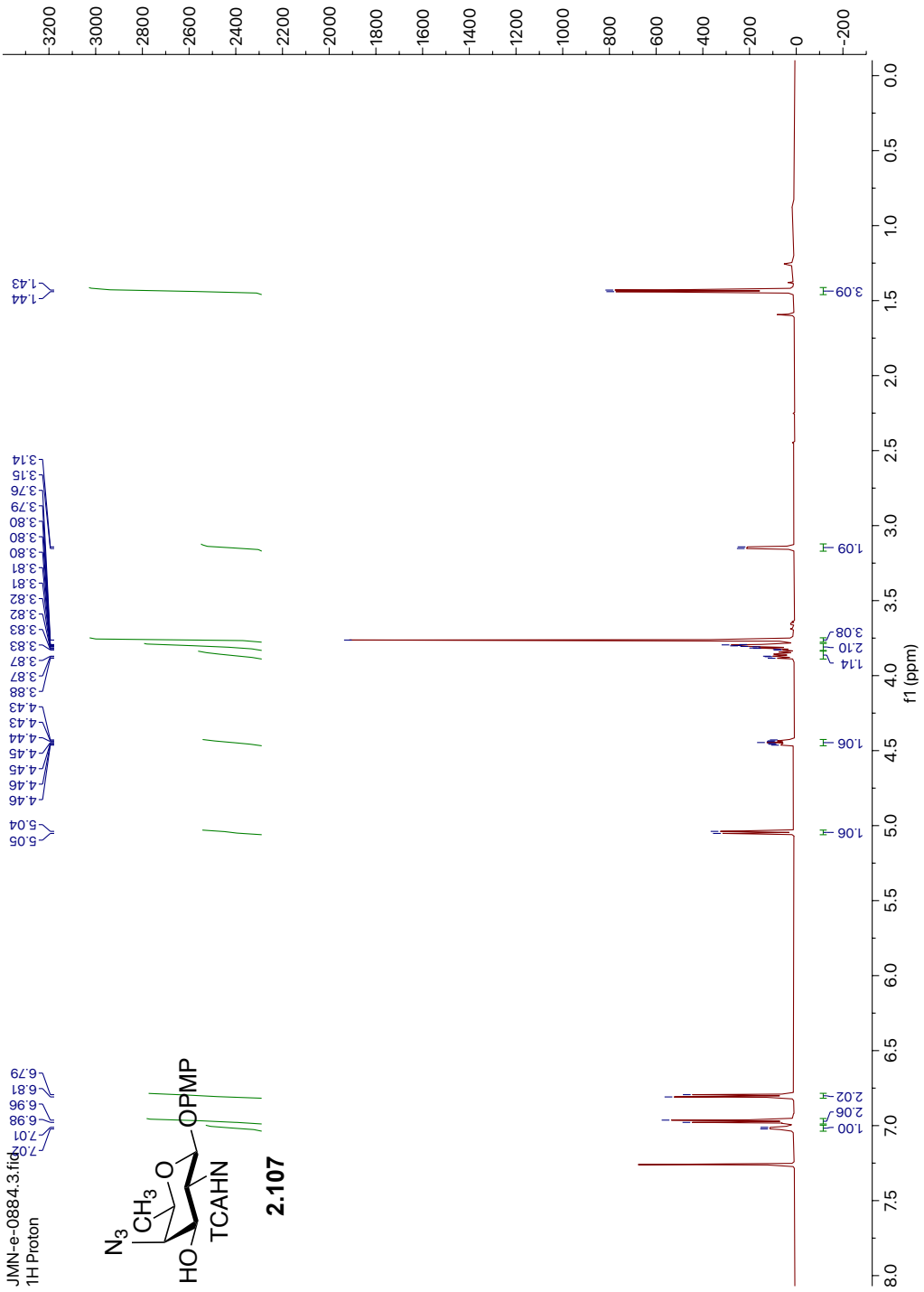

Figure A2.22. ^{1}H NMR (600 MHz, $CDCl_3$) of compound **2.107.**

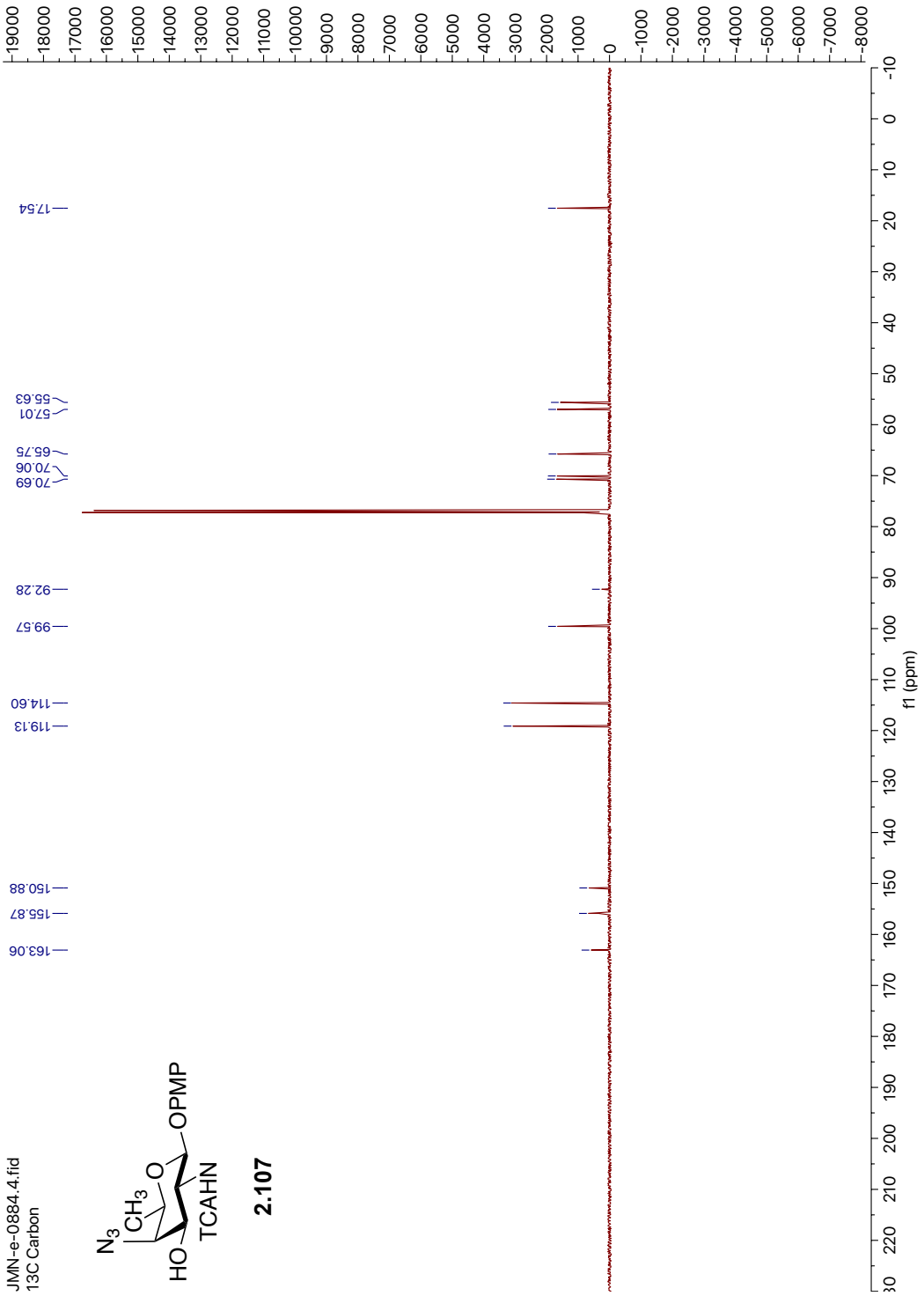

Figure A2.23. ^{13}C NMR (151 MHz, $CDCl_3$) of compound **2.107**

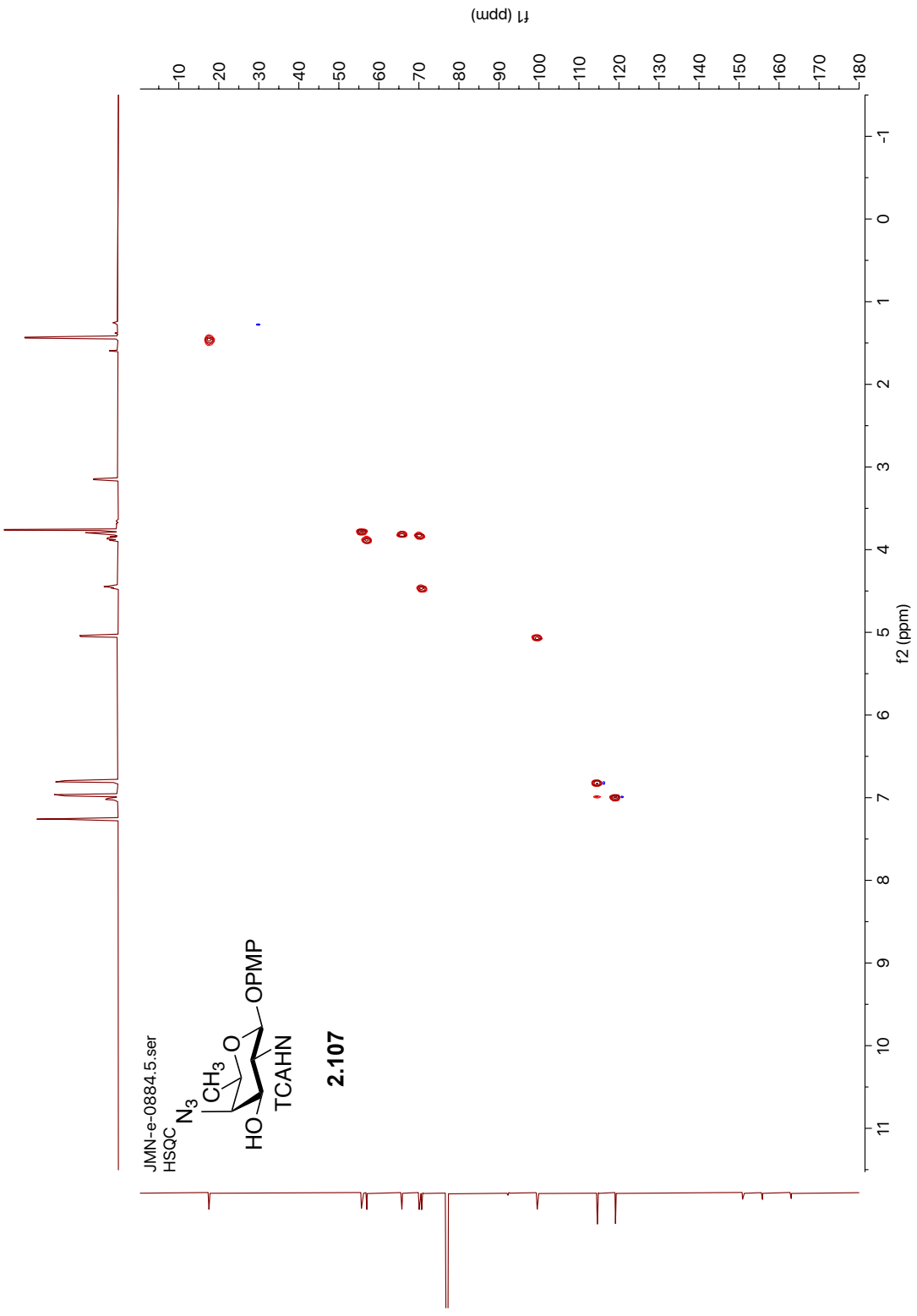

Figure A2.24. ^{1}H-^{13}C HSQC NMR (600 MHz, $CDCl_3$) of compound **2.107**

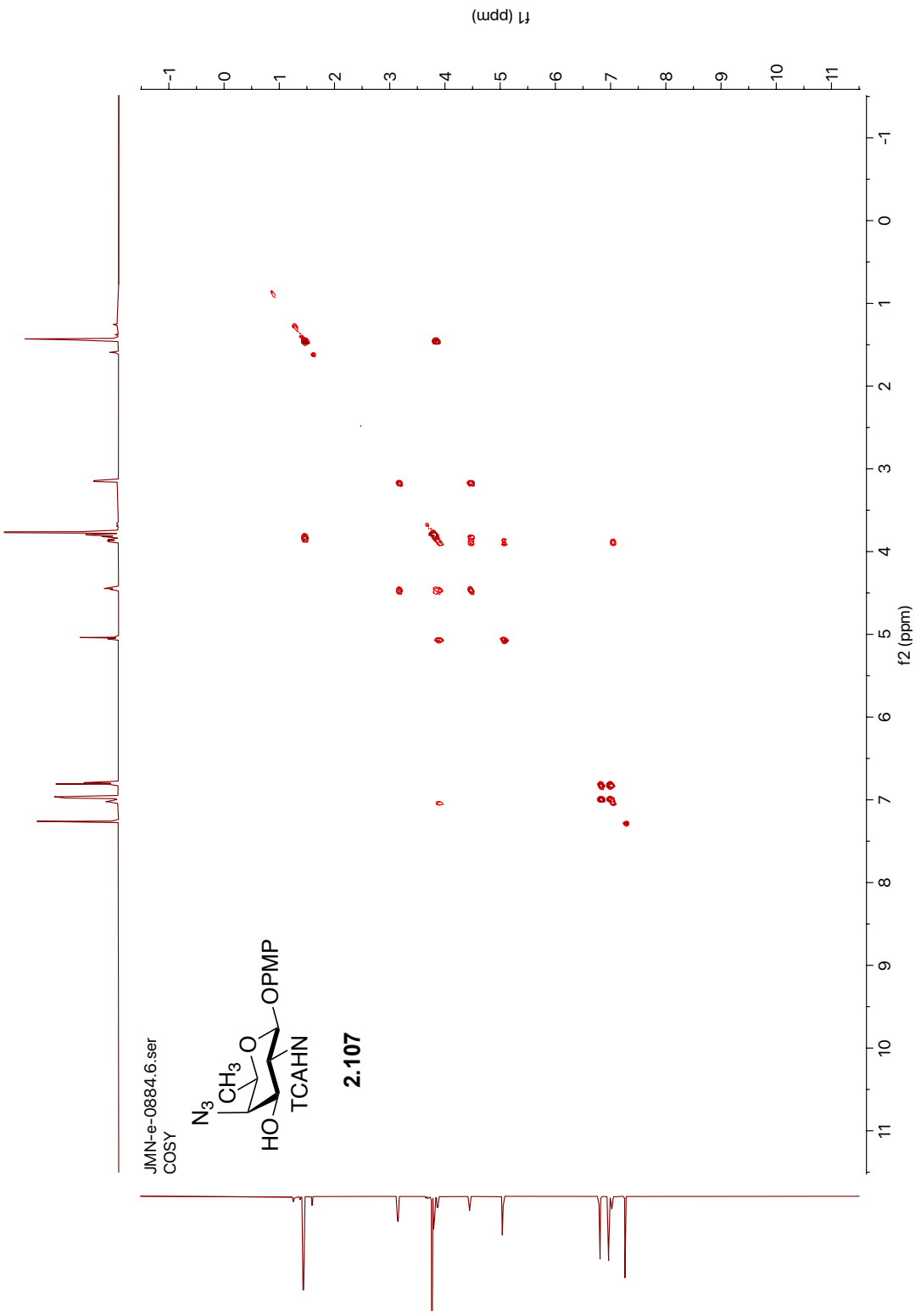

Figure A2.25. ^{1}H-^{1}H COSY NMR (600 MHz, $CDCl_3$) of compound **2.107**.

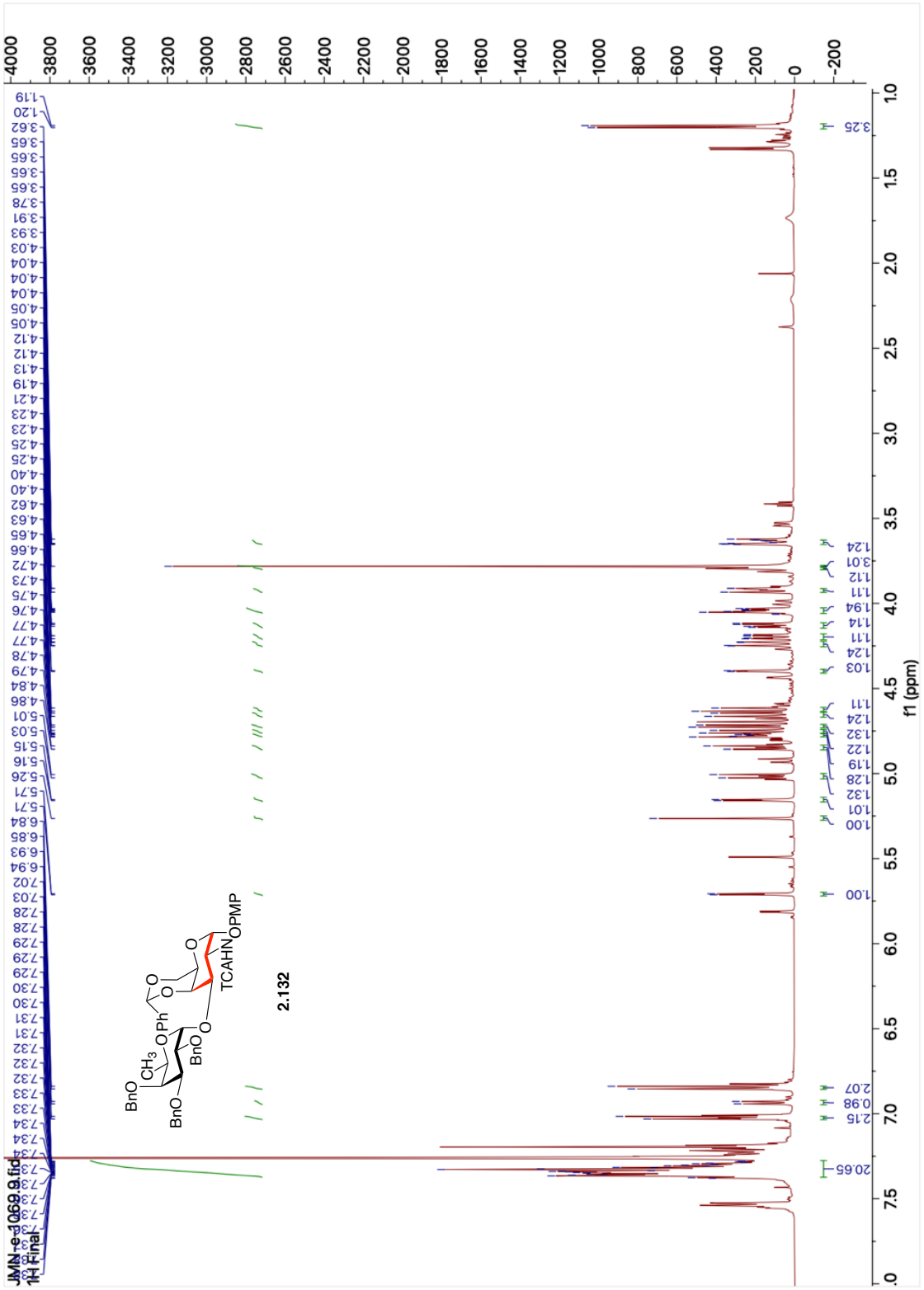

Figure A2.26. ^{1}H NMR (600 MHz, $CDCl_3$) of compound **2.132**.

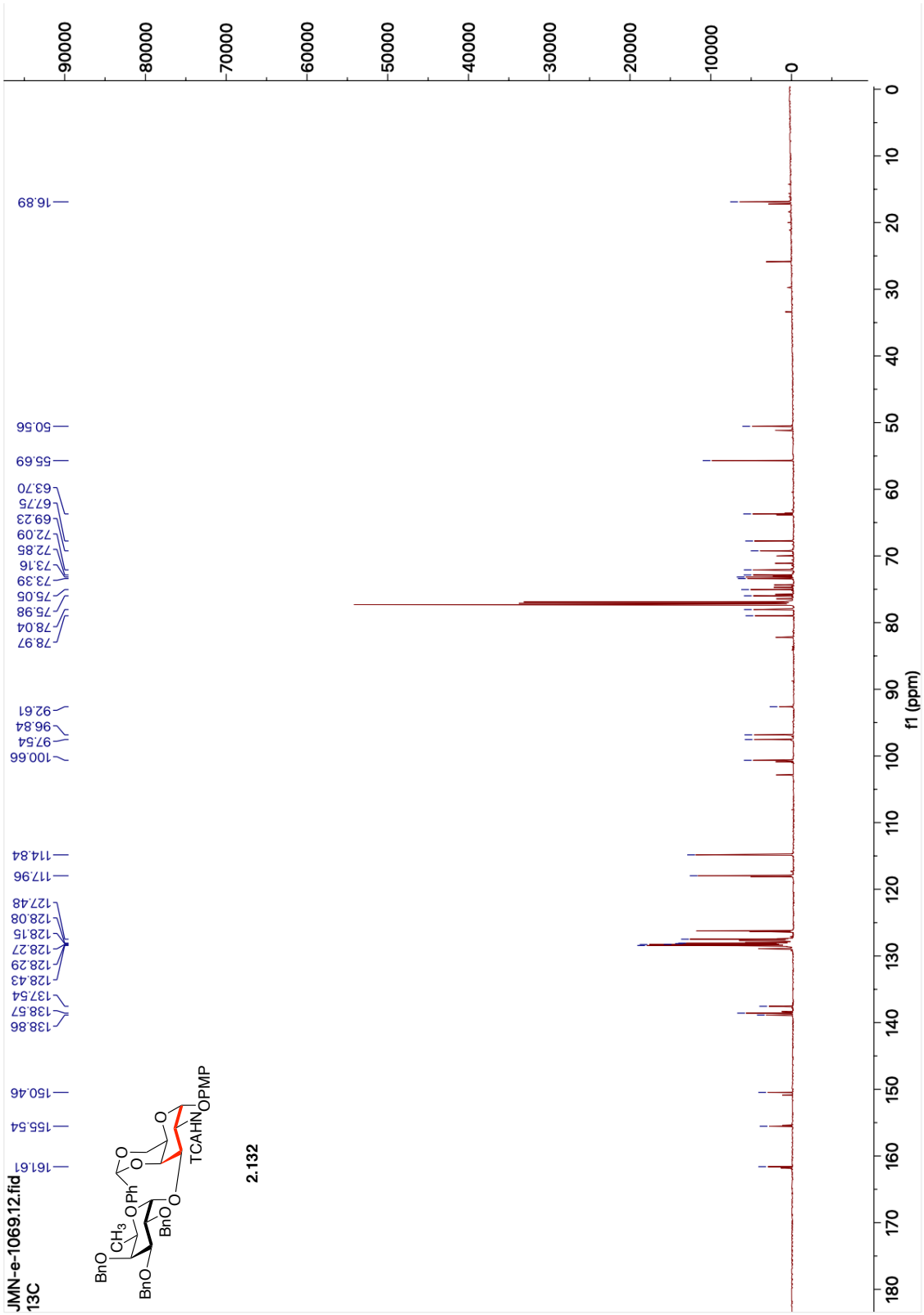

Figure A2.27. ^{13}C NMR (151 MHz, $CDCl_3$) of compound **2.132**.

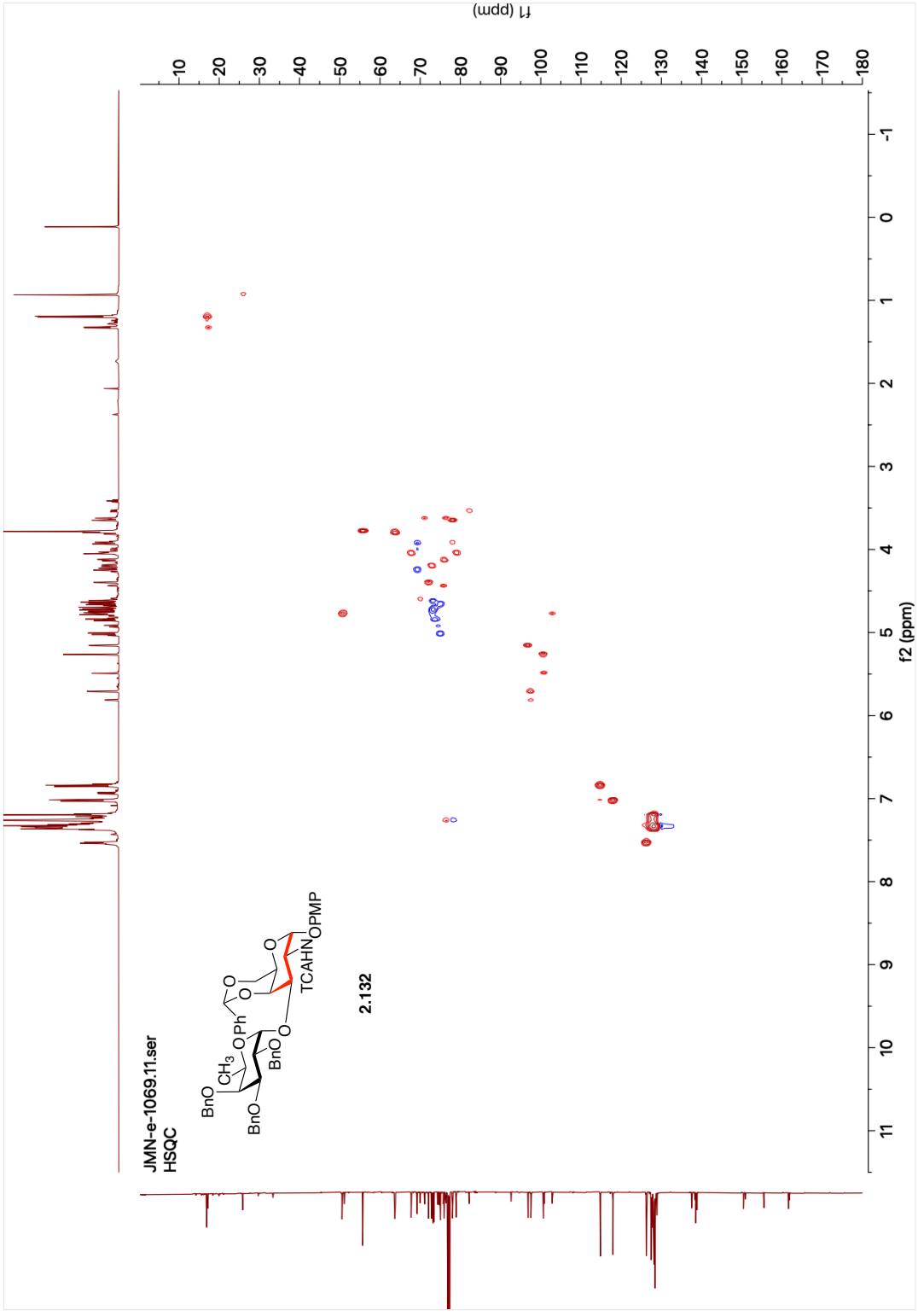

Figure A2.28. ^{1}H-^{13}C HSQC NMR (600 MHz, $CDCl_3$) of compound **2.132**.

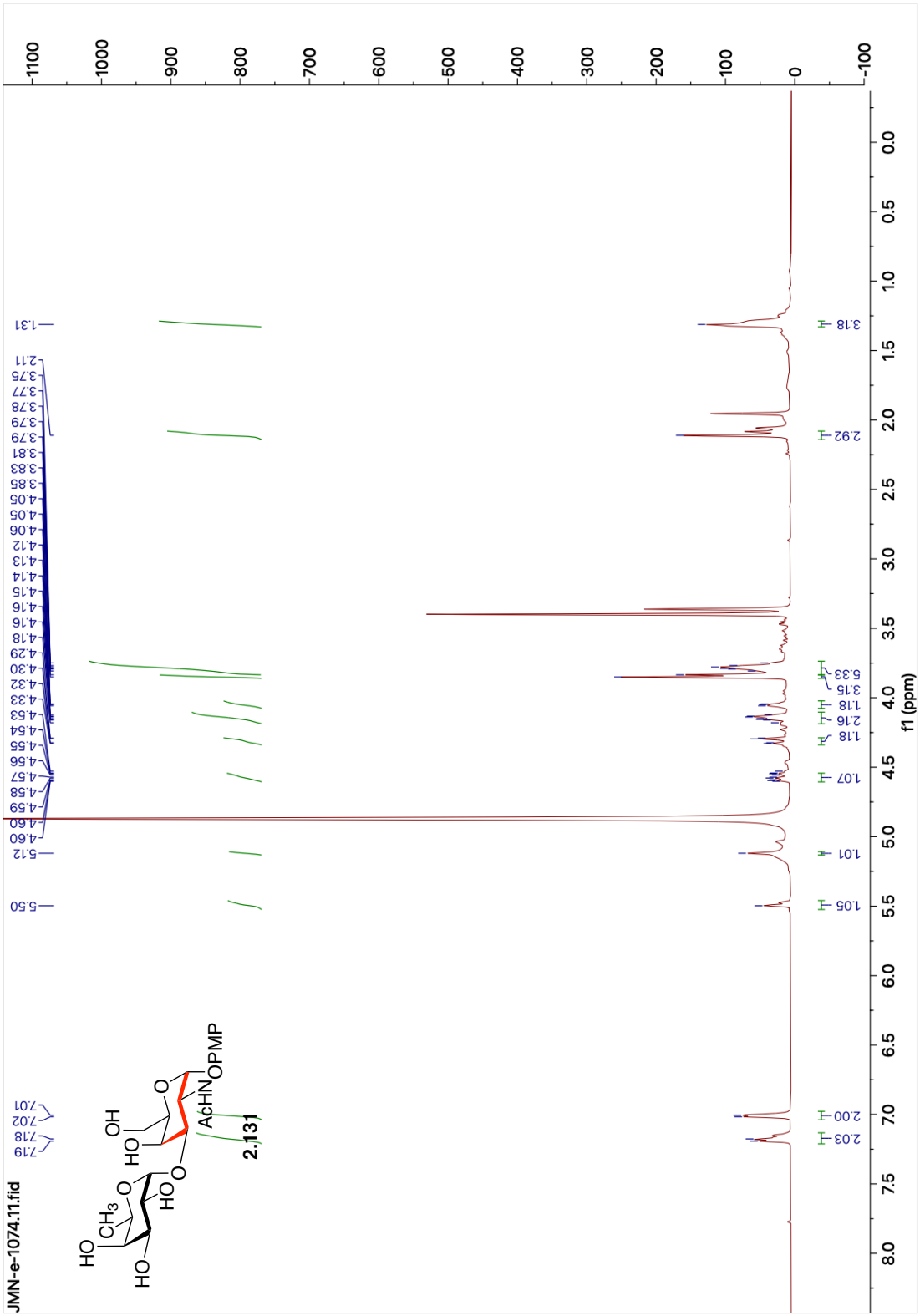

Figure A2.29. ^{1}H NMR (600 MHz, CD_3OD) of compound **2.131**.

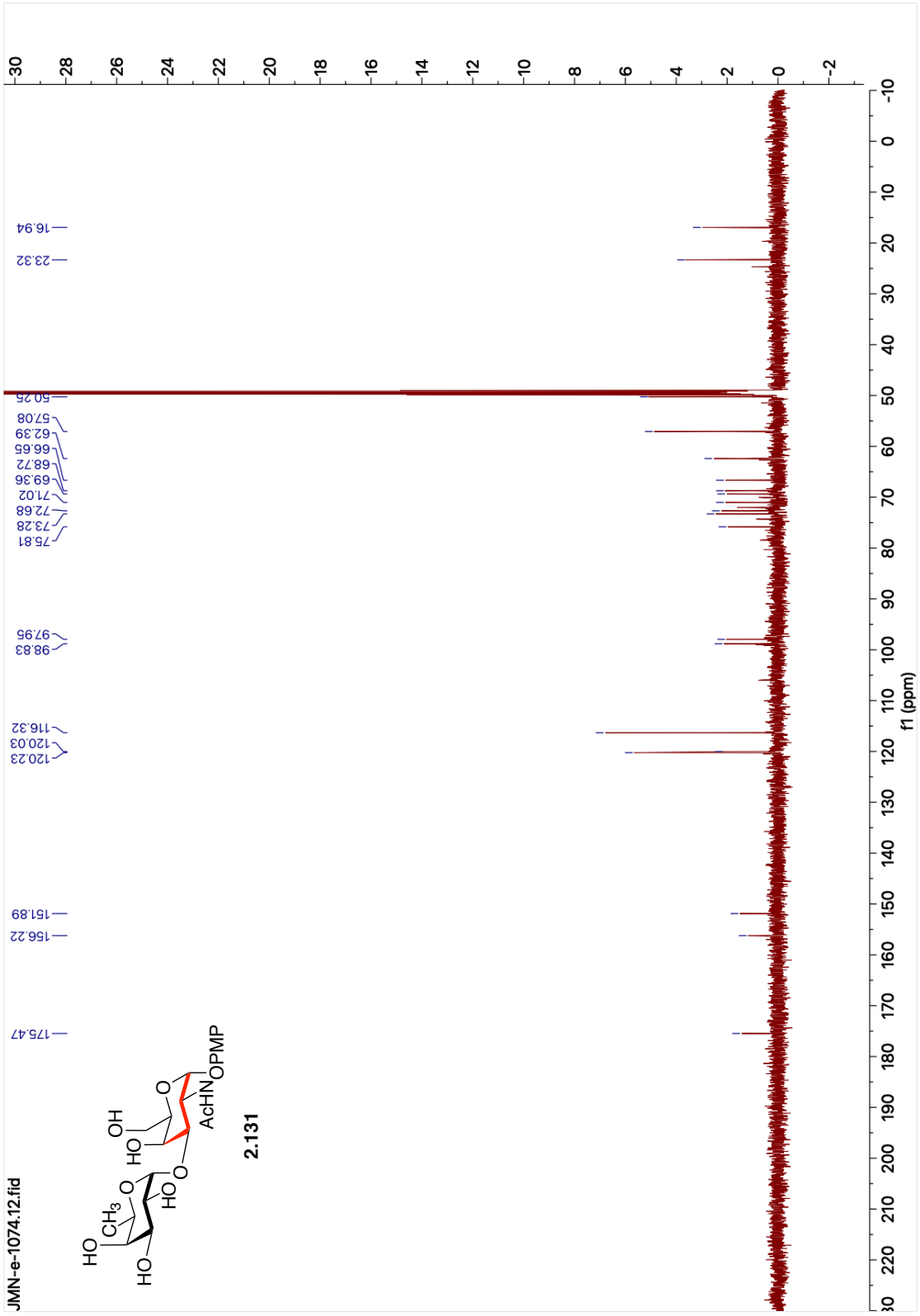

Figure A2.30. ^{13}C NMR (151 MHz, CD_3OD) of compound **2.131**.

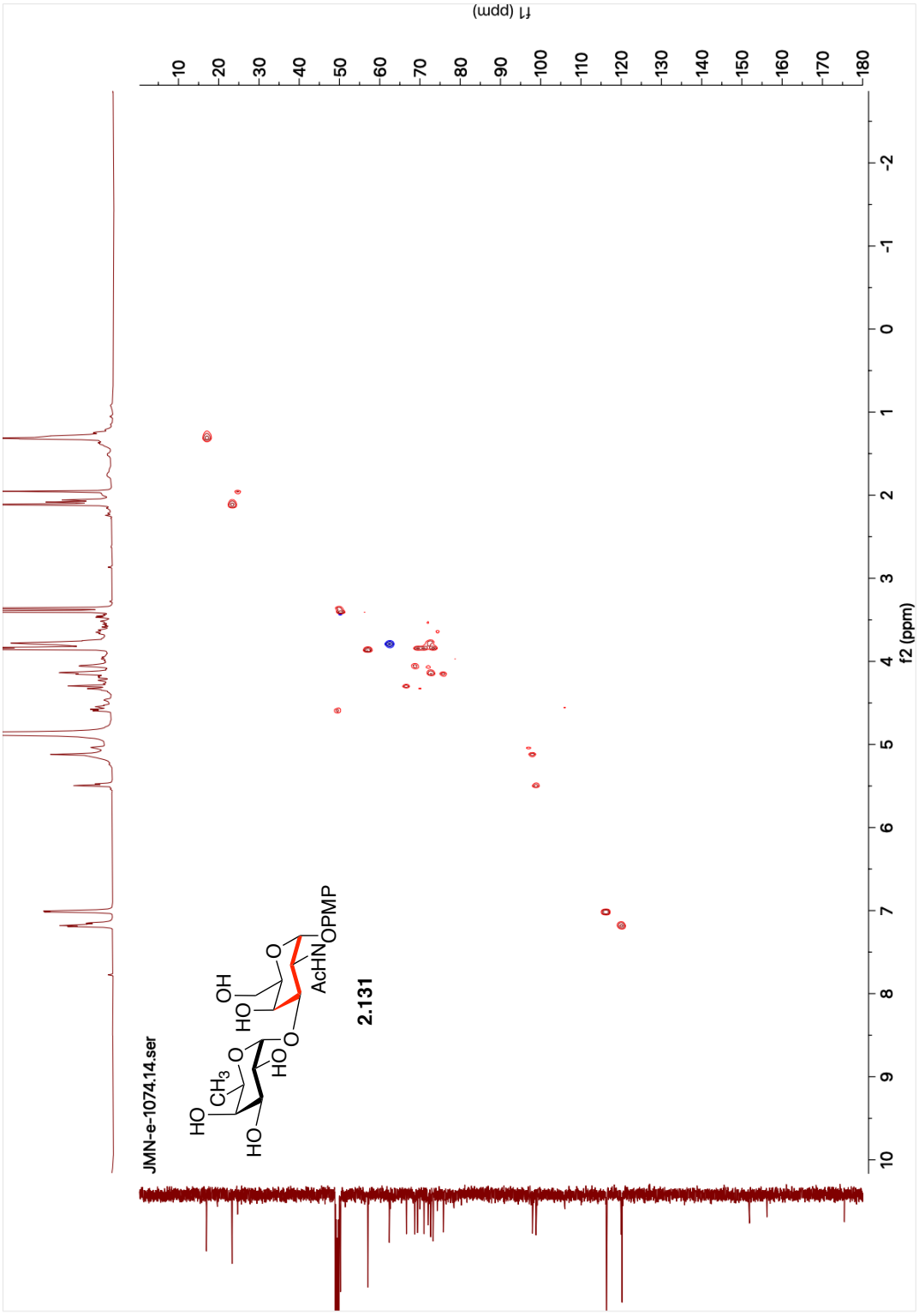

Figure A2.31. ^{1}H-^{13}C HSQC NMR (600 MHz, CD_3OD) of compound **2.131**.

Table A2.1. ^{1}H and ^{13}C NMR chemical shifts (ppm) between isolated polysaccharide and synthetic **2.131**.

Residue		Chemical shifts (ppm)					
		H-1/C-1	H-2/C-2	H-3/C-3	H-4/C-4	H-5/C-5	H-6/C-6
→3-α-D-Fuc*p*-(1→	Isolated	5.04	3.88	3.88	4.06	4.00	1.24
		97.2	68.0	80.7	72.7	68.0	16.6
→3-β-D-Gal*p*NAc-(1→	Isolated	4.60	4.10	3.81	4.16	3.69	3.80
		104.2	52.3	77.3	65.6	76.0	62.1
→3-α-D-Fuc*p*-(1→	Synthetic	5.10	4.05	3.83	3.82	3.84	1.31
		97.9	68.7	73.2	71.0	69.3	16.9
→3-β-D-Gal*p*NAc-(1→	Synthetic	5.50	4.62	4.30	4.14	3.75	3.79
		98.8	50.2	66.7	75.8	72.6	62.3
Chemical shifts for NAc are ^{1}H 2.11 and ^{13}C 23.3/175.4							

Chapter 3

Total Syntheses of Zwitterionic Polysaccharide Repeating Units

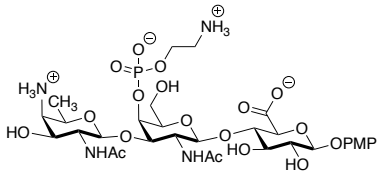

***Photorhabdus temperata ssp.* Cinereal 3240 ZPS Repeating Unit**

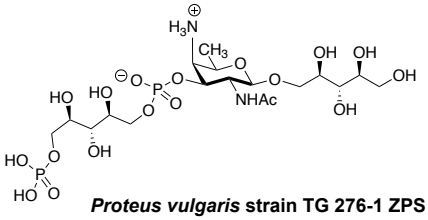

***Proteus vulgaris* strain TG 276-1 ZPS Repeating Unit**

3.1 Introduction

Zwitterionic polysaccharides (ZPSs), an emerging class of carbohydrate antigens with novel T-cell activation capability, have gained interest from the scientific community due to the role of cell surface glycans in pathogenesis.[1-7] Advances in glycobiology have shown how glycan-protein molecular recognition processes play a role in the body's adaptive immune response to pathogens.[3-4] Contrary to nonspecific innate immune responses that prevent the spread of foreign pathogens throughout the body, the adaptive immune response mounts a pathogen-specific response by initiating the production and activation of T-cells and B-cells. In the adaptive immune response, carbohydrates were conventionally thought to be T-cell independent antigens due to their inability to modulate a T-cell response. These carbohydrates activate B-cells through cross-linking of cell receptors, which leads to the production of low affinity immunoglobulin M (IgM) antibodies (Figure 3.1).[5-6] T-cell independent responses are less robust than T-cell dependent responses and short-lived.

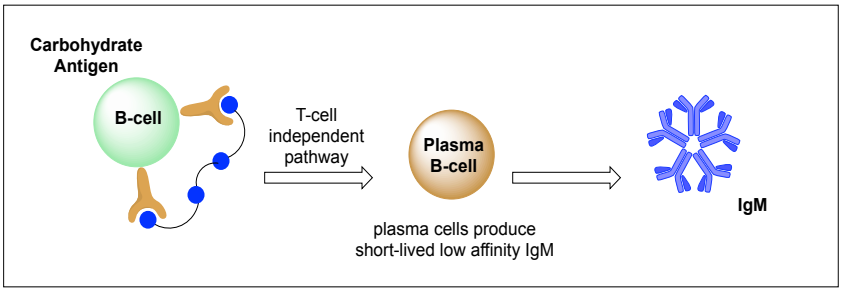

Figure 3.1. Carbohydrates bind B-cell receptors, initiating a weak T-cell independent response.

To access high-affinity immunoglobulin G (IgG) antibodies, class switching from IgM to IgG antibodies must be accomplished, in which B-cells must interact with helper T-cells. To overcome this challenge, carbohydrates have been

conjugated to carrier proteins, such as keyhole limpet hemocyanin (KLH), which induces a T-cell dependent immune response that results in the production of IgG antibodies and memory B-cells.[8-13] However, carrier proteins can be deleterious to carbohydrate immunity as protein-based immune responses can invalidate antibodies directed at the targeted carbohydrate antigens. This results in suppression of immunity of the carbohydrate-specific antigens.[14-16]

A novel insight into glycan recognition by T-cells was disclosed by the Kasper group, when ZPSs were shown to bind to and be presented by major histocompatibility complex II (MHCII) to T-cells.[17] ZPSs have both a positive and negative charge in each repeating unit and can be processed by antigen-presenting cells (APCs) (Figure 3.2). Moreover, Kasper et al. confirmed that removal of either the negative or positive charge, or both, on ZPSs will lead to a T-cell independent pathway, which will cause ZPSs to lose its ability to activate T-cells.

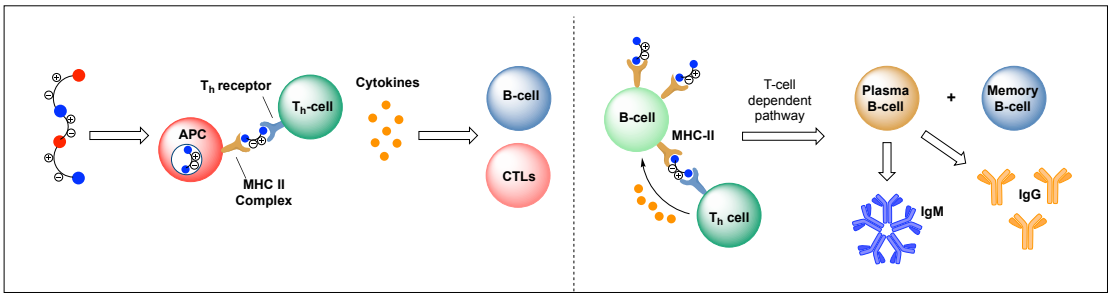

Figure 3.2. Zwitterionic polysaccharides induce a robust T-cell dependent response.

ZPSs are consumed, fragmented by APCs, and bound to MHCII complex via electrostatic interactions. Presentation on the cell surface allows the T-cell receptor of helper T-cells (T_h-cells) to bind to the antigen/MHCII complex resulting in a release of cytokines that activate cytotoxic T-cells (CTLs) and B-cells.[18-22] To acquire high affinity IgG antibodies, additional stimulation from activated T_h-cells to

antigen-bound B-cells leads to B-cell maturation and induces immunoglobulin class switching from IgM to polysaccharide-specific IgG and memory B-cell production. Production of memory B-cells is essential to acquiring a long-lasting immune response.

Zwitterionic glycan modifications, such as the incorporation of a phosphorus residue, govern host-pathogen interactions. Although it is recognized that this transformation play an important role to stimulate the host immune response, the purpose of phosphorus modifications on glycan remains unexplored in the literature. The inherent biological activity of ZPSs can be attributed to the three-dimensional structure of the polysaccharides with each repeating unit having a zwitterionic/alternating charge functionality in contrast to negative or neutral charge polysaccharides. Apart from the charge characteristic, the repeating units of these bacterial glycans are rich with highly immunodominant sugars like D-AAT (2-acetamido-4-amino-2,4,6-trideoxy-D-Galactosamine), D-GalNAc, D-Ribitol, and D-Gal (Figure 3.3). Specifically, D-AAT, as previously mentioned in Chapter 2, is an exclusively rare bacterial sugar that is not present in the human metabolism. Since the discoveries of ZPSs, various research groups around the world have taken up the challenging task of synthesizing these complex ZPSs, to acquire tools to study T-cell activation mechanism. Although these compounds' biological activity is striking, it is truthfully their molecular structure that piqued our group's interest as targets for total synthesis. Our group completed the first total syntheses of two zwitterionic repeating units, such as a 32-step synthesis of *P. temperata*[23-24] and a 33-step synthesis *P. vulgaris* repeating units, both with alternating charges adjacent

monosaccharides, which we believe is pertinent for immunological activity.

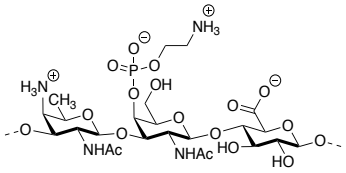

***Photorhabdus temperata ssp.* Cinereal 3240 ZPS**
3.1

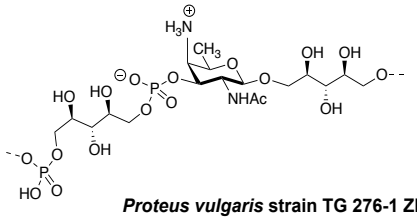

***Proteus vulgaris* strain TG 276-1 ZPS**
3.2

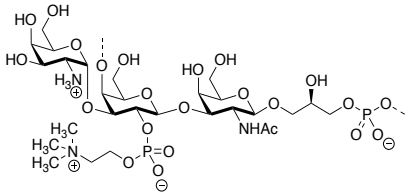

***Morganella morganii* ZPS**
3.3

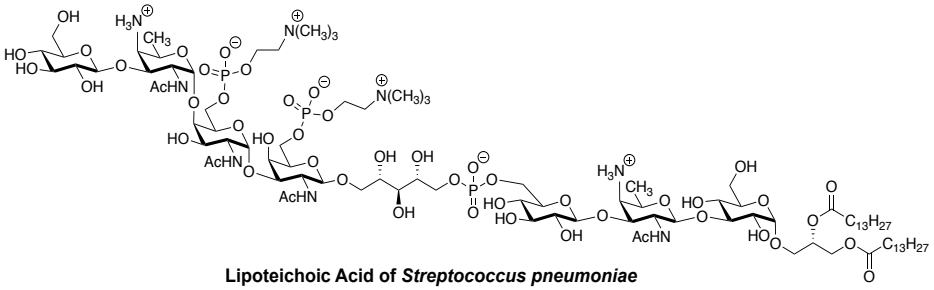

Lipoteichoic Acid of *Streptococcus pneumoniae*
3.4

Figure 3.3. Zwitterionic bacterial glycan structures featuring phosphorus residues.

3.2 Total Synthesis of Photorhabdus temperata ssp. Cinereal 3240 Trisaccharide Repeating Unit

Zwitterionic polysaccharides (ZPSs), such as PT-ZPS, is isolated from *Photorhabdus temperata*, a gram-negative bacterium through a tedious and strenuous multi-step procedure with low yield. The grand limitation of using naturally isolated PT-ZPS in studying the mechanistic details of T-cell activation at the micro level is its heterogenous polymer consisting of unknown lengths and sizes.[1-3] To better understand antigen uptake, processing, and presentation of PT-ZPS regarding MHC II by antigens presenting cells (APCs), acquiring well-characterized tools of defined lengths are the utmost of importance. The completion of a well-thought and executed synthetic route to access ZPS fragments for mechanistic studies will be the overarching theme of this chapter.

In 2019, phosphorylated zwitterionic polysaccharides, namely the *P. temperata* trisaccharide repeating unit, was selected as a formidable synthetic target for our group. Initially, we choose to pursue the total synthesis of PT-ZPS cassette predominantly because we wanted to build upon and apply the chemistry that was developed by our group, as well as to synthesize these complex ZPS fragments bearing unique phosphorus residues. Structurally, the trisaccharide cassette of PT-ZPS is composed of glucuronic acid (GlcA), *N*-Acetyl galactosamine (GalNAc), and the deoxy-amino sugar 2-acetamido-4- amino-2,4,6-trideoxy-D-galactopyranose (AAT). Our initial forays into PT-ZPS repeating unit synthesis began with a structural analysis of the molecule (Scheme 3.1).[24]

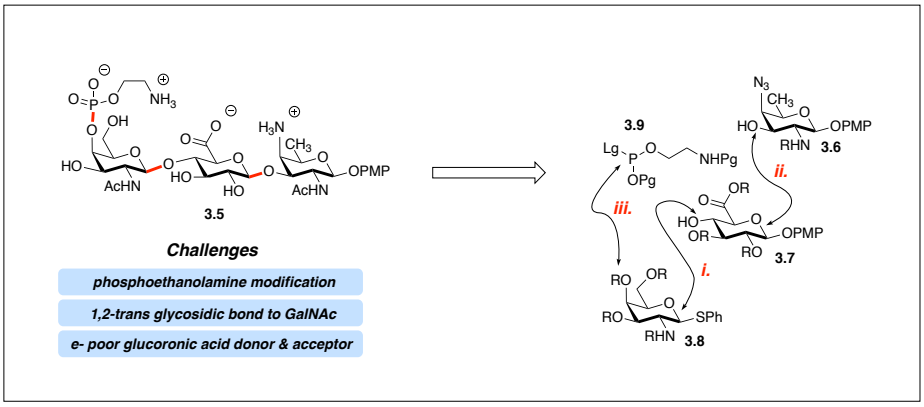

Scheme 3.1. First-generation analysis of PT-ZPS repeating unit.

When considering the structure of PT-ZPS repeating unit, several synthetic challenges become apparent. The repeating unit of *P. temperata* possesses two 1,2-trans-β-glycosidic bonds, which would require anchimeric assistance from an ester at C2 to govern the diastereoselectivity during this type of glycosidic bond formation reaction. In particular, we anticipated that installing phosphoethanolamine (PEtN) on the poorly nucleophilic and sterically hindered axial alcohol of the GalNAc residue would be puzzling.[25-26] While pioneering studies have clarified the difficulties in achieving such a transformation, most of these methods are not amendable to our synthetic route. Notwithstanding this bleak outlook, we hypothesized that we could mask the C2 amine as a trichloroacetamide to control diastereoselectivity and unmasking to reveal the native amide. The repeating unit have an unusual architecture featuring a PEtN and a glucuronic acid residue. Incorporation of these residues into the repeating unit of complex ZPSs are known to be synthetically challenging with limited chemistry that have been developed for these key transformations. Thus, we hope to develop a strategy for the preparation of phosphorylated ZPSs that would be amenable to the synthesis of other complex

ZPSs, such as the repeating unit of *P. vulgaris.*

A retrosynthetic strategy for the synthesis of PT-ZPS repeating unit is presented in Scheme 3.1. As a critical maneuver, we choose to introduce the PEtN (**3.9**) moiety at a late stage in the synthesis to facilitate the handling of key precursors and to avoid the early introduction of diastereomers affected by the central phosphorus residue. Thus, our first-generation approach to the repeating unit centered on the synthesis of frame **3.5**, where PEtN-modified sugar is at the nonreducing end to minimize steric hindrance related to the C4 alcohol. Furthermore, this route relied on the synthesis of three key building blocks (**3.6**, **3.7**, and **3.8**), which were readily available from carbohydrate starting materials (Scheme 3.1).

Our initial efforts toward the total synthesis of the repeating unit **3.5** focused on a linear [1+1] glycosylation strategy with donor **3.13** and acceptor **3.17**. The synthesis of the orthogonally protected D-galactosamine donor **3.13** began with TCA protection of the C2 amine of D-galactosmine **3.10**, followed by peracetylation of the intermediate provided compound **3.11** in 80% yield over two steps. Installation of thiophenol or thiotoluene at the anomeric position using the Lewis-acid BF_3•Et_2O gave **3.12**. Next, compound **3.12** was then subjected to Zemplén deprotection conditions to afford the triol. The triol was then regioselectively masked as its benzylidene acetal by means of benzaldehyde dimethyl acetal (BDMA) under camphorsulfonic acid (CSA). Finally, the compound was then protected with acetic anhydride in pyridine to obtain the desired donor **3.13** in 50-55% yield over three steps (Scheme 3.2A).

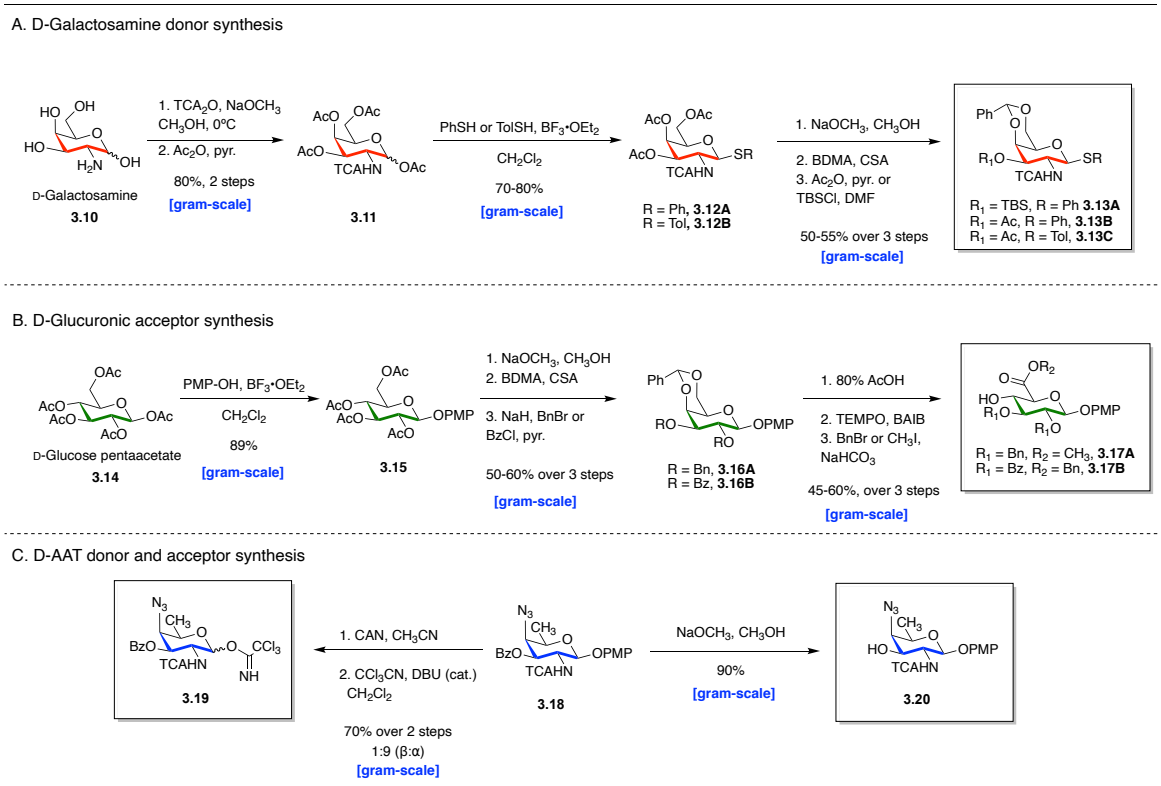

Scheme 3.2. Synthesis of building blocks **3.13**, **3.17**, and **3.19**.

In preparation for the union of **3.13** and **3.17**, it was necessary to synthesize analogues of acceptor **3.17** to find a compatible coupling partner that was not too electron deficient and rich in character. The second building block was synthesized from D-glucose pentaacetate **3.14**, which was converted to its *p*-methoxy phenol derivative **3.15**. Deprotection of the compound **3.15** led to the formation of tetraol. Similar to the synthesis of building block **3.13**, a benzylidiene acetal protection of the tetraol was required and completed under acidic conditions. Subsequent benzylation or benzoylation provided compound **3.16** in 50-60% over three steps. At this juncture, we decided that we needed to install the carboxylic acid functionality early on in our building block synthesis phase to avoid a late-stage oxidation step

that could be deleterious to a more complex trisaccharide scaffold. A reliable method for the synthesis of the glucuronic acid acceptor **3.17** would entail a tempo-catalyzed oxidation with (Diacetoxyiodo) benzene (BAIB). Removal of the benzylidene acetal followed by oxidation and esterification of the intermediate gave **3.17**, which can be unmasked to provide the carboxylic moiety during the final global deprotection steps (Scheme 3.2B).

One of the early challenges that we faced in our synthesis of the PT-ZPS repeating unit was the procurement of the rare deoxy-amino sugar, AAT (**3.18**). Although a quick survey of the literature showed that this building block was

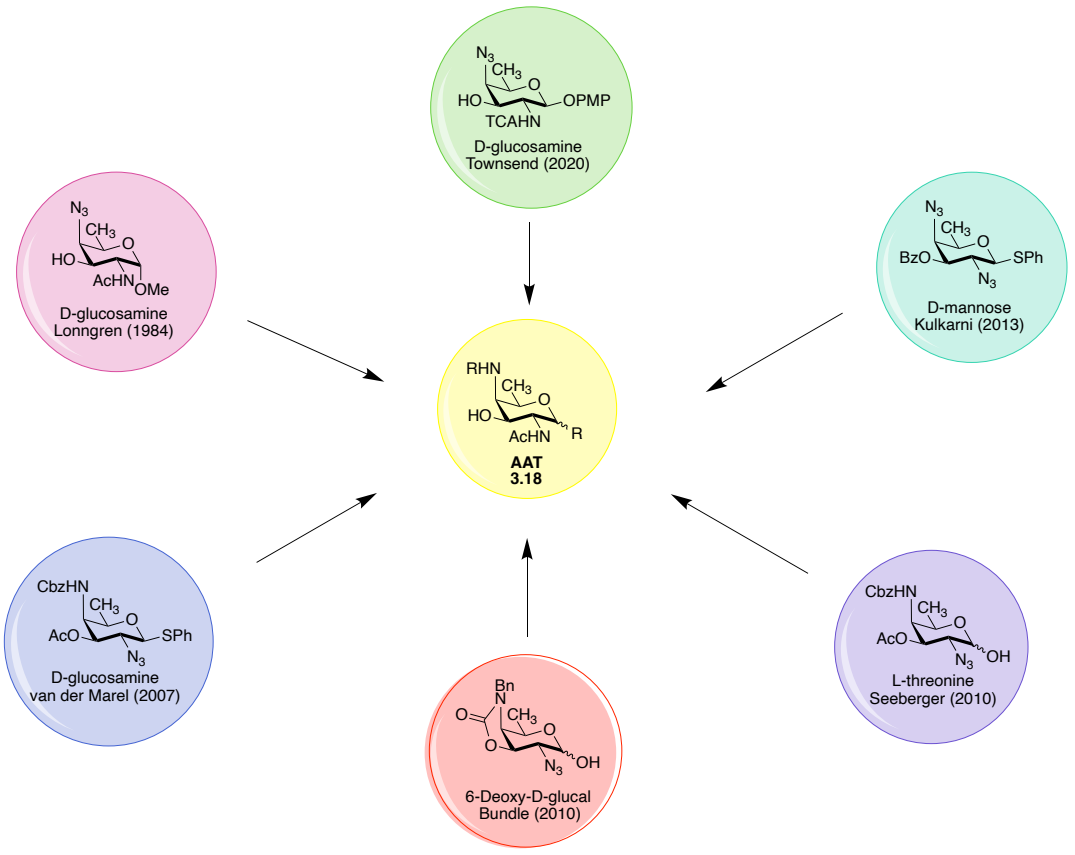

Figure 3.4. Previous syntheses of AAT building block

previously synthesized by various groups, there was minimal examples shown of a participating group at C2 for β-selective glycosylation.[27-33] Majority of the known published route relied on a late-stage reduction of an azide followed by acetylation to access the amide in the native polymer (Figure 3.4). The disadvantage in this strategy comprises of harsh reaction conditions that are incompatible with several functional groups and the incorporation of additional concession steps. Our initial endeavor for the synthesis of AAT resulted in three strategies that ended in disappointment, whereas the reserve strategy, though it teetered on the edge of despair, proved to be successful. In fact, the first glimmer of hope came nearly after 7 months of darkness. Our successful route toward AAT was previously mentioned in chapter 2, where we disclose an efficient and scalable method to access both AAT donor (**3.19**) and acceptor (**3.20**, Scheme 3.2C).

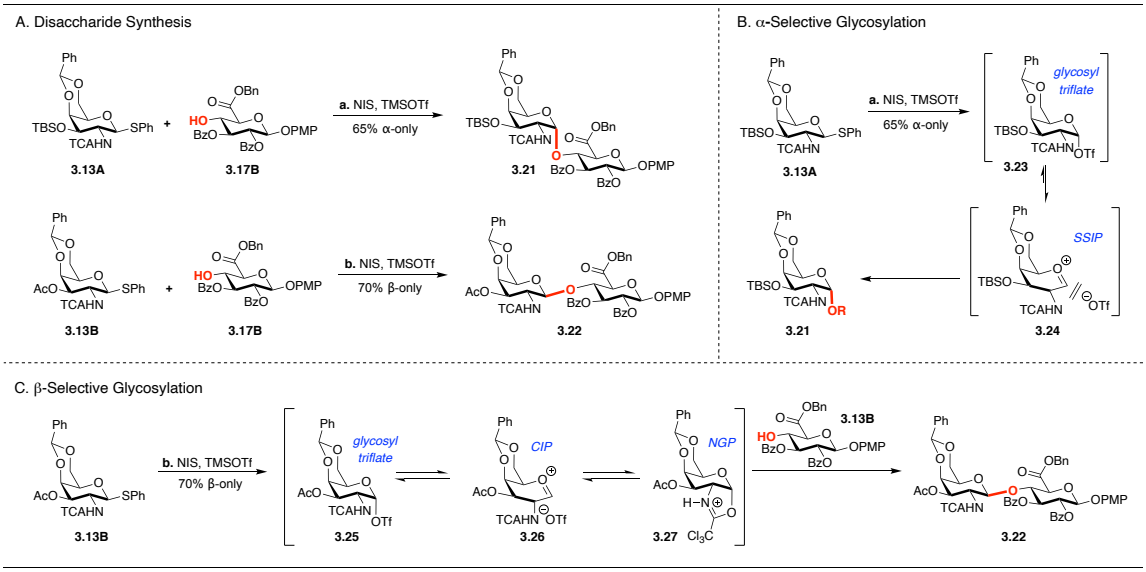

Scheme 3.3. C-3 directed glycosylation

With all the key fragments in hand, we next investigated the viability of the glycosylation reaction (Scheme 3.3A). Upon exposure to NIS/TMSOTf mediated conditions, thioglycoside donor **3.13A** and glucuronic acceptor **3.17B**[33] underwent a [1+1] glycosylation to afford disaccharide **3.21** in 65 % yield. While the glycosylation reaction was successful, it did not provide the desired β-selectivity that one would have hoped for with a C-2 trichloroacetamide participating group. Instead, an α-anomer as the sole diastereomer was isolated.[34-35] Despite this uninviting outlook, we hypothesized that the selectivity was guided by a torsional effect from the 4,6-*O*-benzylidene acetal, modification of the donor **3.13** (i.e., exchange of the silyl ether for an electron withdrawing acetate) generated the desired β-anomer **3.22** in 70% yield. Although protecting groups shields undesired sites from reaction during a reaction, it is known that they can have a deleterious effect on the reactivity of the molecule. With the initial success, a more detailed study and optimization of the direct coupling was pursued. The undesired α-selectivity had previously been documented by Fraser-Reid and co-workers, where they reasoned that observed 4,6-*O* benzylidene acetals have a disarming (retarding oxocarbenium ion formation) effect on the hydrolysis of *O*-pentenyl glycosides.[36-37]

Nevertheless, this effect was accredited to the increased torsional strain in the fused bicyclic system as the chair−chair glycosyl donor collapses to an intermediate chair−boat oxocarbenium ion.[38-41] Regrettably, employing this logic to the selectivity observed in the synthesis of **3.21** and **3.22** is contradictory since both donors **3.13A** and **3.13B** contain a benzylidene acetal protecting group. As a result, we postulated that an electronic element from C3 was governing the

diastereoselectivity. In detail, the plausible mechanism is shown in Scheme 3.3B, upon activation of the thioglycoside donor **3.13A** by NIS/TMSOTf, we speculated that an electron donating silyl ether at C-3 would destabilize the intermediate glycosyl triflate **3.23**. Consequently, we expected a shift in the covalent α-glycosyl triflate **3.24** solvent-separated ion pair (SSIP) equilibria to favor an α-selective SSIP.

Further analysis would suggest that in the β-selective case (Scheme 3.3C), the result is best described as the C3 acetate imparting a moderate electron-withdrawing effect, which acts to increase the energetic barrier between a covalent glycosyl triflate and the oxocarbenium ion, resulting in a diminished concentration of the SSIP. While disappointing, we did acquire some intelligence into the shortcomings of this reaction. Analysis of the β-selective pathway suggests that one would anticipate the reactive intermediate to be present in the form of a α-glycosyl triflate **3.25**, contact ion pair (CIP) **3.26**, or an oxocarbenium ion **3.27** stabilized through anchimeric assistance. Therefore, we believe that in each of these cases, an increased in β-selectivity would be observed. We mention that this analysis is hypothetical at this juncture and spectroscopic studies are ongoing to characterize the pathways involved in producing the diverging selectivity.

Returning to the synthesis of trisaccharide **3.29**, the methods of Adamo and co-workers for oxidative cleavage of the PMP acetal was successful upon exposure to ceric ammonium nitrate (CAN) to release the anomeric alcohol.[42] Since the use of trichloroacetimidate are adorned in the literature, we had hoped it might be possible to unite donor **3.28** with AAT acceptor **3.19** (Scheme 3.4).

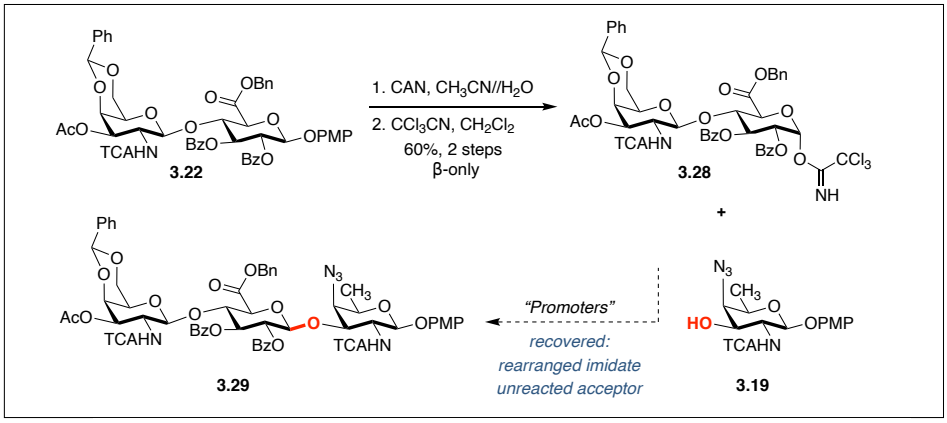

Scheme 3.4. Failed synthesis of the trisaccharide core **3.29**

Chemistry developed and elegantly presented by Boons and co-worker showed trichloroacetimidate donors would allow for productive glycosylation.[43] Following the conversion to donor **3.28**, we were surprised by our inability to unite donor **3.28** with AAT acceptor **3.19** under a multitude of Lewis and Brønsted acidic reaction conditions. It is tempting to consider that the presence of a uronic acid moiety could impart an electronic element in destabilizing the oxocarbenium ions. It was quickly discovered that the ester protecting groups at C2 and C3 would also render the Boons approach intractable. Furthermore, exchange of all benzoates for electron-rich benzyl ethers also failed to furnish any of the desired coupled product. Thus, we realized that a frame shift in the repeating unit would be needed for a successful total synthesis of PT-ZPS repeating unit.

After the next frame shift was selected, a screen of new building blocks and optimal solvent conditions to promote a β-selective glycosylation was undertaken. Our new retrosynthetic analysis is shown in Scheme 3.5. A defining aspect of the second-generation approach consists of moving the AAT building block to the nonreducing end of the repeating unit **3.30**, a maneuver that jettisoned the

glucuronic acid monosaccharide as both an acceptor and donor. While we had carefully tackled the glucuronic acid glycosylation issue, we would now need to

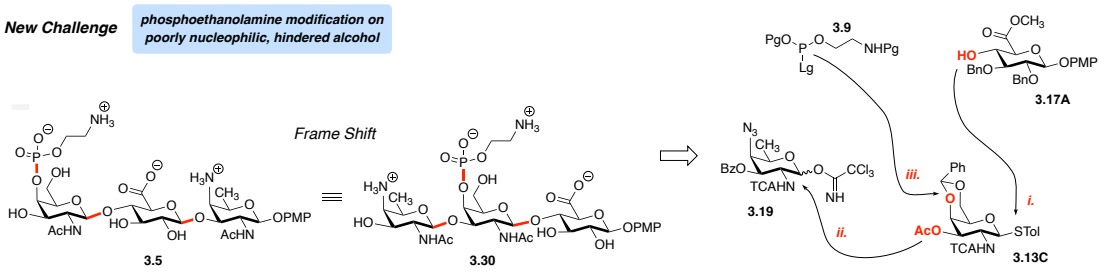

Scheme 3.5. Successful second-generation approach

install the phosphorus residue on a very sterically hindered alcohol.

Undeterred, individual monosaccharides were designed to be more reactive and surpass previous problems encountered during our first-generation approach. While we were able to form the β-linkage of **3.31** with donor **3.13C** and acceptor **3.17A**, the resultant diastereomeric ratio was not appreciated. An assessment of the coupling system showed that extended reaction time did not provide better diastereoselectivity nor improve the overall yield. Although conducting the coupling at warmer temperatures was significantly more productive (72%), the diastereoselectivity suffered, dropping to 2:1. After several abortive attempts, we were able to access a tractable route to **3.31** by using TfOH as the promoter at −78

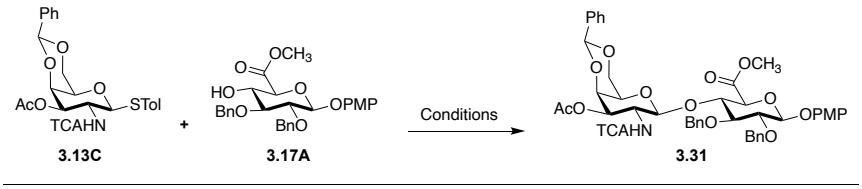

Entry	Conditions	Yield %	β, α-ratio
1	TMS-OTf, -78ºC, CH_2Cl_2	48	β
2	TMS-OTf, 0ºC-rt, CH_2Cl_2	72	2:1
3	TfOH, -78ºC, CH_2Cl_2-CH_3CH_2CN (4:1)	91	4:1

Table 3.1. Optimization of glycosylation reaction

°C in a CH_2Cl_2/CH_3CN solvent system with a 4:1 β/α ratio in 91% yield (Table 3.1). With **3.31** in hand, an acetate deprotection could be accomplished under Zemplén condition to obtain acceptor **3.32** in near quantitative yield (Scheme 3.6).

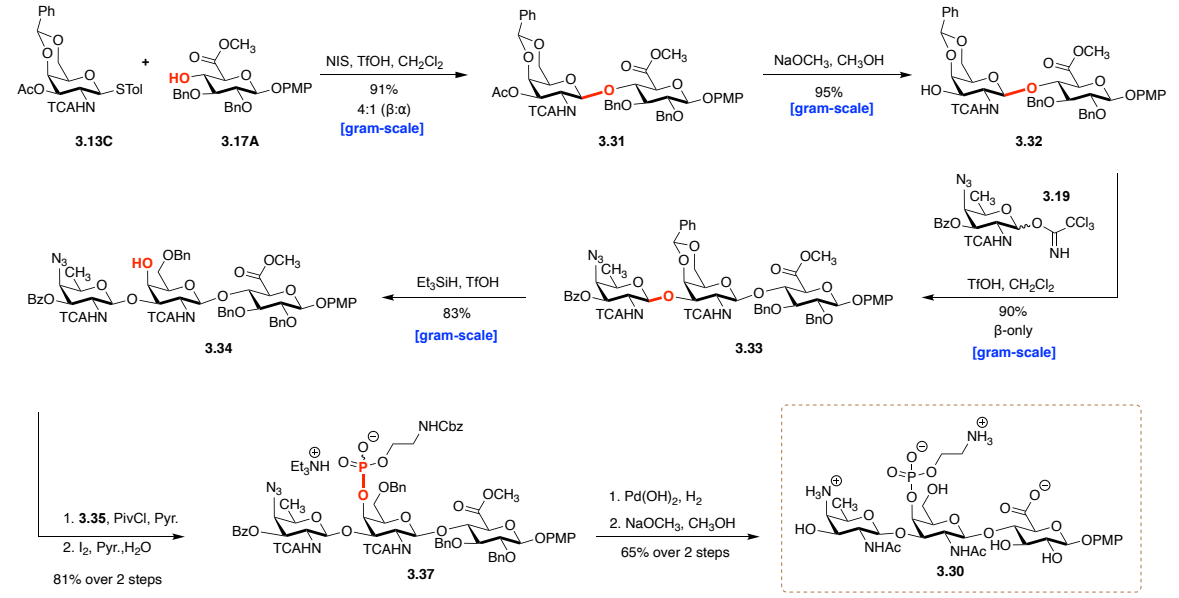

Scheme 3.6. Completion of the total synthesis of PT-ZPS repeating unit

Next, the assembly of the trisaccharide repeating unit commenced with a [2+1] glycosylation of trichloroacetimidate donor **3.19** with acceptor 3.32 at −78 °C using TfOH as the promoter provided **3.33** as the β-anomer in 90% yield. Inspired by the work done by Ellervik and co-workers regarding the reductive opening of the benzylidene acetal, we wondered if analogy could be made to the problem at hand with our more complex substrate.[44] In the case of the reductive opening, exhaustive attempts were made prior to successful attainment of the desired regioselectivity (Table 3.2). Accordingly, trisaccharide **3.34** was isolated with a free axial C4″ alcohol in 83% yield. The synthetic challenge posed by the reductive opening of galactosamine residues in complex carbohydrate synthesis has been answered by

an $Et_3SiH-TfOH$ reducing system.[45-50] Having obtained the desired intermediate, additional assessment for installing the phosphorus arm were made. Given that the acceptor is fixed on the central residue, it is in a 1,2-cis relationship with the terminal monosaccharide, and is axial, we suspected that phosphorylation would be challenging.

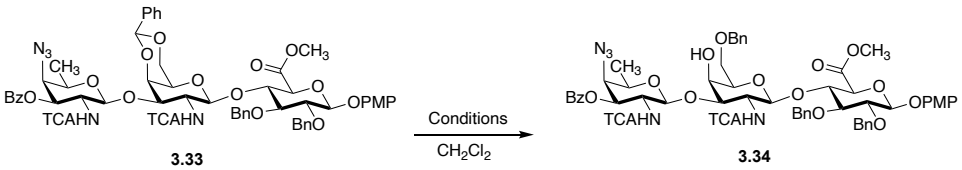

Entry	Conditions	Yield %
1[a]	Et_3SiH, $BF_3{\cdot}OEt_2$, 0°C - rt	0
2[a]	Et_3SiH, I_2, 0°C - rt	0
3	Et_3SiH, TfOH, -78°C	83

a. observed the cleavage of the trisaccharide starting material

Table 3.2. Optimization of regioselective reductive opening of benzylidene acetal

Previous experience from our lab has shown that electrophiles of type **3.36** are suitable reagents to install phosphocholine onto hindered nucleophiles.[51-52] Regrettably, the coupling of phosphoramidite **3.36** with **3.34** (under a range of reaction conditions), using 1*H*-tetrazole as the activator failed to form any desired O−P bonds. Undeniably, the only productive reaction (33% yield) observed in our early studies was when 4,5-dichloroimidazole (DCI) was used as the activator to provide phosphorylated compound **3.37**. While we had some success, we ultimately decided to diverge from the initial protocol and sought other means to incorporate the phosphorus residue. A very small summary of our failures can be seen in Table 3.3.

With a quick inquiry of the known literature, we discovered that a common strategy to form O-P bonds is to leverage the reactivity of H-phosphonates.[53-55] We postulated that we could use reagent **3.35** to install the phosphoethanolamine moiety. H-phosphonate chemistry work according to the following proposed mechanism. First, the phosphonate is activated by pivaloyl chloride, which generates a system in which the electron-withdrawing character of the pivaloyl ester makes the phosphorus(V) center sufficiently electrophilic. Furthermore, upon reaction with an alcohol nucleophile, rapid transesterification leads to the formation of the O−P bond. Next, oxidation leads to the desired functionality. Pleasingly, coupling between **3.34** and **3.35** was indeed executed in the presence of pivaloyl chloride and pyridine to form the O−P bond. At this juncture, oxidation with I_2 provided the phosphorylated trisaccharide **3.37** in 81% yield (Scheme 3.6).

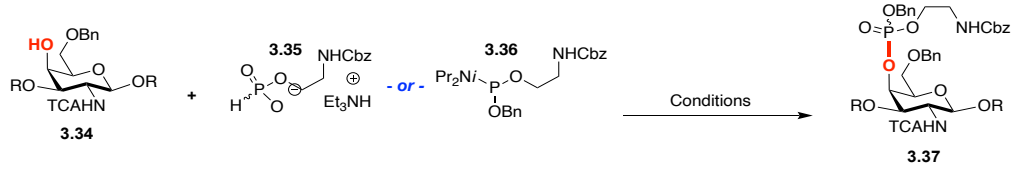

Entry	Conditions	Yield %
1	**3.34** (2.0 equiv), *1H*-tetrazole, rt, then *m*CPBA	0
2	**3.34** (10 equiv), *1H*-tetrazole, rt, then *m*CPBA	0
3	**3.34** (2.0 equiv), *1H*-tetrazole, 40°C, then *m*CPBA	0
4	**3.34** (2.0 equiv), DCI, rt, then *m*CPBA	33
5.	**3.33** (2.0 equiv), PivCl, pyr., then I_2	81

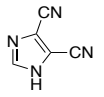

4,5-dicyanoimidazole (DCI)

1H-tetrazole

Table 3.3. Screening of phosphorylation conditions

With the fully protected repeating unit in hand, we began our monumental descent from this exhaustive endeavor by initiating a global deprotection sequence. First, hydrogenolysis over Pearlman's catalyst was employed to remove three benzyl ethers and a carbamate. The reducing environment also reduced two trichloroacetamides to their corresponding acetamide and one azide to its corresponding amine. Removing organic soluble impurities by means of a short column, the material was carried forward and exposed to $NaOCH_3$ in aqueous CH_3OH at ambient temperature to saponify the methyl ester and remove a single benzoate.

Following purification of the material via size exclusion chromatography, **3.30** was isolated as a white solid after lyophilization. Moreover, the characterization of the repeating unit using ^{1}H, ^{13}C, and ^{31}P NMR provided spectra analogous to those of the native polymer. In conclusion, we developed the first concise and diastereoselective synthesis of the *Photorhabdus temperata ssp. Cinereal* 3240 zwitterionic trisaccharide repeating unit. Our synthesis of PT-ZPS highlights a scalable synthesis of AAT donor and the use of an H-phosphonate donor to install the desired phosphoethanolamine moiety on a poorly nucleophilic and sterically hindered alcohol.

3.3 Total Synthesis of a Ribitol Teichoic Acid Zwitterionic Repeating Unit from Proteus vulgaris strain TG 276-1

Having completed the total synthesis of PT-ZPS repeating unit, my initial goals were to prepare a thorough review of deoxy-amino sugars, and possibly explore the syntheses of other rare bacterial sugars. However, upon examining the literature for other repeating units consisting of an AAT residue, I came across the repeating unit of *P. vulgaris*. Steve, not unexpectedly, had agreed to let me pursue an additional two total synthesis projects, knowing my time was almost up. As an advocate for collaborative projects, I organized the junior members of the group to synthesize building blocks, while I orchestrated the assembly of the desired repeating units at hand. I encouraged Ms. C. Elizabeth Adams (hereafter referred to just as Elizabeth) to join me on this new endeavor. Like PT-ZPS, *P. vulgaris* repeating unit is zwitterionic; however, the cassette features two phosphorous residues. In fact, our group had previously synthesized a bis-phosphorylated trisaccharide ZPS back in 2019[51], whereby we developed new phosphorus chemistry to install this key residue. Although Steve had agreed to let me work on this new project, the rest of the planning fell on Elizabeth's and my shoulders. The initial strategy, developed after some minor investigative work in the laboratory (and coffee at FIDO), turned to be conceptually close to the final working route.

As mentioned in previous chapters, in gram-negative organisms, the outer membrane provides protection from the environment, provides a barrier from toxins, and forms the periplasm, which holds the extra-cytoplasmic enzymes required for cell-wall growth and degradation. To contrast, gram-positive organisms lack an outer

membrane. Consequently, the peptidoglycan layer is very thick compared to the thin layer present in gram-negative organisms.[55] Peptidoglycan stabilizes the cell membrane and provides many sites to which extracellular conjugates can attach. For example, gram-positive peptidoglycan is heavily modified with charged polysaccharides that are critical to membrane integrity. Intriguingly, this anionic polymer layer appears to function in a similar manner as the outer membrane: they govern membrane permeability, facilitate extracellular interactions, provide stability to the plasma membrane, and, along with peptidoglycan, serve as scaffolds for extra-cytoplasmic enzymes required for cell-wall growth and degradation.

A major class of cell wall macromolecules in gram-positive organisms are the teichoic acids (TAs).[56-60] TAs are made up of anionic polymers of glycerol phosphate or ribitol phosphate linked via an ester to either D-alanine or a monosaccharide. There are two types of teichoic acids. The first are wall teichoic acids (WTAs), which are covalently bound via a phosphodiester bond to C-6 of *N*-acetylmuramic acid in the peptidoglycan layer. The second type are lipoteichoic acids (LTAs), which contain a terminal glycolipid that functions as an anchor in the cytoplasmic membrane.[61] Several central physiological functions have been assigned to teichoic acids ranging from cation homeostasis to ion trafficking. Overall, LTAs are essential for microbial cell growth and play an important role in host-pathogen interactions.

Enterobacteriaceae are a large family of opportunistic, gram-negative pathogens of the genus *Proteus*.[62] These bacteria are a common cause of urinary tract infections and related kidney and urological illnesses in patients who have undergone procedures involving catheterization of the urinary tract. *P. vulgaris* is

among the most virulent species in the clinic and is known to employ several virulence factors that govern the infectious process - such as swarming, flagella, capsule, and outer membrane lipopolysaccharide (LPS). Recently, Knirel *et al*. have characterized the structure of a cell surface *O*- zwitterionic polysaccharide with a repeating unit containing 2-acetamido-4-amino-2,4,6-trideoxy-d-galactose (D-FucNAc4N or AAT) and two D-ribitol phosphate (D-Rib-ol-5-P) residues.[63]

Compelled by the biological importance of ZPSs, together with the unanswered questions regarding their minimum polymer length to elicit an immune response, our group embarked on the total synthesis of *P. vulgaris* ZPS (PV-ZPS) repeating unit **3.38**, aiming for a concise approach from commercially available carbohydrates. Corollary to these goals was our group's ongoing interest in phosphorylated zwitterionic polysaccharides and the synthesis of rare-deoxy amino sugars. An important structural component of the repeating unit is the AAT residue, which was expected to allow for straightforward elaboration to the trisaccharide repeating unit.

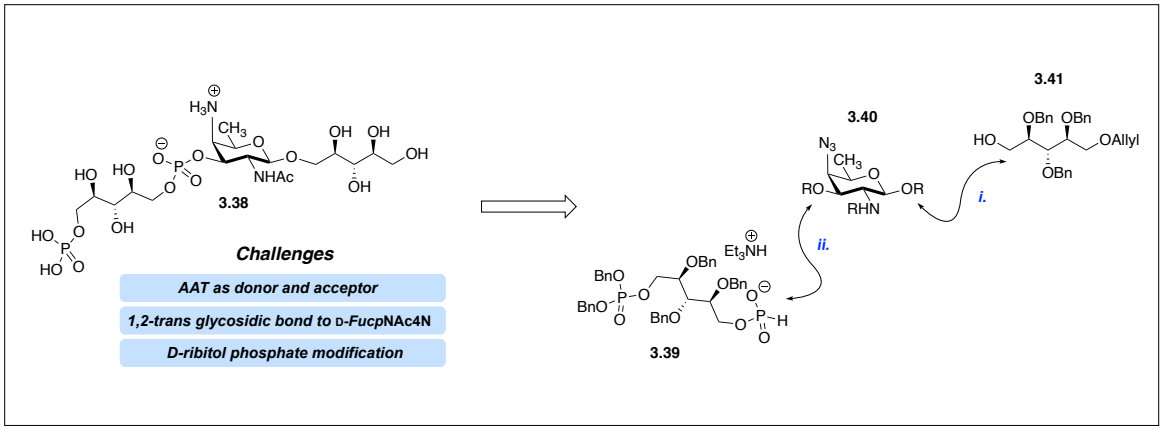

Scheme 3.7. PV-ZPS repeating unit synthetic target and key common intermediates

After careful considerations, a synthetic route to PV-ZPS repeating unit beginning from readily available carbohydrate precursors was deemed a suitable approach for the following reasons: 1) the opportunity to apply chemistry developed in our group for the synthesis of ZPSs containing AAT residues; and 2) the occasion to synthesize new phosphorylated sugars with H-phosphonate chemistry. However, several challenges must be addressed, including the use of AAT as both an acceptor and donor, the diastereoselective formation of 1,2-trans-β glycosidic linkage, and the installation of two phosphorus residues.

To access PV-ZPS repeating unit, monosaccharide building blocks were functionalized and protected with various protecting groups to provide the respective acceptors and donors. During the planning stage, Elizabeth was tasked with the synthesis of the bis-phosphorylated D-ribitol piece **3.39**, while I worked on the AAT (**3.40**) and allyl protected D-ribitol (**3.41**) building blocks (**Scheme 3.7**).

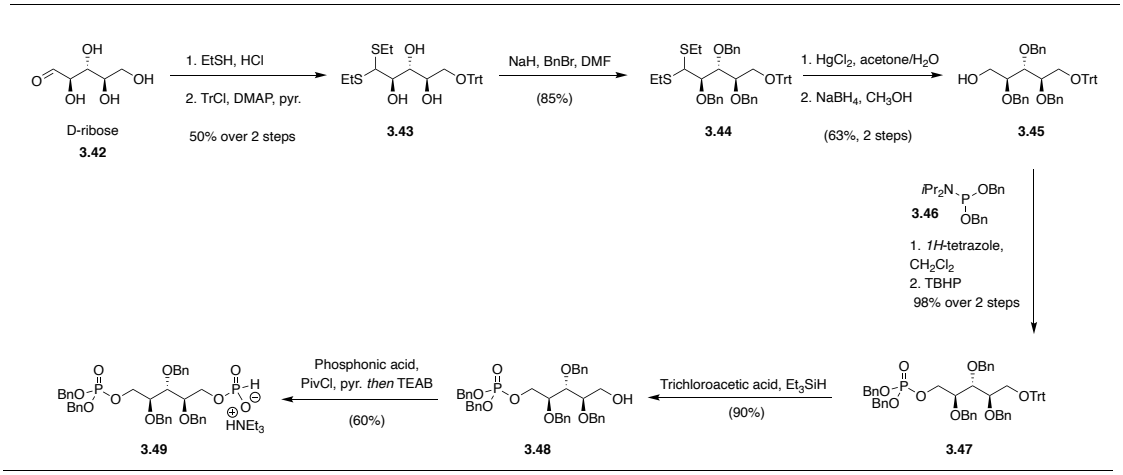

Scheme 3.8. Synthesis of bis-phosphorylated building block **3.49**

Elizabeth had previously found that preparation of building block **3.49** can be derived from D-ribose **3.42**. Thus, treatment of **3.42** with ethanethiol with the aid of

hydrochloric acid and consequent reaction with trityl chloride under the promotion of 4-dimethylaminopyridine (DMAP) and pyridine afforded trityl protected D-ribose derivative **3.43** in 50% yield over two steps. The triol **3.43** was then benzylated with benzyl bromide and sodium hydride in DMF to give fully protected compound **3.44** in 85% yield. Exposure of **3.44** to a solution of mercury (II) chloride in acetone and water led to the cleavage of the dithioacetal, providing an aldehyde, which was subsequently reduced with sodium borohydride to afford **3.45** in 63% yield over two steps. Gratifyingly, reaction with phosphorous reagent **3.46** with tetrazole gave the monophosphorylated intermediate and further oxidation with *tert*-Butyl hydroperoxide (TBHP) provided **3.47** in 98% yield over two steps. Next, selective trityl removal under trichloroacetic acid and triethyl silane gave alcohol **3.48**. Finally, treatment of monophosphorylated intermediate with phosphonic acid and pivaloyl chloride in pyridine delivered the bis-phosphorylated D-ribitol piece **3.49** in 60% yield (Scheme 3.8).

Considering the convenience of this approach for the synthesis of bis-phosphorylated D-ribitol building block **3.49** from D-ribose, we adopt a similar strategy to prepare the known allyl protected D-ribitol fragment **3.41**. Furthermore, the AAT donor **3.19** was synthesized using chemistry previously developed in our group. To demonstrate the utility of the three key building blocks, assembly of the unique core of trisaccharide **3.38** of *P. vulgaris* was carried out (Scheme 3.9).

To access the desired frameshift, a linear glycosylation approach was used adapting previous methods in the total synthesis of PT-ZPS. Synthesis of the bis-phosphorylated zwitterionic repeating unit **3.38** started with [1+1] glycosylation using AAT trichloroacetimidate donor **3.19** and allyl protected ribitol acceptor **3.41**. The TCA donor **3.19** and ribitol acceptor **3.41** were coupled using TfOH as the activator in dichloromethane at −78 °C to afford the disaccharide and subsequent treatment under Zemplén conditions provided acceptor **3.50** exclusively as the β-product in 90% yield over two steps. Based on our work related to the other phosphorylated ZPSs (see PT-ZPS section above), the bis-phosphorylated D-ribitol derivative **3.49** could be successfully coupled with disaccharide **3.50** in the presence of pivaloyl chloride and pyridine followed by oxidation with I_2 to furnish the phosphorylated trisaccharide **3.51** in 53% yield over two steps. In this scenario, allyl removal with an iridium complex followed by Pd $(OH)_2$/C-mediated removal and/or reduction of all remaining protecting groups will provide the trisaccharide repeating of *P. vulgaris* **3.38**.

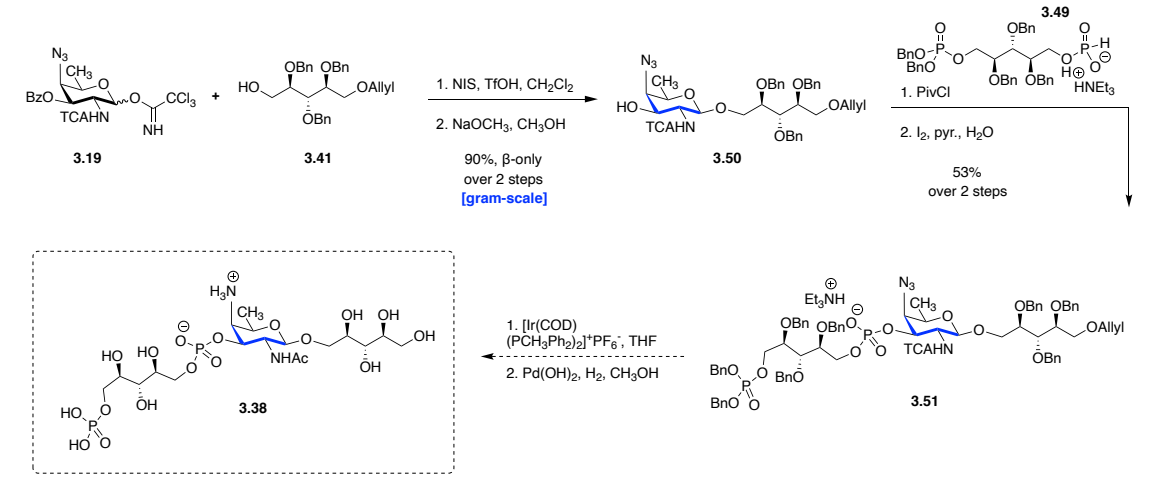

Scheme 3.9. Synthesis of PV-ZPS repeating unit **3.38**

3.4 Conclusion

In summary, we have developed a facile method for the total synthesis of two phosphorylated zwitterionic polysaccharides involving H-phosphonate chemistry for installation of the key phosphorous residue. Viewed within the proper historical context, this protocol represents a significant advance in the field of phosphorus coupling chemistry. Specifically, it has been shown that coupling of poorly nucleophilic and sterically hindered substrates is a challenging process. Thus, work from our laboratory has shown that functionalization of complex glycans through this methodology is possible and efficient. This research program was initiated with the structures of the phosphorylated zwitterionic polysaccharides in mind and with a conscious effort to access rare deoxy-amino sugars, such as AAT.

3.5 References

1. Roberts, I. S. The biochemistry and genetics of capsular polysaccharide production in bacteria*. Annu. Rev. Microbiol*. **1996,** *50,* 285−315.
2. Reid, C. W.; Fulton, K. M.; Twine, S. M. Never take candy from a stranger: the role of the bacterial glycome in host-pathogen interactions. *Future Microbiol*. **2010**, *5* (2), 267−288.
3. Cobb, B. A.; Wang, Q.; Tzianabos, A. O.; Kasper, D. L. Polysaccharide processing and presentation by the MHCII pathway. *Cell* **2004,** *117* (5), 677−687.
4. Avci, F. Y.; Kasper, D. L. How bacterial carbohydrates influence the adaptive immune system. *Annu. Rev. Immunol.* **2010**, *28*, 107−30.
5. Kalka-Moll, W. M.; Tzianabos, A. O.; Bryant, P. W.; Niemeyer, M.; Ploegh, H. L.; Kasper, D. L. Zwitterionic polysaccharides stimulate T cells by MHC class II-dependent interactions. *J. Immunol.* **2002**, *169* (11), 6149−6153.
6. Berti, F.; Adamo, R. Recent mechanistic insights on glycoconjugate vaccines and future perspectives. *ACS Chem. Biol.* **2013**, *8* (8), 1653−1663.
7. Gallorini, S.; Berti, F.; Mancuso, G.; Cozzi, R.; Tortoli, M.; Volpini, G.; Telford, J. L.; Beninati, C.; Maione, D.; Wack, A. Toll-like receptor 2 dependent immunogenicity of glycoconjugate vaccines containing chemically derived zwitterionic polysaccharides. *Proc. Natl. Acad. Sci. U. S. A.* **2009**, *106* (41), 17481−6.
8. Danishefsky, S. J.; Shue, Y. K.; Chang, M. N.; Wong, C. H. Development of Globo-H cancer vaccine. *Acc. Chem. Res.* **2015**, *48* (3), 643−52.

9. Keding, S. J.; Danishefsky, S. J. Prospects for total synthesis: a vision for a totally synthetic vaccine targeting epithelial tumors. *Proc. Natl. Acad. Sci. U. S. A.* **2004**, *101* (33), 11937−42.
10. Slovin, S. F.; Ragupathi, G.; Musselli, C.; Olkiewicz, K.; Verbel, D.; Kuduk, S. D.; Schwarz, J. B.; Sames, D.; Danishefsky, S.; Livingston, P. O.; Scher, H. I. Fully synthetic carbohydrate-based vaccines in biochemically relapsed prostate cancer: clinical trial results with alpha-N-acetylgalactosamine-O-serine/threonine conjugate vaccine. *J. Clin. Oncol.* **2003**, *21* (23), 4292−8.
11. Ragupathi, G.; Koide, F.; Sathyan, N.; Kagan, E.; Spassova, M.; Bornmann, W.; Gregor, P.; Reis, C. A.; Clausen, H.; Danishefsky, S. J.; Livingston, P. O. A preclinical study comparing approaches for augmenting the immunogenicity of a heptavalent KLH-conjugate vaccine against epithelial cancers. *Cancer Immunol. Immunother.* **2003**, *52* (10), 608−16.
12. Wang, Z. G.; Williams, L. J.; Zhang, X. F.; Zatorski, A.; Kudryashov, V.; Ragupathi, G.; Spassova, M.; Bornmann, W.; Slovin, S. F.; Scher, H. I.; Livingston, P. O.; Lloyd, K. O.; Danishefsky, S. J. Polyclonal antibodies from patients immunized with a globo Hkeyhole limpet hemocyanin vaccine: isolation, quantification, and characterization of immune responses by using totally synthetic immobilized tumor antigens. *Proc. Natl. Acad. Sci. U. S. A*. **2000**, *97* (6), 2719−24.
13. Ragupathi, G.; Slovin, S. F.; Adluri, S.; Sames, D.; Kim, I. J.; Kim, H. M.; Spassova, M.; Bornmann, W. G.; Lloyd, K. O.; Scher, H. I.; Livingston, P. O.; Danishefsky, S. J. A Fully Synthetic Globo H Carbohydrate Vaccine Induces a

Focused Humoral Response in Prostate Cancer Patients: A Proof of Principle. *Angew. Chem. Int. Ed.* **1999,** *38* (4), 563−566.

14. Gilewski, T.; Ragupathi, G.; Bhuta, S.; Williams, L. J.; Musselli, C.; Zhang, X. F.; Bornmann, W. G.; Spassova, M.; Bencsath, K. P.; Panageas, K. S.; Chin, J.; Hudis, C. A.; Norton, L.; Houghton, A. N.; Livingston, P. O.; Danishefsky, S. J.; et al. Immunization of metastatic breast cancer patients with a fully synthetic globo H conjugate: a phase I trial. *Proc. Natl. Acad. Sci. U. S. A.* **2001**, *98* (6), 3270−3275.
15. Kudryashov, V.; Glunz, P. W.; Williams, L. J.; Hintermann, S.; Danishefsky, S. J.; Lloyd, K. O. Toward optimized carbohydrate-based anticancer vaccines: epitope clustering, carrier structure, and adjuvant all influence antibody responses to Lewis(y) conjugates in mice. *Proc. Natl. Acad. Sci. U. S. A.* **2001**, *98* (6), 3264−9.
16. Herzenberg, L. A.; Tokuhisa, T. Epitope-specific regulation. I. Carrier-specific induction of suppression for IgG anti-hapten antibody responses. *J. Exp. Med*. **1982**, *155* (6), 1730−40.
17. Surana, N. K.; Kasper, D. L. The yin yang of bacterial polysaccharides: lessons learned from *B. fragilis* PSA. *Immunol Rev.* **2012,** *245* (1), 13−26.
18. De Silva, R. A.; Wang, Q.; Chidley, T.; Appulage, D. K.; Andreana, P. R. Immunological response from an entirely carbohydrate antigen: design of synthetic vaccines based on Tn-PS A1 conjugates. *J. Am. Chem. Soc.* **2009**, *131* (28), 9622−3.

19. De Silva, R. A.; Appulage, D. K.; Pietraszkiewicz, H.; Bobbitt, K. R.; Media, J.; Shaw, J.; Valeriote, F. A.; Andreana, P. R. The entirely carbohydrate immunogen Tn-PS A1 induces a cancer cell selective immune response and cytokine IL-17. *Cancer Immunol. Immunother.* **2012**, *61* (4), 581−5.
20. Nishat, S.; Andreana, P. R. Entirely Carbohydrate-Based Vaccines: An Emerging Field for Specific and Selective Immune Responses. Vaccines (Basel, Switz.) **2016**, *4* (2), 19.
21. Trabbic, K. R.; Bourgault, J. P.; Shi, M.; Clark, M.; Andreana, P. R. Immunological evaluation of the entirely carbohydrate-based Thomsen-Friedenreich - PS B conjugate. *Org. Biomol. Chem.* **2016**, *14* (13), 3350−5.
22. Eradi, P.; Ghosh, S.; Andreana, P. R. Total Synthesis of Zwitterionic Tetrasaccharide Repeating Unit from *Bacteroides fragilis* ATCC 25285/NCTC 9343 Capsular Polysaccharide PS A1 with Alternating Charges on Adjacent Monosaccharides. *Org. Lett.* **2018**, *20* (15), 4526−4530.
23. Nguyen, J.M.; Townsend, S. D. Total Synthesis of the *Photorhabdus temperata ssp.* Cinereal 3240 Zwitterionic Trisaccharide Repeating Unit. *Org. Lett.* **2021**, *23*, 15, 5922-5926.
24. Kondakova, A. N.; Kirsheva, N. A.; Arbatsky, N. P.; Shaikutdinova, R. Z.; Shashkov, A. S.; Ivanov, S. A.; Anisimov, A. P.; Knirel, Y. A. Structure of a zwitterionic O-polysaccharide from *Photorhabdus temperata* subsp. cinerea 3240. *Carbohydr. Res.* **2015**, *407*, 1-4.
25. Pfister, H. B.; Paoletti, J.; Poveda, A.; Jimenez-Barbero, J.; Mulard, L. A. Zwitterionic Polysaccharides of *Shigella sonnei*: Synthetic Study toward a

Ready-for-Oligomerization Building Block Made of Two Rare Amino Sugars. *Synthesis-Stuttgart* **2018,** *50*, 4270-4282.

26. van den Bos, L. J.; Boltje, T. J.; Provoost, T.; Mazurek, J.; Overkleeft, H. S.; van der Marel, G. A. A synthetic study towards the PSA1 tetrasaccharide repeating unit. *Tetrahedron Letters* **2007,** *48*, 2697-2700.
27. Ni Cheallaigh, A.; Oscarson, S. Synthesis of building blocks for an iterative approach towards oligomers of the *Streptococcus pneumoniae* type 1 zwitterionic capsular polysaccharide repeating unit. *Can. J. Chem.* **2016,** *94*, 940-960.
28. Toth, A.; Medgyes, A.; I, B.; Liptak, A.; Batta, G.; Kontrohr, T.; Peterffy, K.; V, P. Synthesis of the repeating unit of the O-specific polysaccharide of *Shigella sonnei* and quantitation of its serologic activity. *Bioorganic & Medicinal Chemistry Letters* **2000,** *10*, 19-21.
29. Gu, G.; Adabala, P. J.; Szczepina, M. G.; Borrelli, S.; Pinto, B. M. Synthesis and immunological characterization of modified hyaluronic acid hexasaccharide conjugates. *J. Org. Chem.* **2013,** *78*, 8004-19.
30. Calin, O.; Pragani, R.; Seeberger, P. H. De novo synthesis of L-colitose and L-rhodinose building blocks. *J. Org. Chem.* **2012,** *77*, 870-7.
31. Iynkkaran, I.; Bundle, D. R. A novel glycosyl donor for synthesis of 2-acetamido-4-amino-2,4,6-trideoxy-alpha-D-galactopyranosides. *Carbohydr. Res.* **2010,** *345*, 2323-7.

32. van den Bos, L. J.; Codee, J. D.; van Boom, J. H.; Overkleeft, H. S.; van der Marel, G. A. A novel strategy towards the synthesis of orthogonally functionalized 4-aminoglycosides. *Org. Biomol. Chem.* **2003,** *1*, 4160-5.
33. Lopin, C.; Jacquinet, J. C. From polymer to size-defined oligomers: An expeditious route for the preparation of chondroitin oligosaccharides. *Angew. Chem. Int. Edit.* **2006,** *45*, 2574-2578.
34. Belot, F.; Jacquinet, J. C. Intermolecular aglycon transfer of a phenyl 1-thiogalactosaminide derivative under trichloroacetimidate glycosylation conditions. *Carbohydr. Res.* **1996,** *290*, 79-86.
35. Moume-Pymbock, M.; Furukawa, T.; Mondal, S.; Crich, D. Probing the Influence of a 4,6-O-Acetal on the Reactivity of Galactopyranosyl Donors: Verification of the Disarming Influence of the trans-gauche Conformation of C5-C6 Bonds. *J. Am. Chem. Soc.* **2013,** *135*, 14249-14255.
36. Fraserreid, B.; Wu, Z. F.; Andrews, C. W.; Skowronski, E.; Bowen, J. P. Torsional Effects in Glycoside Reactivity - Saccharide Couplings Mediated by Acetal Protecting Groups. *J. Am. Chem. Soc.* **1991,** *113*, 1434-1435.
37. Mootoo, D. R.; Konradsson, P.; Udodong, U.; Fraserreid, B. Armed and Disarmed N-Pentenyl Glycosides in Saccharide Couplings Leading to Oligosaccharides. *J. Am. Chem. Soc.* **1988,** *110*, 5583-5584.
38. Bohe, L.; Crich, D. A propos of glycosyl cations and the mechanism of chemical glycosylation; the current state of the art. *Carbohydr. Res.* **2015,** *403*, 48-59.

39. Ranade, S. C.; Demchenko, A. V. Mechanism of Chemical Glycosylation: Focus on the Mode of Activation and Departure of Anomeric Leaving Groups. *J. Carbohydr. Chem.* **2013,** *32*, 1-43.
40. Huang, M.; Garrett, G. E.; Birlirakis, N.; Bohe, L.; Pratt, D. A.; Crich, D. Dissecting the mechanisms of a class of chemical glycosylation using primary C-13 kinetic isotope effects. *Nature Chemistry* **2012,** *4*, 663-667.
41. Bohe, L.; Crich, D. A propos of glycosyl cations and the mechanism of chemical glycosylation. *Cr Chim* **2011**, *14*, 3-16.
42. Cattaneo, V.; Oldrini, D.; Corrado, A.; Berti, F.; Adamo, R. Orthogonal cleavage of the 2-napthylmethyl group in the presence of the p-methoxy phenyl-protected anomeric position and its use in carbohydrate synthesis. *Organic Chemistry Frontier.* **2016,** *3(6)*, 753-758.
43. Dhamale, O. P.; Zong, C. L.; Al-Mafraji, K.; Boons, G. J. New glucuronic acid donors for the modular synthesis of heparan sulfate oligosaccharides. *Org. Biomol. Chem.* **2014,** *12*, 2087-2098.
44. Johnsson, R.; Ohlin, M.; Ellervik, U. Reductive openings of benzylidene acetals revisited: a mechanistic scheme for regio- and stereoselectivity. *J. Org. Chem.* **2010,** *75*, 8003-11.
45. Ohlin, M.; Johnsson, R.; Ellervik, U. Regioselective reductive openings of 4,6-benzylidene acetals: synthetic and mechanistic aspects. *Carbohydr. Res.* **2011,** *346*, 1358-70.
46. Johnsson, R.; Cukalevski, R.; Dragen, F.; Ivanisevic, D.; Johansson, I.; Petersson, L.; Wettergren, E. E.; Yam, K. B.; Yang, B.; Ellervik, U. Reductive

openings of benzylidene acetals. Kinetic studies of borane and alane activation by Lewis acids. *Carbohydr. Res.* **2008,** *343*, 2997-3000.

47. Sherman, A. A.; Mironov, Y. V.; Yudina, O. N.; Nifantiev, N. E. The presence of water improves reductive openings of benzylidene acetals with trimethylaminoborane and aluminium chloride. *Carbohydr. Res.* **2003,** *338*, 697-703.
48. Vohra, Y.; Vasan, M.; Venot, A.; Boons, G. J. One-pot synthesis of oligosaccharides by combining reductive openings of benzylidene acetals and glycosylations. *Org. Lett.* **2008,** *10*, 3247-50.
49. Wang, C. C.; Lee, J. C.; Luo, S. Y.; Fan, H. F.; Pai, C. L.; Yang, W. C.; Lu, L. D.; Hung, S. C. Synthesis of biologically potent alpha1-->2-linked disaccharide derivatives via regioselective one-pot protection-glycosylation. *Angew. Chem. Int. Edit.* **2002,** *41*, 2360-2.
50. Sakagami, M.; Hamana, H. A selective ring opening reaction of 4,6-O-benzylidene acetals in carbohydrates using trialkylsilane derivatives. *Tetrahedron Letters* **2000,** *41*, 5547-5551.
51. Keith, D. J.; Townsend, S. D. Total Synthesis of the Congested, Bisphosphorylated Morganella morganii Zwitterionic Trisaccharide Repeating Unit. *J. Am. Chem. Soc.* **2019**, *141*, 12939−12945.
52. Xu, L. L.; Berg, L. J.; Jamin Keith, D.; Townsend, S. D. An effective reagent to functionalize alcohols with phosphocholine. *Org. Biomol. Chem.* **2020,** *18*, 767-770.

53. Cieslak, J.; Jankowska, J.; Kers, A.; Kers, I.; Sobkowska, A.; Sobkowski, M.; Stawinski, J.; Kraszewski, A. Synthetic applications of aryl H-phosphonates in nucleotide chemistry. *Collect. Czech. Chem. C.* **1996,** *61*, S242-S245.

54. Tsai, Y. H.; Gotze, S.; Vilotijevic, I.; Grube, M.; Silva, D. V.; Seeberger, P. H. A general and convergent synthesis of diverse glycosylphosphatidylinositol glycolipids. *Chemical Science* **2013,** *4*, 468-481.

55. Romaniuk, J. A. H.; Celgelski, L. Peptidoglycan and Teichoic Acid Levels and Alterations in *S. aureus* by Cell-Wall and Whole-Cell NMR. *Biochemistry*, **2018**, *57*(26), 3966-3975.

56. Brown, S.; Santa Maria, Jr., J. P.; Walker, S. Wall Teichoic Acids of Gram-Positive Bacteria. *Annu. Rev. Microbiol*. **2013**, 67.

57. Allison, S.E.; D'Elia, M.A.; Arar, S.; Monteiro, M.A.; Brown, E.D. Studies of the genetics, function, and kinetic mechanism of TagE, the wall teichoic acid glycosyltransferase in *Bacillus subtilis* 168. *J Biol Chem.* **2011**, *286*, 23708–23716.

58. Aly, R.; Shinefield, H.R.; Litz, C.; Maibach, H.I. Role of teichoic acid in the binding of *Staphylococcus aureus* to nasal epithelial cells. *J Infect Dis.* **1980**, *141*, 463–465.

59. Anderson AJ, Green RS, Sturman AJ, Archibald AR. Cell wall assembly in *Bacillus subtilis*: location of wall material incorporated during pulsed release of phosphate limitation, its accessibility to bacteriophages and concanavalin A, and its susceptibility to turnover. *J Bacteriol.* **1978**, *136*, 886– 899.

60. Andre G, Deghorain M, Bron PA, van S II, Kleerebezem M, et al. Fluorescence and atomic force microscopy imaging of wall teichoic acids in *Lactobacillus plantarum*. *ACS Chem Biol*. **2011**, *6*, 366–376.

61. Percy, M. G.; Grundling, A. Lipoteichoic Acid Synthesis and Function in Gram-Positive Bacteria. *Annual Review of Microbiology*. **2014**, *68*, 81-100.

62. Nordmann, P. Carbapenemase-producing Enterobacteriaceae: overview of a major public health challenge. *Med. Mal. Infect.* **2014**, *44*(2), 51-6.

63. Arbatsky, N. P.; Kondakova, A. N.; Senchenkova, S. N.; Siwinska, M.; Shashkov, A. S.; Zych, K.; Knirel, Y. A., Zygmunt, S. Structure of a new ribitol teichoic acid-like O-polysaccharide of a serologically separate *Proteus vulgaris* strain, TG 276-1, classified into a new *Proteus* serogroup O53. *Carbohydr. Res.* **2007**, *342* (14), 2061-2066.

3.6 Experimental Methods

General. All non-aqueous reactions were performed in flame-dried or oven dried round-bottomed flasks under an atmosphere of nitrogen or argon, unless otherwise noted. Stainless steel syringes or cannula were used to transfer air- and moisture-sensitive liquids. Reaction temperatures were controlled using a thermocouple thermometer and analog hotplate stirrer. Reactions were conducted at room temperature (rt, approximately 23 °C) unless otherwise noted. The anhydrous solvents used in the reactions were obtained from an MBraun MB-SPS 800 anhydrous Solvent System. Solvent for chromatography were of analytical grade and distilled under reduced pressure prior to use. Commercially available reagents were obtained from Aldrich, Fisher, TCI, TRC, and Carbosynth. Flash column chromatography was conducted as described Still et. al. using silica gel 230-400 mesh.[1] Where necessary, silica gel was neutralized by treatment of the silica gel prior to chromatography with the eluent containing 1% triethylamine. TEAB buffer was prepared by filling TEA (7 mL) in a measuring cylinder and adding water until the total volume reached 500mL. The solution was transferred to a flask and CO_2 was bubbled through the solution for 2 h at 0 °C. The buffer was stored at 4 °C. Thin layer chromatography (TLC) was performed using glass backed 60-F254 silica gel plates obtained from Silicycle. Visualization of TLC plates was performed by UV (215 nm and 254 nm), CAM stain (5% (w/v) ammonium molybdate, 1% (w/v) cerium (II) sulfate and 10% (v/v) sulfuric acid in water) or ninhydrin stain (1.5% (w/v) ninhydrin and 3% (v/v) acetic acid in n-butanol) dipping solutions. Size exclusion chromatography (SEC) was performed using Bio Gel ® P-2 Gel (Bio-Rad).

Powdered 4 Å molecular sieves were obtained from Sigma-Aldrich and used for reactions. Sieves were activated by iterative heating (to 180 °C) and cooling (to 25 °C) cycles (minimum of 3 times). Heating was carried out by microwave irradiation and cooling took place in a desiccator equipped with Drierite™ and P_2O_5.

Instrumentation: ^{1}H NMR, ^{13}C NMR, ^{31}P and 2D NMR spectra were recorded in the Vanderbilt Small Molecule NMR Facility on a Bruker 400 and 600 MHz. Chemical shifts are reported in parts per million (ppm) of the δ scale. Spectra were recorded in $CDCl_3$ by using the solvent residual peak chemical shift as the internal standard ($CDCl_3$: S7 7.26 ppm ^{1}H, 77.0 ppm ^{13}C) or in D_2O using the solvent as the internal standard in ^{1}H NMR (D_2O: 4.79 ppm 1H) unless otherwise stated. ^{31}P NMR spectra 1% H_3PO_4 in D_2O was used as an external standard. 1H NMR spectral data are presented as follows: Chemical shifts (δ ppm), multiplicity (s = singlet, d = doublet, dd = doublet of doublets, dq = doublet of quadruplet, ddd = doublet of doublet of doublet, t = triplet, q = quartet, p = pentet, br = broad, m = multiplet) coupling constants (Hz), integration. High-resolution mass spectra (HRMS) were obtained from the Department of Chemistry, Vanderbilt University using an LTQ-Orbitrap XL mass spectrometer. Optical rotations (OR) were measured with on a AUTOPOL IV digital polarimeter. Concentrations (c) in g/100 mL and solvent are given in parentheses and the reported value is an average of n = 3 independent measurements.

Proton and Carbon assignment based on the following figure:

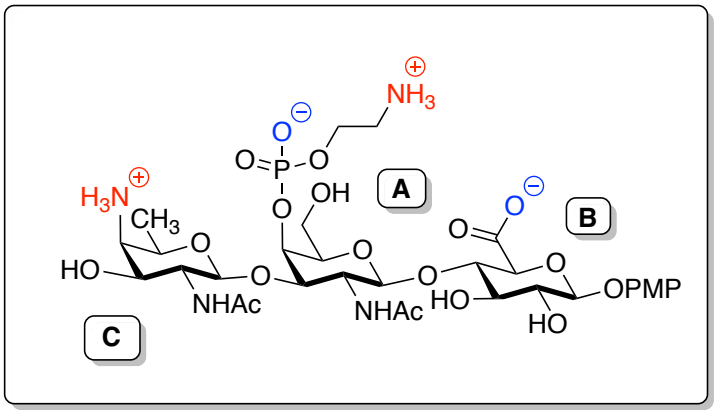

phenyl (4,6-*O*-benzylidene-3-*O*-acetyl-2-deoxy-2-trichloroacetamido-1-thio-β-D- galactopyranoside (3.13B):

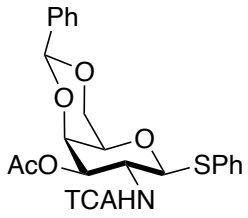

3.13B

To a solution of known phenyl 4,6-O-benzylidene acetal-2-deoxy-2-trichloracetamido-1-thio-β-D-galactopyranoside[6] (4.0 g, 7.92 mmol, 1 equiv.) in pyridine (35 mL) was cooled to 0 °C under an argon atmosphere and added acetic anhydride (3.7 mL, 39.6 mmol, 5 equiv.) and DMAP (0.1 equiv.). The reaction was stirred at room temperature. At 1 h, TLC indicated that the starting material was completely consumed. The reaction was cooled to 0 °C and the excess acetic anhydride was quenched by the addition of CH_3OH (5.0 mL). After 5 min at 0 °C, the crude reaction mixture was stirred at room temperature for 5 min and then transferred to a separatory funnel with EtOAc (100 mL). The reaction was washed with 1 N HCl (3 x 25 mL), satd. aq. $NaHCO_3$ (1 x 25 mL), brine (1 x 125 mL), dried ($NaSO_4$) and filtered through a glass fritted vacuum filter funnel to remove drying agent. The filtrate was concentrated to a crude oil which was purified by flash column chromatography (1:3 to 1:1 EtOAc/hexanes) then was crystalized from hot EtOAc and hexanes to give product (3.50 g, 6.40 mmol, 81%) as white crystals. R_f = 0.55 (EtOAc/Hexane 1:1) visualized with ceric ammonium molybdate stain; $[\alpha]D^{25}$ = +4.2° (c = 0.0012, $CHCl_3$); ^{1}H NMR (600 MHz, $CDCl_3$) δ 7.69 – 7.62 (m, 2H, Ar), 7.45-7.42 (m, 2H, Ar), 7.41 – 7.35 (m, 3H, Ar), 7.35-7.31 (m, 1H, Ar), 7.29 – 7.26 (m, 2H, Ar), 6.69 (d, *J* = 8.3, 1H, NH), 5.53 (s, 1H, PhC*H*), 5.44 (dd, *J* = 10.9, 3.3 Hz, 1H, H-3), 5.18 (d, *J* = 10.0 Hz, 1H, H-1), 4.40 (dd, *J* = 12.3, 1.7 Hz, 1H, H-6), 4.37 (dd, *J* = 3.3, 1.0 Hz, 1H, H-4), 4.14 (td, *J* = 10.5, 8.3 Hz, 1H, H-2), 4.06 (dd, *J* = 12.4, 1.6 Hz, 1H, H-6), 3.67 (s, 1H, H-5), 2.03 (s, 3H, COC*H*$_3$); ^{13}C NMR (151 MHz, $CDCl_3$) δ 170.7 (*C*OCH_3), 161.4

(NH*C*O), 137.6, 134.0, 130.9, 129.3, 129.1, 128.6, 128.3, 126.5, 101.0 (Ph*C*H/benzylidene), 92.4 (*C*Cl_3), 84.4 (C-1), 73.4 (C-4), 70.9 (C-3), 70.0 (C-5), 69.3 (C-6), 50.9 (C-2), 20.9 (CO*C*H_3); HRMS (ESI) calcd. for $C_{23}H_{22}O_6Cl_3NSNa$ $(M+Na)^+$ 568.0133, found 568.0126 *m/z*.

***p*-Methoxyphenyl methyl 2,3-di-*O*-benzyl-β-D-glucopyranosidurinate (3.17A):**

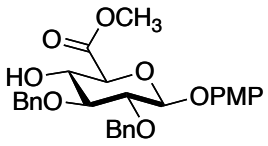

3.17A

To a solution of known diol[4b] (3.75 g, 8.04 mmol, 1.0 equiv.) in CH_2Cl_2/H_2O (3/1 v/v, 100 mL) under an argon atmosphere was added 2,2,6,6-tetramethyl-1-piperidinyloxy (TEMPO) (377 mg, 2.41 mmol, 0.3 equiv.) and (Diacetoxyiodo) benzene (BAIB) (6.45g, 20.1 mmol, 2.5 equiv.). The biphasic mixture was stirred vigorously for 3 h and quenched by the addition of satd. aq. $Na_2S_2O_3$ (20 mL). The layers were separated, and the aqueous layer was acidified with 1M aqueous HCl to pH 2 and extracted with CH_2Cl_2 (50 mL × 3. The combined organic layers were dried over anhydrous Na_2SO_4, filtered, and concentrated *in vacuo*. The residue was dissolved in 65.0 mL of anhydrous DMF. To this solution was added sequentially $KHCO_3$ (3.23 g, 32.3 mmol, 5.0 equiv.) and CH_3I (0.44 mL, 7.10 mmol, 1.1 equiv.) at 0 °C and the solution was stirred at 25 °C for about 12 h. The solvents were concentrated *in vacuo,* and the residue was purified by flash silica gel chromatography (50:50 EtOAc/Hexanes) to provide the glucuronic acid methyl ester 31 (3.00 g, 6.45 mmol, 94% yield) as a white amorphous solid. Glucuronic acid methyl ester had R_f 0.40 (EtOAc/Hexane 1:1) visualized with ceric ammonium molybdate stain; $[\alpha]D^{25}$ = +9.2 ° (c = 0.0024, $CHCl_3$); ^{1}H NMR (600 MHz, $CDCl_3$) δ 7.38 – 7.28 (m, 10H, Ar), 7.02 (d, *J* = 9.0 Hz, 2H, Ar),

6.84 (d, *J* = 9.0 Hz, 2H, Ar), 5.02 (d, *J* = 10.9 Hz, 1H, PhC*H*H), 4.93 (d, *J* = 7.7 Hz, 1H, H-1), 4.92 (d, *J* = 11.4 Hz, 1H, PhCH*H*), 4.85 (d, *J* = 11.4 Hz, 1H, PhC*H*H), 4.82 (d, *J* = 10.9 Hz, 1H, PhCH*H*), 3.99 – 3.94 (m, 1H, H-4), 3.91 (m, 1H, H-5), 3.81 (s, 3H, CO_2CH_3), 3.79 (s, 3H, OCH_3), 3.74 – 3.68 (m, 1H, H-2), 3.59 (t, *J* = 8.9 Hz, 1H, H-3), 2.88 (s, 1H, O*H*); ^{13}C NMR (151 MHz, $CDCl_3$) δ 169.6 (CO_2CH_3), 155.7, 151.3, 138.5, 138.1, 128.6, 128.5, 128.3, 128.1, 128.0, 118.7, 114.7, 103.2 (C-1), 83.1 (C-3), 81.0 (C-2), 75.6 (PhCH_2), 75.26 (PhCH_2), 74.2 (C-5), 71.7 (C-4), 55.8 (OCH_3), 52.9 (CO_2CH_3); HRMS (ESI) calcd. for $C_{28}H_{30}O_8Na$ $(M+Na)^+$ 517.1833, found 517.1836 *m/z*.

_p_-Methoxyphenyl benzyl 2,3-di-_O_-benzoyl-β-D-glucopyranosidurinate (3.17B):

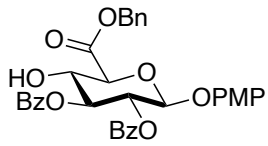

3.17B

To a solution of known diol (1.00 g, 1.97 mmol, 1.0 equiv.) in CH_2Cl_2/H_2O (3/1 v/v, 100 mL) under an argon atmosphere was added 2,2,6,6-tetramethyl-1-piperidinyloxy (TEMPO) (92.2 mg, 0.59 mmol, 0.3 equiv.) and (Diacetoxyiodo) benzene (BAIB) (1.37, 4.92 mmol, 2.5 equiv.). The biphasic mixture was stirred vigorously for 3 h and quenched by the addition of satd. aq. $Na_2S_2O_3$ (20 mL). The layers were separated, and the aqueous layer was acidified with 1M aqueous HCl to pH 2 and extracted with CH_2Cl_2 (50 mL × 3. The combined organic layers were dried over anhydrous Na_2SO_4, filtered, and concentrated *in vacuo*. The residue was dissolved in 65.0 mL of anhydrous DMF. To this solution was added sequentially $KHCO_3$ (1.00 g, 9.83 mmol, 5.0 equiv.) and BnBr (0.25 mL, 2.16 mmol, 1.1 equiv.) at 0 °C and the solution was stirred at 25 °C for about 12 h. The solvents were concentrated *in vacuo,* and

the residue was purified by flash silica gel chromatography (50:50 EtOAc/Hexanes) to provide the glucuronic acid benzyl ester 31 (0.95 g, 1.60 mmol, 81% yield) as a white amorphous solid. Glucuronic acid benzyl ester had R_f 0.44 (EtOAc/Hexane 1:1) visualized with ceric ammonium molybdate stain; $[\alpha]D^{25}$ = +11.7° (c = 0.011, $CHCl_3$); ^1H NMR (600 MHz, $CDCl_3$) δ 8.00 (dd, *J* = 8.4, 1.3 Hz, 1H, Ar), 7.97 (dd, *J* = 8.4, 1.4 Hz, 1H, Ar), 7.55 – 7.48 (m, 2H, Ar), 7.43 – 7.34 (m, 9H, Ar), 6.95 (d, *J* = 9.0 Hz, 2H, Ar), 6.74 (d, *J* = 9.1 Hz, 2H, Ar), 5.67 (dd, *J* = 9.6, 7.6 Hz, 1H, H-2), 5.60 (t, *J* = 9.4 Hz, 1H, H-3), 5.39 – 5.23 (m, 2H, PhCH_2), 5.17 (d, *J* = 7.6 Hz, 1H, H-1), 4.33 (t, *J* = 9.4 Hz, 1H, H-4), 4.20 (d, *J* = 9.6 Hz, 1H, H-5), 3.74 (s, 3H, OCH_3); ^{13}C NMR (151 MHz, $CDCl_3$) δ 168.2 (*C*O_2Bn), 166.6 (*C*OPh), 165.1 (*C*OPh), 155.9, 150.9, 134.8, 133.5, 133.3, 130.0, 129.8, 129.1, 128.9, 128.7, 128.6, 128.4, 128.1, 119.3, 114.5, 101.2 (C-1), 74.8 (C-3), 74.6 (C-5), 71.2 (C-2), 70.3 (C-4), 67.7 (Ph*C*H_2), 55.6 (O*C*H_3); HRMS (ESI) calcd. for $C_{30}H_{30}O_{10}Na$ $(M+Na)^+$ 621.1731, found 621.1732 *m/z*.

***p*-Methoxyphenyl (4,6-*O*-benzylidene-3-*O*-*tert*. Butyldimethylsiyl-2-deoxy-2-trichloroacetamido-α-D- galactopyranosyl)-(1→ 4)-(methyl 2,3-di-*O*-benzyl-β-D-glucopyranosid)uronate (3.21):**

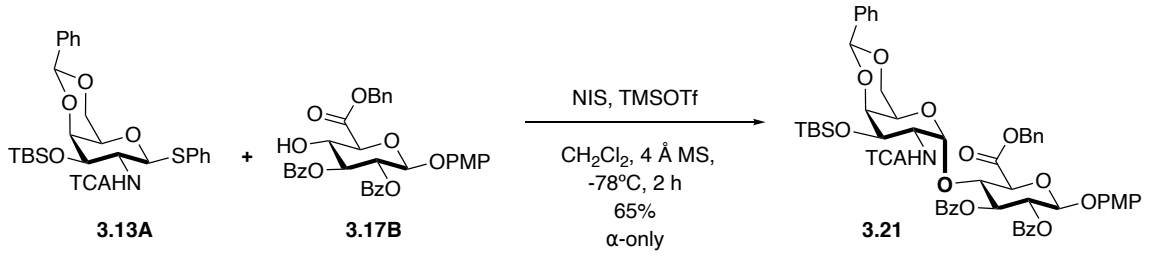

A solution of known acceptor **17.B** (250 mg, 0.42 mmol, 1.0 equiv.) and donor **3.13A** (284 mg, 0.46 mmol, 1.1 equiv.) in anhydrous CH_2Cl_2 (5 mL) under an argon atmosphere was added 4 Å MS (0.5 g) at room temperature and allowed to stir for 1 h. The reaction mixture was cooled to -78 °C and added NIS (188 mg, 0.83 mmol, 2.0 equiv.). After 1 min, a solution of TMSOTf (0.15 equiv., 2.0 mL, 5% in anhydrous CH_2Cl_2) was added dropwise. The reaction was stirred at -78 °C for 2 h when TLC indicated complete consumption of the alcohol **17** starting material. The reaction was quench by the addition of dilute Et_3N in CH_2Cl_2 while warming to room temperature. The reaction was filtered through a glass fritted filter funnel equipped with a pad of Celite to remove the 4 Å MS and then concentrated *in vacuo*. The crude oil was then diluted with EtOAc and transferred to a separatory funnel and washed with satd. aq. $Na_2S_2O_3$ (20 mL x 1), brine (20 mL x 1), and dried over anhydrous Na_2SO_4. The mixture was filtered and concentrated to a crude oil. Flash chromatography of the crude material eluting with EtOAc/Hexane (2:3) gave α product: (300 mg, 0.27 mmol, 65%) as a yellow foam. R_f = 0.55 (EtOAc/Hexane 2:3) visualized with ceric ammonium molybdate stain; $[\alpha]D^{25}$ = +37.5° (c = 0.015, $CHCl_3$); ^{1}H NMR (600 MHz, $CDCl_3$) δ 7.99 – 7.92 (m, 2H, Ar), 7.93 – 7.85 (m, 2H, Ar), 7.63

– 7.49 (m, 4H, Ar), 7.45 – 7.31 (m, 12H, Ar), 7.29 – 7.12 (m, 2H, Ar), 6.91 (d, *J* = 9.1 Hz, 2H, Ar), 6.75 (d, *J* = 9.1 Hz, 2H, Ar), 6.36 (d, *J* = 8.8 Hz, 1H, NH), 5.75 (t, *J* = 9.2 Hz, 1H, H-3b), 5.65 (dd, *J* = 9.3, 6.9 Hz, 1H, H-2b), 5.50 (s, 1H, PhC*H*), 5.32 (d, *J* = 3.3 Hz, 1H, H-1a), 5.24 (d, *J* = 7.7 Hz, 1H, H-1b), 5.22 (d, *J* = 12.1 Hz, 1H, PhC*H*H), 5.17 (d, *J* = 12.1 Hz, 1H, PhC*H*H), 4.69 (t, *J* = 8.8 Hz, 1H, H-4a), 4.50 – 4.39 (m, 1H, H-2a), 4.28 (d, *J* = 8.8 Hz, 1H, H-5b), 4.20 (d, *J* = 10.7, 1H, H-6a), 4.07-4.02 (m, 2H, H-3a, H-4b), 3.95 (d, *J* = 10.6,1H, H-6a), 3.75 (s, 3H, OC*H*$_3$), 3.68 (s, 1H, H-5a), 0.84 (s, 9H, TBS), 0.09 (s, 3H, TBS), 0.07 (s, 3H, TBS); ^{13}C NMR (151 MHz, $CDCl_3$) δ 167.0 (*C*O_2Bn), 165.9 (*C*OPh), 165.1(*C*OPh), 161.8 (NH*C*O), 155.9, 150.8, 137.6, 134.8, 133.9, 133.5, 130.2, 129.8, 128.9, 128.8, 128.8, 128.7,128.6,128.6,128.5, 128.5, 128.2, 126.2, 118.9, 114.6, 100.9 (Ph*C*H), 100.7 (C-1a GalN*)*, 98.0 (C-1b GluA), 92.0 (*C*Cl_3), 76.0 (C-4b), 75.6 (C-5b), 74.6 (C-4a), 73.7 (C-3b), 71.8 (C-2b), 69.1 (C-6a), 68.0 (PhC*H*$_2$), 67.8 (C-3a), 64.3 (C-5a), 55.7 (O*C*H_3), 51.8 (C-2a), 25.7 (TBS), 18.0 (TBS), -4.1 (TBS), -4.5 (TBS); HRMS (ESI) calcd. for $C_{55}H_{58}O_{15}NCl_3SiNa$ $(M+Na)^+$ 1128.2534, found 1128.2566 *m/z*.

***p*-Methoxyphenyl (4,6-*O*-benzylidene-3-*O*-acetyl-2-deoxy-2-trichloroacetamido-β-D- galactopyranosyl) -(1→ 4)-(methyl 2,3-di-*O*-benzoyl-β-D-glucopyranosid)uronate (3.22):**

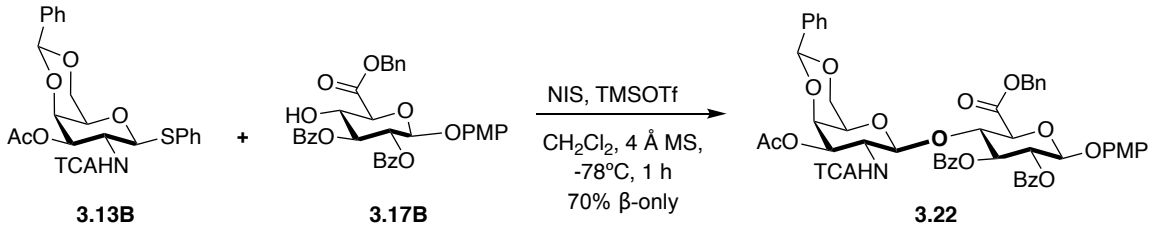

A solution of acceptor **3.17B** (0.90 g, 1.50 mmol, 1.0 equiv.) and donor **3.13B** (0.95 g, 1.73 mmol, 1.1 equiv.) in anhydrous CH_2Cl_2 (20 mL) under an argon atmosphere was added 4 Å MS (0.50 g) at room temperature and allowed to stir for 1 h. The reaction mixture was cooled to -78 °C and added NIS (0.52 g, 3.0 mmol, 2.0 equiv.). After 1 min, a solution of TMSOTf (0.15 equiv., 2.0 mL, 5% in anhydrous CH_2Cl_2) was added dropwise. The reaction was stirred at -78 °C for 2 h when TLC indicated complete consumption of the alcohol **31** starting material. The reaction was quench by the addition of dilute Et_3N in CH_2Cl_2 while warming to room temperature. The reaction was filtered through a glass fritted filter funnel equipped with a pad of Celite to remove the 4 Å MS and then concentrated *in vacuo*. The crude oil was then diluted with EtOAc and transferred to a separatory funnel and washed with satd. aq. $Na_2S_2O_3$ (20 mL x 1), brine (20 mL x 1), and dried over anhydrous Na_2SO_4. The mixture was filtered and concentrated to a crude oil. Flash chromatography of the crude material eluting with EtOAc/Hexane (2:3) gave separable β product:(1.10 g, 1.06 mmol, 70%) as white foam. The β-anomer had R_f = 0.45 (EtOAc/Hexane 2:3) visualized with ceric ammonium molybdate stain; $[\alpha]D^{25}$ = +17.3° (c = 0.012, $CHCl_3$); ^{1}H NMR (600 MHz, $CDCl_3$) δ 7.97-7.92 (m, 4H, Ar), 7.48 – 7.24 (m, 14H, Ar), 7.20

(t, *J* = 7.8 Hz, 2H, Ar), 6.92 (d, *J* = 9.1 Hz, 2H, Ar), 6.71 (d, *J* = 9.2 Hz, 2H, Ar), 5.77 (t, *J* = 9.1 Hz, 1H, H-3b), 5.61 (dd, *J* = 9.2, 7.0 Hz, 1H, H-2b), 5.30 (d, *J* = 12.4 Hz, 1H, PhCH*H*), 5.28 (s, 1H, PhC*H*), 5.21 (d, *J* = 7.0 Hz, 1H, H-1a), 5.14 (d, *J* = 12.2 Hz, 1H, PhC*H*H), 5.03 (dd, *J* = 11.2, 3.4 Hz, 1H, H-3a), 4.85 (d, *J* = 8.3 Hz, 1H, H-1b), 4.50 (t, *J* = 9.1 Hz, 1H, H-4b), 4.28 (d, *J* = 9.2 Hz, 1H, H-5b), 4.18 – 4.11 (m, 1H, H-2a), 4.10 (d, *J* = 3.4 Hz, 1H, H-4a), 3.73 (s, 1H, OC*H*$_3$), 3.65 (d, *J* = 12.5 Hz, 1H, H-6a), 3.60 (d, *J* = 12.4 Hz, 1H, H-6a), 3.09 (s, 1H, H-5a), 2.02 (s, 3H, COC*H*$_3$); ^{13}C NMR (151 MHz, $CDCl_3$) δ 170.9 (*C*OCH_3), 168.1(*C*O$_2$Bn), 165.5 (*C*OPh), 165.3 (*C*OPh), 161.6 (NH*C*O), 155.9, 150.8, 137.6, 134.9, 133.4, 132.9, 130.0, 129.9, 129.0, 128.8, 128.8, 128.7, 128.5, 128.3, 128.2 128.0, 126.6, 119.0, 114.6, 100.9 (Ph*C*H*)*, 100.8 (C-1a GalN), 100.1 (C-1b GlcA), 92.6 (*C*Cl_3), 76.1 (C-4b), 74.4 (C-5b), 72.8 (C-4a), 72.5(C-3b), 72.0 (C-2b), 70.7 (C-3a), 68.1 (C-6a), 67.9 (PhC*H*$_2$), 66.5 (C-5a), 55.7 (O*C*H_3), 52.6 (C-2a), 20.8 (CO*C*H_3); HRMS (ESI) calcd. for $C_{51}H_{46}O_{16}Cl_3NNa$ $(M+Na)^+$ 1056.1774, found 1056.1789 *m/z*.

***p*-Methoxyphenyl (4,6-*O*-benzylidene-3-*O*-acetyl-2-deoxy-2-trichloroacetamido-β-D- galactopyranosyl)-(1→ 4)-(methyl 2,3-di-*O*-benzyl-β-D-glucopyranosid)uronate (3.31):**

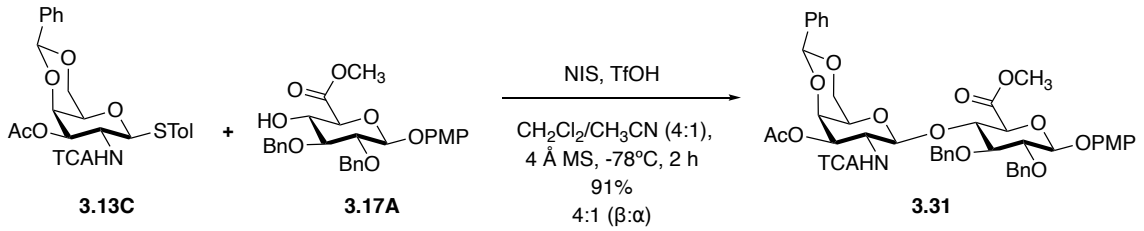

A solution of acceptor **3.17A** (1.75 g, 3.50 mmol, 1.0 equiv.) and donor **3.13C** (2.46 g, 4.36 mmol, 1.5 equiv.) in anhydrous CH_2Cl_2 (30 mL) under an argon atmosphere was added 4 Å MS (5.0 g) at room temperature and allowed to stir for 1 h. The reaction mixture was cooled to -78 °C and added NIS (1.59 g, 7.08 mmol, 2.0 equiv.). After 1 min, a solution of TMSOTf (0.15 equiv., 2.0 mL, 5% in anhydrous CH_2Cl_2) was added dropwise. The reaction was stirred at -78 °C for 2 h when TLC indicated complete consumption of the alcohol **3.17A** starting material. The reaction was quench by the addition of dilute Et_3N in CH_2Cl_2 while warming to room temperature. The reaction was filtered through a glass fritted filter funnel equipped with a pad of Celite to remove the 4 Å MS and then concentrated *in vacuo*. The crude oil was then diluted with EtOAc and transferred to a separatory funnel and washed with satd. aq. $Na_2S_2O_3$ (20 mL x 1), brine (20 mL x 1), and dried over anhydrous Na_2SO_4. The mixture was filtered and concentrated to a crude oil. Flash chromatography of the crude material eluting with EtOAc/Hexane (1:4) gave separable β/α (4:1) products: β **32** (2.40 g, 2.53 mmol, 74%) and α (0.60g, 0.64 mmol, 18%) as both yellow foams. The combine yield is 91%. The β-anomer had R_f = 0.45 (EtOAc/Hexane 1:1) and α-anomer had R_f = 0.55 (EtOAc/Hexane 1:1), both visualized with ceric ammonium molybdate stain; β-anomer: $[\alpha]D^{25}$ = +46.7° (c = 0.0018, $CHCl_3$); ^{1}H NMR (600 MHz,

$CDCl_3$) δ 7.55 – 7.47 (m, 2H, Ar), 7.44 – 7.38 (m, 2H, Ar), 7.37 – 7.26 (m, 9H, Ar), 7.17 (m, 2H,Ar), 6.97 (d, *J* = 9.1 Hz, 2H, Ar), 6.85 (d, *J* = 9.0 Hz, 1H, NH), 6.82 (d, *J* = 9.1 Hz, 2H, Ar), 5.55 (s, 1H, PhC*H*), 5.20 (d, *J* = 10.7 Hz, 1H, PhC*H*H), 5.13 (dd, *J* = 11.2, 3.4 Hz, 1H, H-3a), 5.02 (d, *J* = 8.5 Hz, 1H, H-1a), 4.95 (d, *J* = 6.8 Hz, 1H, H-1b), 4.94 (d, *J* = 11.0 Hz, 1H, PhC*H*H), 4.79 (d, *J* = 11.1 Hz, 1H, PhCH*H*), 4.76 (d, *J* = 10.7 Hz, 1H, PhCH*H*), 4.42 (dt, *J* = 11.2, 8.6 Hz, 1H, H-2a), 4.31 (d, *J* = 2.4 Hz, 1H, H-4a), 4.26 (d, *J* = 10.9 Hz, 1H, H-6a), 4.21 (t, *J* = 9.0 Hz, 1H, H-4b), 3.99 (d, *J* = 10.8 Hz, 1H, H-6a), 3.97 (d, *J* = 9.4 Hz, 1H, H-5b), 3.78 (s, 3H, OC*H*$_3$), 3.75 (s, 3H, CO_2C*H*$_3$), 3.73 (d, *J* = 8.7 Hz, 1H, H-3b), 3.69 (dd, *J* = 8.9, 6.8 Hz, 1H, H-2b), 3.50 (s, 1H, H-5a), 2.08 (s, 3H, COC*H*$_3$); ^{13}C NMR (151 MHz, $CDCl_3$) δ 171.2 (*C*OCH_3), 170.1(*C*O_2CH_3), 161.9 (NH*C*O), 155.6, 151.2, 138.6, 138.2, 137.7, 129.1, 128.6, 128.5, 128.3, 128.2, 128.1, 127.8, 127.5, 126.5, 118.5, 118.4, 114.7, 102.7 (C-1a GalN), 101.0 (Ph*C*H), 100.6 (C-1b GlcA), 92.7 (*C*Cl_3), 82.2 (C-3b), 81.3 (C-2b), 78.5 (C-4b), 76.39 (Ph*C*H_2), 75.0 (Ph*C*H_2), 74.1 (C-5b), 73.2 (C-4a), 71.4 (C-3a), 68.8 (C-6a), 66.9 (C-5a), 55.8 (O*C*H_3), 53.1 (CO_2*C*H$_3$), 52.7 (C-2a), 20.9 (CO*C*H_3); HRMS (ESI) calcd. for $C_{45}H_{46}O_{14}NCl_3Na$ $(M+Na)^+$ 952.1876, found 952.1877 *m/z*.

***p*-Methoxyphenyl (4,6-di-*O*-benzylidene-2-deoxy-2-trichloroacetamido-β-D-galactopyranosyl) -(1→4)-(methyl 2,3-di-*O*-benzyl-β-D-glucopyranosid)uronate (3.32):**

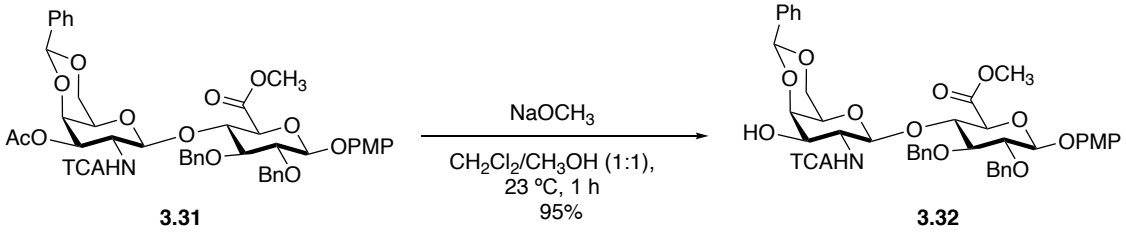

3.31 **3.32**

A solution of **3.31** (1.40 g, 1.54 mmol, 1.0 equiv.) in anhydrous CH_3OH/CH_2Cl_2 (20 mL) under an argon atmosphere was added $NaOCH_3$ solution (1.00 mL, 1.5 mmol, [1.5 M] in CH_3OH) dropwise at room temperature. At 1 h, the pH of the reaction mixture was still >12 and TLC indicated that the starting material had been completely consumed for a more polar spot. The reaction was neutralized by the addition of acidic form Amberlite IR 120 (H+) ion exchange resin. The solution was filtered through a glass fritted funnel with a pad of Celite to remove the resin. The filtrate was concentrated *in vacuo* to give **3.32** (1.28 g, 1.44 mmol, >95%) as a yellow foam in quantitative yield. Rf = 0.25 (EtOAc/Hexanes 1:1) visualized with ceric ammonium molybdate stain; $[\alpha]D^{25}$ = +12.8° (c = 0.0015, $CHCl_3$); ^{1}H NMR (600 MHz, $CDCl_3$) δ 7.54 – 7.43 (m, 4H, Ar), 7.40 – 7.26 (m, 9H, Ar), 7.26 – 7.14 (m, 2H, Ar), 6.99 (d, *J* = 9.1 Hz, 2H, Ar), 6.84 (d, *J* = 9.1 Hz, 2H, Ar), 5.59 (s, 1H, PhC*H*), 5.21 (d, *J* = 10.4 Hz, 1H, PhC*H*H), 4.96 (d, *J* = 6.74, 1H, H-1b), 4.95 (d, *J* = 11.0 Hz, 1H, PhC*H*H), 4.86 (d, *J* = 8.4 Hz, 1H, H-1a), 4.81 (d, *J* = 11.0 Hz, 1H, PhCH*H*), 4.75 (d, *J* = 10.4 Hz, 1H, PhCH*H*), 4.26 (d, *J* = 12.7 Hz, 1H, H-6a), 4.24 – 4.16 (m, 2H, H-2a, H-4a), 4.14 (t, *J* = 9.0 Hz, 1H, H-4b), 4.03-4.00 (m, 2H, H-6a, H-5b), 3.83-3.79 (m, 1H, H-3a), 3.78 (s, 3H, OC*H*$_3$), 3.77 (s, 3H, CO_2CH_3), 3.74 – 3.69 (m, 2H, H-2b,

H-3b), 3.48 (s, 1H, H-5a), 2.78 (s, 1H, O*H*); ^{13}C NMR (151 MHz, $CDCl_3$) δ 170.7 (*C*O_2CH_3), 163.3 (NH*C*O), 155.7, 151.2, 138.5, 138.1, 137.6, 129.3, 128.7, 128.5, 128.3, 128.1, 127.9, 127.7, 126.5,126.2, 118.5, 114.7, 102.73 (Ph*C*H), 101.44 (C-1b GlcA), 100.7 (C-1a GalN), 92.8 (*C*Cl_3), 82.3 (C-3b), 81.3 (C-2b), 78.9 (C-4b), 76.6 (Ph*C*H_2), 75.1 (Ph*C*H_2), 75.0 (C-4a), 74.0 (H-5b), 72.6 (H-3a), 68.7 (C-6a), 67.2 (C-5a), 55.8 (O*C*H_3), 55.7 1 (CO_2*C*H_3), 53.2 (C-2a); HRMS (ESI) calcd. for $C_{43}H_{44}O_{13}NCl_3Na$ $(M+Na)^+$ 910.1770, found 910.1769 *m/z*.

***p*-Methoxyphenyl (3-*O*-benzoyl-4-azido-2,4,6-trideoxy-2-trichloroacetamido-β-D-galactopyranosyl)-(1→3)-(4,6-di-*O*-benzylidene-2-deoxy-2-trichloroacetamido-β-D- galactopyranosyl)-(1→4)-(methyl 2,3-di-*O*-benzyl-β-D-glucopyranosid)uronate (3.33):**

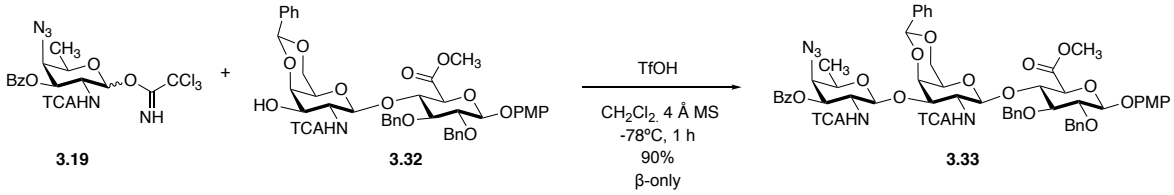

3.19 3.32 3.33

A solution of acceptor **3.32** (1.10 g, 1.24 mmol, 1.0 equiv.) and donor **3.19** (0.864 g, 1.49 mmol, 1.2 equiv.) in anhydrous CH_2Cl_2 (12 mL) under an argon atmosphere was added 4 Å MS (3.0 g) at room temperature and allowed to stir for 1 h. The reaction mixture was cooled to -78 °C and a solution of TfOH (0.15 equiv., 2.0 mL, 5% in anhydrous CH_2Cl_2) was added dropwise. The reaction was stirred at -78 °C for 1 h when TLC indicated complete consumption of the alcohol **3.32** starting material. The reaction was quench by the addition of dilute Et_3N in CH_2Cl_2 while warming to room temperature. The reaction was filtered through a glass fritted filter funnel equipped with a pad of Celite to remove the 4 Å MS and then concentrated *in vacuo*. The crude oil was then diluted with EtOAc and transferred to a separatory funnel and washed with satd. aq. $Na_2S_2O_3$ (20 mL x 1), brine (20 mL x 1), and dried over anhydrous Na_2SO_4. The mixture was filtered and concentrated to a crude oil. Flash chromatography of the crude material eluting with EtOAc/Hexane (1:4) gave the **3.33** (1.45g, 1.11 mmol, 90%) as a white foam. The trisaccharide **3.33** had R_f = 0.40 (EtOAc/Hexane 1:1) visualized with ceric ammonium molybdate stain; $[\alpha]D^{25}$ = -27.7° (c = 0.0017, $CHCl_3$); ^{1}H NMR (600 MHz, $CDCl_3$) δ 8.07 – 7.98 (m, 2H, Ar), 7.64 – 7.55 (m, 1H, Ar), 7.52 – 7.42 (m, 4H, Ar), 7.40 – 7.34 (m, 2H, Ar), 7.28 (m, 8H, Ar), 7.20 – 7.11 (m, 3H, Ar), 7.13 (d, *J* = 7.7 Hz, 1H, NH), 6.97 (d, *J* = 9.1 Hz,

2H, Ar), 6.85 (d, *J* = 9.0 Hz, 1H, NH), 6.82 (d, *J* = 9.1 Hz, 2H, Ar), 5.57 (s, 1H, PhC*H*), 5.32 (dd, *J* = 11.0, 3.5 Hz, 1H, H-3c), 5.14 (d, *J* = 10.9 Hz, 1H, PhC*H*H), 5.05 (d, *J* = 8.3 Hz, 1H, H-1a), 4.97 (d, *J* = 6.6 Hz, 1H, H-1b), 4.91 (d, *J* = 11.0 Hz, 1H, PhC*H*H), 4.88 (d, *J* = 8.5 Hz, 1H, H-1c), 4.77 (d, *J* = 11.0 Hz, 1H, PhCH*H*), 4.73 (d, *J* = 11.0 Hz, 1H, PhCH*H*), 4.46 (dt, *J* = 11.0, 8.7 Hz, 1H, H-2c), 4.36 (dd, *J* = 10.8, 3.4 Hz, 1H, H-3a), 4.32 (dd, *J* = 3.5, 1.0 Hz, 1H, H-4a), 4.28 (m, 1H, H-4b), 4.27 (d, *J* = 10.7 Hz, 1H, H-6a), 4.18 – 4.11 (m, 1H, H-2a), 4.01 (d, *J* = 10.7 Hz, 1H, H-6a), 3.98 (d, *J* = 9.1 Hz, 1H, H-5b), 3.95 (dd, *J* = 3.5, 1.3 Hz, 1H, H-4c), 3.84 (qd, *J* = 7.3, 1.8 Hz, 1H, H-5c), 3.78 (s, 3H, OC*H*$_3$), 3.75 (s, 3H, CO_2C*H*$_3$), 3.75 – 3.67 (m, 2H, H-2b, H-3b), 3.46 (s, 1H, H-5a), 1.43 (d, *J* = 6.3 Hz, 3H, H-6c); ^{13}C NMR (151 MHz, $CDCl_3$) δ 170.0 (*C*O_2CH_3), 166.2 (*C*OPh), 162.5 (NH*C*O), 162.2 (NH*C*O), 155.6, 151.2, 138.6, 138.1, 137.9, 134.0, 130.3, 128.8, 128.7, 128.52, 128.49, 128.3, 128.2, 128.2, 128.1, 127.8, 127.5, 126.4, 118.4, 114.7, 102.7 (C-1b GlcA), 100.6 (Ph*C*H), 99.6 (C-1a GalN), 99.0 (C-1c AAT), 92.9 (*C*Cl_3), 92.2 (*C*Cl_3), 82.2 (C-3b), 81.3 (C-2b), 77.6 (C-4b), 76.0 (Ph*C*H_2), 75.2 (C-4a), 75.0 (Ph*C*H_2), 74.3 (C-5b), 73.4 (C-3c), 72.4 (C-3a), 70.3 (C-5c), 68.7 (C-6a), 67.1 (C-5a), 63.4 (C-4c), 55.8 (O*C*H_3), 54.8 (C-2a), 53.0 (CO_2*C*H_3), 52.5 (C-2c), 17.6 (C-6c); HRMS (ESI) calcd. for $C_{58}H_{56}O_{17}N_5Cl_6$ $(M-H)^-$ 1304.1808, found 1304.1770 *m/z*.

***p*-Methoxyphenyl (3-*O*-benzoyl-4-azido-2,4,6-trideoxy-2-trichloroacetamido-β-D-galactopyranosyl)-(1→3)-(6-*O*-benzyl-2-deoxy-2-trichloroacetamido-β-D-galactopyranosyl)-(1→4)-(methyl 2,3-di-*O*-benzyl-β-D-glucopyranosid)uronate (3.34):**

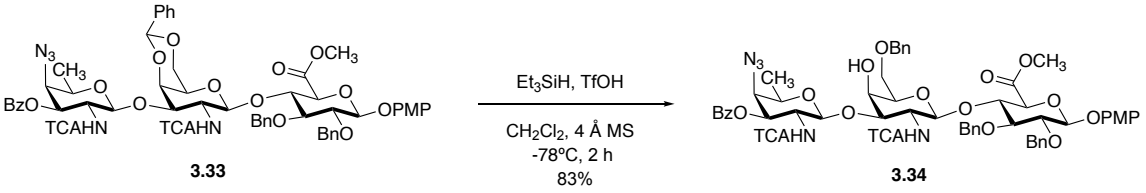

3.33 3.34

The trisaccharide **3.33** (1.40 g, 1.07 mmol, 1 equiv.) in CH_2Cl_2 (11 mL) and Et_3SiH (0.520 mL, 3.21 mmol, 3.0 equiv.) was stirred with preactivated 4Å MS (3.0 g) for 30 min under an argon atmosphere. After cooling to −78 °C, the mixture was treated with TfOH (0.330 mL, 3.74 mmol, 3.5 equiv.). The mixture was maintained at that temperature for 2 h. After TLC indicated complete consumption of the starting material, CH_3OH (3 mL) and then NEt_3 (1 mL) were added in this order. The mixture was diluted with EtOAc (50 mL), washed with H_2O (2 x 50 mL), dried over anhydrous Na_2SO_4, and concentrated *in vacuo* to yield the crude alcohol. Flash chromatography of the crude material eluting with EtOAc/Hexane (3:7) gave the alcohol **3.34** (1.20 g, 0.915 mmol, 86%) as a white foam. The trisaccharide **3.34** had R_f = 0.30 (EtOAc/Hexane 1:1) visualized with ceric ammonium molybdate stain; $[\alpha]D^{25}$ = -15.0° (c = 0.002, $CHCl_3$); ^{1}H NMR (600 MHz, $CDCl_3$) δ 8.05 (dd, *J* = 8.4, 1.4 Hz, 2H, Ar), 7.63 – 7.53 (m, 1H, Ar), 7.50 – 7.42 (m, 2H, Ar), 7.41 – 7.36 (m, 2H, Ar), 7.36 – 7.23 (m, 13H, Ar), 7.13 (d, *J* = 7.5 Hz, 1H, NH), 7.01 (d, *J* = 8.7 Hz, 1H, NH), 6.97 (d, *J* = 9.1 Hz, 2H, Ar), 6.82 (d, *J* = 9.1 Hz, 2H, Ar), 5.42 (dd, *J* = 11.1, 3.5 Hz, 1H, H-3c), 4.98 (d, *J* = 10.7 Hz, 1H, PhC*H*H), 4.95 – 4.89 (m, 3H, PhC*H*H, H-1a, H-1b), 4.84 (d, *J* = 8.3 Hz, 1H, H-1c), 4.78 (d, *J* = 11.0 Hz, 1H, PhCH*H*), 4.74 (d, *J* = 10.6 Hz, 1H, PhCH*H*), 4.46 (d, *J* = 11.9 Hz, 1H, PhC*H*H), 4.42 – 4.37 (m, 1H,

H-2c), 4.37 (d, *J* = 11.8 Hz, 1H, PhCH*H*), 4.26 (dd, *J* = 10.4, 3.2 Hz, 1H, H-3a), 4.19 (ddd, *J* = 9.1, 5.9, 3.0 Hz, 1H, H-4b), 4.12 (s, 1H, H-4a), 3.97-3.90 (m, 3H, H-2a, H-4c, H-5b), 3.85 – 3.79 (m, 1H, H-5c), 3.78 (s, 3H, OC*H*$_3$), 3.74 (s, 3H, CO_2C*H*$_3$), 3.72 (dd, *J* = 9.7, 6.6 Hz, 1H, H-6a), 3.68 – 3.61 (m, 3H, H-2b, H-3b, H-5a), 3.54 (dd, *J* = 9.7, 5.5 Hz, 1H, H-6a), 2.71 (s, 1H, OH), 1.40 (d, *J* = 6.3 Hz, 3H, H-6c); ^{13}C NMR (151 MHz, $CDCl_3$) δ 169.7 (*C*O_2CH_3), 166.4 (*C*OPh), 162.6 (NH*C*O), 162.2 (NH*C*O), 155.6, 151.2, 138.6, 138.2, 138.1, 134.1, 130.3, 128.8, 128.5, 128.3, 128.3, 128.2, 127.9, 127.79, 127.62, 118.5, 114.7, 102.8 (C-1b GlcA), 99.7 (C-1c AAT), 98.9 (C-1a GalN), 92.9 (*C*Cl_3), 92.3 (*C*Cl_3), 82.1 (C-3b), 81.2 (C-2b), 76.8 (C-4b), 76.1 (C-3a), 75.9 (Ph*C*H_2), 75.1 (Ph*C*H_2), 74.2 (C-5b), 73.7 (C-5a), 73.5 (Ph*C*H_2), 72.8 (C-3c), 70.1 (C-5c), 68.6 (Ph*C*H_2), 67.9 (C-4a), 63.5 (C-4c), 55.8 (OCH_3), 55.7 (C-2a), 53.2 (CO_2*C*H_3), 53.1 (C-2c), 17.5 (C-6c); HRMS (ESI) calcd. for $C_{58}H_{58}O_{17}N_5Cl_6$ $(M-H)^-$ 1306.1964, found 1306.1930 *m/z*.

***p*-Methoxyphenyl (3-*O*-benzoyl-4-azido-2,4,6-trideoxy-2-trichloroacetamido-β-D-galactopyranosyl)-(1→3)-(4-(N-benzyloxycarbonyl)aminoethyl-phosphonato-6-*O*-benzyl-2-deoxy-2-trichloroacetamido-β-D-galactopyranosyl)-(1→4)-(methyl 2,3-di-*O*-benzyl-β-D-glucopyranosid)uronate (3.37):**

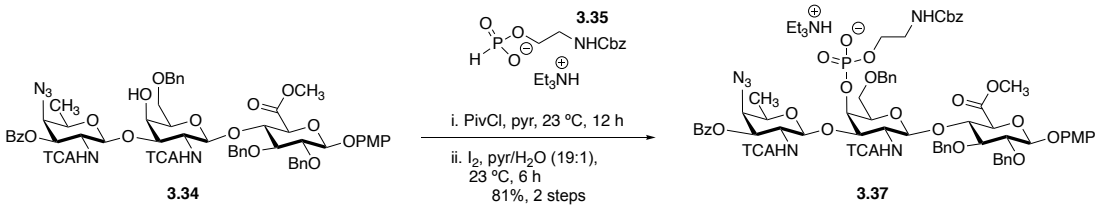

Ethanolamine H-phosphonate **3.35** (208 mg, 0.58 mmol, 2.0 equiv.) and trisaccharide **3.34** (108 mg, 0.082 mmol, 1.0 equiv.) were co-evaporated with anhydrous pyridine (3 × 5 mL) in two separate portions of 10 mL of RBF and dried under high vacuum overnight. The ethanolamine H-phosphonate **3.35** was dissolved in anhydrous pyridine (1 mL) followed by the addition of pivaloyl chloride (0.070 mL, 0.58 mmol, 2.0 equiv.) stirring for 15 min at room temperature under an argon atmosphere. To that mixture, a solution of trisaccharide **3.34** in anhydrous pyridine (1.5 mL) was added, and the resulting mixture was stirred at room temperature for 12 h. Iodine (158 mg, 0.62 mmol, 2.5 equiv.) in a mixture of pyridine and H_2O (19:1, 0.5 mL) was added to oxidize P(III) to P(V) and stirred for additional 6 h at room temperature. The reaction mixture was diluted with CH_2Cl_2 (50 mL) and the organic layer washed with satd. aq. $Na_2S_2O_3$ (20 mL x 1), followed by 1M TEAB (triethylammonium bicarbonate) (20 mL x 1) buffer solution, and dried over anhydrous Na_2SO_4. Solvents were concentrated *in vacuo*, and the crude was purified by flash column chromatography with $E_{t3}N$ deactivated silica gel to give **3.37** (118 mg, 0.082 mmol, 86%) as a white sticky liquid. Phosphorated **3.37** had R_f = 0.5 (CH_2Cl_2/CH_3OH = 9:1) visualized with ceric ammonium molybdate stain; $[\alpha]D^{25}$ = -

5.7° (c = 0.0017, $CHCl_3$); ^1H NMR (600 MHz, $CDCl_3$) δ 8.05 (d, *J* = 7.7 Hz, 2H, Ar), 7.55 (t, *J* = 7.4 Hz, 1H, Ar), 7.49 – 7.20 (m, 22H, Ar), 7.01 (d, *J* = 8.7 Hz, 1H, NH), 6.97 (d, *J* = 9.0 Hz, 2H, Ar), 6.81 (d, *J* = 9.1 Hz, 2H, Ar), 6.50 (d, *J* = 5.0 Hz, 1H, NH), 6.13 (d, *J* = 9.7 Hz, 1H, H-4a), 5.32 (d, *J* = 8.1 Hz, 1H, H-1c), 5.13 – 4.98 (m, 2H, PhC*H*H, PhC*H*$_2$), 4.96 (d, *J* = 6.8 Hz, 1H, H-1b), 4.90 – 4.83 (m, 2H, H-3c, PhCH*H*), 4.80 (d, *J* = 8.2 Hz, 1H, H-1a), 4.74 (d, *J* = 11.1 Hz, 1H, PhC*H*H), 4.66 (d, *J* = 10.8 Hz, 1H, PhCH*H*), 4.50 (d, *J* = 11.8 Hz, 1H, PhC*H*H), 4.43 (d, *J* = 12.0 Hz, 1H, PhCH*H*), 4.36 (d, *J* = 8.2 Hz, 1H, H-5c), 4.28 (t, *J* = 8.4 Hz, 1H, H-4b), 4.02 – 3.95 (m, 4H, H-3a, H-5b, H-2c, H-4c), 3.93 – 3.80 (m, 4H, H-2a, H-6a, PEtN-C*H*$_2$), 3.77 (s, 3H, OC*H*$_3$), 3.74-3.73 (m, 1H, H-5a), 3.72 (s, 3H, CO_2C*H*$_3$), 3.70 – 3.58 (m, 3H, H-2b, H-3b, H-6a), 3.41 – 3.32 (m, 2H, PEtN-C*H*$_2$), 1.38 (d, *J* = 6.3 Hz, 3H, H-6c); ^{13}C NMR (151 MHz, $CDCl_3$) δ 169.4 (*C*O_2CH_3), 165.9 (*C*OPh), 163.5 (NH*C*O), 162.5 (NH*C*O), 156.6, 155.5, 151.2, 138.8, 138.4, 138.2, 136.8, 133.6, 130.2, 128.7, 128.6, 128.5, 128.4, 128.4, 128.4, 128.3, 128.1, 128.1, 127.7, 127.7, 127.6, 127.5, 118.36, 114.66, 102.4 (C-1b GlcA), 100.7 (C-1a GalN), 96.5 (C-1c AAT), 92.9 (*C*Cl_3), 92.7 (*C*Cl_3), 82.1 (C-3b), 81.0 (C-2b), 77.0 (C-4b), 75.3 (Ph*C*H_2), 74.9 (Ph*C*H_2), 74.8 (C-5a), 74.4 (C-5b), 73.8 (Ph*C*H_2), 73.5 (C-3c), 70.7 (C-5c), 70.3 (C-4a), 69.7 (C-6a), 69.5 (C-3a), 66.6 (Ph*C*H_2), 64.3 (PEtN-*C*H_2), 63.3 (C-4c), 55.7 (OCH_3), 54.1 (C-2a), 53.9 (C-2c), 52.8 (CO_2C*H*$_3$), 42.6 (PEtN-*C*H_2), 17.9 (C-6c); ^{31}P NMR (162 MHz, $CDCl_3$) δ -0.28; HRMS (ESI) calcd. for $C_{68}H_{70}O_{22}N_6Cl_6P$ $(M-H)^-$ 1563.2383, found 1563.2417 *m/z*.

***p*-Methoxyphenyl 2-acetamido-4-amino-2,4,6-trideoxy-β-D-galactopyranosyl-(1→3)-4-*O*-aminoethyl-phospho-nato-β-D-galactopyranosyl-(1→4)-*O*-β-D-Glucopyranosyluronic acid (3.30):**

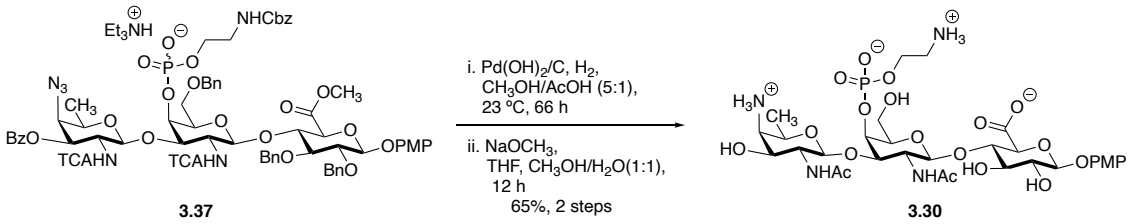

3.37 **3.30**

Protected trisaccharide **3.37** (36 mg, 0.022 mmol, 1.0 equiv.) was placed under argon. To this flask was wet Pd $(OH)_2$/C (20% Pd by weight, 110 mg, 0.15 mmol, 7.0 equiv.). CH_3OH (5 mL) and AcOH (1 mL) was added to this mixture, and then, H_2 gas was bubbled through the solution at 23 °C for 30 min.[10] After the H_2 atmosphere was established, the reaction was stirred for 66 h (progress monitored by MS). The mixture was then, filtered over Celite and concentrated *in vacuo* to yield the crude product. The crude material was dissolved in THF (3 mL) at 23 °C and then, treated dropwise, with a 1.5 M $NaOCH_3$ solution in 1:1 CH_3OH/H_2O (5.0 mL, 1.95 mmol). After stirring for 12 h (progress monitored by MS), AcOH was added until neutral pH was achieved. The crude material was concentrated *in vacuo* and was purified by size exclusion chromatography (Bio-Gel P2 gel) using deionized H_2O as an eluant. Fractions containing the desired product (determined from MS) were combined and lyophilized to **3.30** (12.0 mg, 0.015 mmol, 68%) as a white powder; $[\alpha]D^{25}$ = -29.1° (c = 0.003, H_2O); ^1H NMR (600 MHz, D_2O) δ 7.11 (d, *J* = 9.1 Hz, 2H), 6.99 (d, *J* = 9.1 Hz, 2H), 5.01 (d, *J* = 7.9 Hz, 1H), 4.72 (dd, *J* = 9.2, 2.8 Hz, 1H), 4.60 (d, *J* = 8.4 Hz, 1H), 4.54 (d, *J* = 8.4 Hz, 1H), 4.24 – 4.15 (m, 2H), 4.09 – 4.00 (m, 2H), 3.97 (q, *J* = 6.0 Hz, 1H), 3.91 – 3.83 (m, 4H), 3.82 (s, 3H), 3.81 – 3.76 (m, 3H), 3.71 (t, *J* = 8.7 Hz, 1H), 3.62 (dd, *J* = 9.5, 7.9 Hz, 1H), 3.55 (d, *J* = 4.7

Hz, 1H), 3.30 (t, *J* = 5.5 Hz, 2H), 2.10 (s, 3H), 2.02 (s, 3H), 1.34 (d, *J* = 6.6 Hz, 3H); ^{13}C NMR (151 MHz, D_2O) δ 175.3, 175.1, 155.8, 152.0, 119.2, 116.1, 103.9, 102.3, 102.1, 80.9, 79.2, 77.7, 75.9, 75.3, 74.8, 73.6, 69.0, 68.4, 63.2, 62.2, 56.8, 55.6, 53.1, 52.0, 41.3, 23.7, 23.4, 16.8; ^{31}P NMR (162 MHz, D_2O) δ -0.30; HRMS (ESI) calcd. for $C_{31}H_{48}O_{19}N_4P$ $(M-H)^-$ 811.2656, found 811.2631 *m/z*. Our spectroscopic data strongly matched previously reported data.[11]

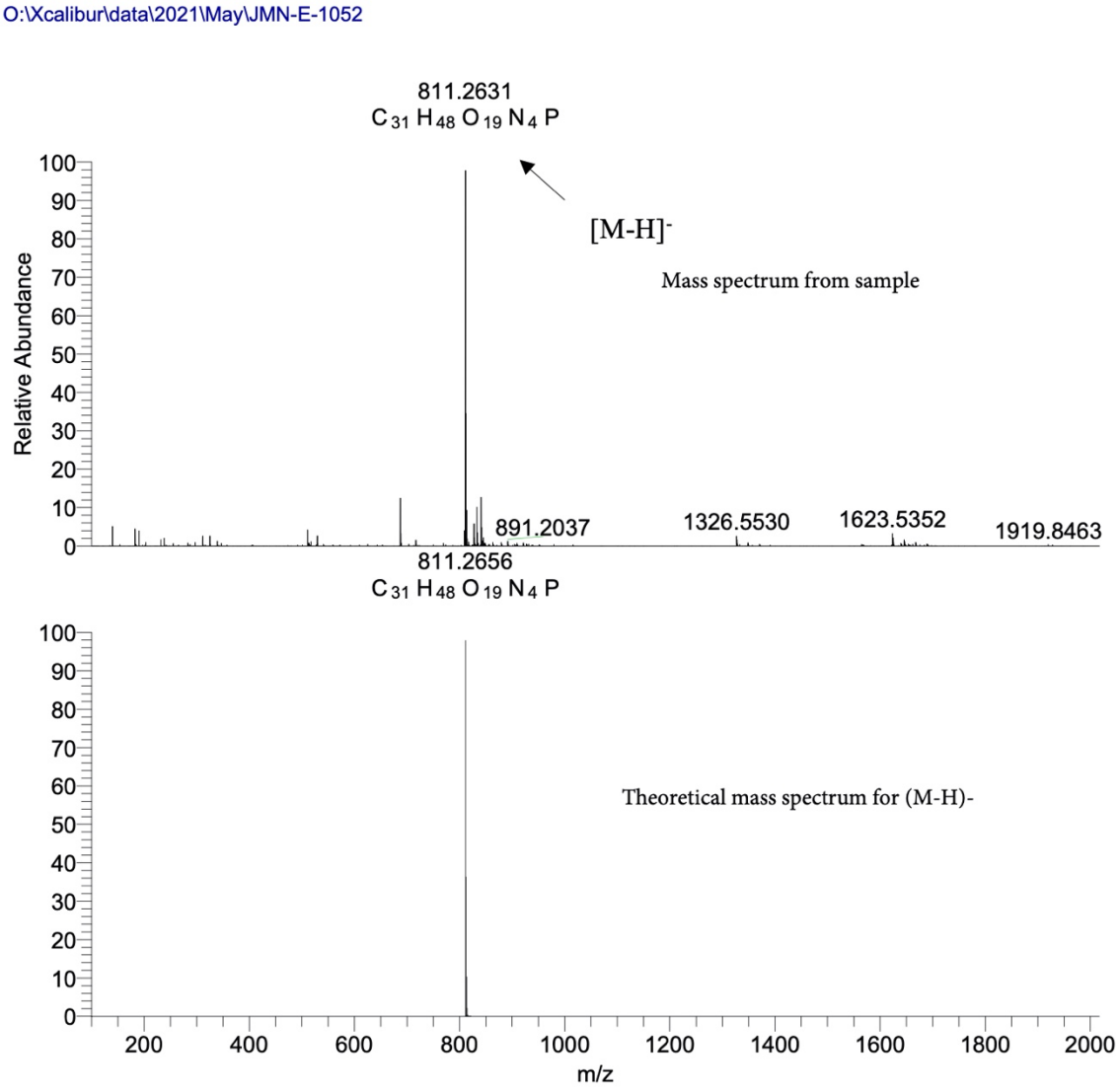

Appendix A3:

Spectra and Table Relevant to Chapter 3

Table A3.1. Comparison of ^{1}H and ^{13}C NMR chemical shifts (ppm) between isolated and synthetic 3.30

Residue		Chemical shifts (ppm)							
		C1/H1	C2/H2	C3/H3	C4/H4	C5/H5	C6/H6	NAc	C=O
→3)-β-D Fuc*p*NAc4N-(1→	isolated[a]	103.8	51.9	78.8	55.5	68.3	16.8	23.5	175.6-
		4.56	3.87	4.11	3.77	3.94	1.30	2.01	176.0
	synthetic	103.9	53.1	69.0	55.7	68.4	16.8	23.5	175.4-
		4.54	3.79	4.02	3.54	3.97	1.34	2.02	175.3
→3)-β-D-Gal*p*NAc-(1→	isolated[a]	102.2	52.1	79.3	75.4	76.1	62.3	23.8	175.6-
		4.53	4.00	3.82	4.68	3.76	3.79, 3.75	2.04	176.0
	synthetic	102.1	52.0	79.2	75.3	75.9	62.2	23.7	175.4-
		4.60	4.04	3.86	4.72	3.80	3.83, 3.78	2.10	175.3
→4)-β-D-Glc*p*A-(1→	isolated[a]	105.6	73.4	74.9	81.1	77.5	175.6		
		4.51	3.36	3.58	3.74	3.73			
	synthetic	102.3	73.6	74.8	80.9	77.8	175.1		
		5.01	3.62	3.71	3.86	3.85			
PEtN	isolated[a]	63.3	41.4						
		4.16	3.27						
	synthetic	63.3	41.3						
		4.20	3.30						

[a]Data from isolation ref: *Carbohydrate Res.* **2015**, 1-4.

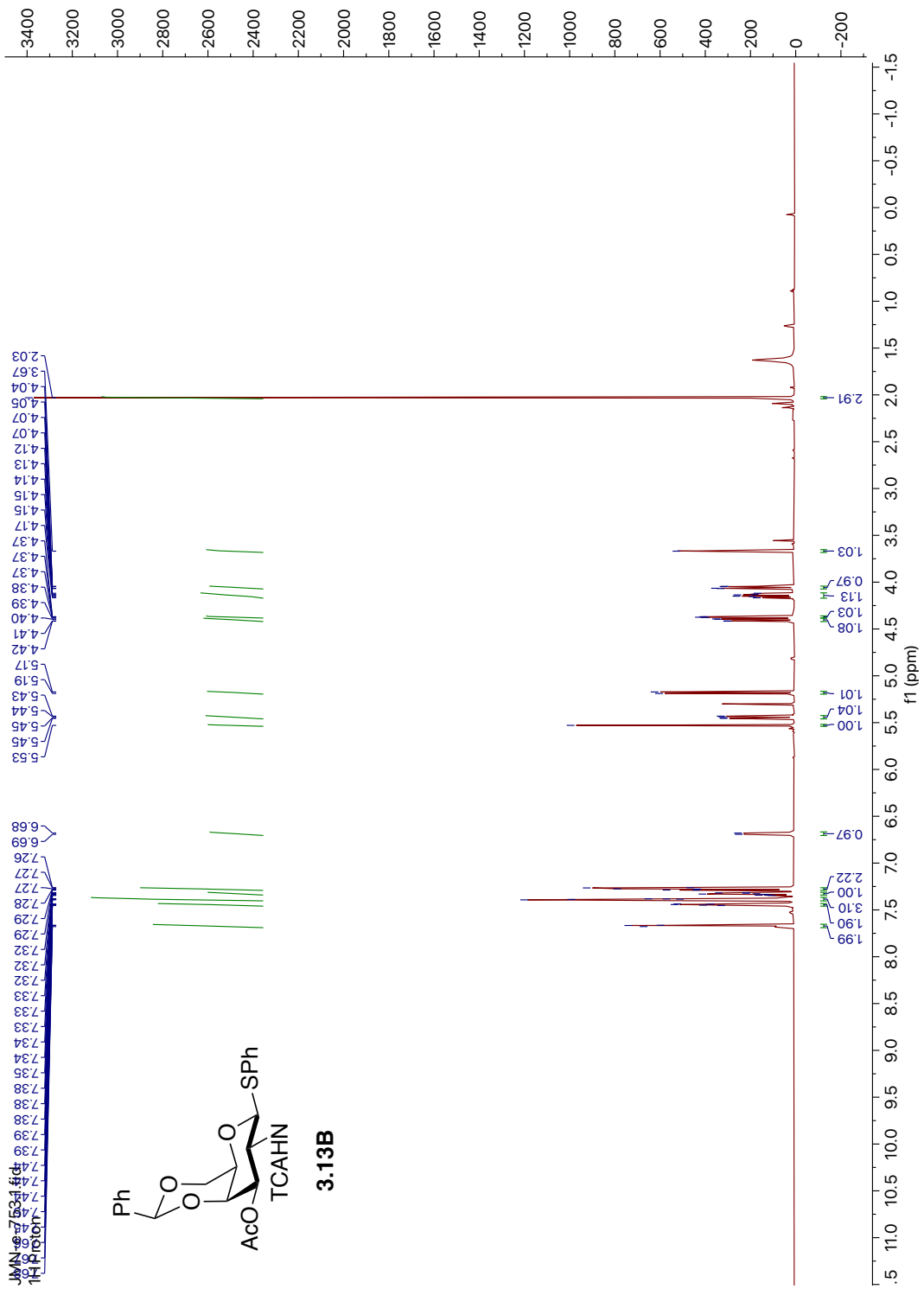

Figure A3.1. ^{1}H NMR (600 MHz, $CDCl_3$) of compound **3.13B**

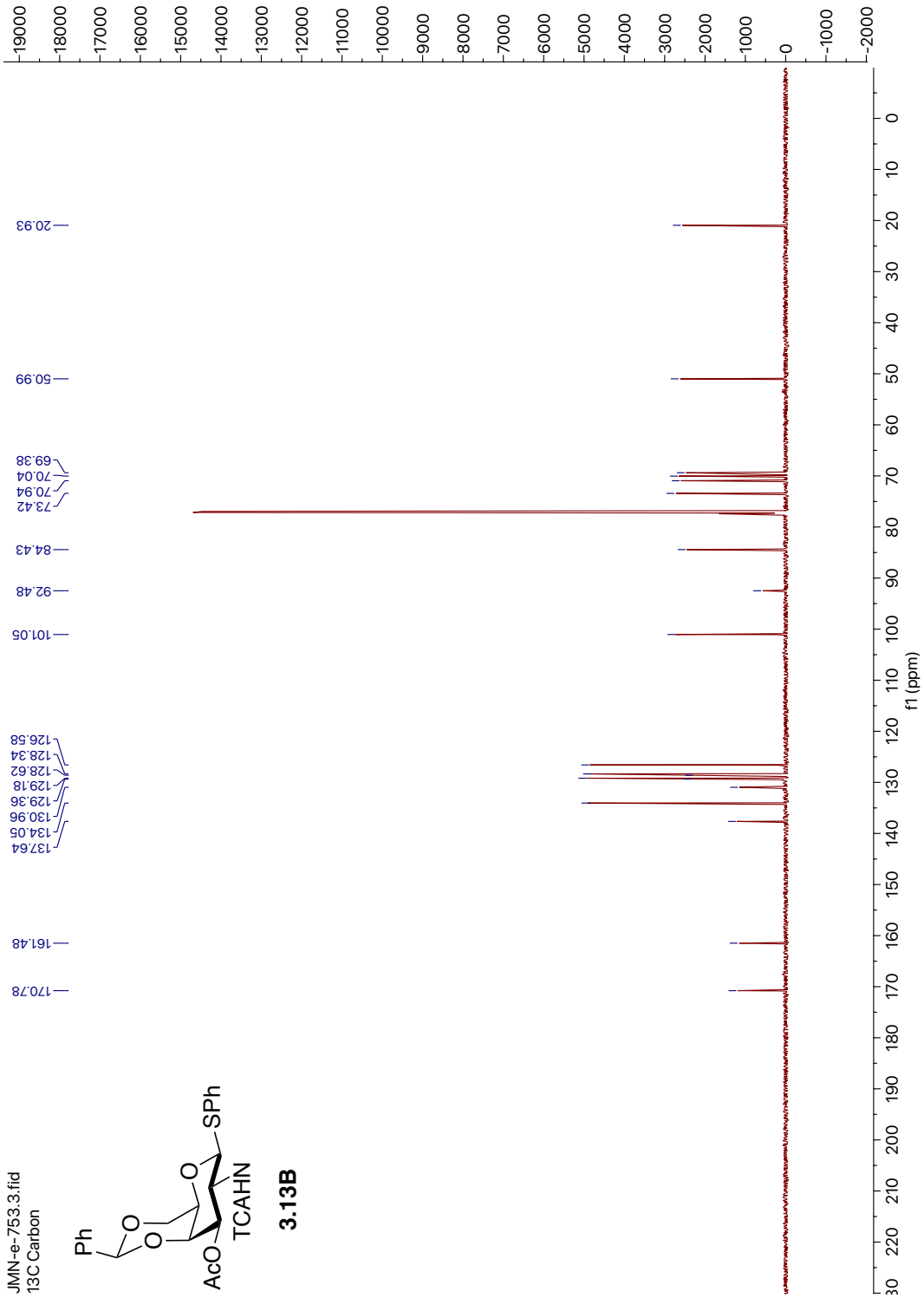

Figure A3.2. ^{13}C NMR (151 MHz, $CDCl_3$) of compound **3.13B**.

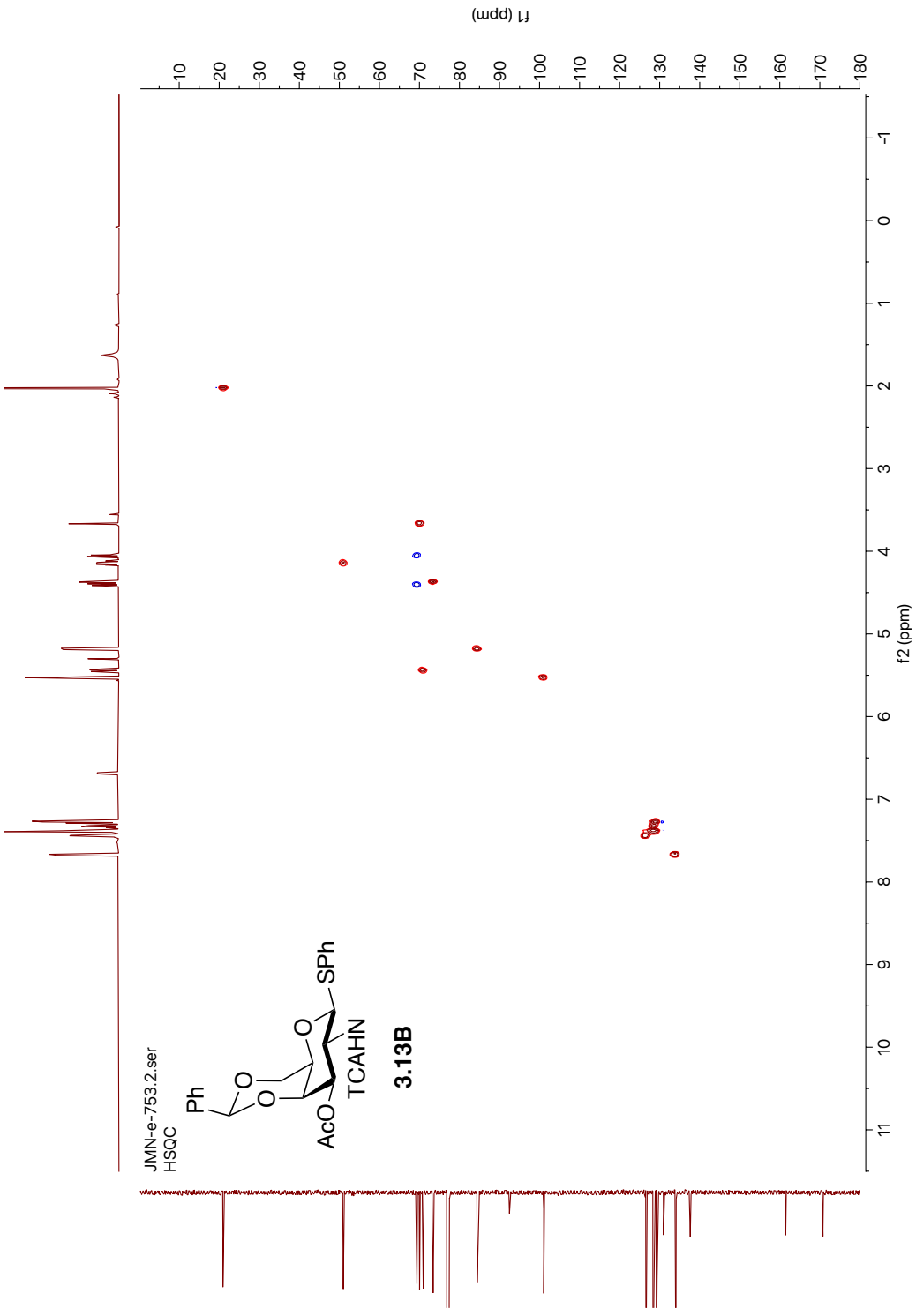

Figure A3.3. ^{1}H-^{13}C HSQC NMR (600 MHz, $CDCl_3$) of compound **3.13B**.

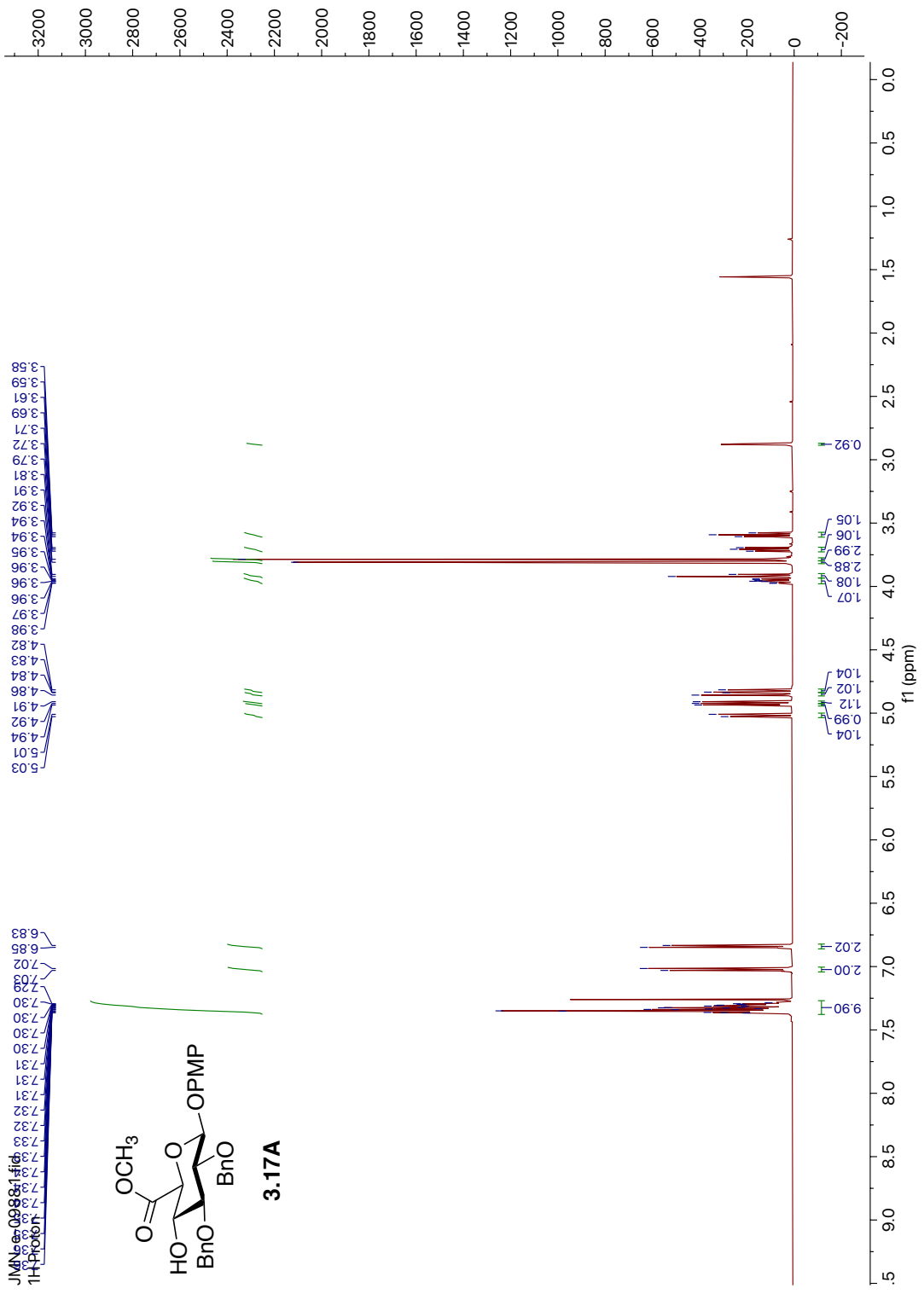

Figure A3.4. ^{1}H NMR (600 MHz, $CDCl_3$) of compound **3.17A**.

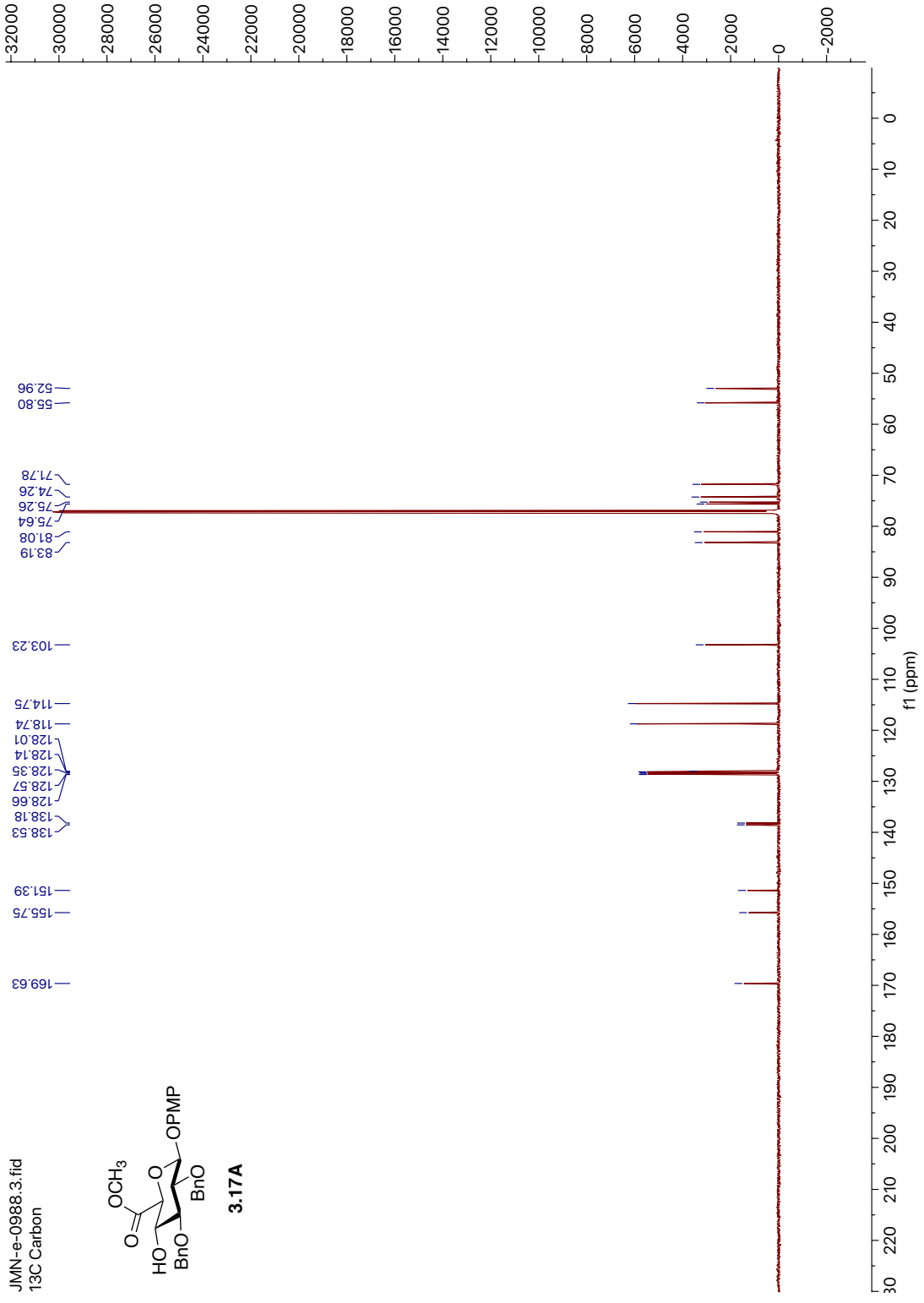

Figure A3.5. ^{13}C NMR (151 MHz, $CDCl_3$) of compound **3.17A**.

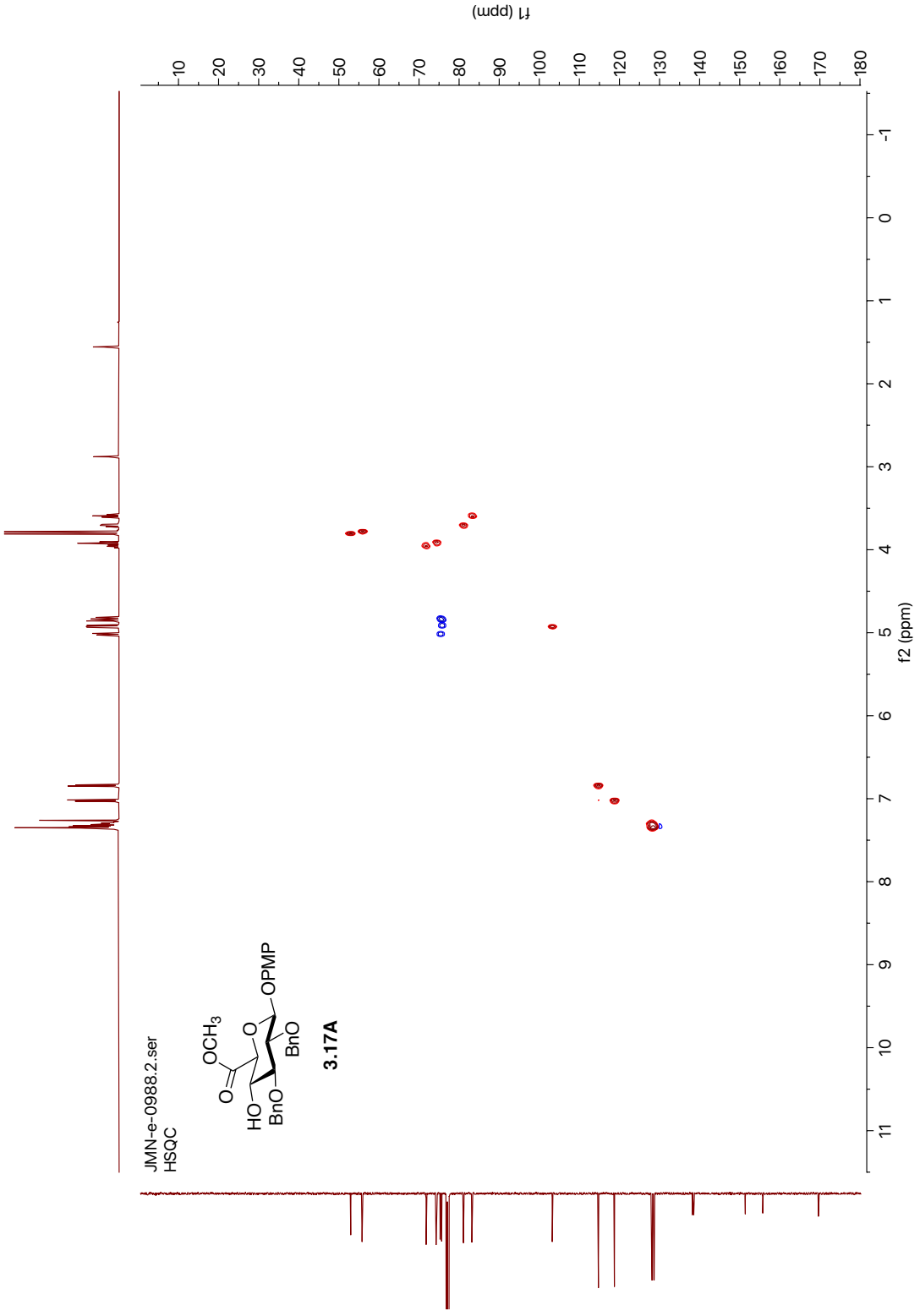

Figure A3.6. ^{1}H-^{13}C HSQC NMR (600 MHz, $CDCl_3$) of compound **3.17A.**

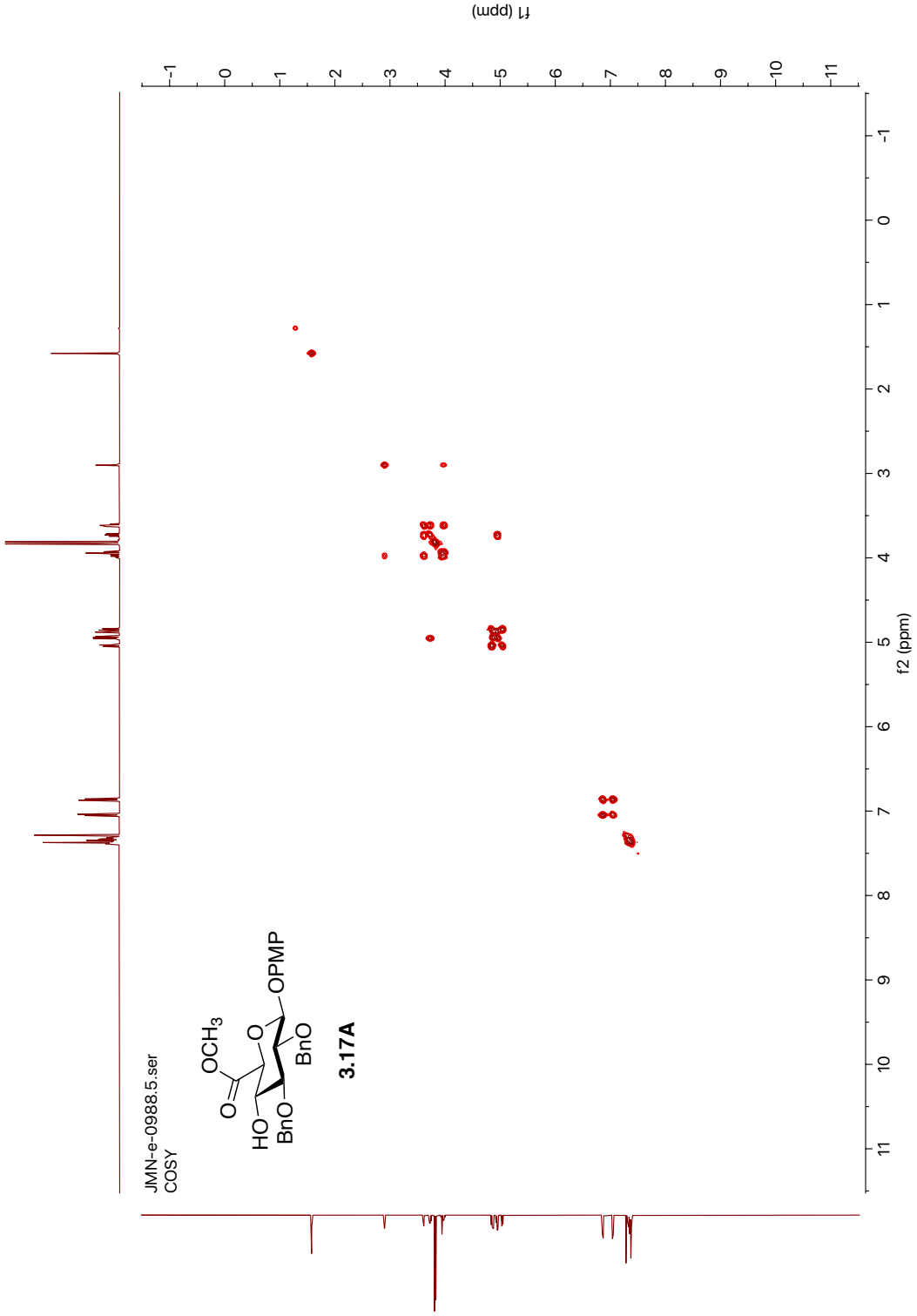

Figure A3.7. ^{1}H-^{1}H COSY NMR (600 MHz, $CDCl_3$) of compound **3.17A**.

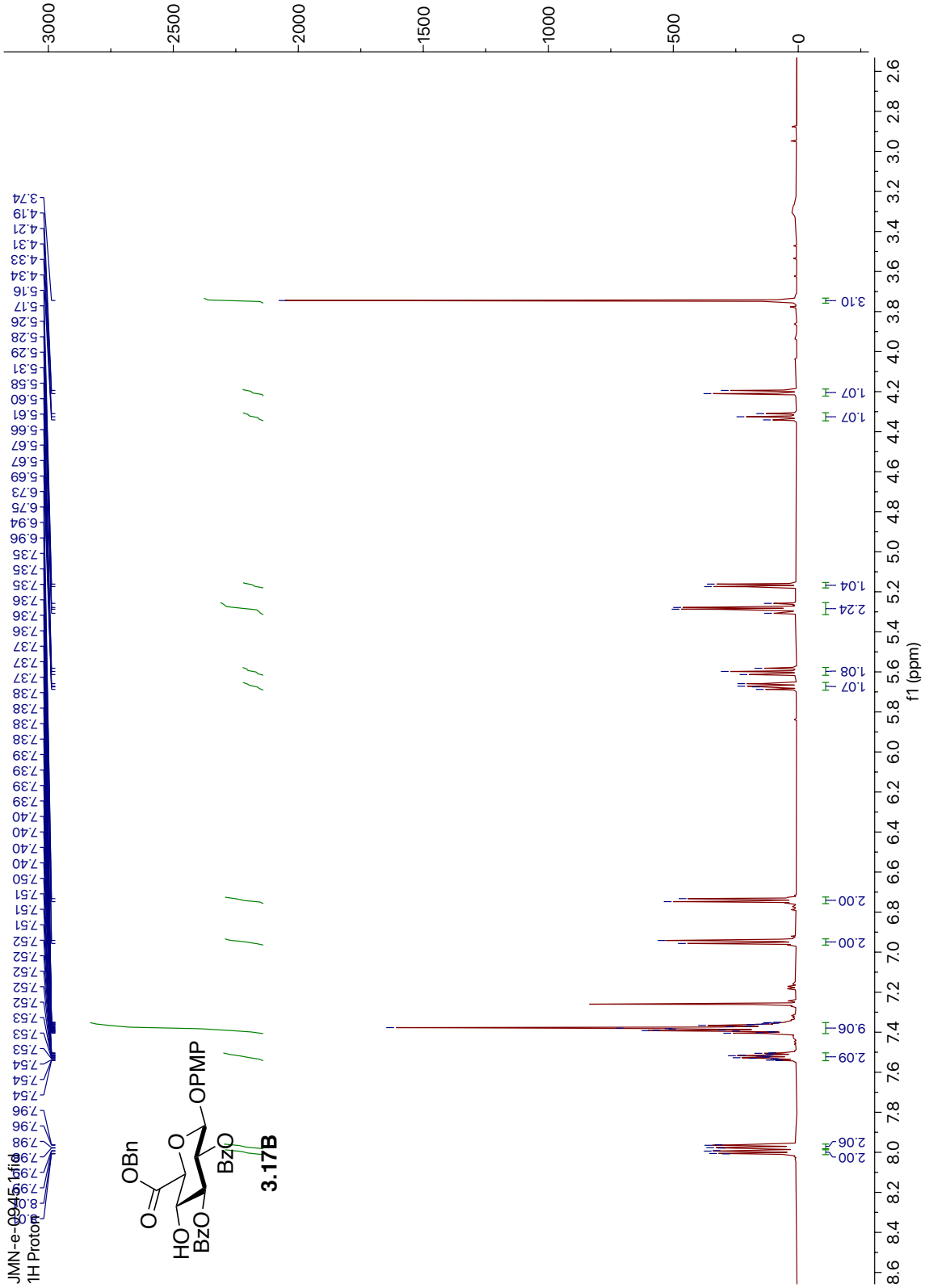

Figure A3.8. ^{1}H NMR (600 MHz, $CDCl_3$) of compound **3.17B**.

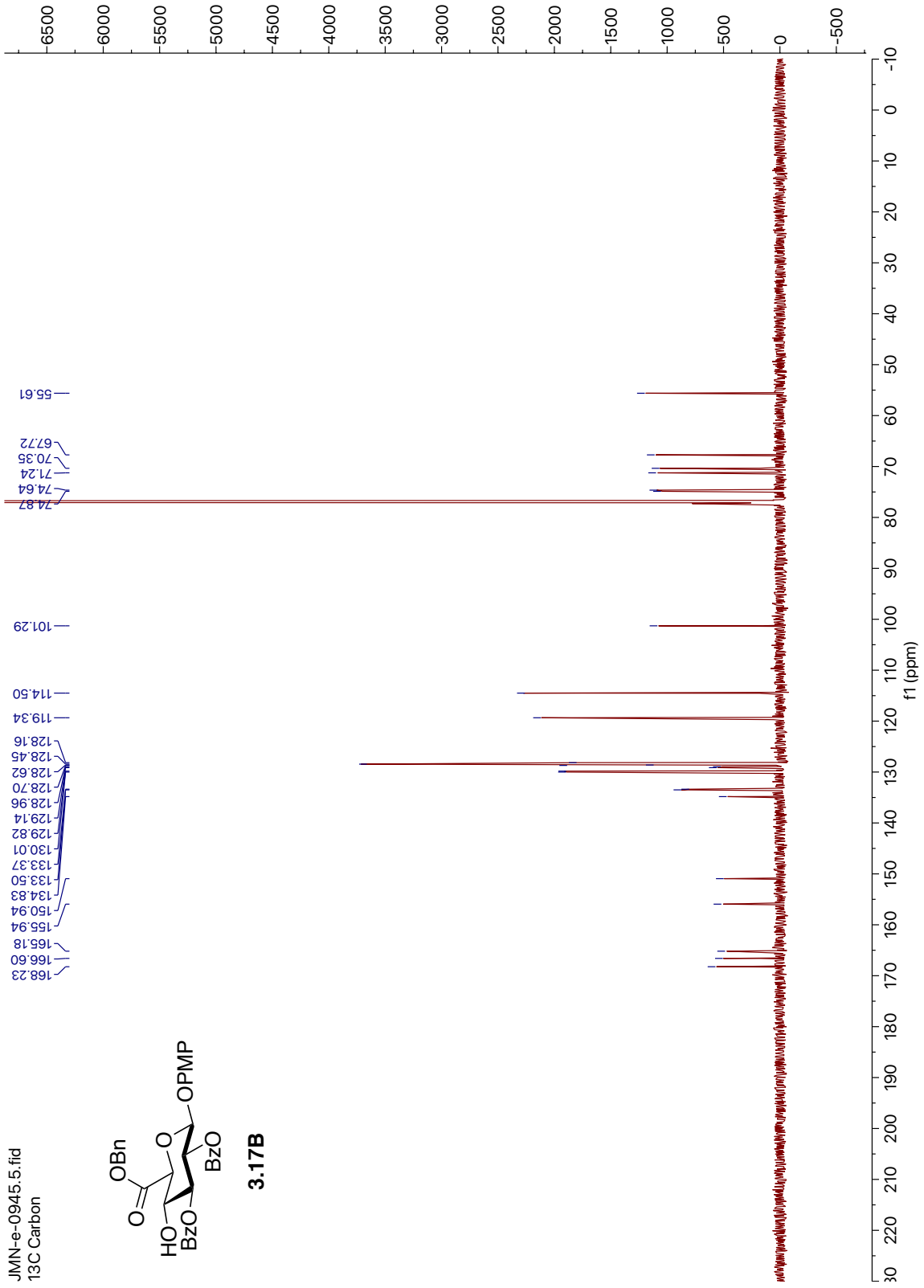

Figure A3.9. ^{13}C NMR (151 MHz, $CDCl_3$) of compound **3.17B**.

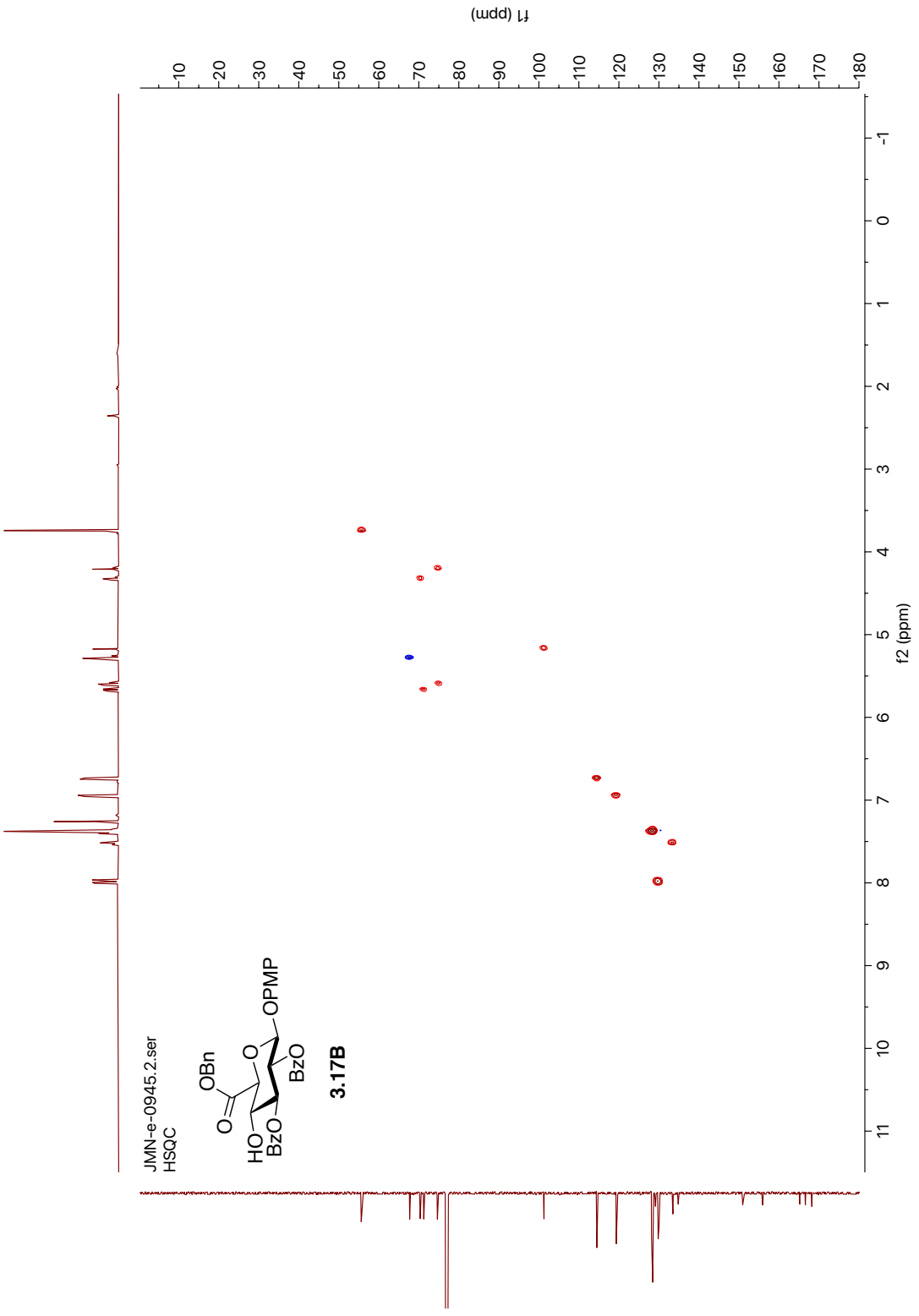

Figure A3.10. ^{1}H-^{13}C HSQC NMR (600 MHz, $CDCl_3$) of compound **3.17B**.

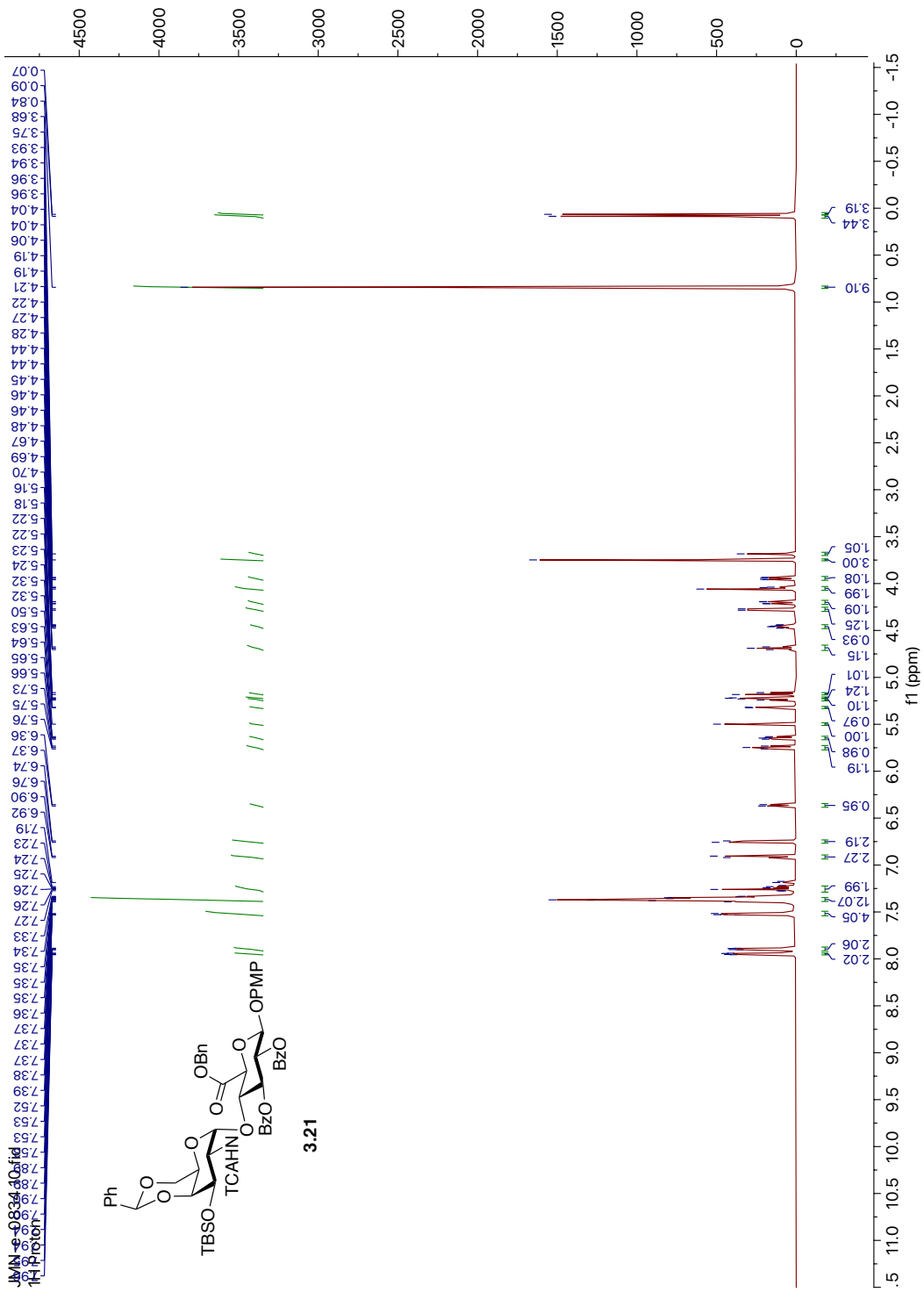

Figure A3.11. ^{1}H NMR (600 MHz, $CDCl_3$) of compound **3.21**.

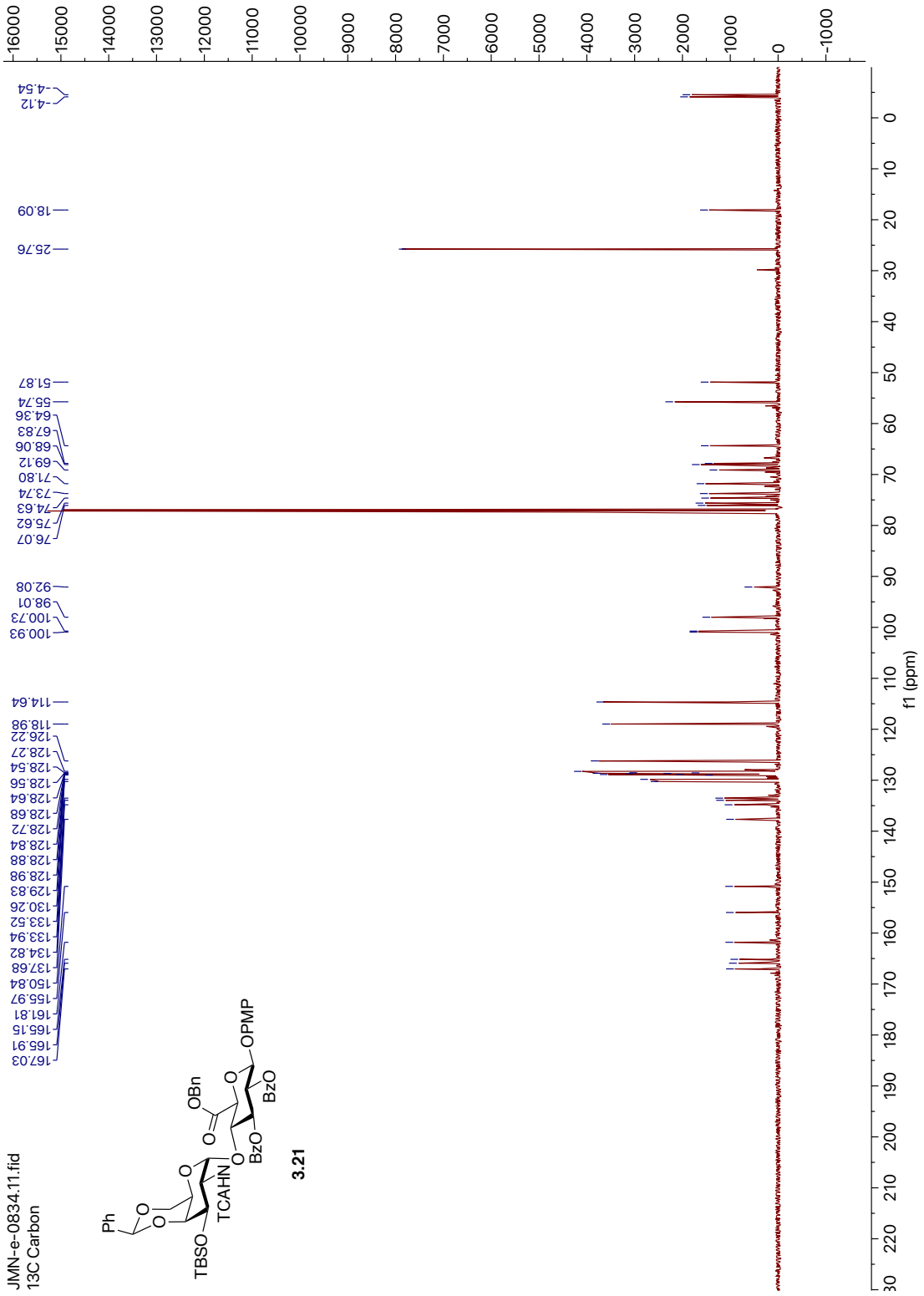

Figure A3.12. ^{13}C NMR (151 MHz, $CDCl_3$) of compound **3.21.**

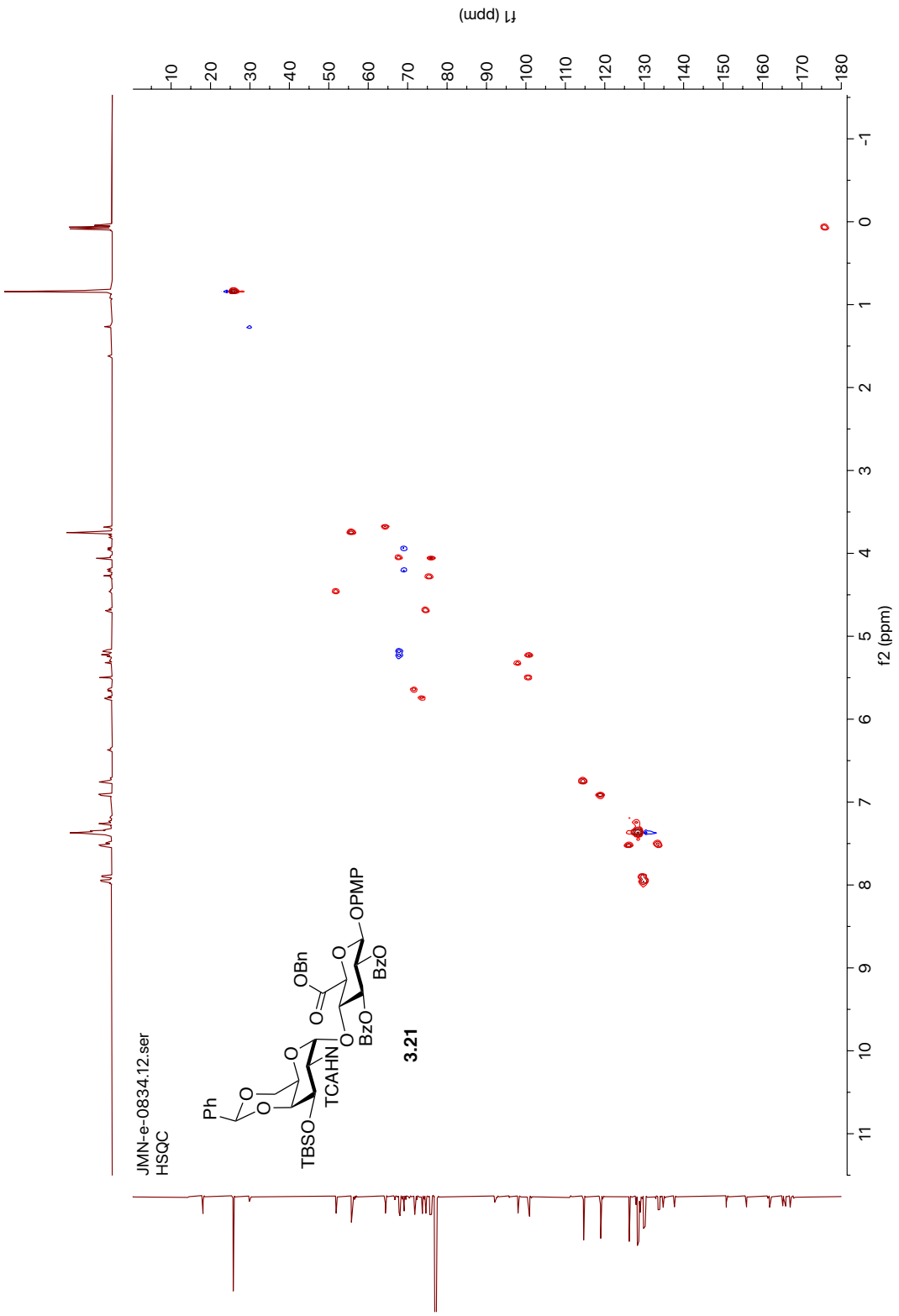

Figure A3.13. ^{1}H-^{13}C HSQC NMR (600 MHz, $CDCl_3$) of compound **3.21**.

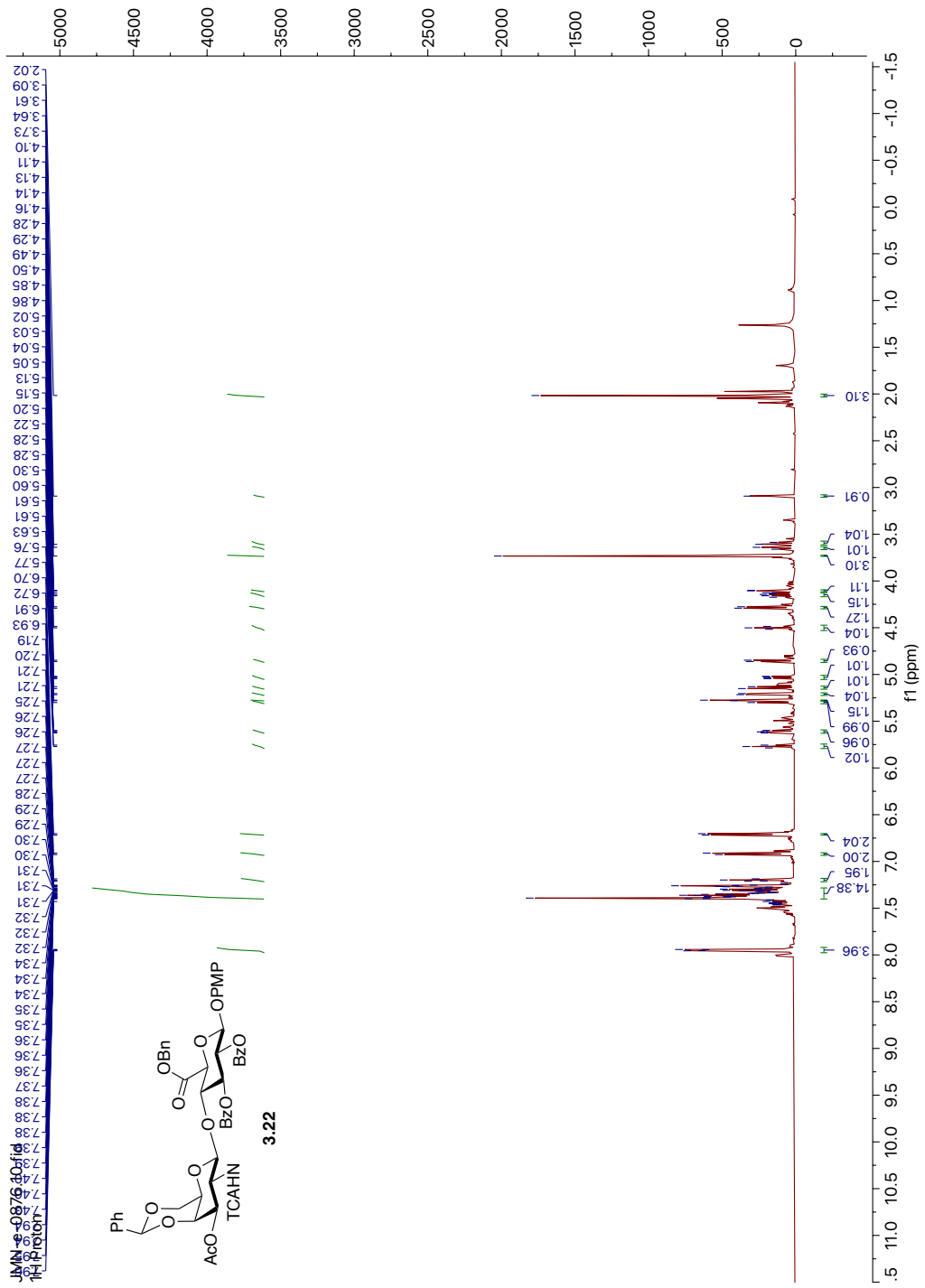

Figure A3.14. ^{1}H NMR (600 MHz, $CDCl_3$) of compound **3.22**.

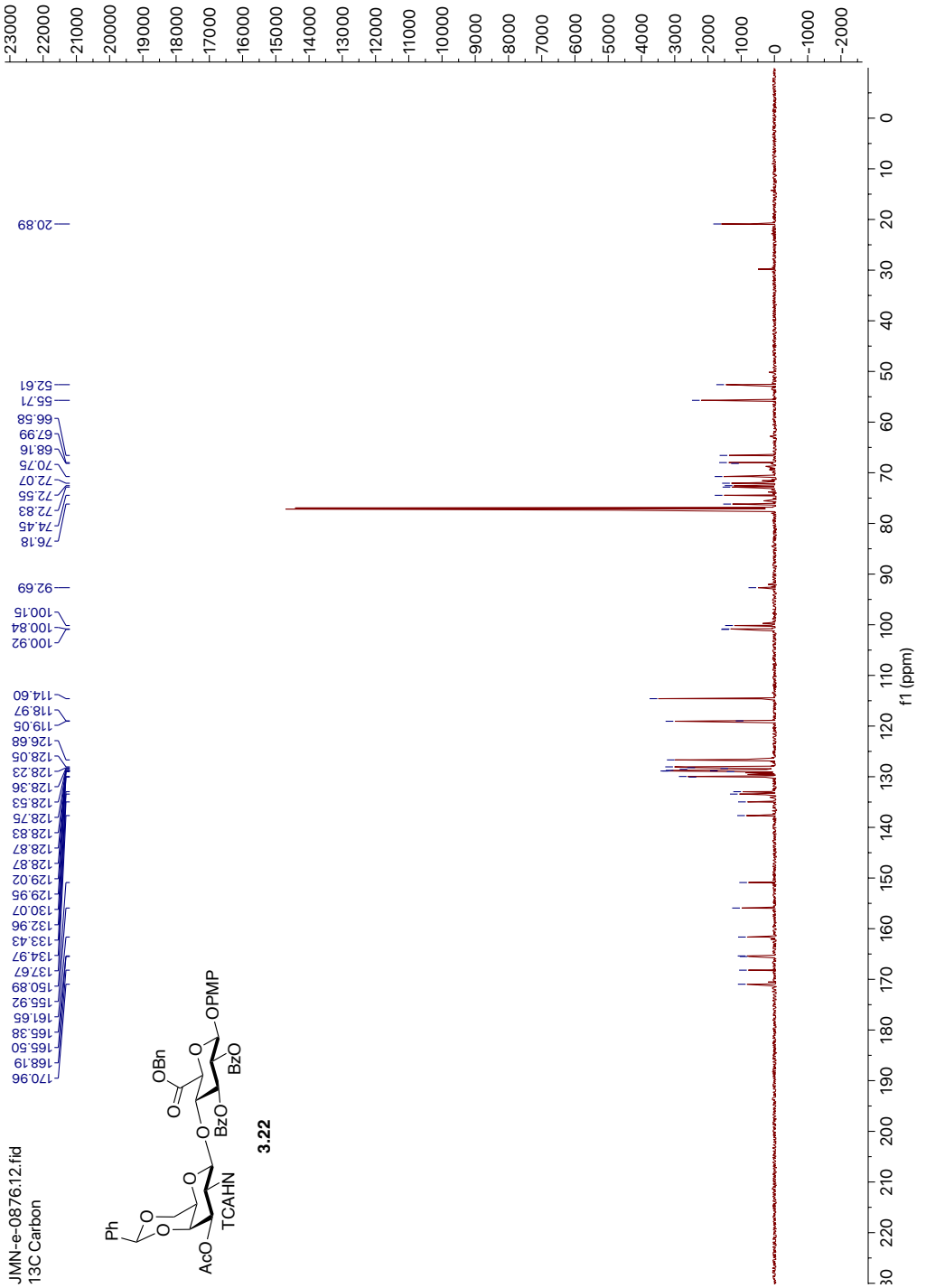

Figure A3.15. ^{13}C NMR (151 MHz, $CDCl_3$) of compound **3.22**.

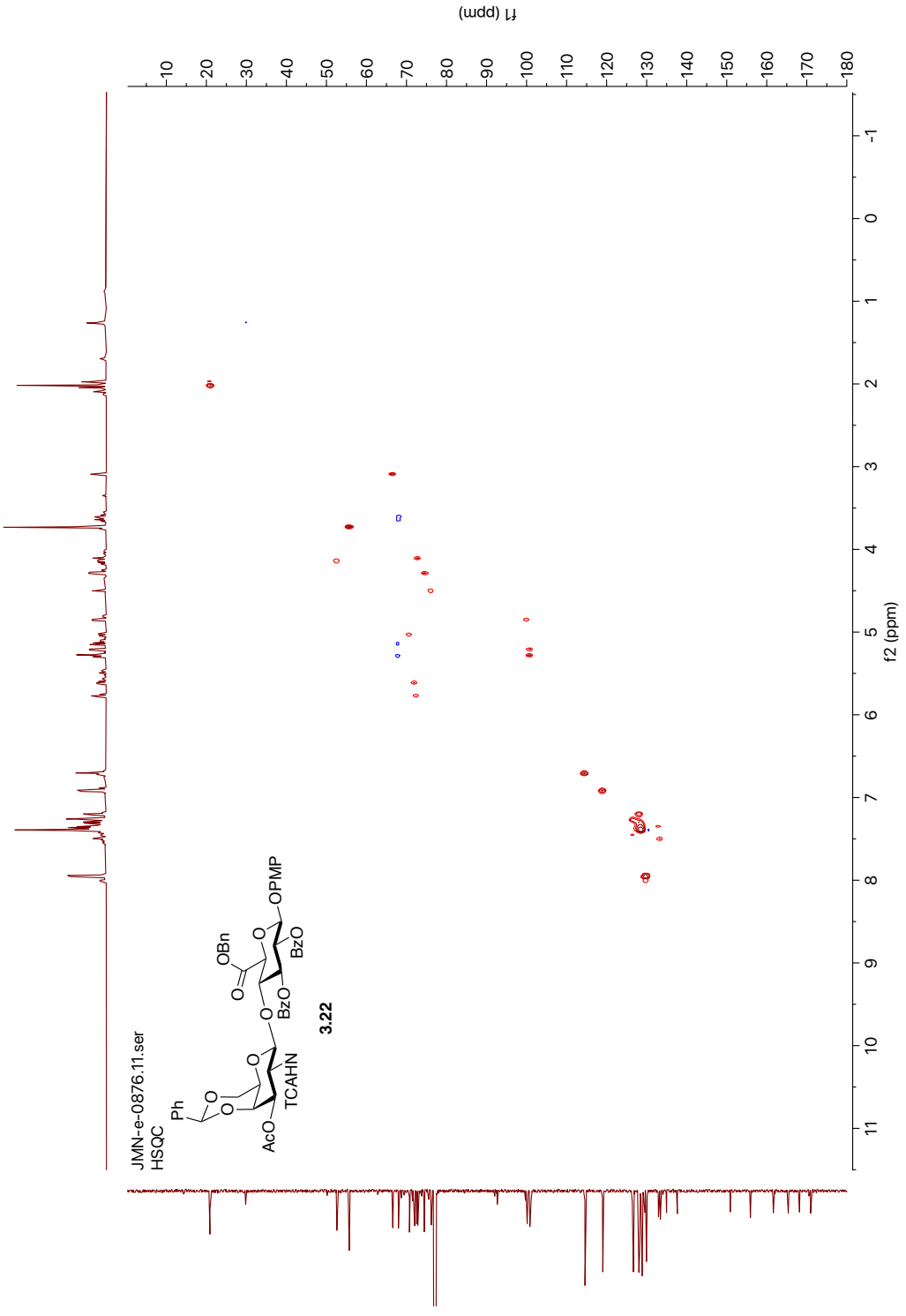

Figure A3.16. ^{1}H-^{13}C HSQC NMR (600 MHz, $CDCl_3$) of compound **3.22**.

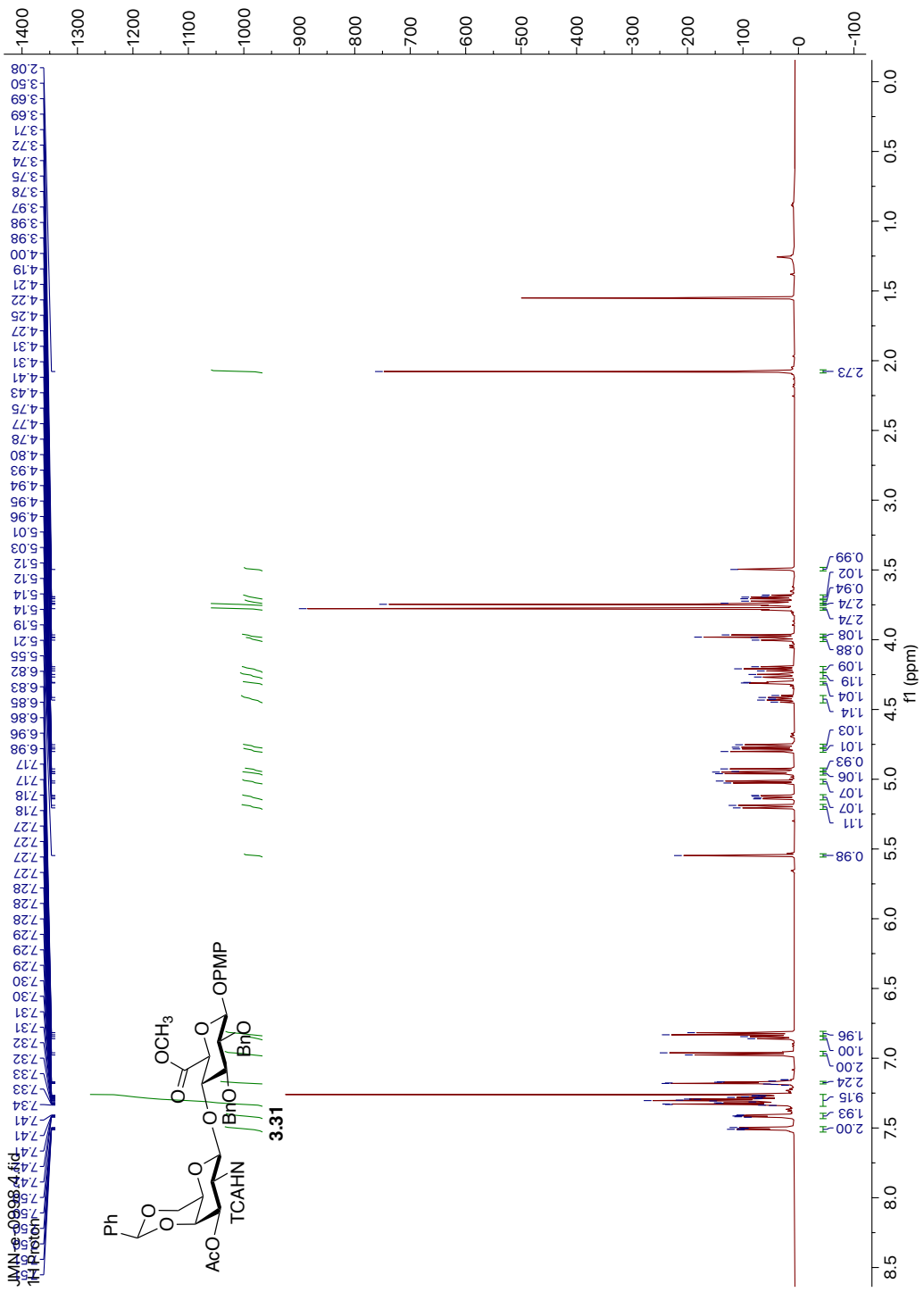

Figure A3.17. ^{1}H NMR (600 MHz, $CDCl_3$) of compound **3.31**.

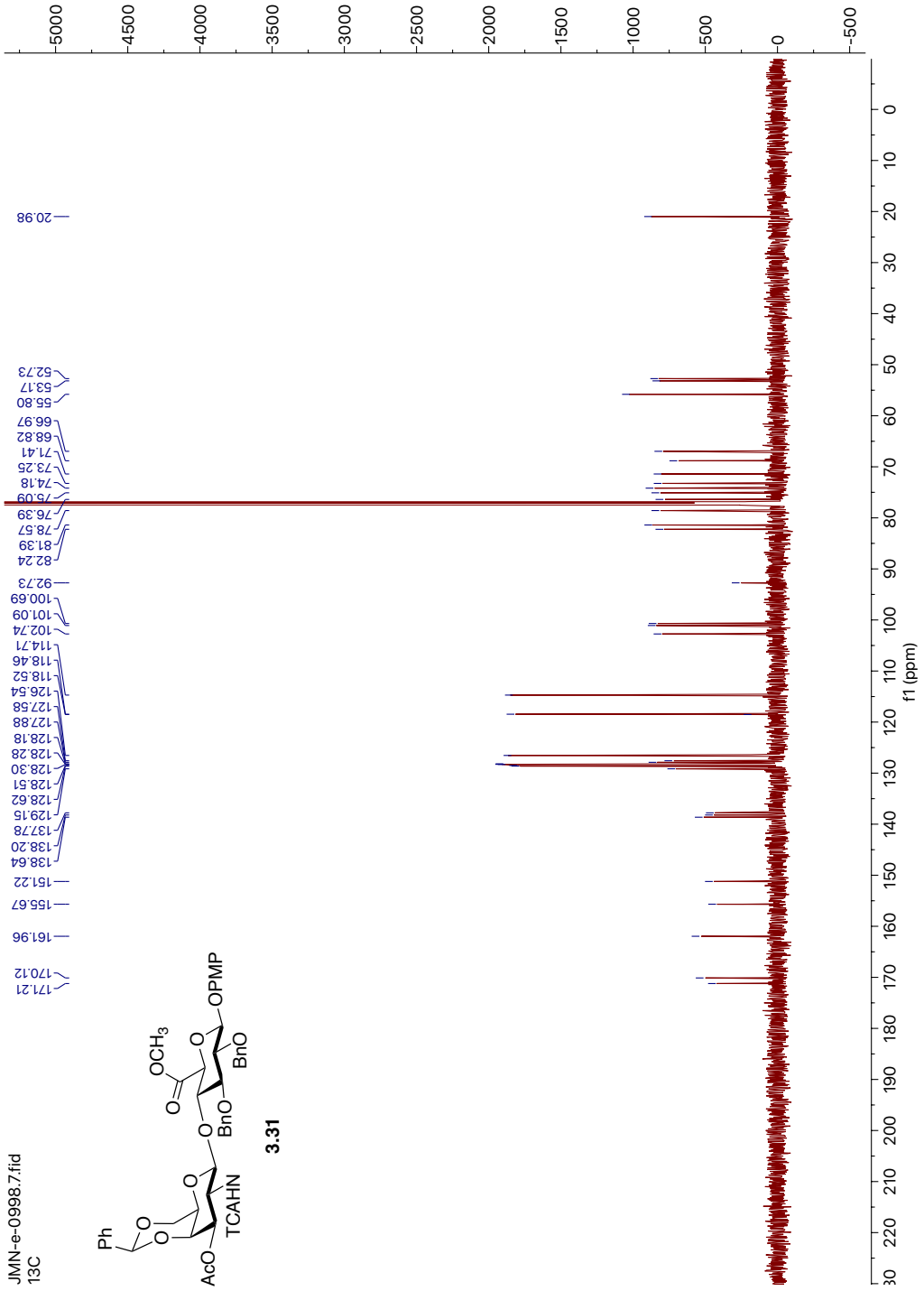

Figure A3.18. ^{13}C NMR (151 MHz, $CDCl_3$) of compound **3.31**.

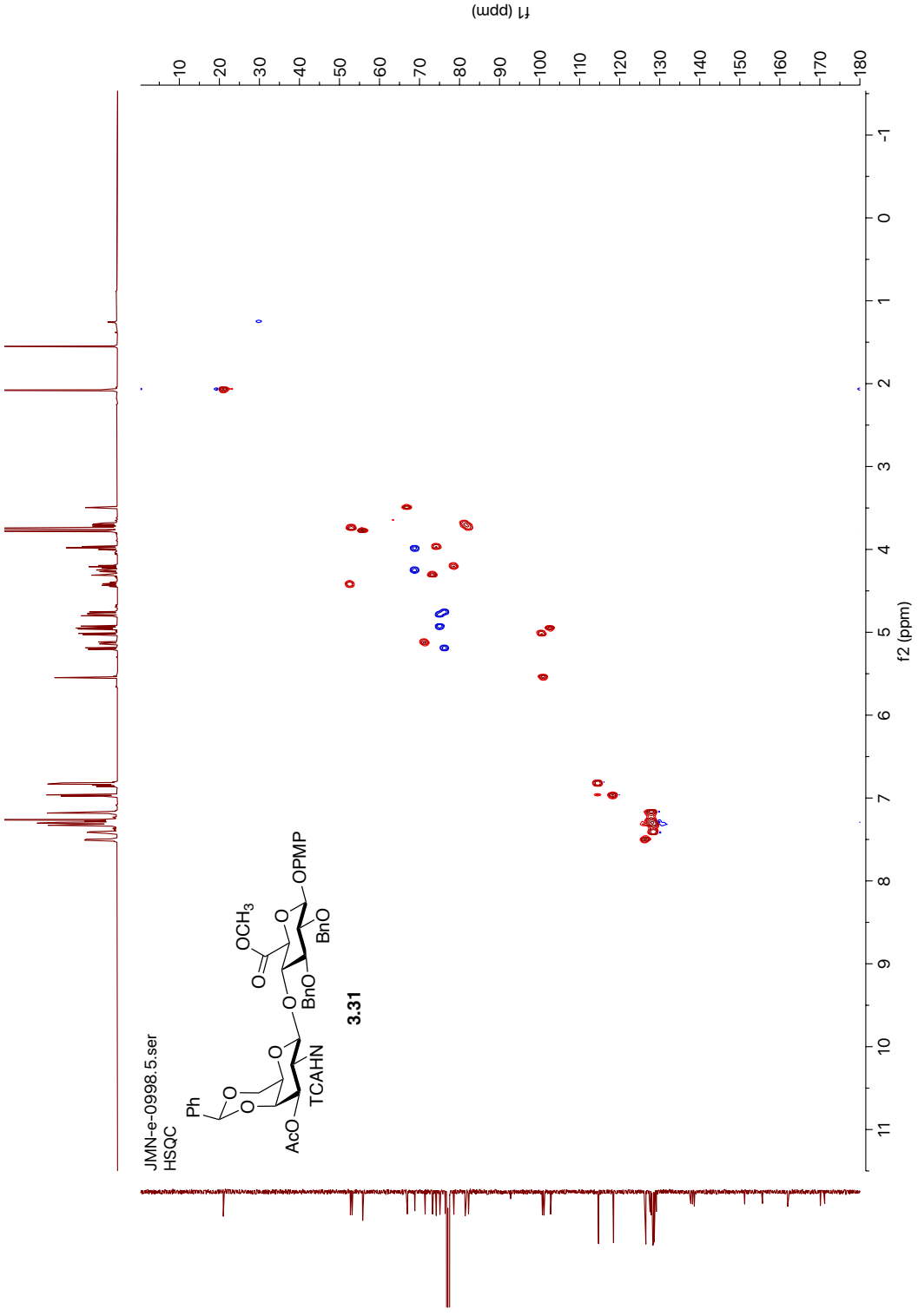

Figure A3.19. ^{1}H-^{13}C HSQC NMR (600 MHz, $CDCl_3$) of compound **3.31**.

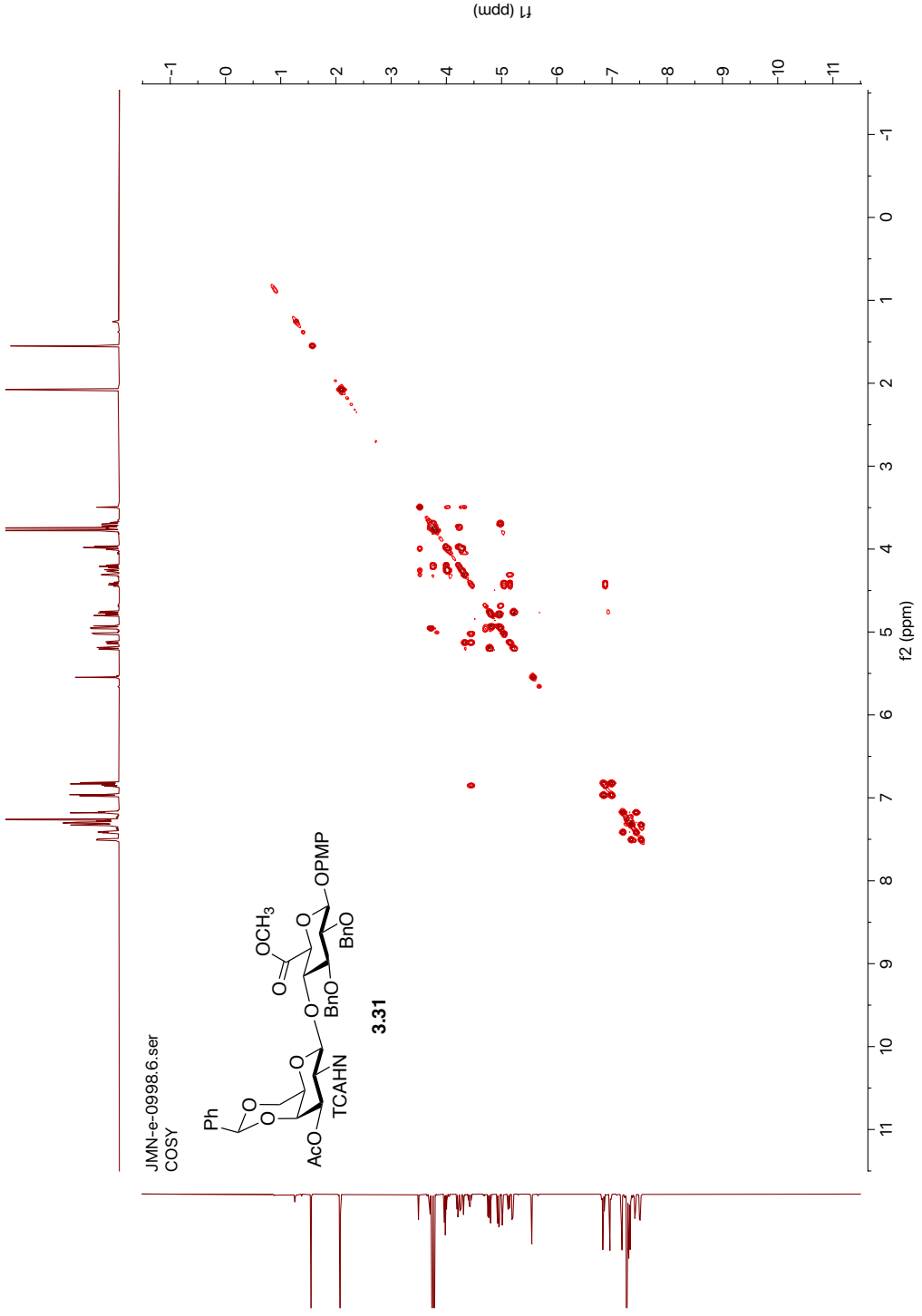

Figure A3.20. ^{1}H-^{1}H COSY NMR (600 MHz, $CDCl_3$) of compound **3.31**.

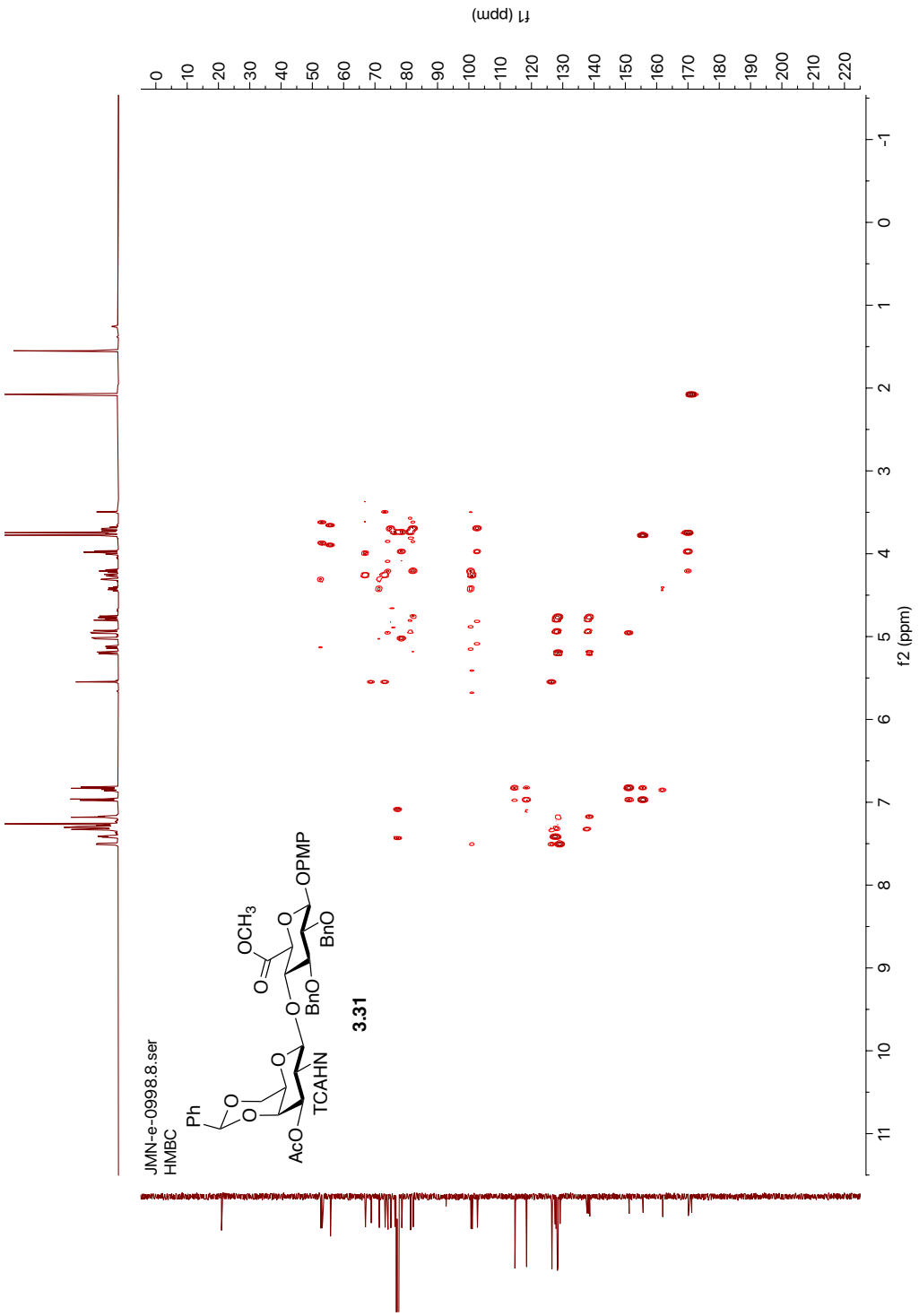

Figure A3.21. ^{1}H-^{13}C HMBC NMR (600 MHz, $CDCl_3$) of compound **3.31**.

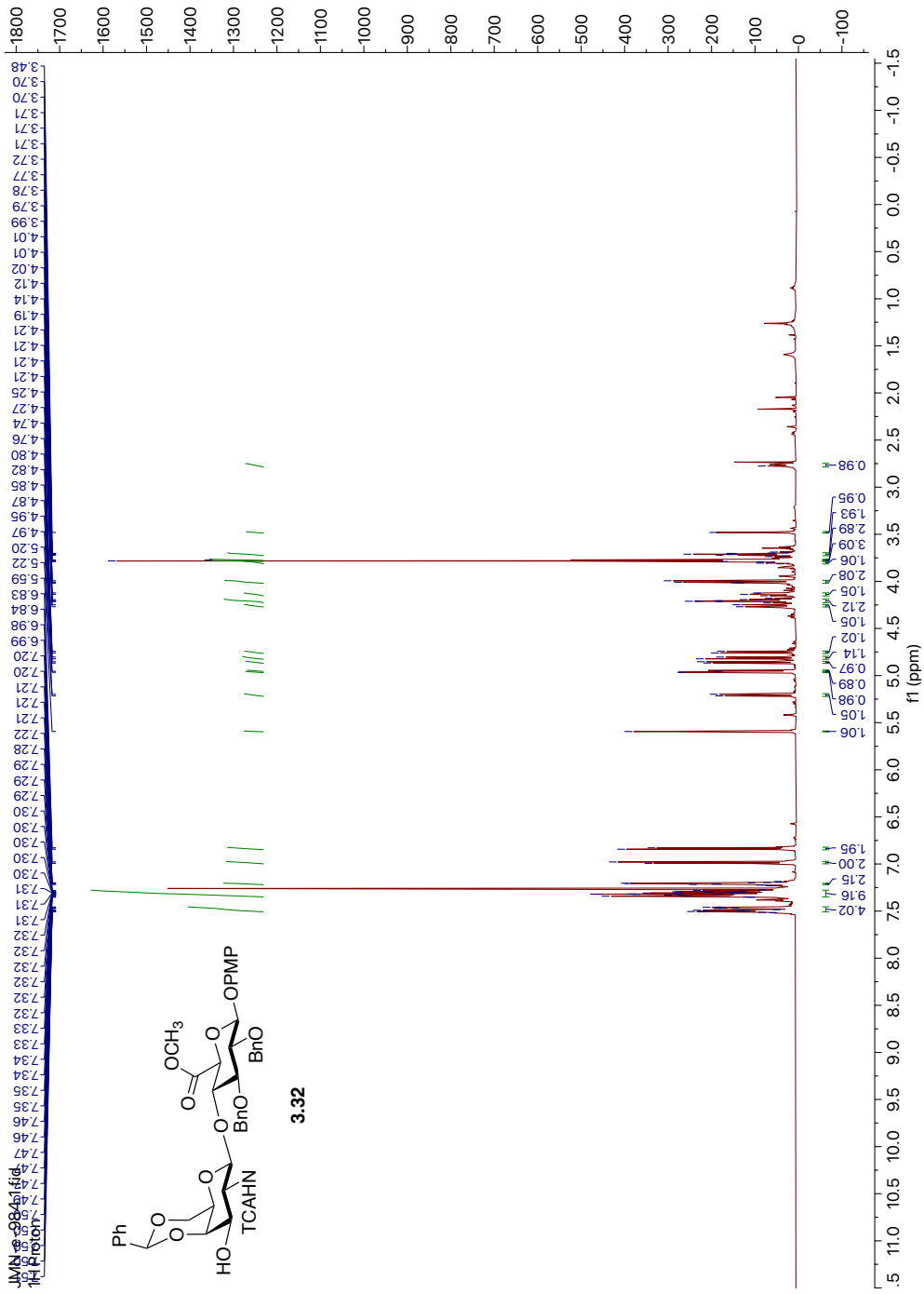

Figure A3.22. ^{1}H NMR (600 MHz, $CDCl_3$) of compound **3.22**.

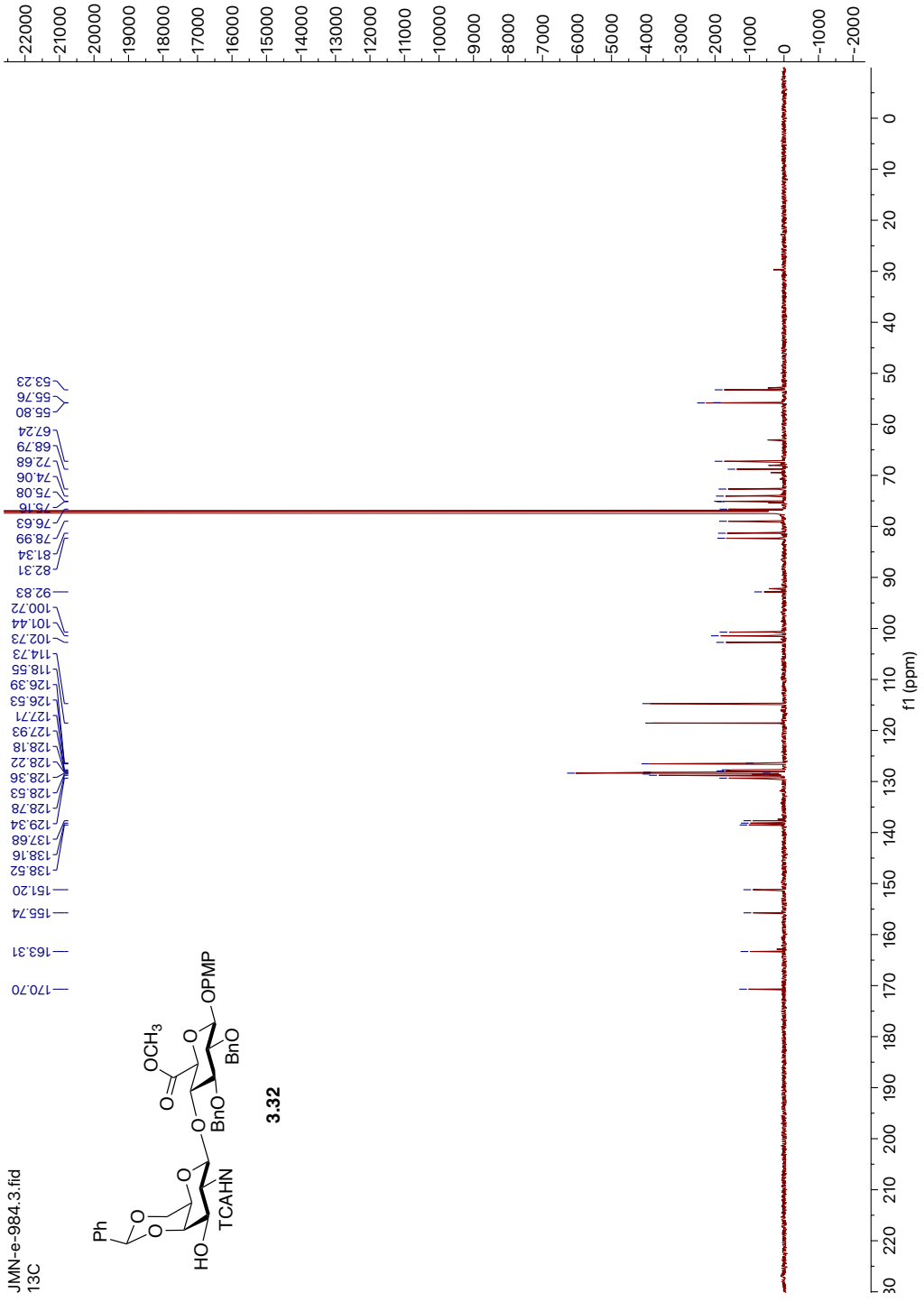

Figure A3.23. ^{13}C NMR (151 MHz, $CDCl_3$) of compound **3.22.**

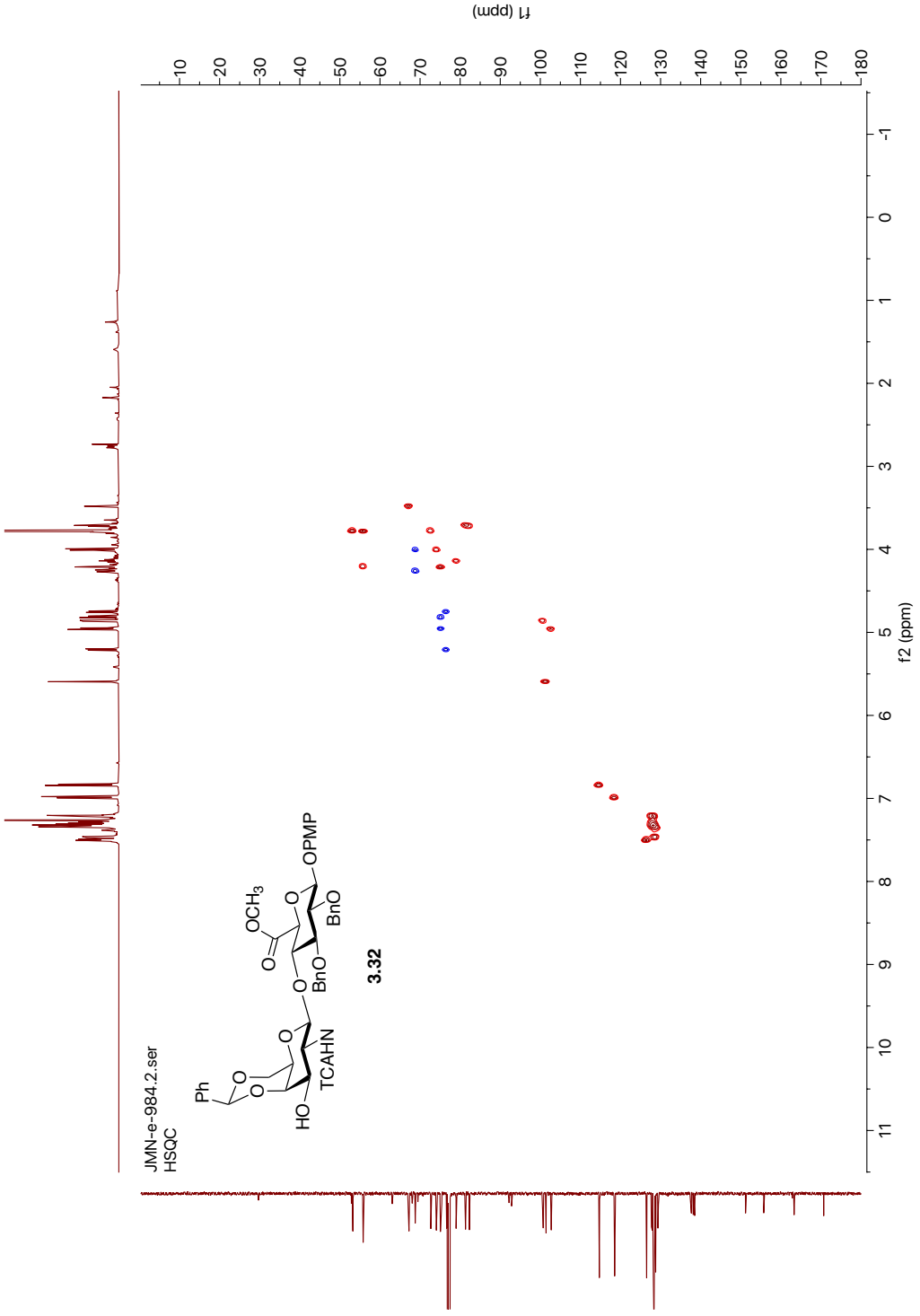

Figure A3.24. ^{1}H-^{13}C HSQC NMR (600 MHz, $CDCl_3$) of compound **3.32**.

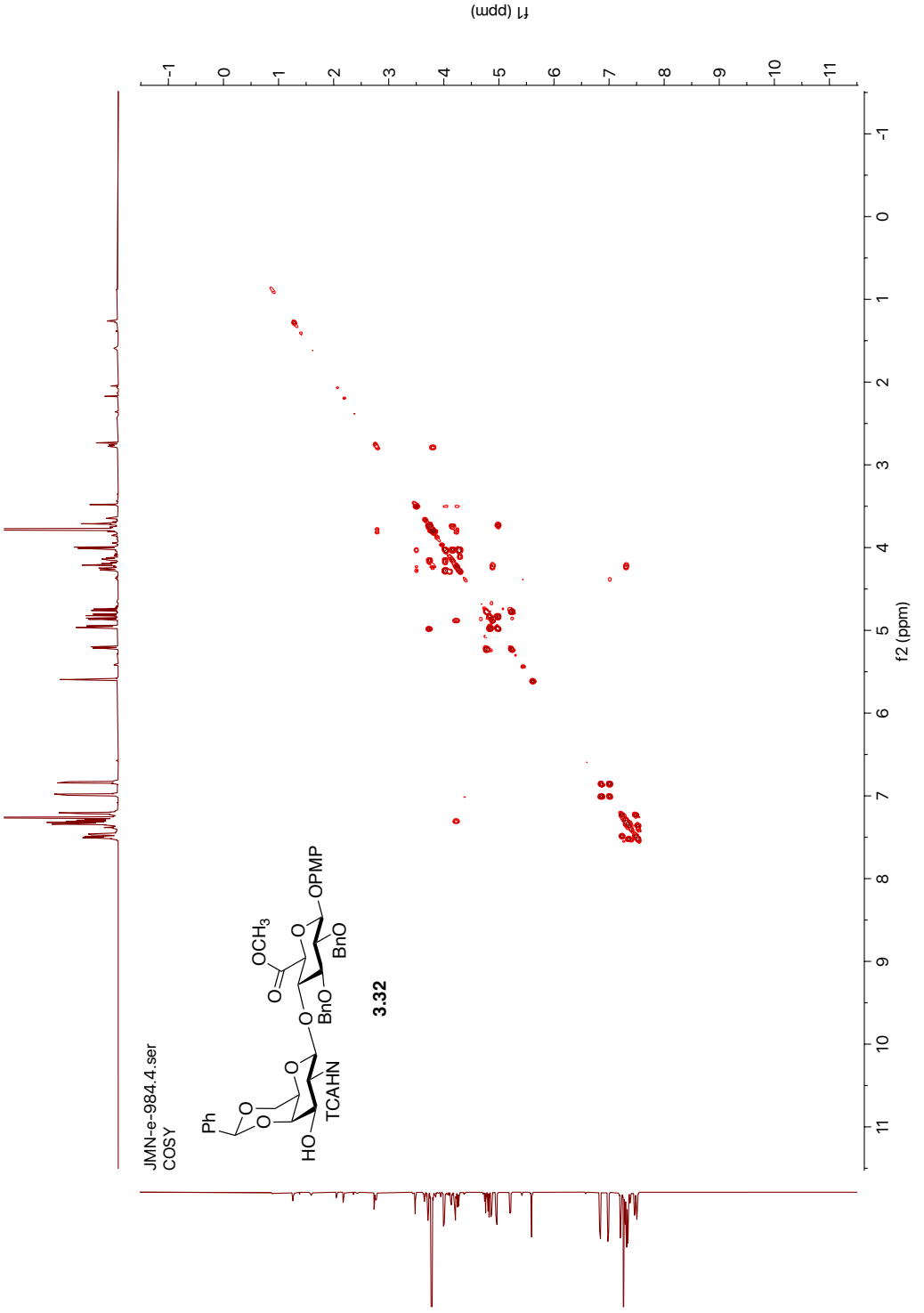

Figure A3.25. ^{1}H-^{1}H COSY NMR (600 MHz, $CDCl_3$) of compound **3.32**.

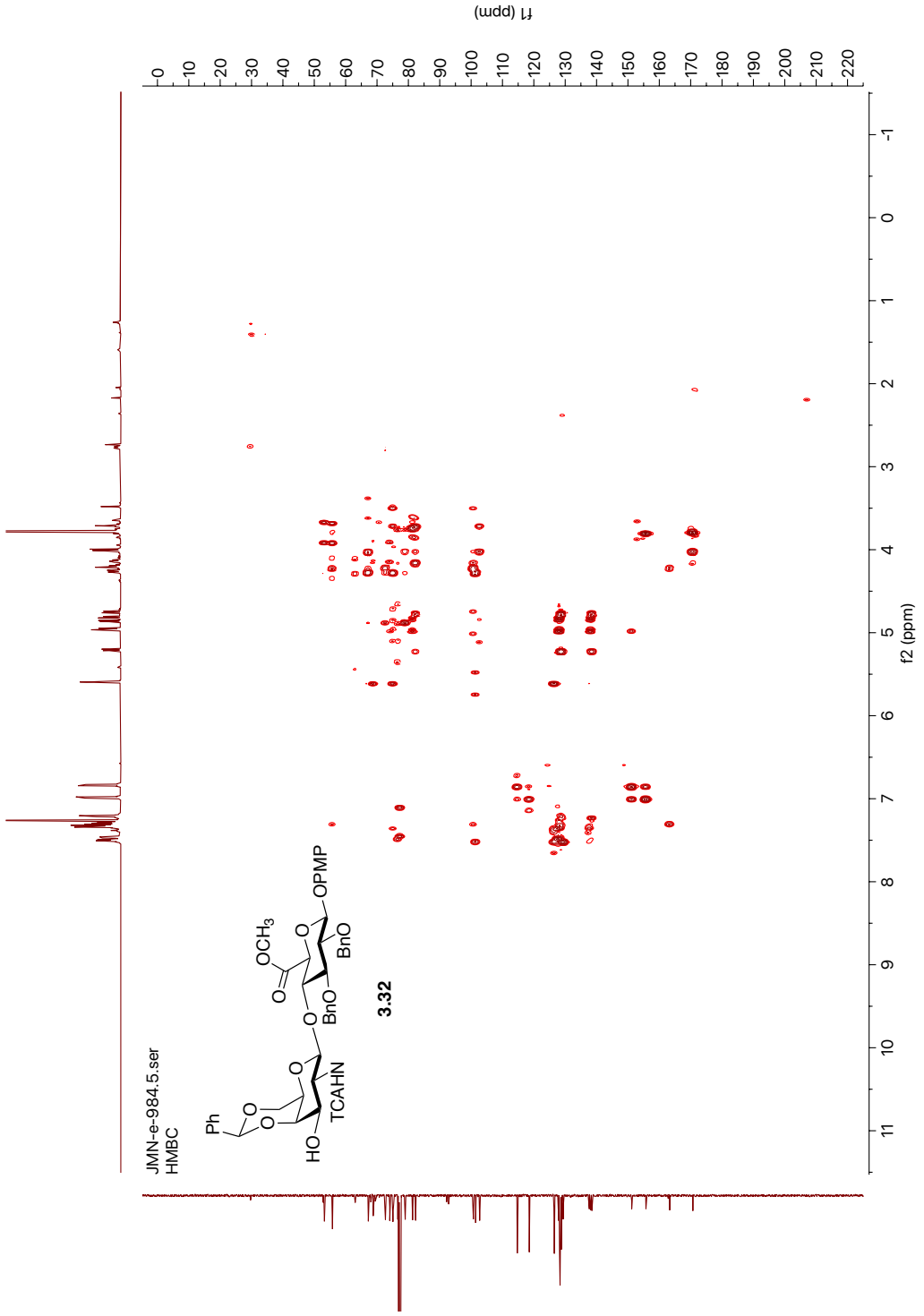

Figure A3.26. ^{1}H-^{13}C HMBC NMR (600 MHz, $CDCl_3$) of compound **3.32**.

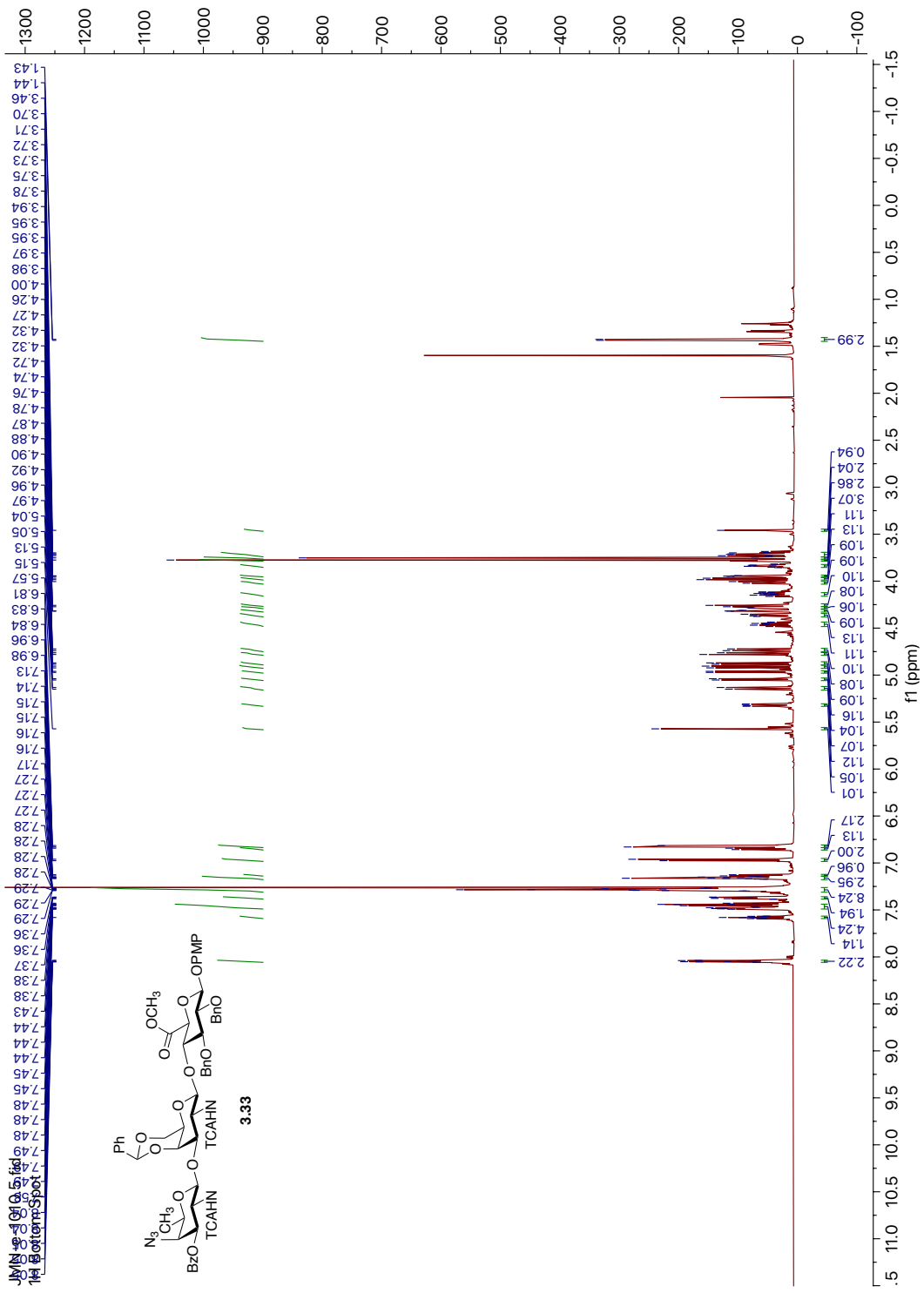

Figure A3.27. ^{1}H NMR (600 MHz, $CDCl_3$) of compound **3.33**.

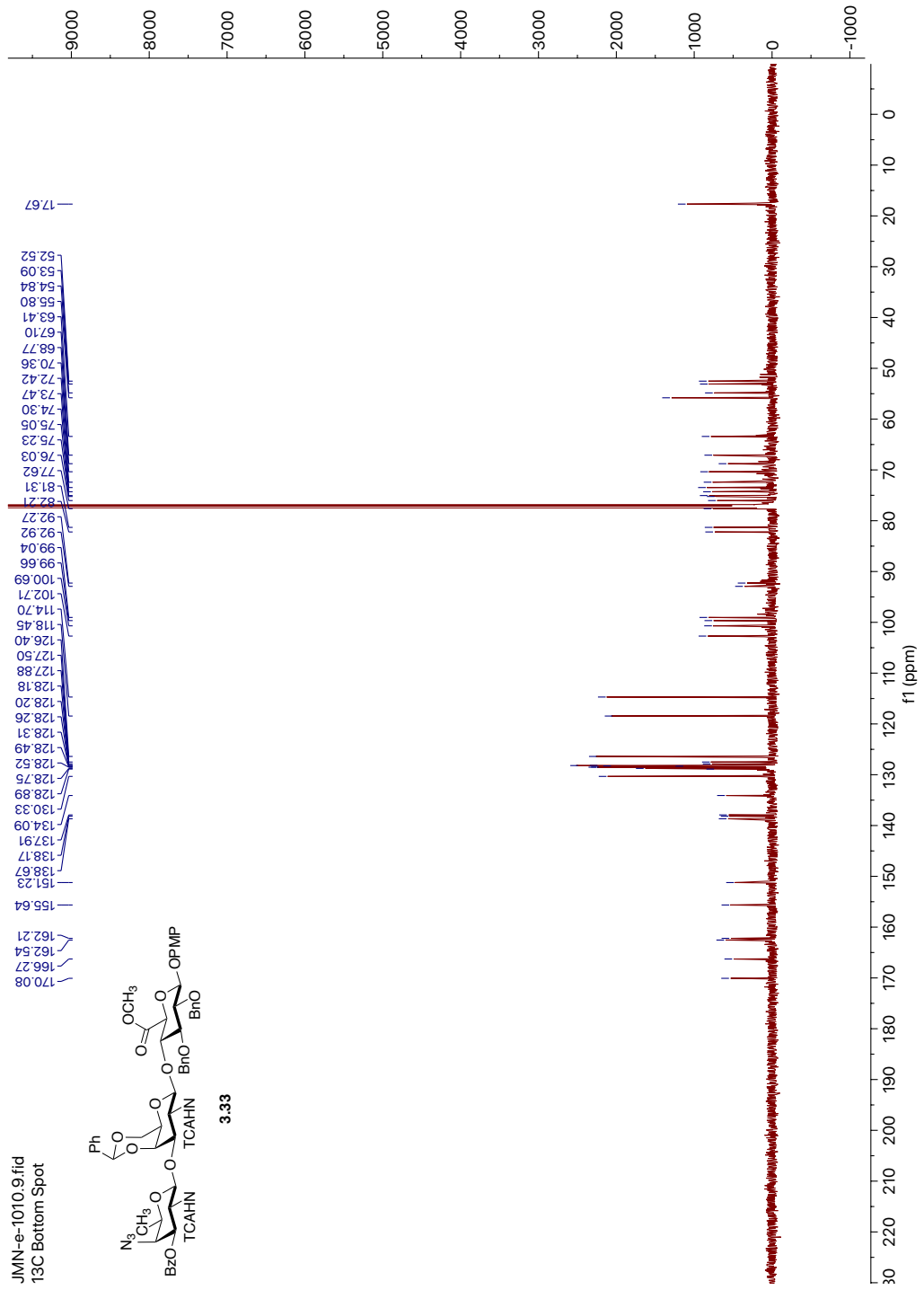

Figure A3.28. ^{13}C NMR (151 MHz, $CDCl_3$) of compound **3.33.**

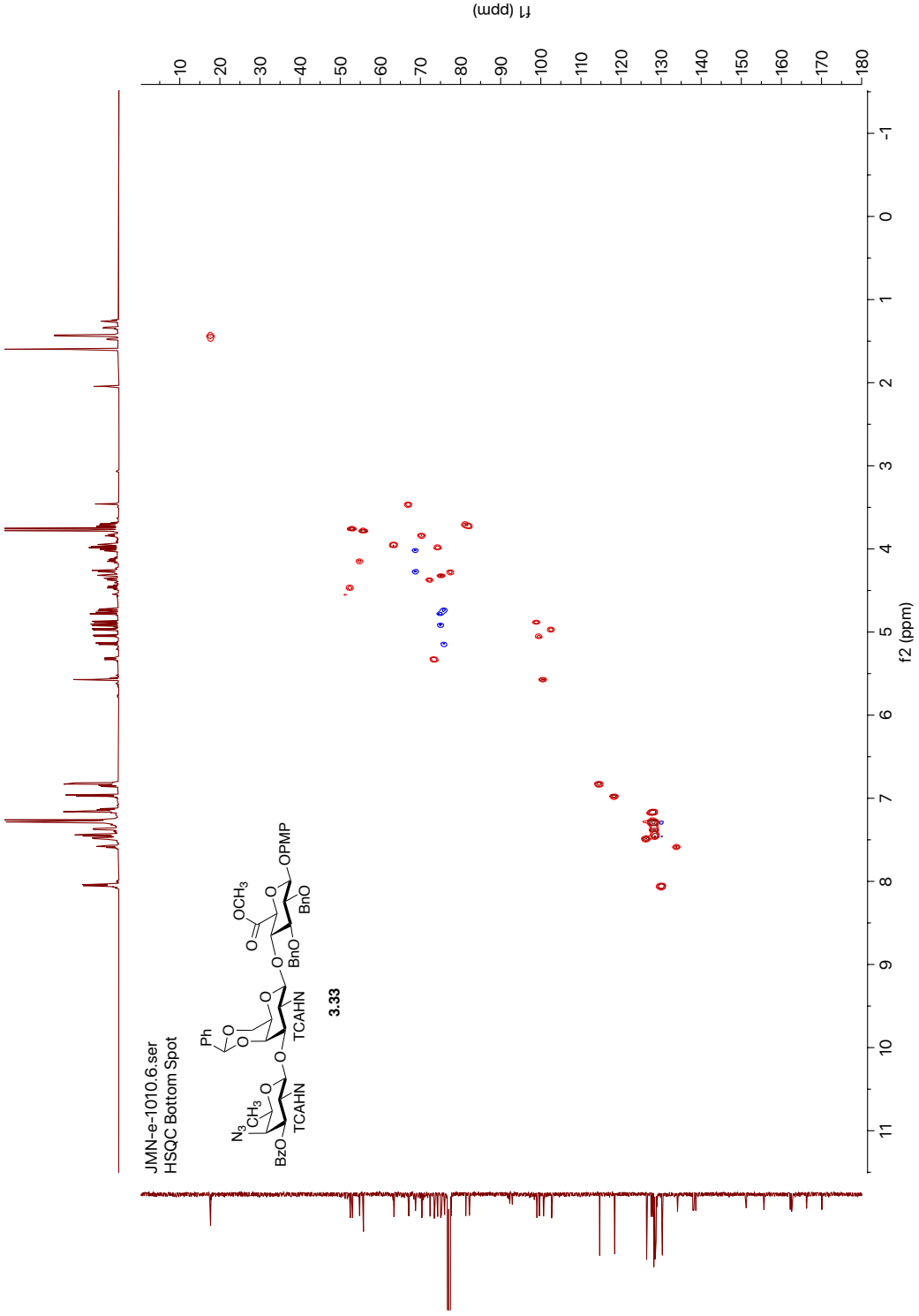

Figure A3.29. ^{1}H-^{13}C HSQC NMR (600 MHz, $CDCl_3$) of compound **3.33**.

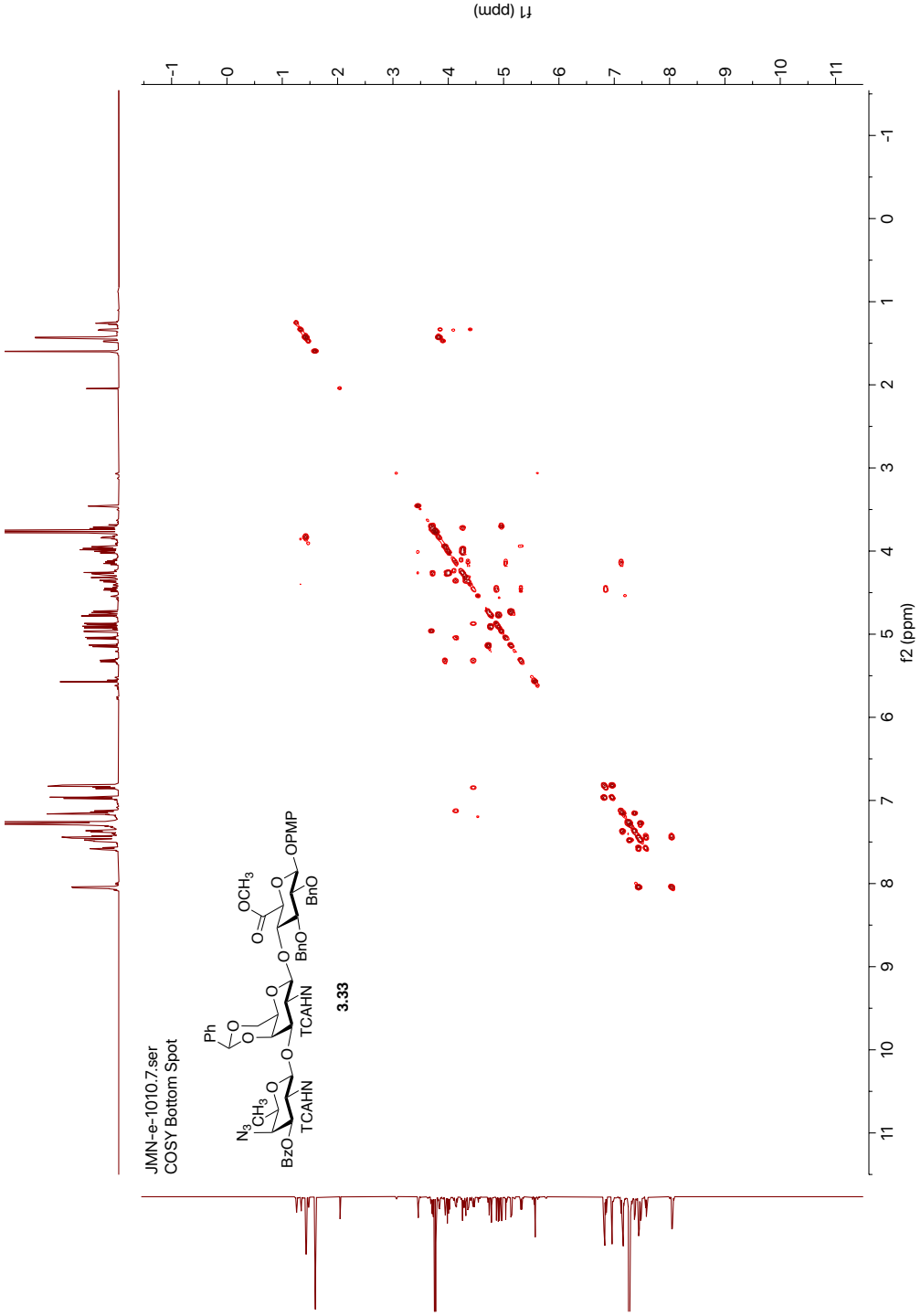

Figure A3.30. ^{1}H-^{1}H COSY NMR (600 MHz, $CDCl_3$) of compound **3.33.**

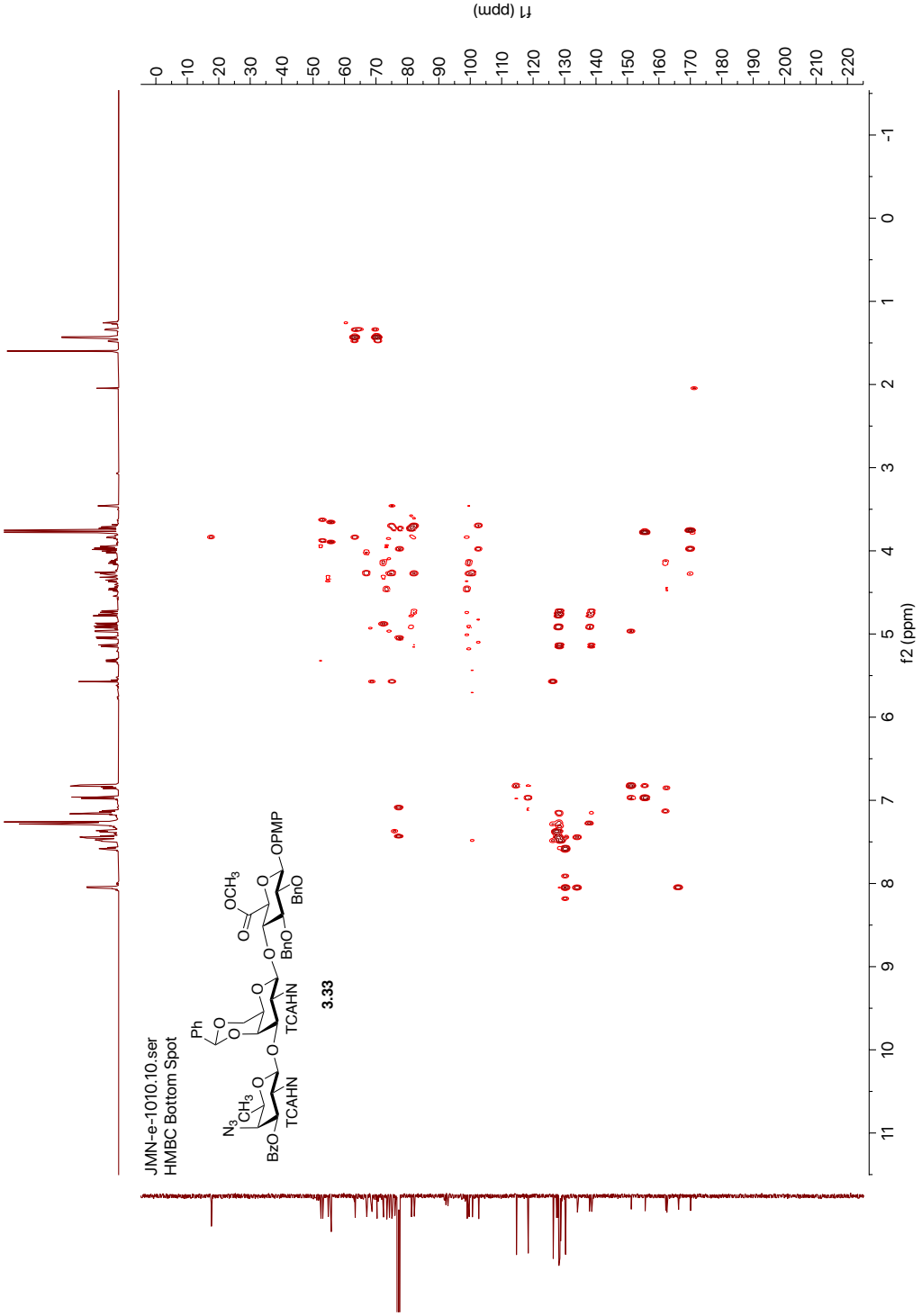

Figure A3.31. ^{1}H-^{13}C HMBC NMR (600 MHz, $CDCl_3$) of compound **3.33**.

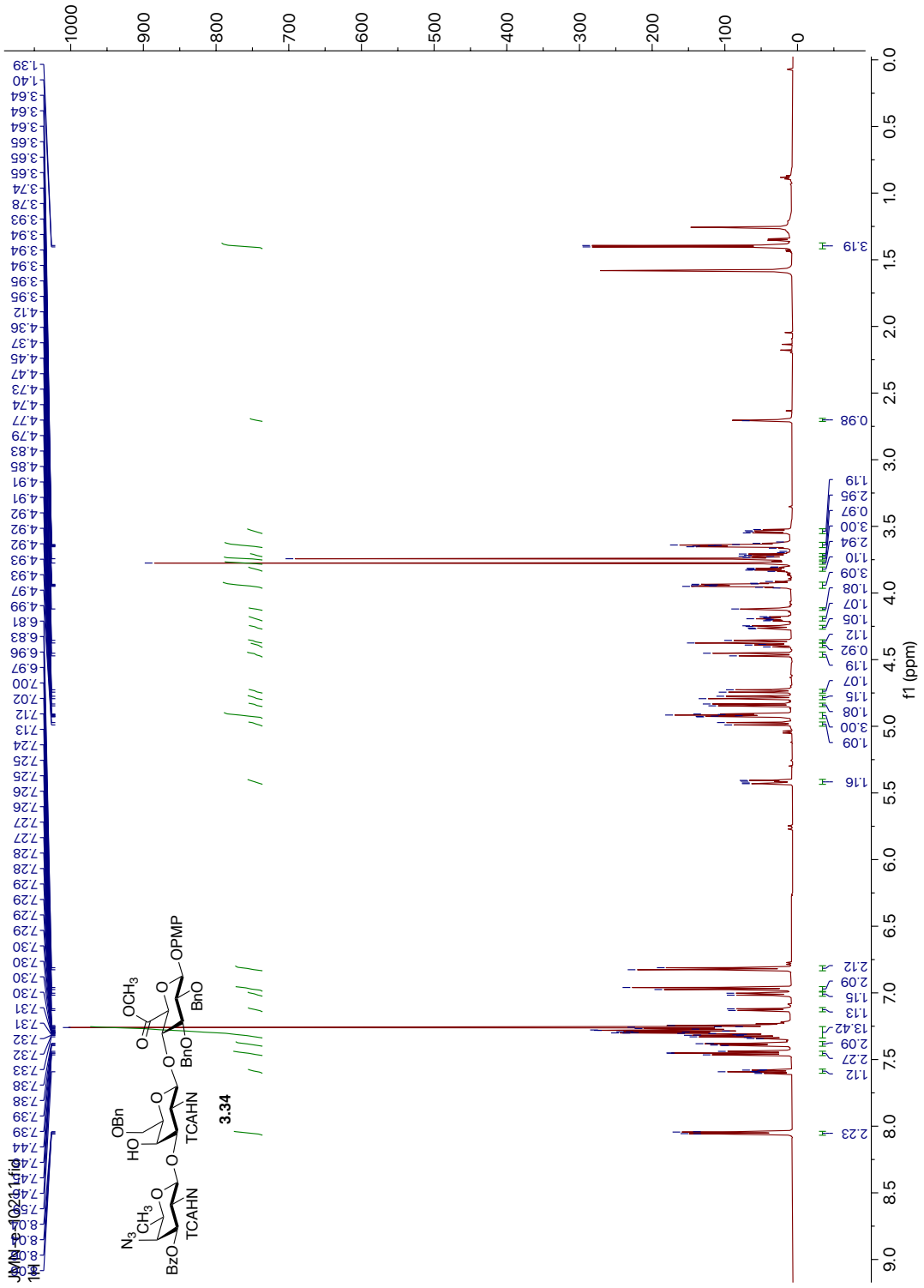

Figure A3.32. ^{1}H NMR (600 MHz, $CDCl_3$) of compound **3.34**.

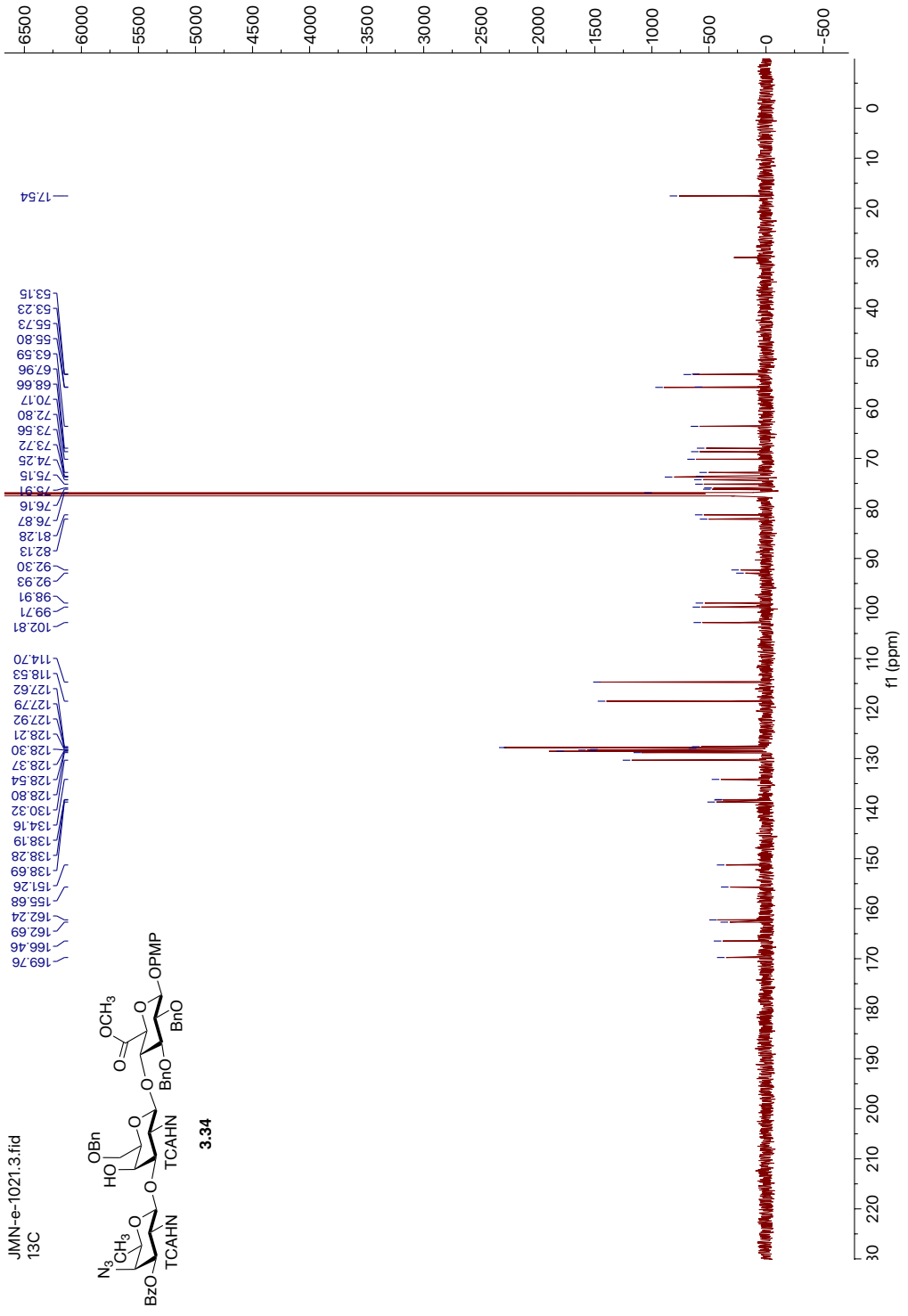

Figure A3.33. ^{13}C NMR (151 MHz, $CDCl_3$) of compound **3.34**.

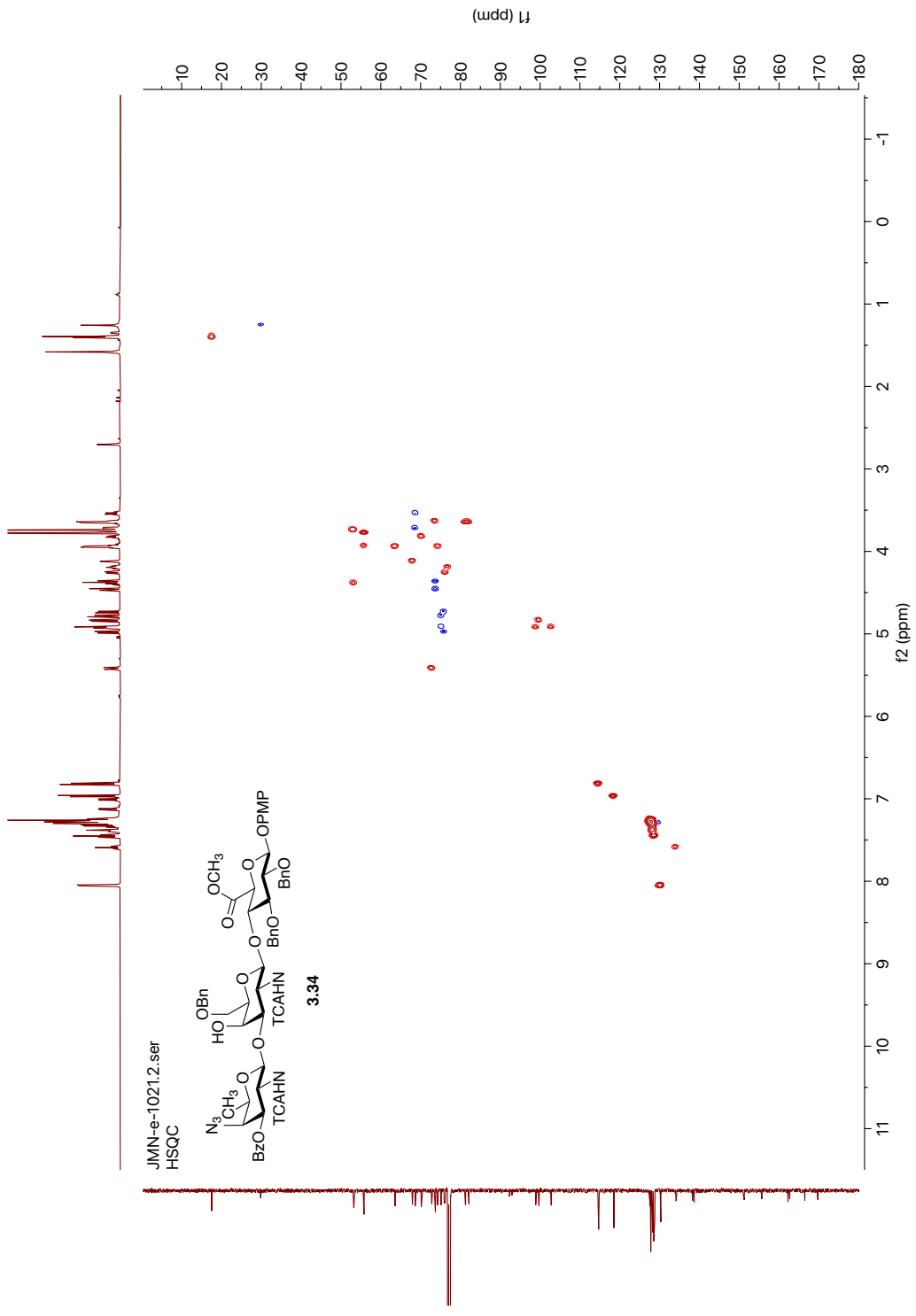

Figure A3.34. ^{1}H-^{13}C HSQC NMR (600 MHz, $CDCl_3$) of compound **3.34**.

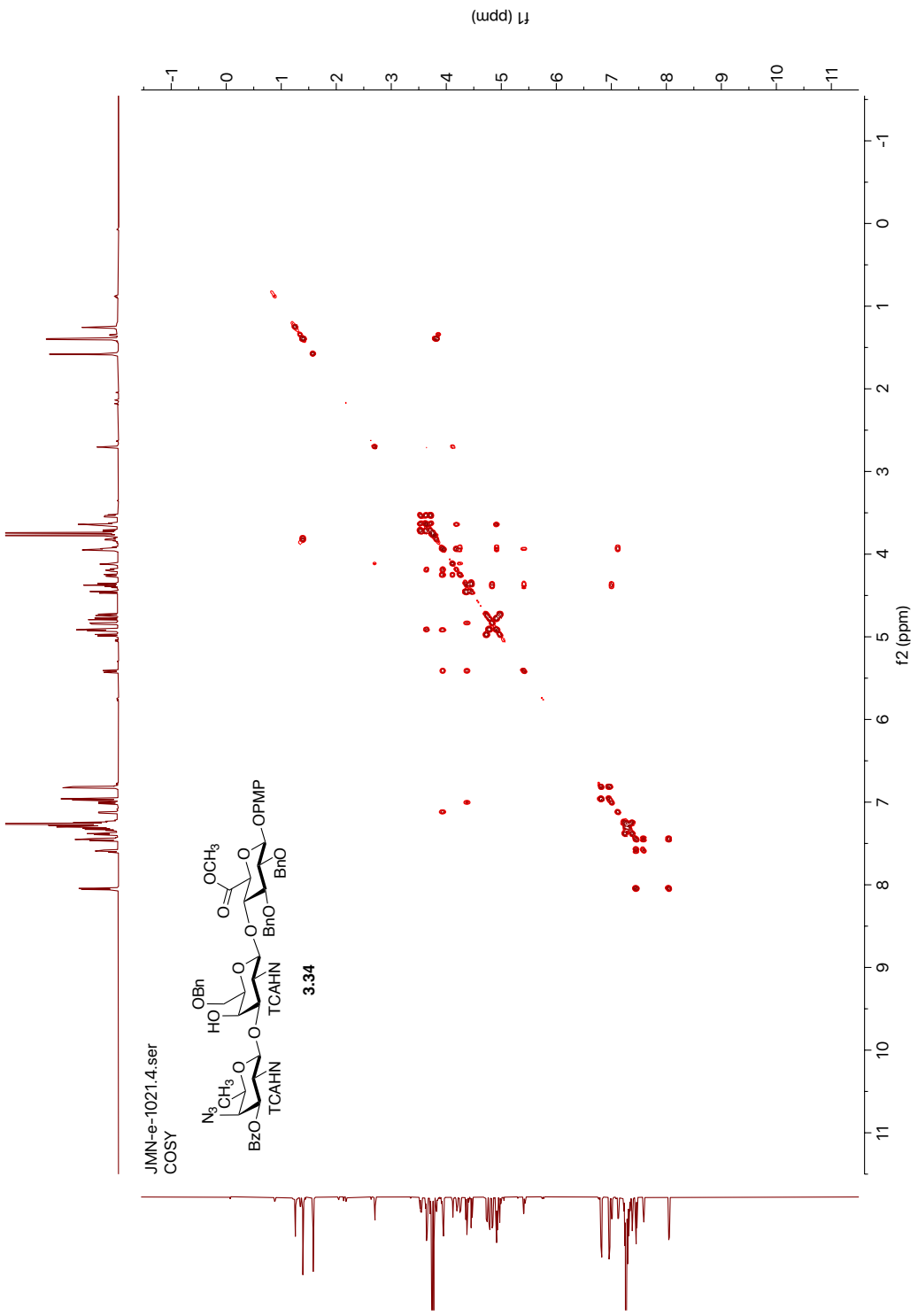

Figure A3.35. ^{1}H-^{1}H COSY NMR (600 MHz, $CDCl_3$) of compound **3.34**.

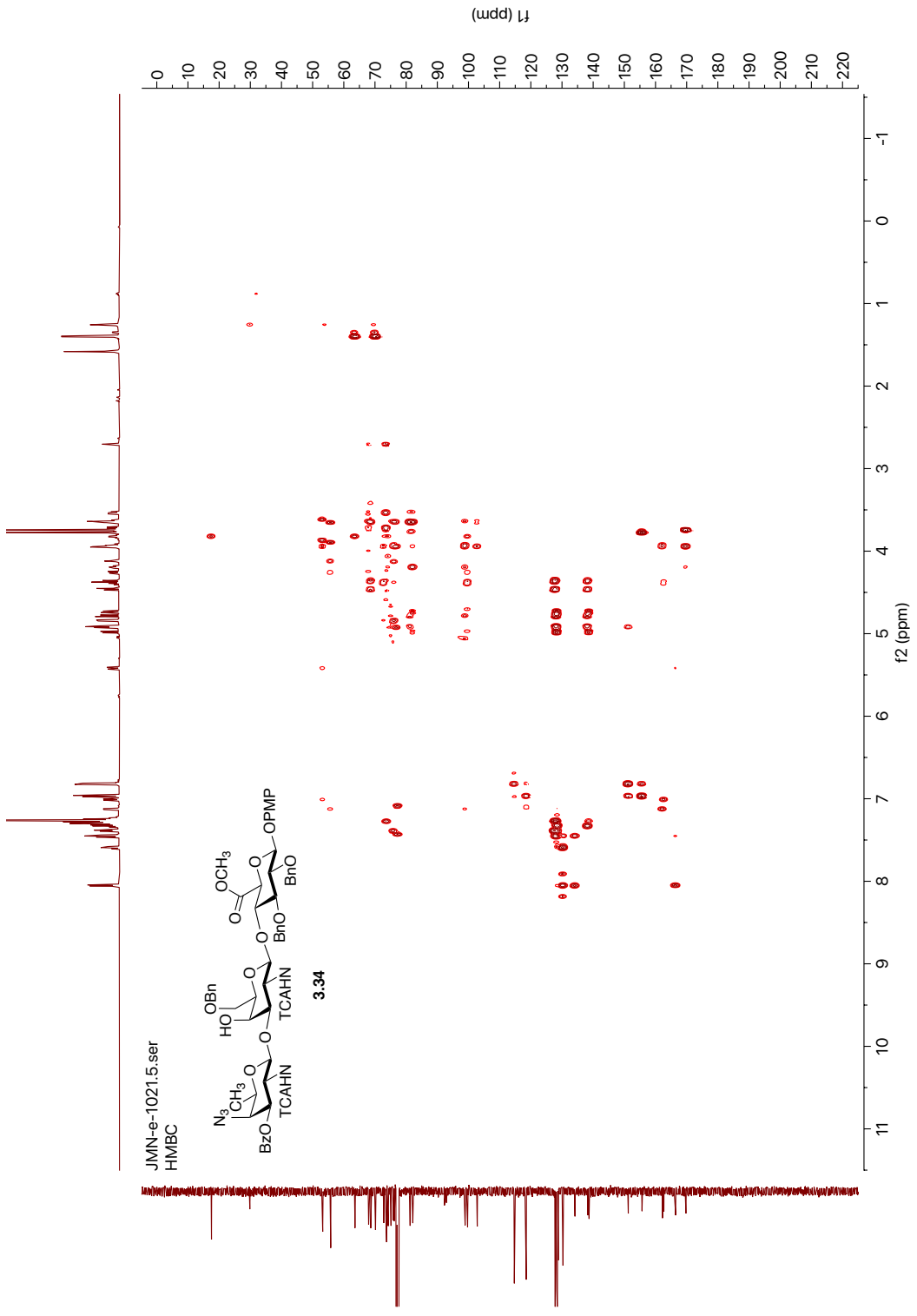

Figure A3.36. ^{1}H-^{13}C HMBC NMR (600 MHz, $CDCl_3$) of compound **3.34**.

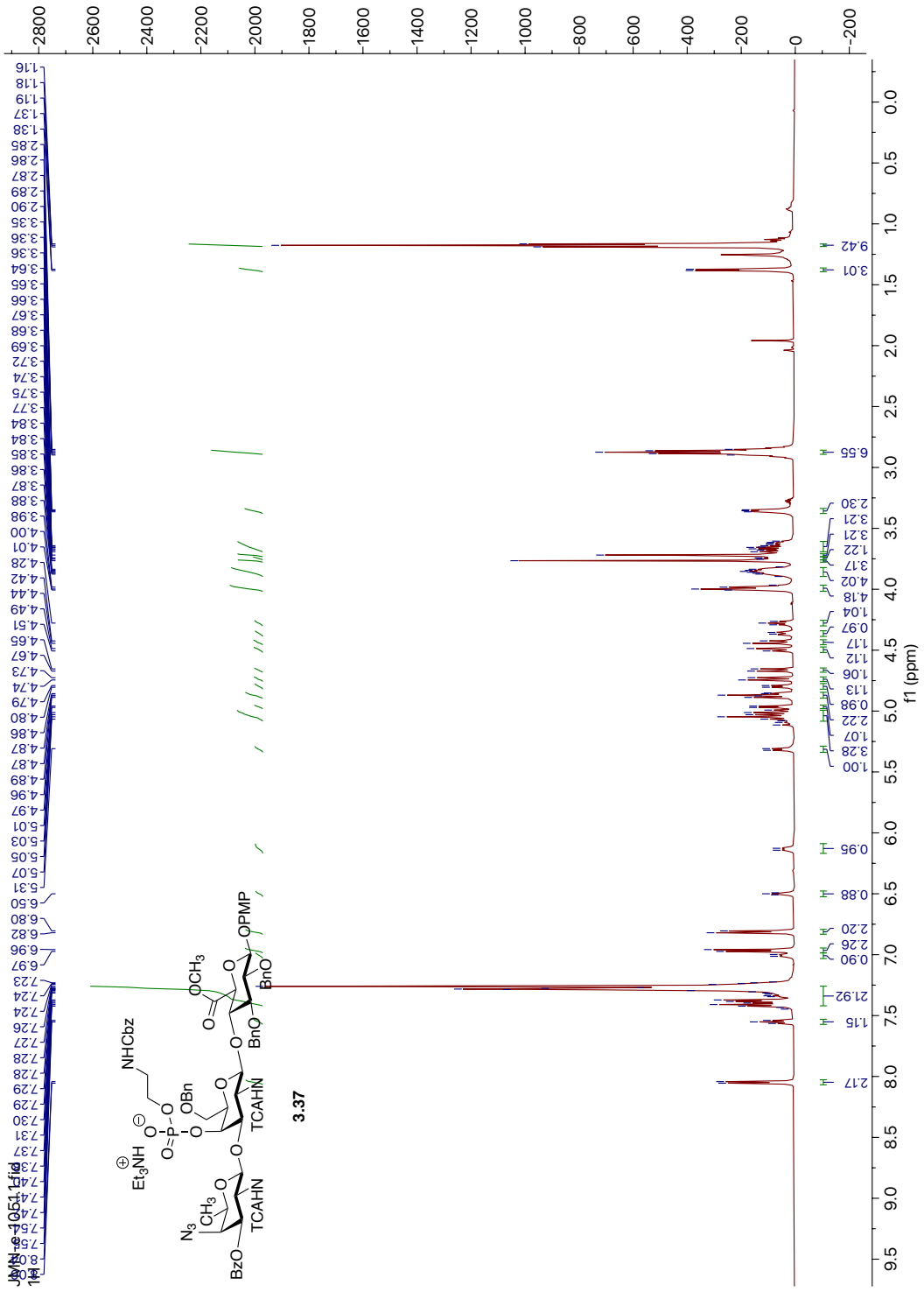

Figure A3.37. ^{1}H NMR (600 MHz, $CDCl_3$) of compound **3.37**

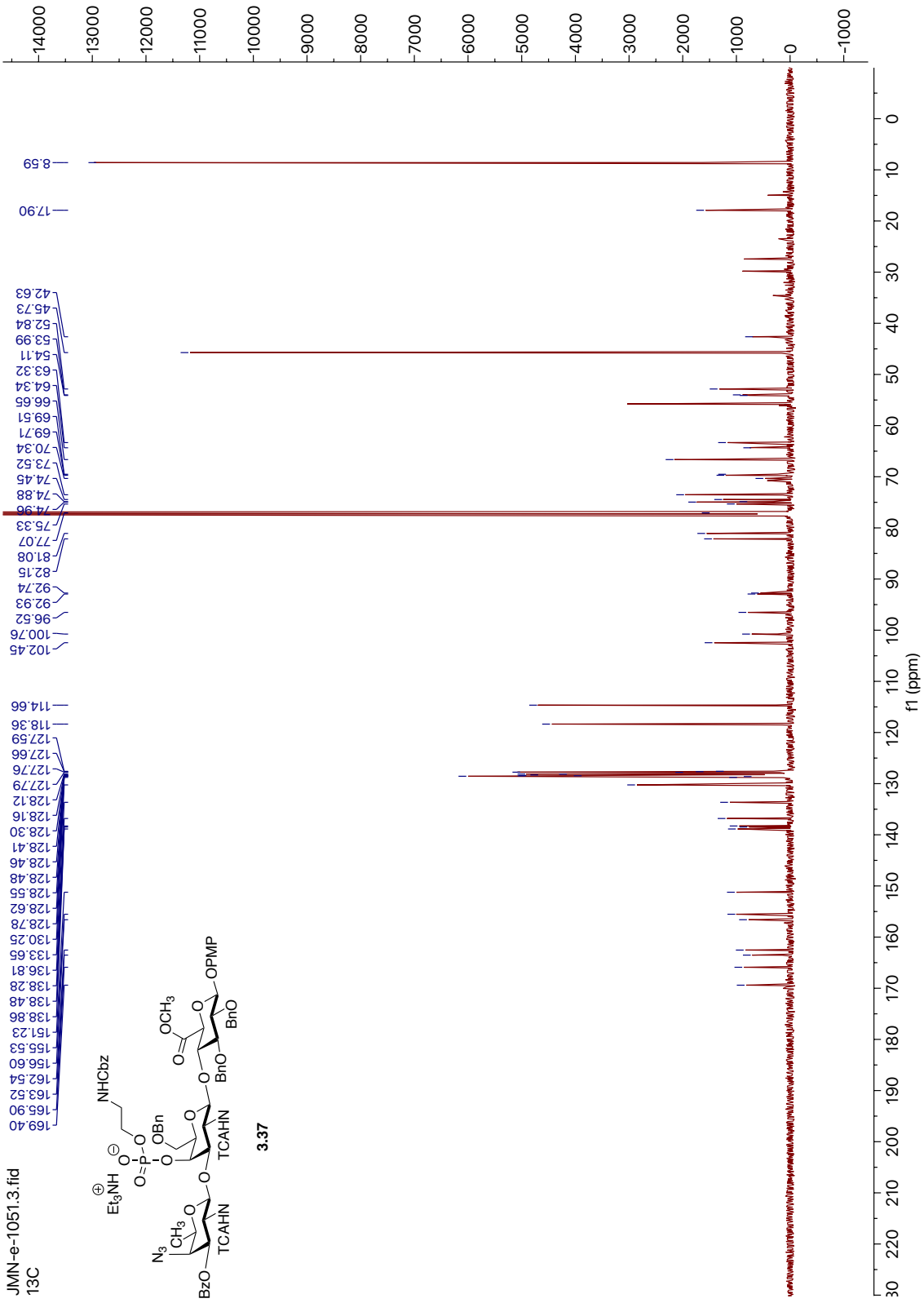

Figure A3.38. ^{13}C NMR (151 MHz, $CDCl_3$) of compound **3.37**.

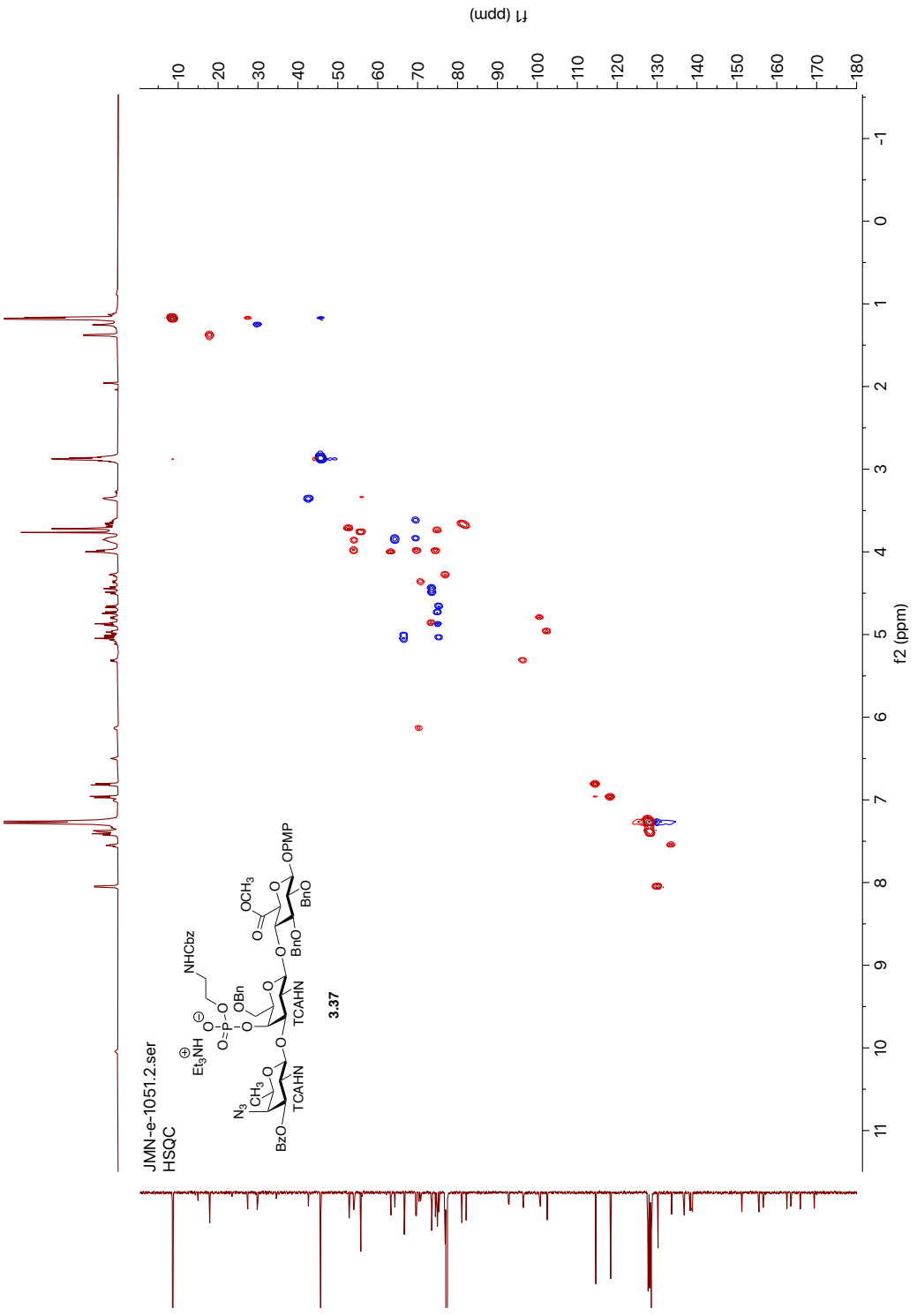

Figure A3.39. ^{1}H-^{13}C HSQC NMR (600 MHz, $CDCl_3$) of compound **3.37**.

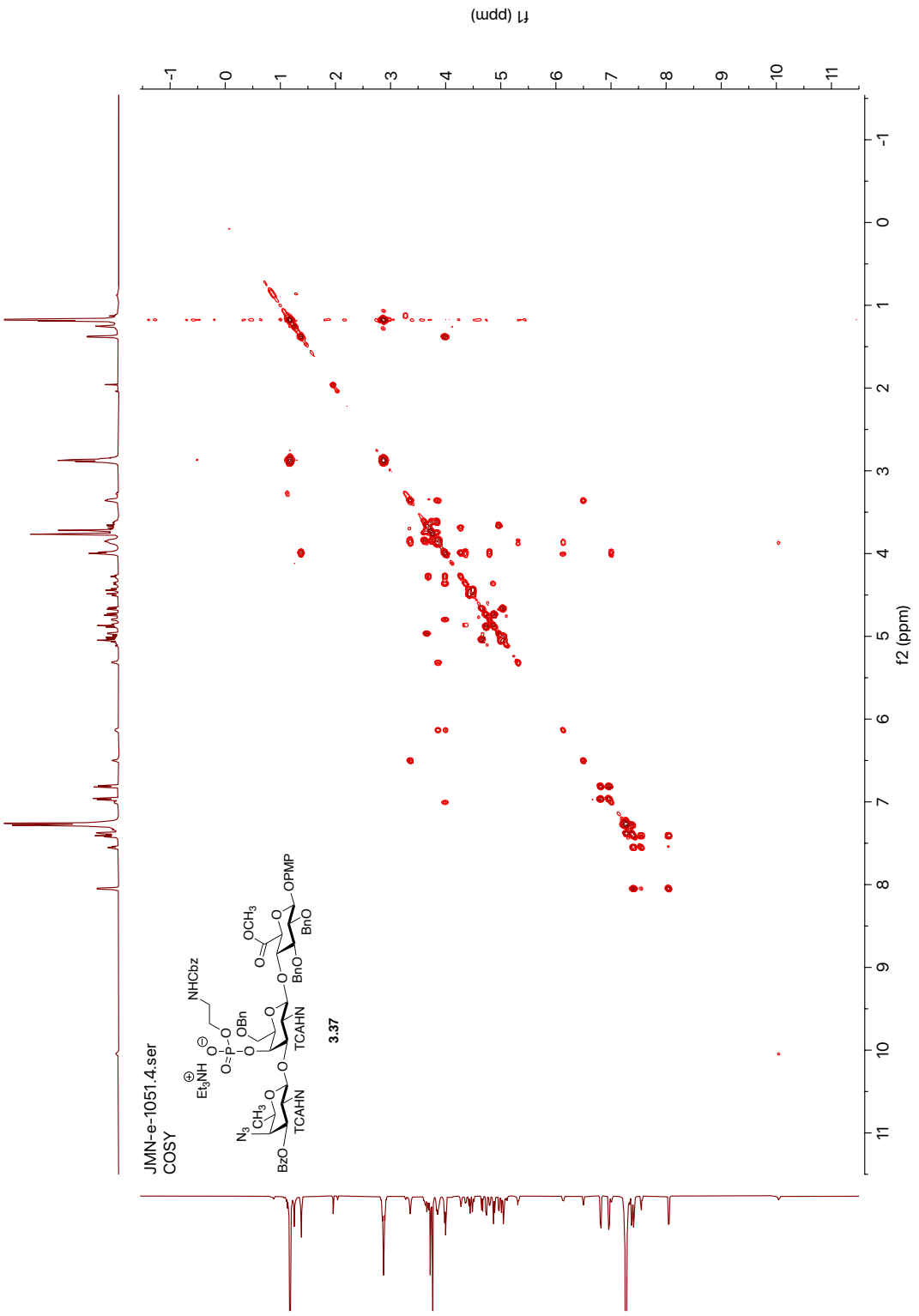

Figure A3.40. ^{1}H-^{1}H COSY NMR (600 MHz, $CDCl_3$) of compound **3.37**.

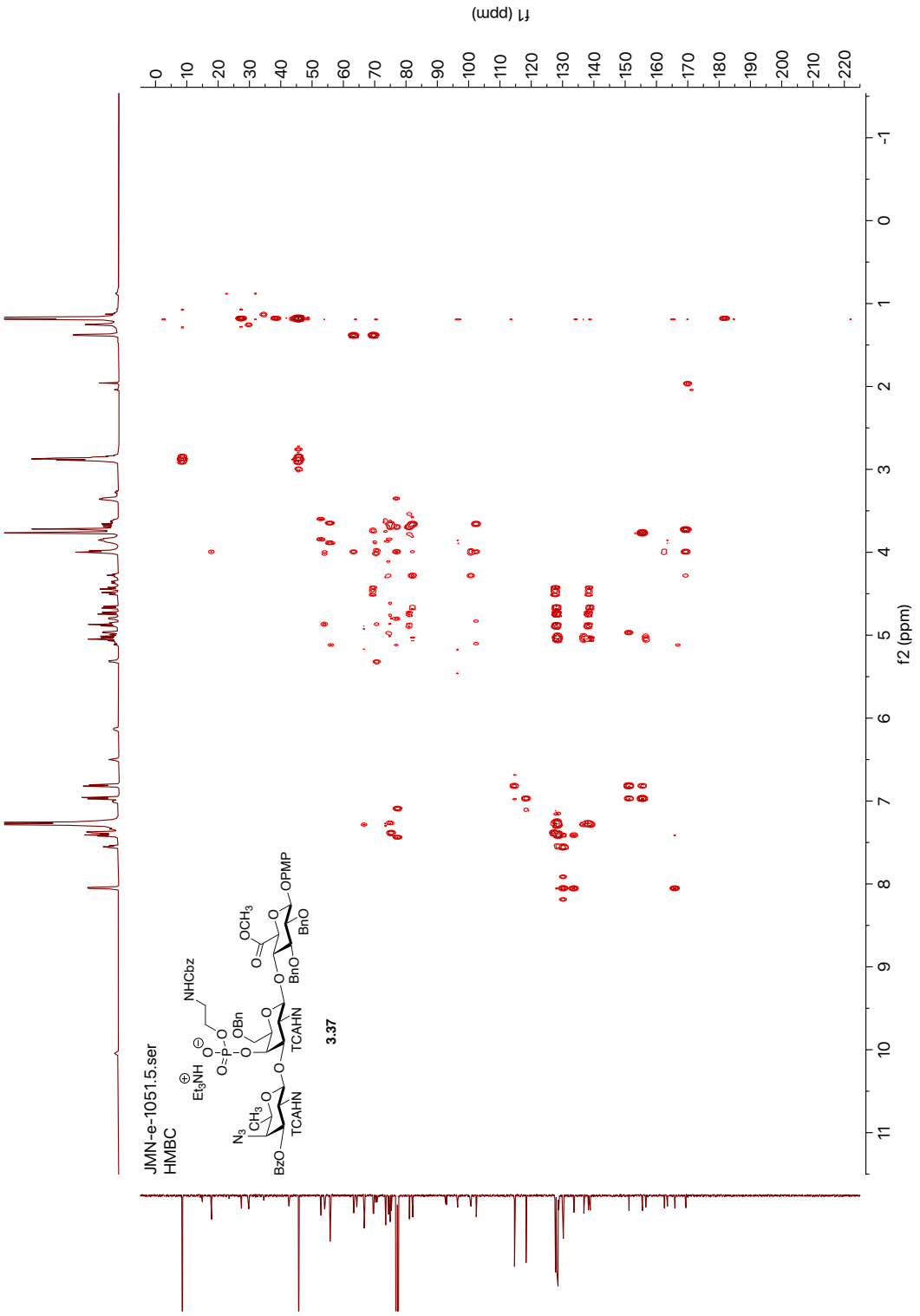

Figure A3.41. ^{1}H-^{13}C HMBC NMR (600 MHz, $CDCl_3$) of compound **3.37**.

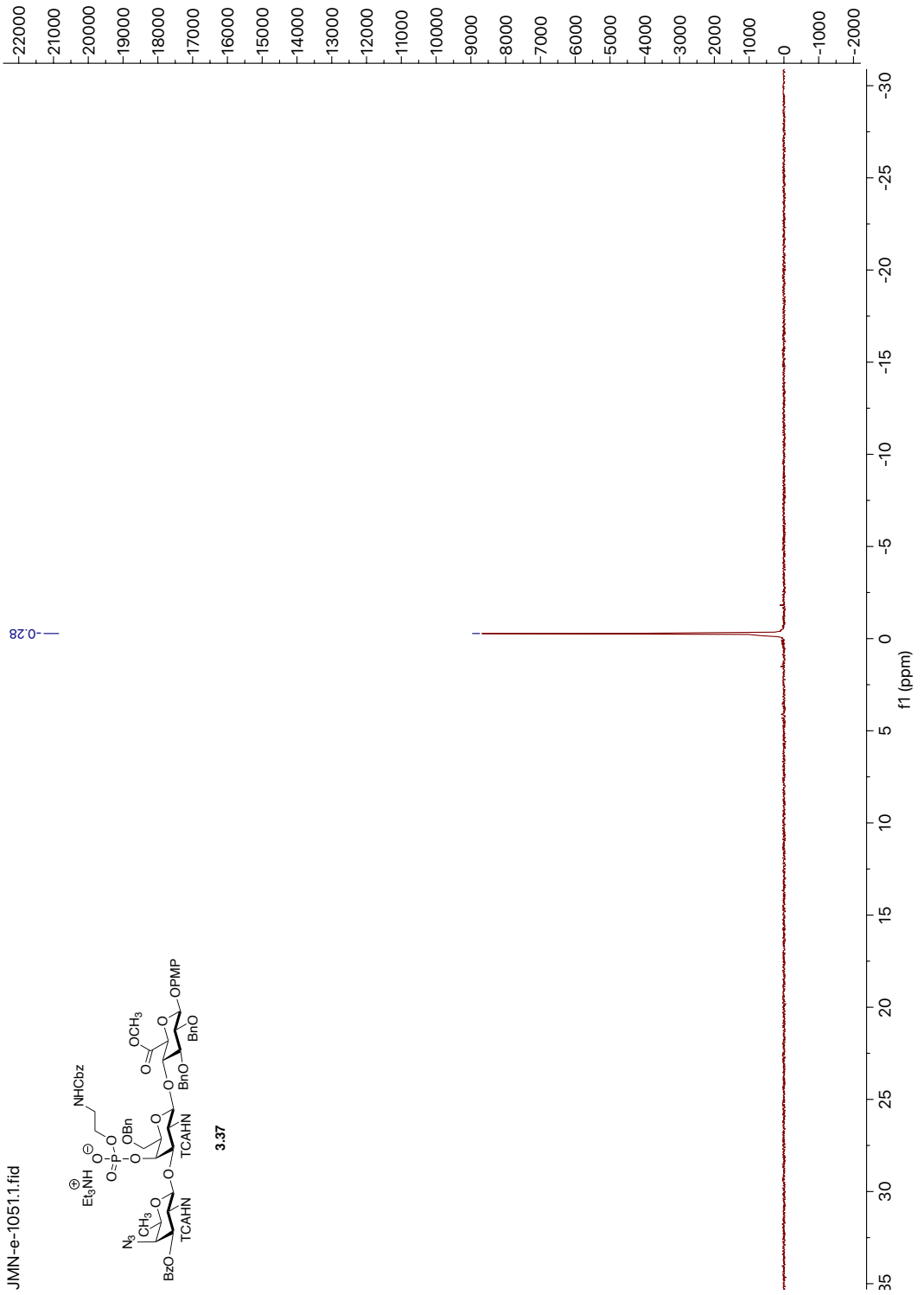

Figure A3.42. ^{31}P NMR (162 MHz, $CDCl_3$) of compound **3.37**.

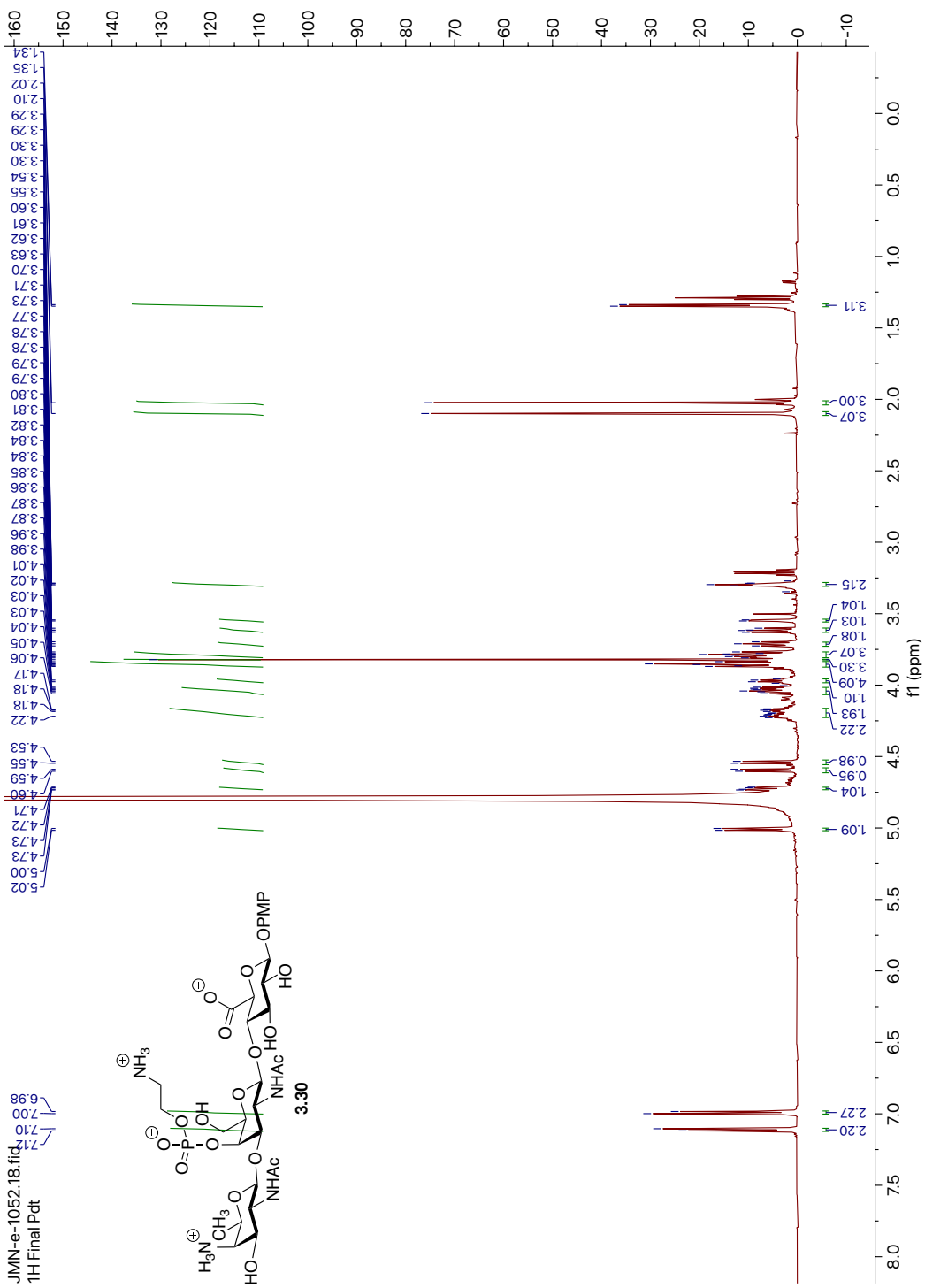

Figure A3.43. ^{1}H NMR (600 MHz, D_2O) of compound **3.30**.

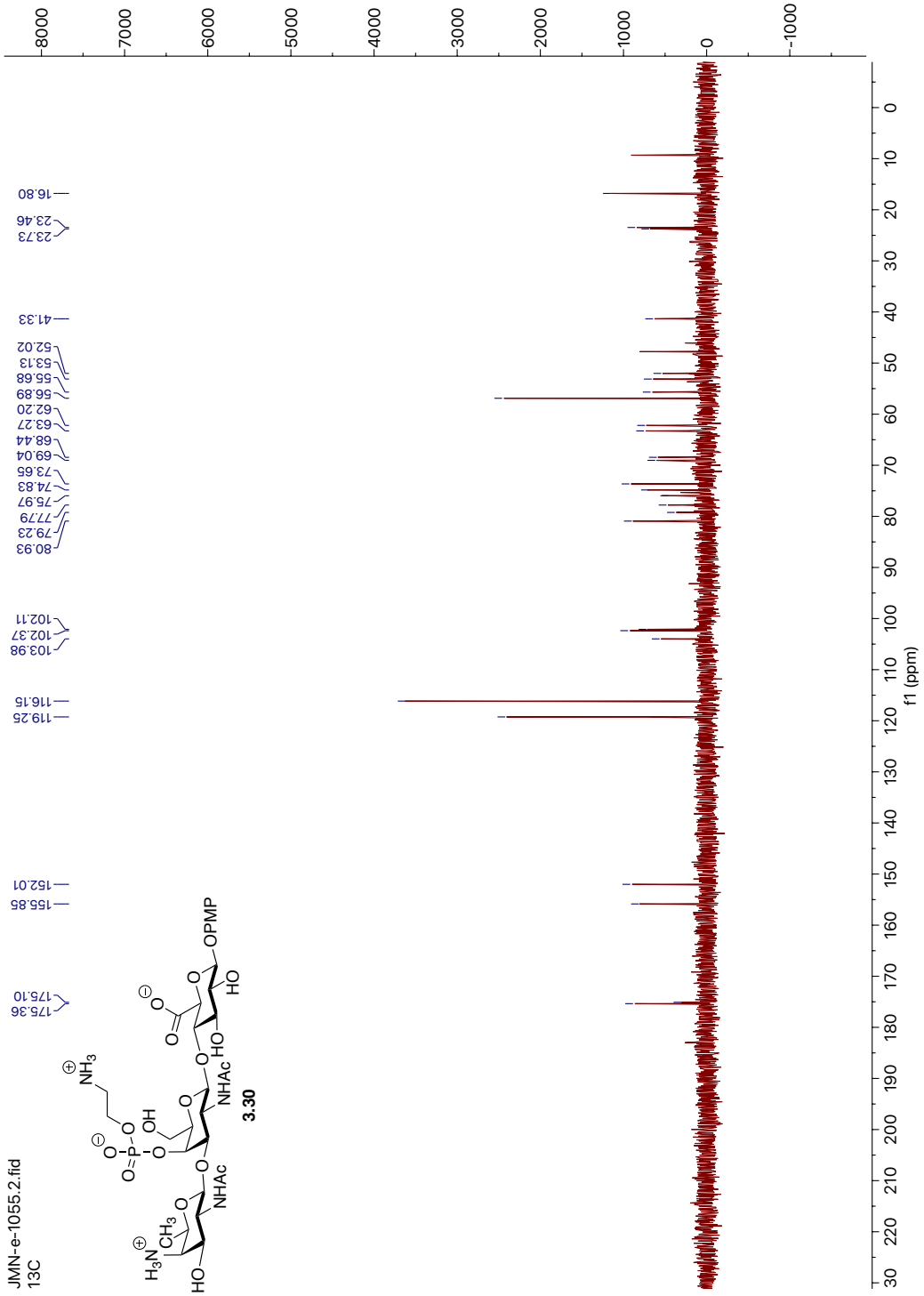

Figure A3.44. ^{13}C NMR (151 MHz, D_2O) of compound **3.30**.

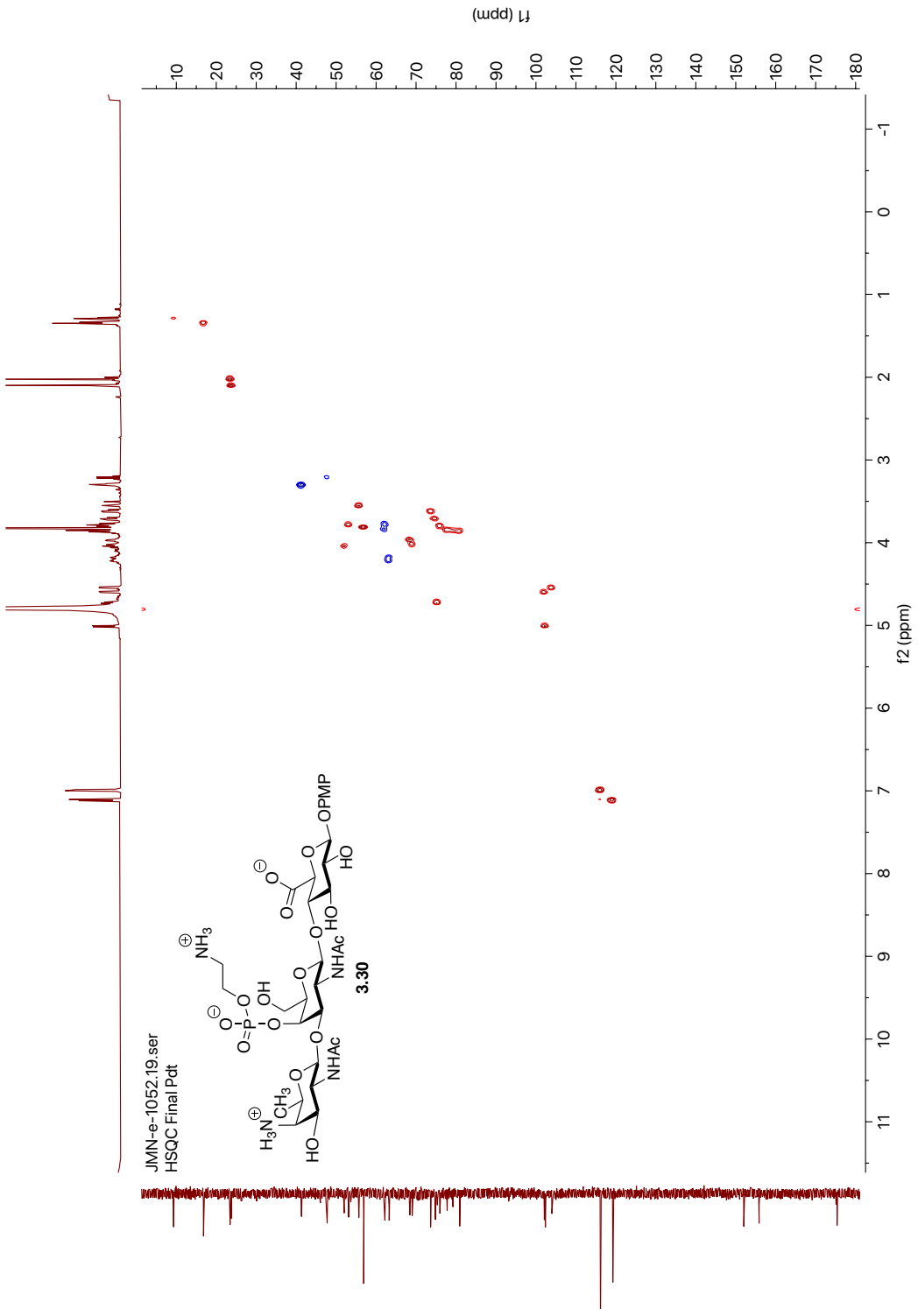

Figure A3.45. ^{1}H-^{13}C HSQC NMR (600 MHz, D_2O) of compound **3.30**.

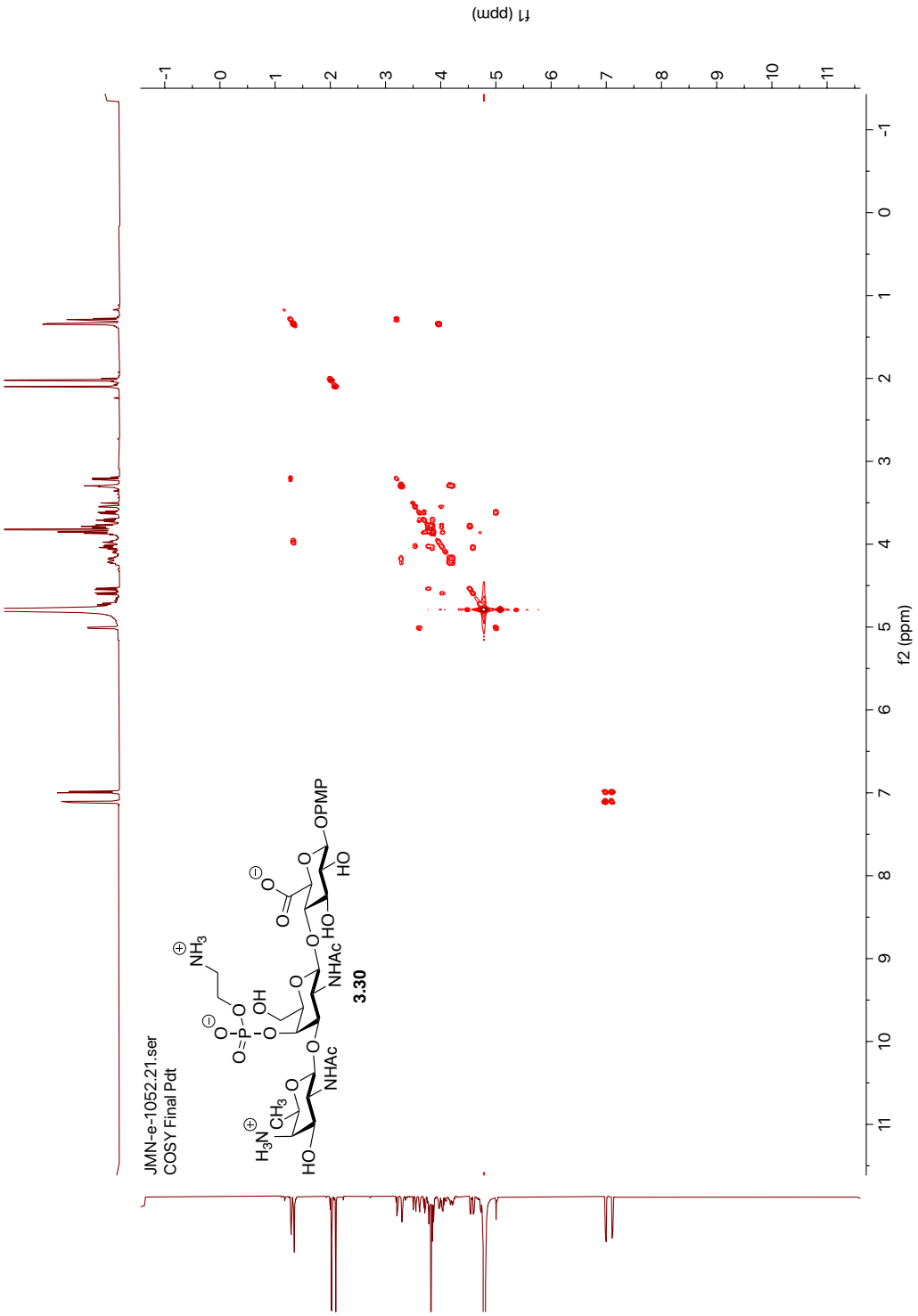

Figure A3.46. ^{1}H-^{1}H COSY NMR (600 MHz, D_2O) of compound **3.30**.

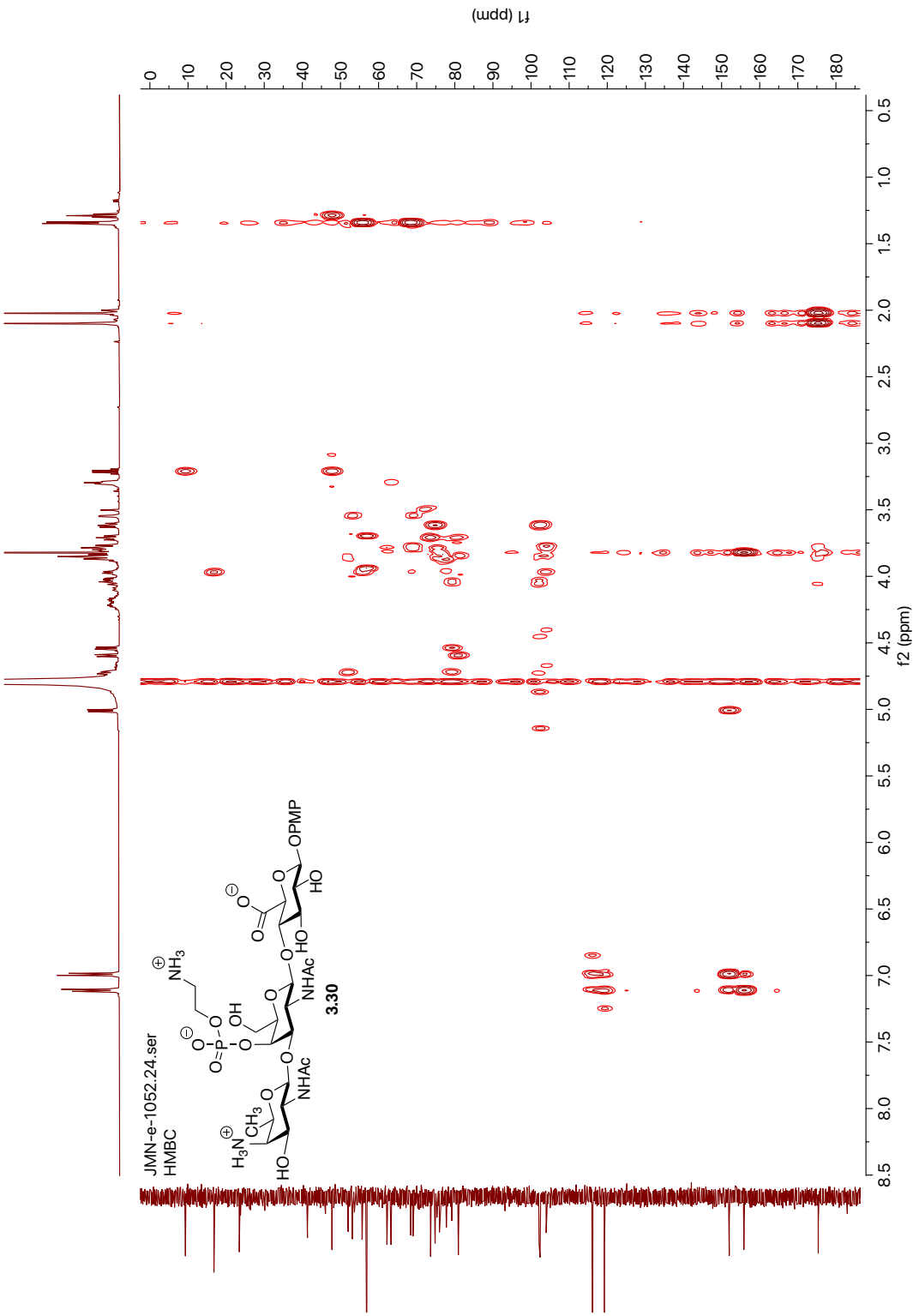

Figure A3.47. ^{1}H-^{13}C HMBC NMR (600 MHz, D_2O) of compound **3.30**.

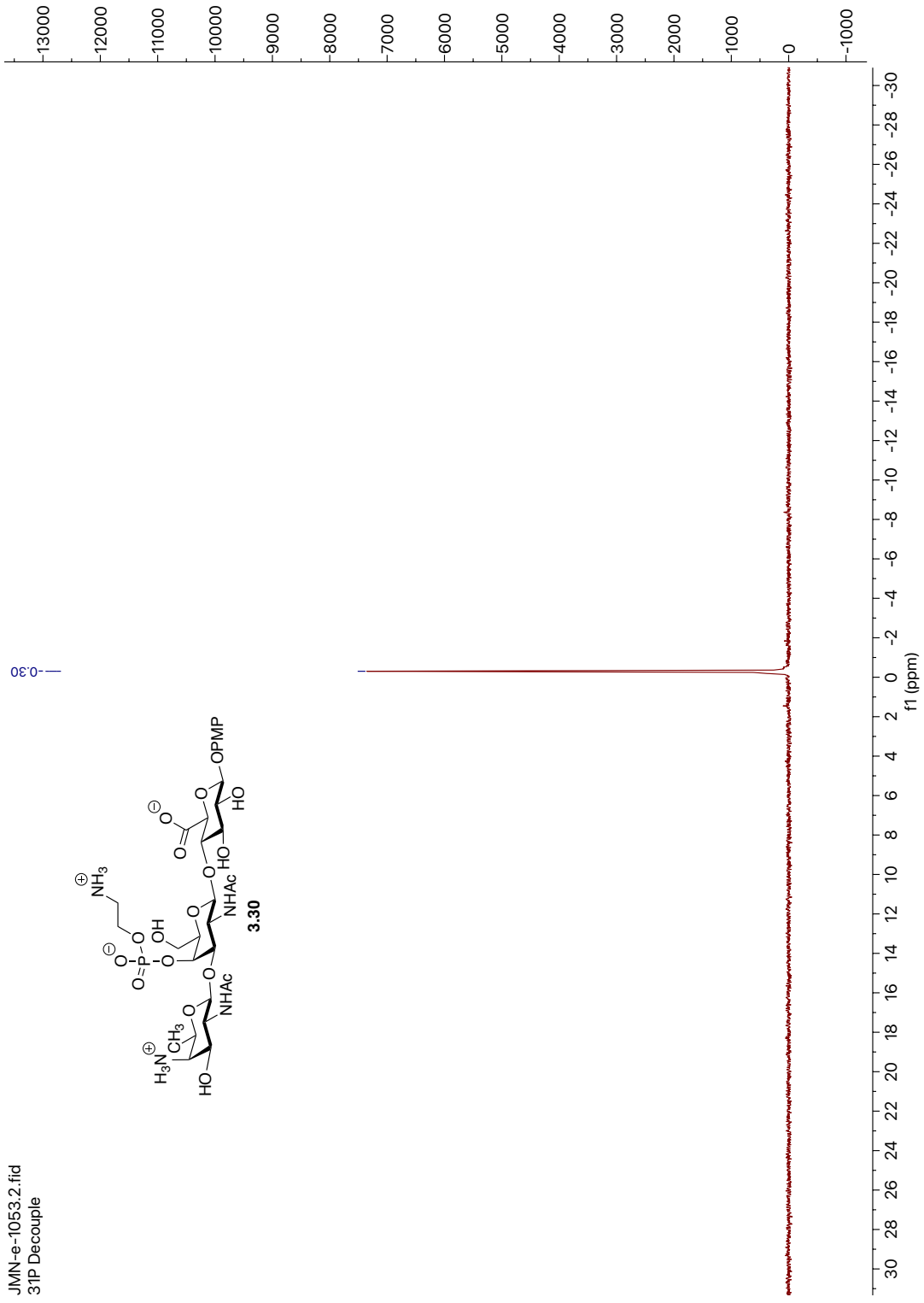

Figure A3.48. ^{31}P NMR (162 MHz, D_2O) of compound **3.30**.

Chapter 4

Future Directions

4.1 Introduction

Carbohydrates pervade the cell surfaces of viruses, parasites, and bacteria. Due to the prevalence of these biomolecules, glycan-protein molecular recognition processes are crucial in understanding the immune response to pathogens. Traditionally, carbohydrates were considered T-cell independent antigens that did not directly activate T-cells nor induce a protective immune response.[1-3] However, a class of carbohydrate antigens called “zwitterionic polysaccharides” (ZPSs) were discovered to be effective immune modulators. ZPSs are characterized by the presence of both positive and negative charged functionalities.[2-3] In recent years, the discovery of phosphorylated ZPSs have become an interesting synthetic target for the synthetic community. These polysaccharides often feature both a rare deoxyamino sugar AAT and a phosphorus residue. Moreover, glycopolymers of ZPSs of defined length are of interest to investigate the minimum polymer length necessary to stimulate an immune response. Our proposed methods will also grant access to glycopolymers of phosphorylated ZPS by leveraging a metal mediated ring-opening metathesis polymerization (ROMP) strategy to provide tool compounds for biological activity evaluation.

4.2 Proposed Synthesis of Haemophilus parainfluenzae strain 20 ZPS

Having achieved the synthesis of *P. temperata* (**4.1**) and *P. vulgaris* (**4.2**) zwitterionic repeating units, our next task is completing the synthesis of *Haemophilus parainfluenzae* (HP) strain 20 ZPS repeating unit (**4.3**).[4] Below, we describe our current progress toward the total synthesis of HP-ZPS as well as our proposed strategy.

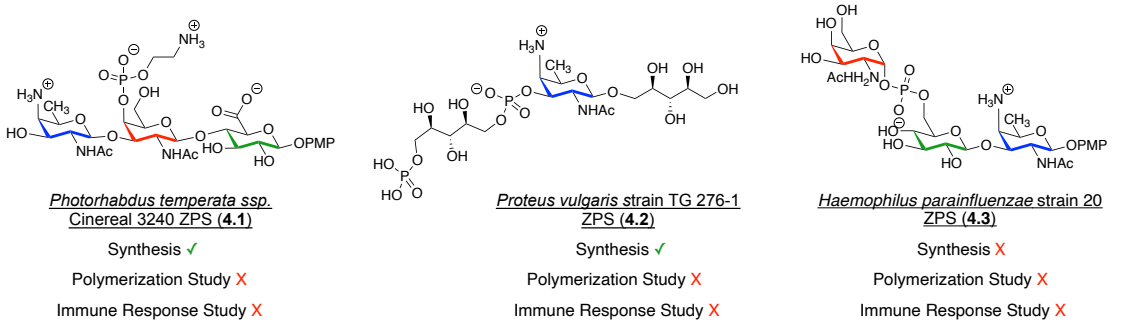

Figure 4.1. Current State of Our Efforts toward the Synthetic Targets Pursued in this Thesis.

4.1.1. Proposed Synthesis of H. parainfluenzae strain 20 ZPS repeating unit

Haemophilus parainfluenzae strain 20 ZPS repeating unit **4.3** shares an AAT residue similar to the one portrayed in the synthesis of **4.1** and **4.2**. As such, we reasoned that the synthesis of HP-ZPS can be accomplished through the use of chemistry developed in the group. Structurally, the trisaccharide repeating unit is composed of an *N*-Acetylgalactosamine (**4.4**), glucose (**4.5**), and AAT (**4.6**) residues. Based on this preliminary evaluation, the molecule incorporates a 1,2-*trans*-β-glycosidic linkage and would require a regioselective reductive ring opening of the benzylidene acetal to free the C'-6 alcohol for future phosphorus coupling. Our efforts toward the synthesis of **4.3** began with the synthesis of the three building blocks **4.4**, **4.5**, and **4.6**, which can be accessed from commercially available carbohydrate starting materials (Scheme 4.1).

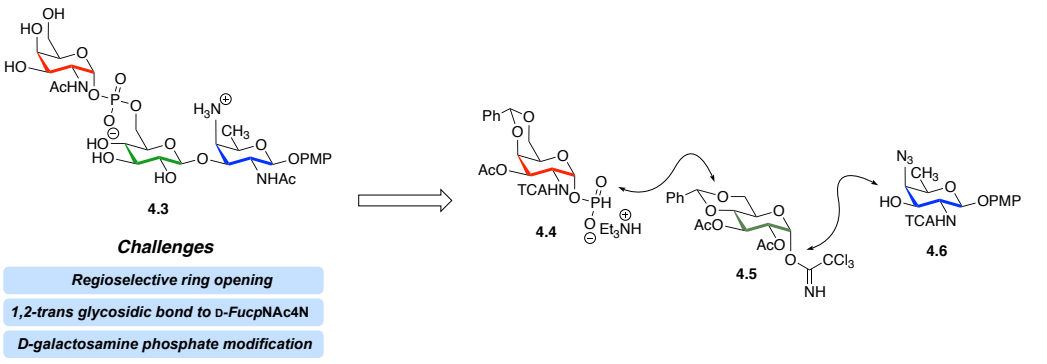

Scheme 4.1. HP-ZPS repeating unit synthetic target and key common intermediates

We envision that union of acceptor **4.4** and donor **4.6** can be possible via TfOH mediated glycosylation to give disaccharide **4.7**. Next, we will subject **4.7** to a regioselective reductive ring-opening with borane-tetrahydrofuran and Lewis-acid to obtain **4.8** as described by Ellervik *et.al*.[5] Subsequent phosphorus coupling with **4.4** will yield **4.9** which should afford the desired repeating unit **4.3** upon hydrogenolysis and saponification with Pearlman's catalyst and sodium methoxide (Scheme 4.2).

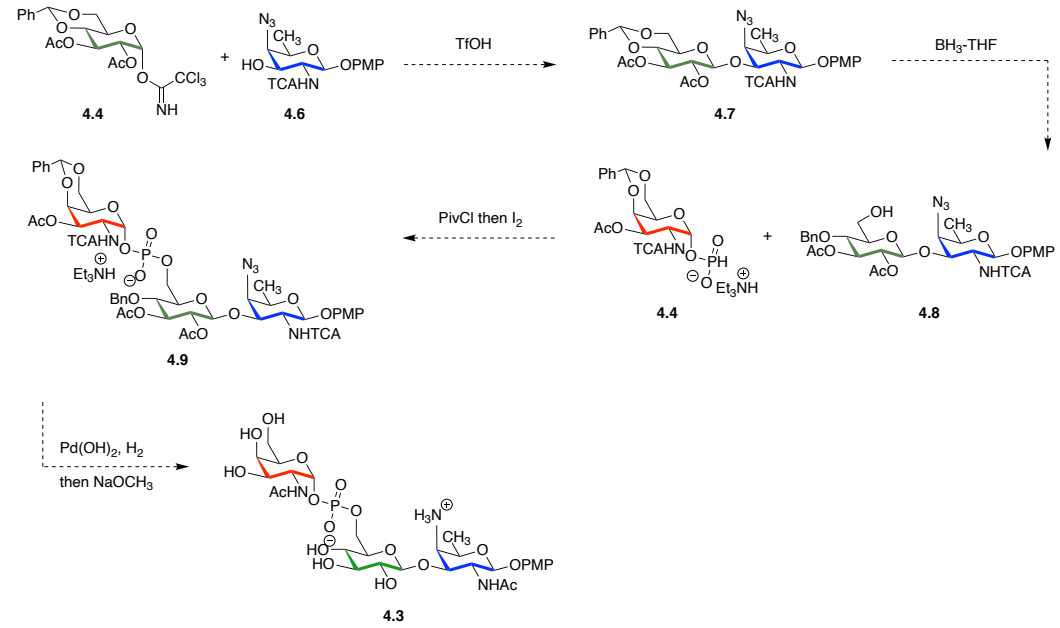

Scheme 4.2. Proposed Synthesis of HP-ZPS repeating unit (**4.3**)

4.3 Polymerization of ZPS derivatives

For the synthesis of the target glycopolymers by ROMP, we will explore the ability of Grubbs II ruthenium alkylidene catalyst to polymerize an end-functionalized norbornene PT-ZPS repeating unit. To our knowledge, ZPS repeating units have not been polymerized or studied before. With this work, we hope not only to better understand how ZPSs can be used as vaccine adjuvants but also to identify the minimum polymer length needed to elicit an immune response. To gain further insight into the bioactivity of the PT-ZPS compounds, we propose the synthesis of glycopolymers of PT-ZPS through end-functionalized ring-opening metathesis polymerization (ROMP) studies. Furthermore, we hope to apply this methodology towards the synthesis of other norbornene functionalized ZPSs.

To assemble glycopolymers of PT-ZPS, we will use Grubbs II ruthenium carbene catalyst to promote ring-opening metathesis polymerization (ROMP), a powerful technique that tolerates many functional groups, especially polar moieties observed on carbohydrates.[6] Kiessling and Hsieh-Wilson have demonstrated ROMP of carbohydrates; however, these examples are limited to neutral and anionic functionalized monosaccharides and disaccharides.[7-8] To our knowledge, ZPS repeating units have not been polymerized or studied before. Thus, we propose a strategy to couple complex ZPS repeating units with a norbornene-based backbone to provide multivalent display of the polysaccharide chains (Figure 4.2).

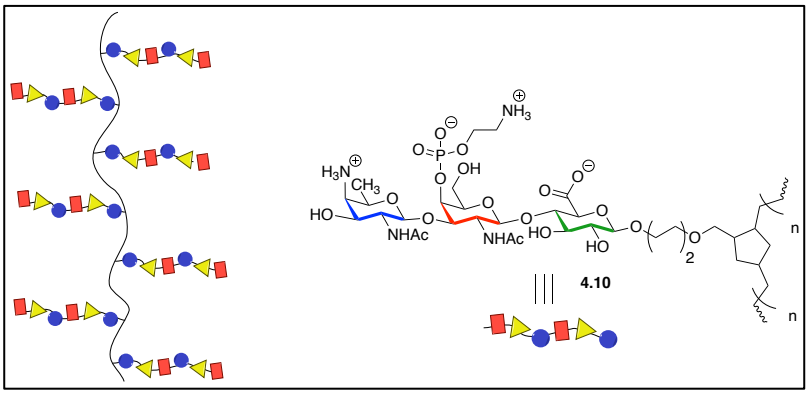

Figure 4.2. PT-ZPS ROMP polymer (**4.10**)

ROMP is highly efficient for strained cycloalkenes, such as norbornenes because the metathesis equilibrium is shifted toward the ring opening process in order to release the ring strain.[9] We chose ROMP for this work because of the living polymerization of nobornenes to produce polymers of a narrow polydispersity index (PDI) and good molecular weight control. PDI is used to describe the distribution of polymer chain molecular weight in a given polymer. As the PDI value increases, the chain length will vary. Living polymerization is a form of chain growth polymerization that does not undergo a termination step.[10] This type of reaction continues until the monomer supply has been consumed completely. Because the supply of monomers is controlled, the chain length can be manipulated to serve the need of a specific application.

Central to this work, key intermediate **4.11** will be subject to oxidative deprotection, cleaving the PMP group at C-1, followed by anomeric activation of the hemiacetal as the trichloroacetimidate to furnish donor **4.12** (Scheme 4.3A). Next, donor **4.12** will be coupled to norbornene acceptor **4.13** to provide the fully protected trisaccharide **4.14**. Using chemistry previously developed by the

Kiessling and Hsieh-Wilson groups, we envision that trisaccharide **4.14** will undergo ROMP with Grubbs II catalyst and subsequent deprotection to yield desired glycopolymer **4.10**.

To determine the molecular weight and length of the glycopolymers, we will implement gel permeation chromatography (GPC). GPC is a separation method used to determine the molecular weight distribution of polymers and to separate polymers with different degrees of polymerization. Upon completion of the first ROMP study, we will apply this chemistry to synthesize the other ZPS repeating unit glycopolymers, such as **4.15** and **4.16** (Scheme 4.3B).

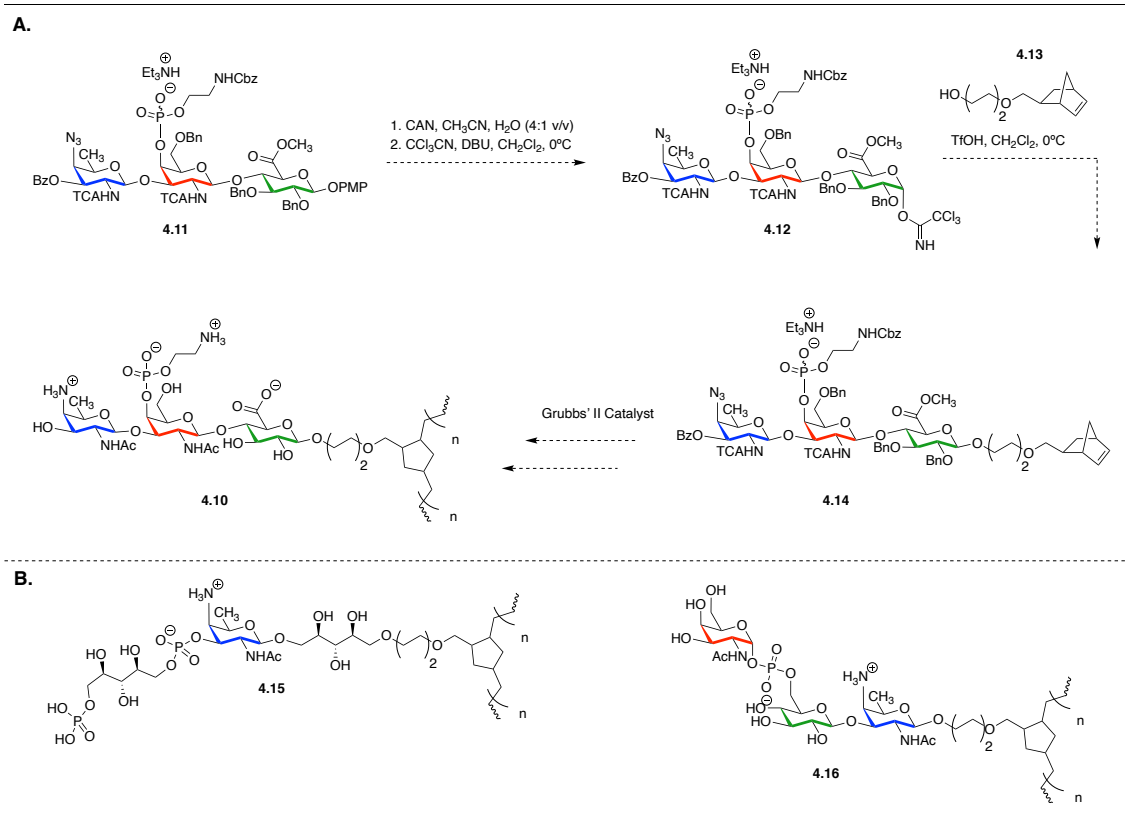

Scheme 4.3. Proposed Synthesis of Norbornene-based Glycopolymers: (A) PT-ZPS (**4.10**) glycopolymer synthesis (B) PV-ZPS (**4.15**) and HP-ZPS (**4.16**) glycopolymers

4.4 Conclusion

The focus of the proposed work is the synthesis and polymerization of the ZPS repeating units for the purpose of determining the minimum polymer length necessary to stimulate an immune response. This work will provide access to three different ZPS repeating units, and future studies using polymerization of zwitterionic polysaccharides will provide a deeper understanding in how ZPS glycopolymers behave and function in the realms of glycobiology. As a result, this work will give new insights key to the design of new carbohydrate-based vaccines.

4.5 References

1. Roberts, I. S. The biochemistry and genetics of capsular polysaccharide production in bacteria*. Annu. Rev. Microbiol*. **1996,** *50,* 285−315.
2. Reid, C. W.; Fulton, K. M.; Twine, S. M. Never take candy from a stranger: the role of the bacterial glycome in host-pathogen interactions. *Future Microbiol*. **2010**, *5* (2), 267−288.
3. Cobb, B. A.; Wang, Q.; Tzianabos, A. O.; Kasper, D. L. Polysaccharide processing and presentation by the MHCII pathway. *Cell* **2004,** *117* (5), 677−687.
4. Vitiazeva, V.; Twelkmeyer, B.; Young, R.; Hood, D. W.; Schweda, E. K. H. Structural studies of the lipopolysaccharide from *Haemophilus parainfluenzae* strain 20. *Carbohydr. Res.* **2011**, *346*(14), 2228-2236.
5. Johnsson, R.; Ohlin, M.; Ellervik, U. Reductive Opening of Benzylidene Acetals Revisited: A Mechanistic Scheme for Regio- and Stereoselectivity. *J. Org. Chem.* **2010**, *75*, 23, 8003-8011.

6. Gordon, E. J.; Sanders, W. J.; Kiessling, L. L. Synthetic ligands point to cell surface strategies. *Nature.* **1998**, *392*, 30–31.
7. Lee, G. S.; Brown, J. M.; Rogers, C. J; Matson, J.B.; Krishnamurthy, C.; Rawat, M.; Hsieh-Wilson, L. C. End-functionalized glycopolymers as mimetics of chondroitin sulfate proteoglycans. *Chem. Sci.* **2010**, *1*, 322-325.
8. Manning, D. D.; Kiessling, L. L. Synthesis of Sulfated Neoglycopolymers: Selective P-Selectin Inhibitors. *J. Am. Chem. Soc*. **1997**, *119*, 3161-3162.
9. Nguyen, S.B.; Johnson, L. K.; Ziller, J. W.; Grubbs, R. H. Ring-opening metathesis polymerization (ROMP) of norbornene by a Group VIII carbene complex in protic media. *J. Am. Chem. Soc*. **1992**, *114*, 3974-3975.
10. Grubbs, R. B.; Grubbs, R. H. 50th Anniversary Perspective: Living Polymerization-Emphasizing the Molecule in Macromolecules. *Macromolecules.* **2017**, *50*, 6979-6997.